Component development for a high fidelity transient simulation of a coal-fired power plant using Flownex SE

Prepared by:

Willie le Grange

LGRWIL001

Department of Mechanical Engineering

University of Cape Town

Supervisor:

DR W.F. Fuls

January 2018

Submitted to the Department of Mechanical Engineering at the University of Cape Town in partial fulfilment of the academic requirements for a Masters of Science degree in Mechanical Engineering

Key Words: Thermo-hydraulic model, Feedwater heater, steam turbine, deaerator, Dynamic simulation, Flownex

Abstract

Large coal-fired power stations are designed to be run predominantly at full load and optimum conditions. The behaviour of plants, operating at low load and varying conditions, is getting more and more attention due to the introduction of variable renewable generation on the grid. Consequently, the need for a fully transient high-fidelity system based model has grown, as this will enable one to study the behaviour of plants under such non-ideal conditions.

This report details the development of a feedwater heater, deaerator and turbine component for such a high-fidelity transient system model using the Flownex Simulation Environment, a one-dimensional thermohydraulic network solver. The components have been modelled all with the aim of using minimal design input data.

The feedwater heater component model includes transient effects and thermodynamic relations to represent aspects such as heater performance, level control and transient inertia. In determining the heat transfer characteristics, the model makes use of plant-performance data and correlates the amount of heat transfer by using the feedwater mass flow as the load indicating parameter. This approach eliminates the need for specific geometrical details to calculate the effective heat transfer area. The level control is modelled by using a level representation built from using heat exchanger design methods.

The turbine component is modelled by using Fuls' Semi-Ellipse law or the pressure drop modelling and Ray's semi-empirical method for the efficiency modelling. The model also contains transient effects, which include thermal inertia due to the shaft and casing, and rotational inertia due to the shaft.

The deaerator component is modelled by adapting the model presented by Banda, and modifying the model to work under various conditions. This involved using curve fit methods in Flownex to use input data to model the pressure drop over the main condensate valve.

Each of the mentioned components was validated and verified with plant data and finally packaged into a compound component which is a component consisting of a subnetwork in Flownex. These compound components further contain design inputs which are easily accessible by the user. The component models were integrated into larger networks in which various scenarios can be run.

A short transient scenario was run on the low-pressure feedwater train of a specific power station. The scenario involved a turbine trip where the bled steam valves for the heaters were closed suddenly. The speed of the valves closing was however unknown and after closing the valves in approximately 10 seconds, results agreed relatively well with plant data. This illustrated the short transient capabilities of the feedwater heater component model.

The three component models (feedwater heater, turbine and deaerator) were finally integrated into a regenerative Rankine cycle and was set up using minimal design data. The boiler, condenser and condensate pump were set as boundary conditions in the network but all extraction points for the network were connected. Steady-state results were obtained for various load cases and the main temperature, flow and pressure results were compared. Results agree well with plant data, even at low load conditions.

Declaration

I, Willie le Grange, hereby declare the work contained in this dissertation to be my own. All information which has been gained from various journal articles, text books or other sources has been referenced accordingly. I have not allowed, and will not allow, anyone to copy my work with the intention of passing it off as their own work or part thereof.

Signed by candidate

Willie le Grange

Acknowledgements

I would first like to acknowledge my sincere gratitude to my supervisor, Prof. Wim Fuls, for his remarkable guidance through the life-span of the project. His support, direction and patience were key to the success of the project.

I would further like to acknowledge my fellow research peers at UCT for their involvement and support during the difficult stages of the project. Valuable life lessons were learned from them and each one made at least a page worthy contribution to the degree. These peers included Patrick Akpan, Excellent Gwebu, Willem van der Meer, Gary de Klerk, Geoff Raikes, Rendi Khobo, Rob Temlett, Gerto Prinsloo, John Clark, Pieter Rosslee, Colin du Sart and Nikki Basson.

My gratitude further extends to my family for their support and continual guidance. It was through their loving influence which made me believe in myself and have confidence in the work which was done. Among them was my Father, Louis le Grange, for his remarkable knowledge in numerical modelling and computation fluid dynamic guidance.

I am also thankful for Eskom and the staff of EPPEI for providing the opportunity to do the Master's degree. It was through them that I could visit three power stations, attend and present at various conferences and meet an amazing network of people through the course of the degree. A special thanks to Priyesh Gosai for his supportive attitude, generosity in knowledge and guidance in various aspects of the project.

I would also like to acknowledge my good friend Henri Branken for his support and shared experience on completing a post-graduate degree ("and there is a friend that sticketh closer than a brother").

Lastly and ultimately, I am grateful for my Lord and saviour Jesus Christ for providing me with the inner strength and abilities to complete the degree.

Table of Contents

Table of Contents (Appendices)

List of Figures

List of Tables

List of Nomenclature

General symbols

d	Diameter	[m]
g	Gravitational acceleration constant	[m/s^2]
h	Enthalpy; Height; convection coefficient	[kJ/kg]; [m]
k	Thermal conductivity	[W/m.K]
$\dot{m}$	Mass flow rate	[kg/s]
p	Pressure	[kPa]
t	Time	[s]
r	Ratio	[-]
v	Velocity; specific volume	[m/s]; [m^3/kg]
x	Direction/increment	[m]
z	Direction/ height	[m]
A	Area	[m^2]
Bi	Biot number	[-]
D	Diameter	[m]
I	Inertia	[kg.m^2]
L	Length; level	[m]
L	Length	[m]
M	Mass fraction	[-]
N	Number; speed	[-]; [rpm]
Pr	Prandtl number	[-]
P	Pitch	[m]
Q	Heat energy	[kJ]
$\dot{Q}$	Heat transfer rate; Volume flow rate	[kW]; [m^3/s]
Re	Reynolds number	[-]
R	Radius	[m]
S	Cross sectional area	[m^2]
T	Temperature	[°C]
UA	Overall heat transfer coefficient with Area	[W/K]
V	Volume	[m^3]

W	Work energy	[kJ]
$\dot{W}$	Work rate	[kW]

Greek symbols

α	Loss coefficient constant	[-]
β	Reactive or impulse constant	[-]
η	Efficiency	[-]
μ	Dynamic viscosity	[N.s/m^2]
ω	Concentration	ppb
ρ	Density	[kg/m^3]

Subscripts

0	Stagnation/Ambient/total
bb	Bundle to shell
e	Exit
fw	Feedwater
f	Fouling
g	Gas
i	Inlet; inside
l	Liquid
lg	Latent heat
mc	Main condensate
o	Outside
otl	Outer tube limit
r	Ratio
rc	Return condensate
s	Diving port; steam; shell; isentropic; steel
t	tube
ts	Tubesheet
tp	Tube plugging
vs	Vent steam
w	Wall
D	Design

EL	Ellipse
L	Losses
M	Machine work
P	Pump
SE	Semi-ellipse
T	Turbine

Acronyms and Abbreviations

BS	Bled Steam
CAS	Cascade
CCC	Convection, Conduction, Convection
CL	Layout Constant
COND	Condensing
CTP	Tube Pass Constant
DA	Deaerator
DC	Drain Cooling
DCA	Drain Cooler Approach
DSH	Desuperheating
H	Heater
HP	High-Pressure
HTC	Heat Transfer Coefficient
IP	Intermediate-Pressure
LP	Low-Pressure
NCG	Non-Condensable Gasses
T	Turbine
TTD	Terminal Temperature Difference

1. Introduction

1.1 Background and motivation for the study

Coal has been the dominant fuel for electricity generation in South Africa. It is estimated by the Electricity Supply Commission of South Africa (ESKOM) that at present the amount of electricity generated from coal is around 77%. This means that more than three-quarters of the nation's electricity supply is generated from the fossil fuel. This number is not likely to decline in the next decade due to insufficient alternative solutions to South Africa's power generation.

One of the main problems that South Africa encountered during the past 7 years was to produce a constant power supply to the nation. Units tripping, unplanned downtime and maintenance on older stations are the primary cause for inconsistent supply. This then results in load fluctuations on working units – which are not designed to run at varying load conditions.

Varying load causes problems throughout the power station. These problems range from large temperature gradients throughout the different components, especially thick-walled components such as the turbine casing, to unstable control due to varying liquid levels. As of yet it is difficult to fully understand and examine these quick transient scenarios due to the complex transient phenomena involved. Consequently, the need for a transient high-fidelity system based model has grown. Such a model will enable one to study the behaviour of plants under such non-ideal conditions.

The generation of this model is key. In the past, computer-aided model generation was used but had the limitation of only being steady-state [1], and was limited largely due to inadequate computer resources. This means that the model was not time-dependent and the monitoring of the power-plant over time due to certain changes in the cycle could not be analyzed. It is now possible to run dynamic simulations which can be used to test different load changes and to analyze plant behaviour.

1.2 Purpose and problem statement of the study

The purpose of the study is to develop specific components for a functioning transient simulation model of a large coal-fired power station within the Flownex Simulation Environment (Flownex SE). Modelling off-design transient conditions require that the models

- are able to capture thermodynamic and hydraulic phenomena realistically,
- have the ability to simulate transient effects such as thermal and rotational inertia,
- use minimal input data,

- be validated and verified with actual plant data,
- and packaged into custom components with the focus of complete cycle integration.

The project's specific components under consideration include the Feedwater heater, the Turbine and the Deaerator. The mentioned components have already been developed, but further refinement (such as transient capabilities, testing and packaging) of these models was still required.

Table 1.1. list the previously developed components

Table 1.1: Previous Flownex and thermal models

Component	Student
Turbine	R. Neerputh [2] (2014)
Deaerator	R. Banda [3]
Feedwater heater	M. Allie [4], M. Thakaso [5] (2016,2014)

The purpose of the component models is to analyse the behaviour of a large coal-fired power stations under various conditions (such as off-design and low-load conditions). The focus will be placed on modelling the components to be integrated with other components in the power station network. By having an integrated network of components, one is able to fully study the effects of varying load conditions and analyse how the components react to each other.

The models will also have the functionality to serve as a tool to train operators, technicians and engineers in the design and use of power plants. It is therefore required to give a detailed documentation of the components as to serve as a user guide/user manual.

1.3 Goals and objectives

The foremost goal of the project is to develop component models to simulate the steam side of a large coal-fired power station using Flownex. The following key objectives have been set for the project.

- Use and enhance existing methodologies for modelling power plant components.
- Develop the models to operate using minimal design inputs.
- Apply transient effects to the models (Effects such as level change where an accumulation of a liquid exists, thermal inertia due to thick-walled components and rotational inertia due to the shaft of a turbine)
- Package the components for further use, with the aim of cycle integration.
- Integrate the models in a complete power station cycle and validate using plant data.

To accomplish the above-mentioned objectives, a literature study will be done on previous dynamic models of power stations. Thereafter, the development of each of the three components will be accomplished through the following steps:

- Literature study on previous thermodynamic models, including Flownex models.
- Development methodology for the current Flownex model of the component.
- Validation and verification of the current Flownex model.
- Description of the final Flownex component, which includes the component family if applicable.

Finally, the three components will be integrated into a complete steam power station network. The plant will be run by designing the components with plant design data and compare the results of the network with plant acceptance or operating data. A conclusion on the project, component and integrated network will be given together with final project recommendations.

1.4 Constraints and boundaries of the project

Modelling a power station on a macro level can be a daunting task if the scope of the modelling is not limited to a certain degree. The following constraints and boundaries are therefore proposed:

- The project will focus on the components of the steam side of a large coal-fired power station.
- Component development will only be done for the Feedwater heater, turbine and the deaerator.
- Auxiliary components such as the valves and pumps are already included in the Flownex and further refinement of those components are not considered.
- Component modelling will be done with the aim of using minimal design inputs.

It is noteworthy to mention that the boiler has a tremendous transient effect on the power station network. Although this component is vital to simulating a complete transient power station network, the project will not include the boiler its scope of work simply due to time constraints. Research has been done in the past on modelling the boiler and reference can be made to the following articles:

1) Transient boiler heat exchanger thermal behaviour analyses by Gwebu E.Z. [6]
2) A Zonal model for radiation heat transfer in coal-fired boiler furnaces by Monnaemang W.O. [7]
3) Boiler system modelling using Flownex by Rossouw A. [8]

2. Literature survey

The literature survey will begin by giving a background of the inner workings of large coal-fired power stations. The review will then move on to the simulation software and briefly explain the conservation equations which is the backbone of the software. A literature review will follow which will focus on previous dynamic simulations of power plants and finally a review of plant data.

2.1 The coal-fired steam power plant

The coal-fired steam power plant, also known as the regenerative Rankine cycle, makes use of energy stored in coal and repeatedly converts the energy into electricity. This process is illustrated in Figure 2.1 where the main working fluid of the cycle is water.

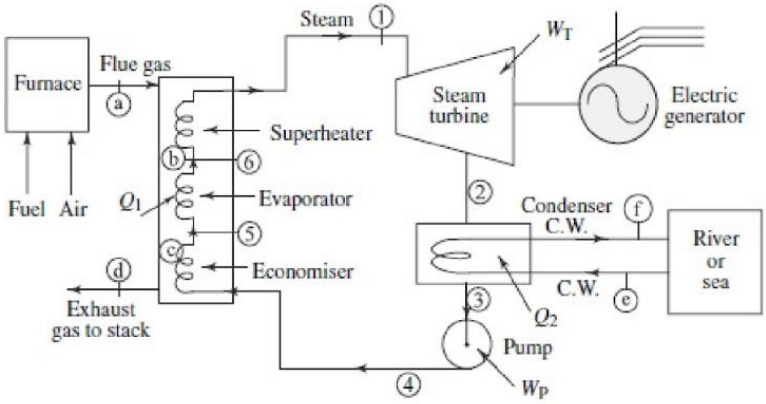

Figure 2.1: The coal-fired power station cycle [6] (modified)

The energy stored in coal is transferred as Q_1 to high-pressure water inside the boiler to turn the liquid water into superheater vapour. This happens primarily in three stages: the water is first heated to saturation temperature in the economizer, evaporation of the water then occurs in the evaporator and finally, the water is superheated in the superheater.

The steam exits the boiler at high-pressure high-temperature conditions and is expanded through the turbines where the kinetic energy inside the steam is transferred through the blades of the turbine to rotate the shaft. This shaft work (W_T) is what drives a generator which produces electricity.

The expanded steam is then condensed into liquid again through a condenser which exchanges heat with a cooling tower. Energy is lost to the environment through this process (Q_2). A pump is then used to pump the water (W_P) back into the furnace and the cycle again repeats itself [6].

The process can also be illustrated by using a temperature-entropy diagram, represented in Figure 2.2, by plotting the working fluid's temperature and enthalpy as it moves through the cycle.

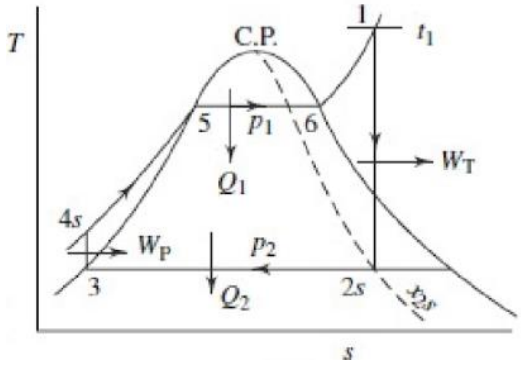

Figure 2.2: T-s diagram of the Rankine cycle [6]

The steam is expanded through state 1 to 2 and condensed from state 2 to 3. The water is pumped from state 3 to 4 and sent through the steam generator from stage 4 to 1. In the steam generator, there are various stages to the heating processes. The first being the economizer where the water is heated to a saturation point from 4 to 5. After this, it is sent to the evaporator from point 5 to 6 and ultimately sent to the super-heater from point 6 to 1.

The most important parameters can be calculated by using the steady flow energy equations. Table 2.1 gives a summary of these parameters. The parameter h is given as the enthalpy with the unit [kJ/kg] and $\dot{m}$ as the mass flow rate [kg/s]

Table 2.1: Most important parameters and equations regarding the regenerative Rankine cycle

Equation		Description
$Q_1 = \dot{m} \cdot (h_1 - h_4)$	(1.1)	The specific heat added by the boiler.
$W_T = \dot{m} \cdot (h_1 - h_2)$	(1.2)	The energy gained from the turbine sets.
$Q_2 = \dot{m} \cdot (h_2 - h_3)$	(1.3)	The energy lost to the environment through the condenser.
$W_P = \dot{m} \cdot (h_4 - h_3)$	(1.4)	The energy needed by the pump.
$\eta = \frac{W_{net}}{Q_1} = \frac{W_T - W_P}{Q_1}$	(1.5)	The efficiency of the Rankine cycle.
Steam rate $= \frac{1}{W_{net}} \frac{kg}{kWs}$	(1.6)	The steam rate or specific steam consumption, this parameter expresses the capacity of the power plant.

It is important to note that Figure 2.2 is a representation of a sub-critical power station, which is the case for most power stations in the ESKOM fleet [7]. There are however two new super-critical power stations that are being built, which is the Kusile and Medupi power station.

The supercritical cycle does not include a two-phase region for the steam, instead, the steam flashes directly into superheated steam in the boiler. This is achieved by pumping the water above the critical pressure point in which the water will change directly into steam (without a notable change in density) if enough heat is added by the boiler, bypassing the two-phase region altogether.

A considerable increase in efficiency is experienced over the entire load range for these types of boilers. The efficiency gain is mostly due to a higher mean temperature as illustrated in the T-s diagram in Figure 2.3.

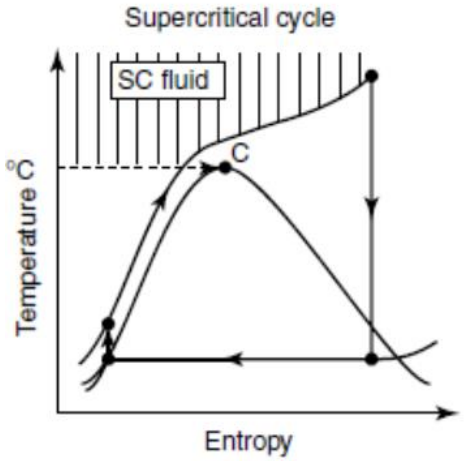

Figure 2.3: T-s diagrams of a subcritical and supercritical cycle [8]

Another method of increasing the efficiency of the steam cycle is by including heat regeneration. Regeneration occurs by extracting some steam from the turbines and exchanging the heat from the extracted steam to the high-pressure liquid flowing into the boiler. By doing this, one reduces the heat required by the economizer section of the boiler to heat up the liquid to saturated liquid conditions before it enters the evaporator section. The component for the steam to liquid heat exchange is call a feed-heater and is of a shell and tube type heater with cross flow condensation on the shell side.

2.1.1 The working fluid

The working fluid for most commercial power plants is water, which can be encountered as liquid, vapour or a combination. The vapour of water is called steam and behaves itself mostly as a real gas, since its properties (temperature, pressure and volume) cannot be described with a simple relation as with a perfect gas such as air. However, under lower pressures water vapour can be assumed to be ideal since the error made in association with the assumption is neglectable. In a Power station, these low pressures are not reached and thus the assumption is invalid.

The following definitions are important to understand the working fluid, these definitions are also illustrated on a T-S diagram in Figure 2.4.

- *Wet steam* is steam which contains moisture.
- *Dry steam* is steam which contains no moisture.
- Subcooled liquid is water-liquid that's temperature is below the saturation temperature.
- *Saturated liquid* is water-liquid that is at its two-phase point.
- *Saturated steam* is water-vapour at its two-phase point.
- *Superheated steam* is dry steam that has been heated above the saturated point.
- *Sensible heat* is the heat needed to heat the steam to boiling point.
- *Latent heat* is the amount of heat required by the water at a specific temperature and pressure to induce a phase change from liquid to vapour.
- *Saturation temperature* is the temperature at which boiling occurs at a specific pressure.

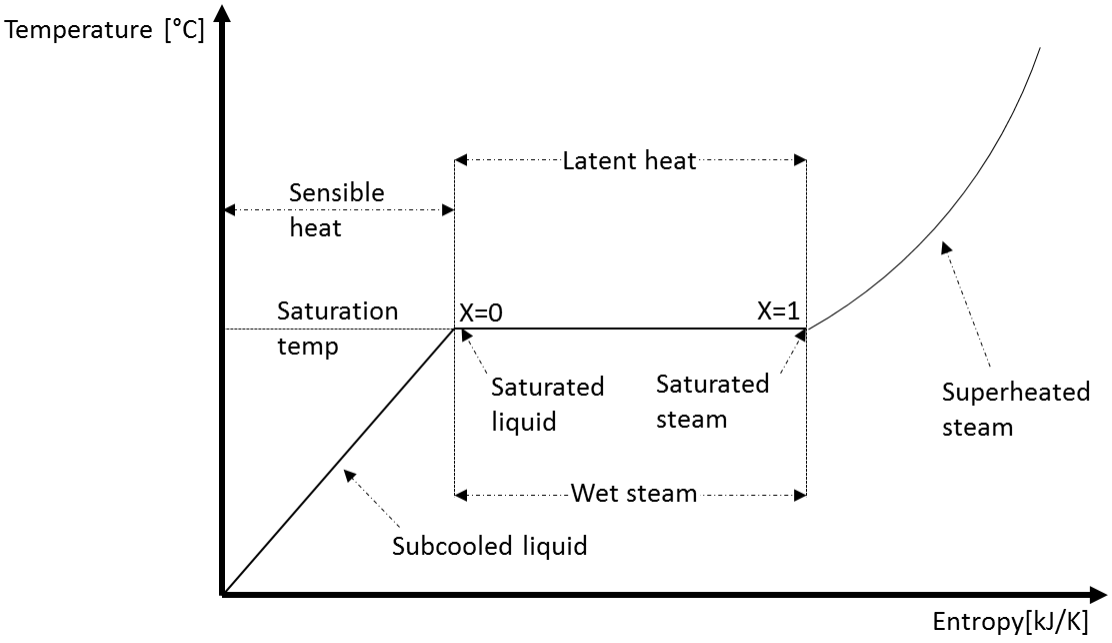

Figure 2.4: Steam definitions on a T-S diagram

The working fluid flows through the Regenerative Rankine cycle changing phase and exchanging heat at various points. The fluid is also given various names at certain points for ease of reference. The fluid identification is shown in the network diagram in Figure 2.5 and the diagram will also be used as a reference for the following sections.

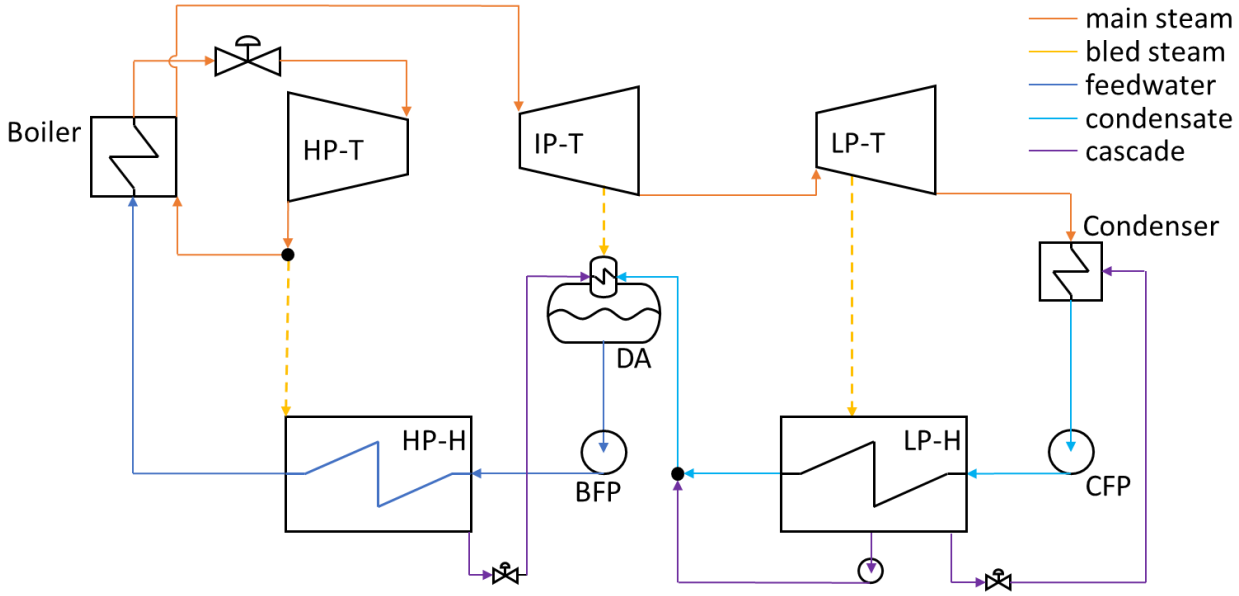

Figure 2.5: Simplified Regenerative Rankine cycle with working fluid identification

*HP-T, IP-T, LP-T: High, Intermediate and Low-pressure turbine; DA: deaerator; HP-H, LP-H: High and Low-pressure turbine; BFP – Boiler feed pump; CFP – Condensate feed pump.

2.1.2 Cycle components

The coal-fired power station consists of five main components, viz., the boiler, the turbine set, the condenser, the boiler feed pump and the feed-heater. Without these five components, the cycle cannot function. The layout, size and number of these main components are dependent on the size of the power plant and the type.

There are additional components, or auxiliary components, which are interconnected to these main components. These components have the purpose of either increasing the efficiency of the cycle and/or to transport or treat the working fluids of the cycle. Some examples of these auxiliary components are the deaerator, mills, furnace drum and extraction fans or pumps.

A complete large coal-fired power station is illustrated in Figure 2.6 where Table 2.2 provides a list of all of the components seen in the illustration.

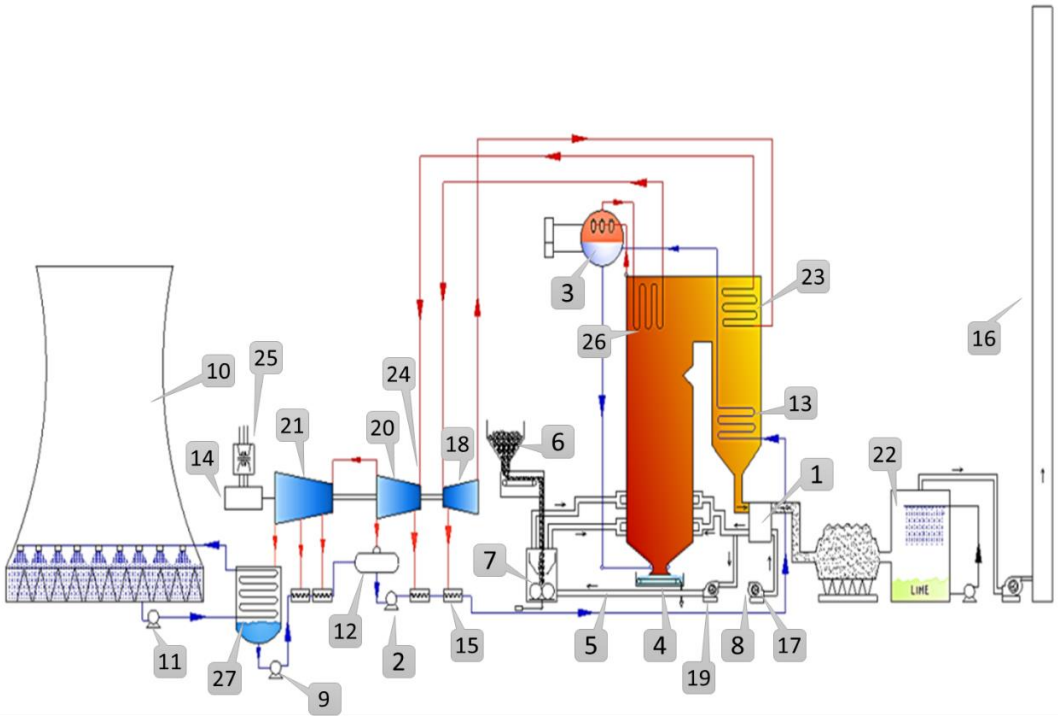

Figure 2.6: Components of a typical large coal-fired power station

Table 2.2 Components of a large coal-fired power station

1. Air preheater	15. Feedwater heater
2. Boiler feedwater pump	16. Flue gas stack
3. Boiler steam drum	17. Forced draught fan
4. Bottom ash hopper	18. High-pressure steam turbine
5. Primary air duct	19. Primary air fan
6. Coal hopper	20. Intermediate pressure steam turbine
7. Coal pulverizer	21. Low-pressure steam turbine
8. Combustion air intake	22. Flue gas desulperization plant
9. Condensate pump	23. Reheater
10. Cooling tower	24. Steam control valve
11. Cooling water pump	25. Step up transformer
12. Deaerator	26. Superheater
13. Economiser	27. Surface condenser
14. Electrical generator	

2.1.3 The Boiler

The boiler is not in the scope of the project, but for completeness will be included in the literature study. The boiler is a steam generator that generates steam at a desired temperature by burning coal in its furnace. The boiler is a complex component consisting of various smaller sections. These sections include the furnace, economiser, evaporator, superheater, reheater and the air preheater. It further compromises of various other auxiliary components such as the burners, pulverisers, stokers, steam attemperators etc. The steam generation mainly occurs in the evaporator where the water is changed from a liquid phase to a gas phase at constant pressure and temperature [6].

Different configurations of boilers exist in industry. Each configuration is built for a specific application with advantages and disadvantages to each. The two most common types of boilers in the ESKOM fleet include the drum-type boiler and the once-through boiler, where the drum-type boiler is the most common [7]. Figure 2.7 and Figure 2.8 presents schematic drawings of these two types of boilers and the water/steam flow through the boilers.

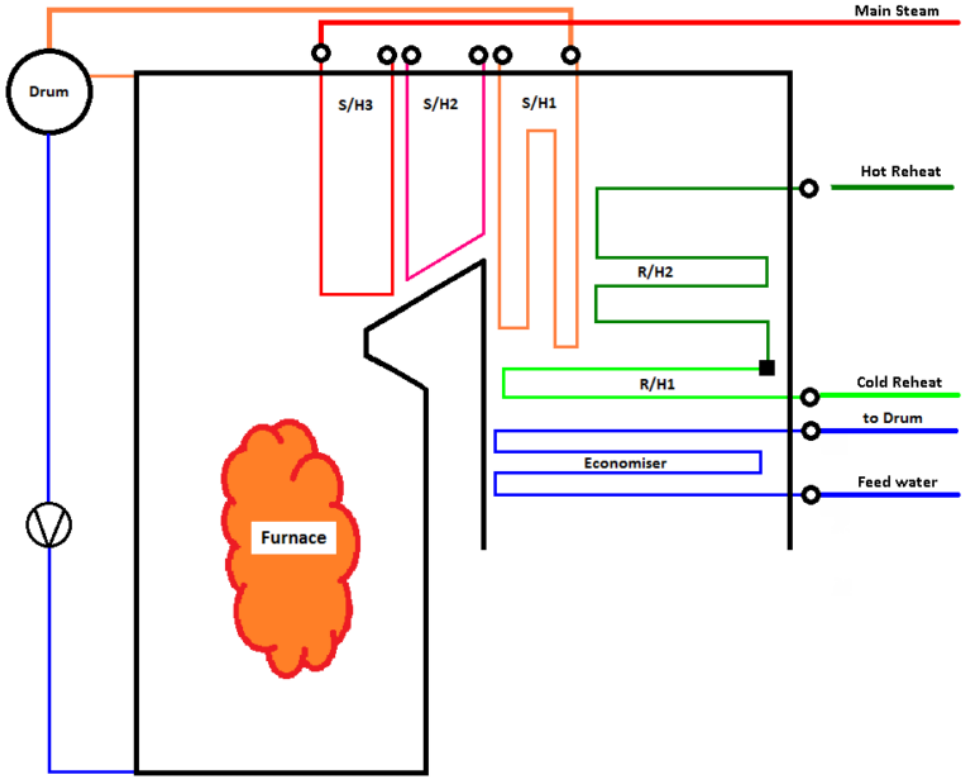

Figure 2.7: Schematic of a drum-type boiler with a reheat cycle [7] (pump below drum used for start-up purposes)

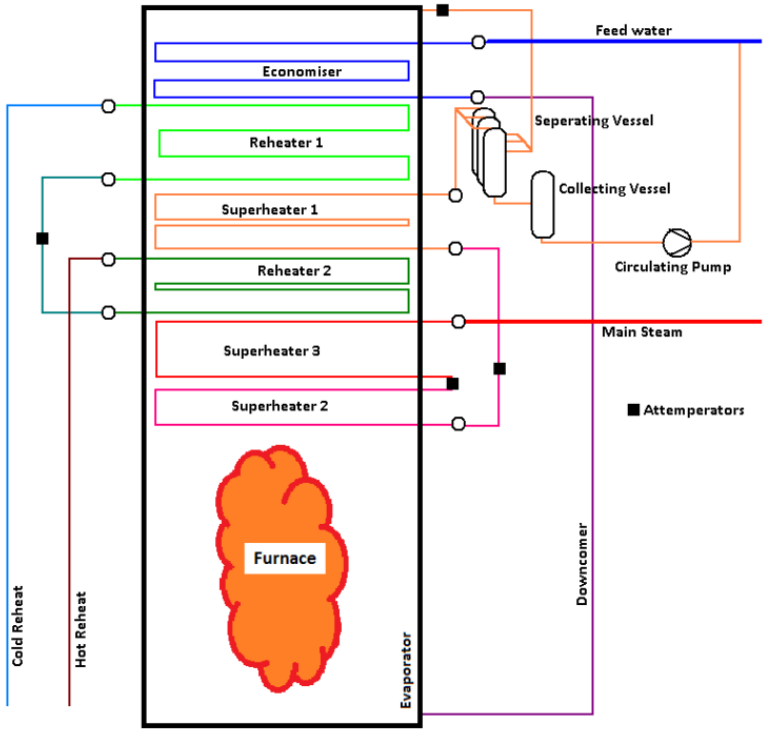

Figure 2.8: Schematic of a once-through boiler with a reheat cycle [7]

Feedwater enters the drum-type boiler through the tube known as the economiser. The temperature is raised, but not enough to change the fluid into steam. The water is then sent to a drum where it collects and exists the drum at the bottom and down through the down-comer tubes. The water then enters a narrow tube section called the water-wall where it is further heated to induce a phase change. The saturated water vapour, along with some water droplets, is again sent to the drum where the separation of the steam and water droplets occurs. The separated steam then enters the superheater tubes where further heating (superheating) occurs. After superheating the steam, it is then sent to the first HP turbine. The steam can then be sent to the boiler's section termed the reheater, mostly for efficiency gains, to increase the temperature of the steam again to the desire superheated temperature. The reheated steam is then sent to the rest of the turbines and the cycle components.

The once-through boiler, or also known as the Benson boiler, works very much the same as drum-type boilers at low loads. However, at higher loads the steam is directly changed into superheated steam and thus these boilers are most commonly found in supercritical power plants. At lower loads, the once-through boiler works very much the same as the drum-type boiler, but where the hot gasses only have one pass. Another difference is that the drum-type boiler utilizes natural circulation to drive the water through the evaporator whereas the once-through boiler uses forced circulation (pumps) to drive the water through the evaporator.

2.1.4 The Turbine

The turbine is the primary component to convert the high-temperature, high-pressure steam into shaft work. This conversation happens primarily in two steps [6]:

1) First, the high-pressure steam is expanded through fixed blades and the potential energy of the steam is converted into kinetic energy.
2) The steam enters the second step where the kinetic energy is transferred to rotating blades, which in turn turns the shaft of the turbine.

The two steps combined is called a stage where an axial turbine usually consists of multiple stages. As the steam moves through the stages of the turbine, the density of the steam decreases as the kinetic energy is transferred to the blades which turn the shaft. To maintain a constant axial flow velocity, the turbine's blade height and shell gradually increase toward the low-pressure end of the turbine [9].

In a large coal-fired power station, there are various turbines positioned throughout the steam cycle. Depending on the layout of the station one would generally find the configuration of a single reheat cycle [6]. This is where the steam enters the HP turbine, exits at a relatively cold temperature, reheated through the boiler and sent back through the IP turbine. The steam is thenthe split through what is called a crossover to two LP turbines. An illustration of this type of configuration is shown in Figure 2.9 and the typical position of the turbine layout is shown in Figure 2.5.

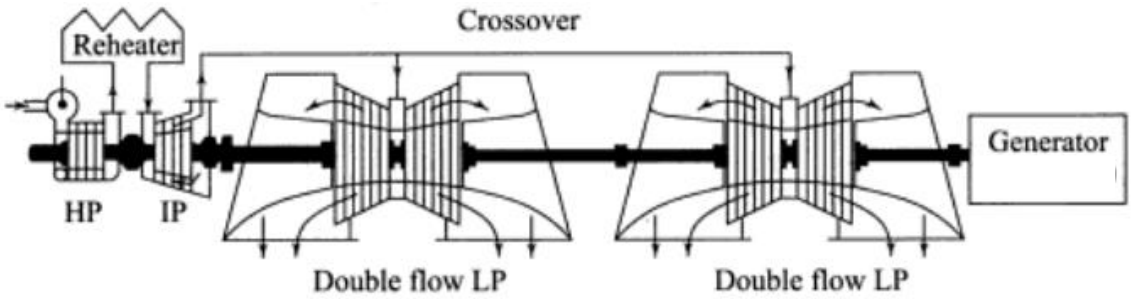

Figure 2.9: Turbine configuration, tandem unit (figure adjusted) [6]

The steam turbine in a power station further contains extraction point which is used to extract steam to the feed-heaters. The amount of extraction points varies where one would usually find the extraction points on the IP and LP turbines of steam cycle.

2.1.5 The Feedwater heater

The feedwater heater is a closed shell-and-tube heater exchanger where extracted steam from the turbine set is sent through the shell to condense over a series of tubes. The heat from the steam is transferred through the walls of the tubes and into the feedwater. The condensed steam is sent as condensate (also known as heater cascade) to the next pressure heater through a trap [6].

The feedwater heaters in a power plant are divided into two sub-categories: LP heaters and HP heaters. The heater is categorised based on the pressure of the feedwater entering the heater. The LP heater is usually positioned between the condensate pump and the deaerator and the HP heater is positioned between the boiler feed pump and the economizer. The positioning of the high and low-pressure heaters is shown in Figure 2.5.

The purpose of the heater is to heat up the feedwater going to the boiler by using steam extracted from the turbine. This has a direct influence on the overall thermal efficiency of the plant since more heat is transferred to the feedwater before it enters the boiler.

The number of heaters is, however, not directly related to the efficiency since there is an optimum degree of regeneration. The optimum degree of regeneration is simply the point where the efficiency gained by the number of heaters do not justify the capital investment of the heater itself. This is illustrated in Figure 2.10, where the cycle efficiency is calculated for the number of heaters in the cycle. There comes a point where the increment of efficiency increase is not justified by the capital cost of the heater, which in the figure is a number of 6 heaters.

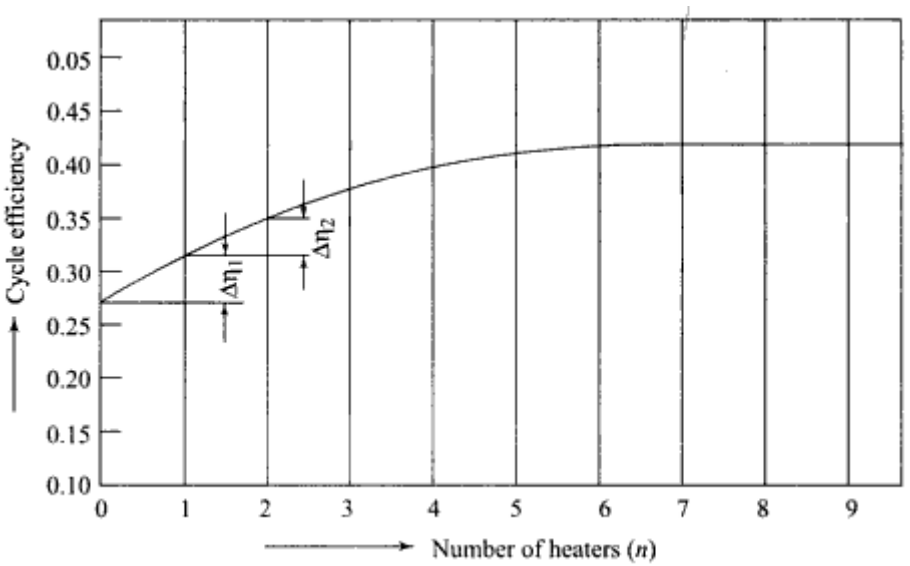

Figure 2.10: Cycle efficiency gain due to an increase in number of heaters [6]

2.1.6 The Deaerator

The deaerator component is an open feedwater heater, which means that the feedwater is in direct contact with the extracted steam. The purpose of the heater is to remove corrosive gases such as oxygen and carbon dioxide [6] in the feedwater. Gasses are dissolved in the feedwater and by heating up the feedwater to saturation temperature, these gases comes out of the solution.

The deaerator performs the functions of [3]:

- storing heated feedwater and
- providing a way of condensation for steam from various sources.

The feedwater enters the heater at the top where it passes through a heat exchanger, commonly called a vent condenser. It is then sprayed through nozzles to atomize the feedwater and thus creating a large surface area for heat exchange. The steam, bled from the turbines, is then fed from the bottom where the steam condenses and the feedwater is heated to saturation temperature. The dissolved gases are then released from the feedwater and vented out of the system.

The location of the deaerator in the steam cycle is just after the low-pressure heaters and before the boiler feed pump. The deaerator is further placed at a relatively elevated position as to provide a Net Positive Suction Head for the boiler feed pump. Figure 2.5 can be referenced to further explain the position of the deaerator in the steam cycle.

Two types of Deaerators are most commonly found in the ESKOM fleet, namely, the spray-tray deaerator and the spray-scrubber (also known as the stork type) deaerator. A study was done on modelling the deaerator component by R. Banda [3] where six ESKOM power stations were under investigation. It was found that 5 of the six power stations contained a spray-tray type deaerator and only one power station contained a spray-scrubber type deaerator.

2.1.7 The Condenser

The condenser is not in the scope of the project as stated in the section 1, but for the completeness of the steam cycle will be included in the literature study. The condenser essentially condenses the steam exiting the turbines and operates at a pressure lower than that of the atmosphere. The condenser serves two purposes:

1. Due to the low temperature of the cooling water, usually around 30 °C, the steam exiting the turbine at 40°C is condensed at saturation pressure (approx. 0.07 bar [6]). This induces a low exhaust pressure for the steam turbine and thus a better performance from the turbine.

2. The condenser condenses the steam back into liquid, only to be pumped back into the system through the condensate extraction pump.

Condensers are generally split up into two classes, namely, surface condensers and direct contact condensers. Surface condenser condenses steam on the outside of tubes where the two streams (hot and cold stream) are never in direct contact but separated by a tube wall.

Direct contact condensers on the other hand work where the two streams, the steam and cooling water, are mixed and exits the condenser in one stream. For the surface condenser, the cooling water is cooled through a cooling tower and flows in a different network to that of the steam cycle's working fluid.

The condenser is positioned between the outlet of the low-pressure turbine and the condensate feed pump. Figure 2.5 illustrates the position of the condenser.

2.2 Flownex

Flownex is a one a one-dimensional network solver, which is applicable to thermo-hydraulic problems. Flownex can simulate various scenarios involving steady-state and dynamic simulations (i.e. liquid systems, gas systems, two-phase systems, heat transfer, two-phase systems with phase changes, etc.) [10]. Flownex is also able to optimize and design various network parameters, and present numerous physical domains into one network (e.g. mechanical systems, electrical circuits, pneumatic systems, etc.) making it ideal for a high-fidelity power plant simulator. The software further enables the creation of custom compound components which can be created to be very user-friendly and easy to implement with the purpose of building a larger power plant network.

Flownex's solver is based on the Implicit Pressure Correction Method, which is a method of solving the fundamental governing equations. These governing equations involve the momentum equation used on the elements of the networks and energy and continuity equations for the nodal points of the network. The steps involved in the IPCM are shown in Figure 2.11 [11].

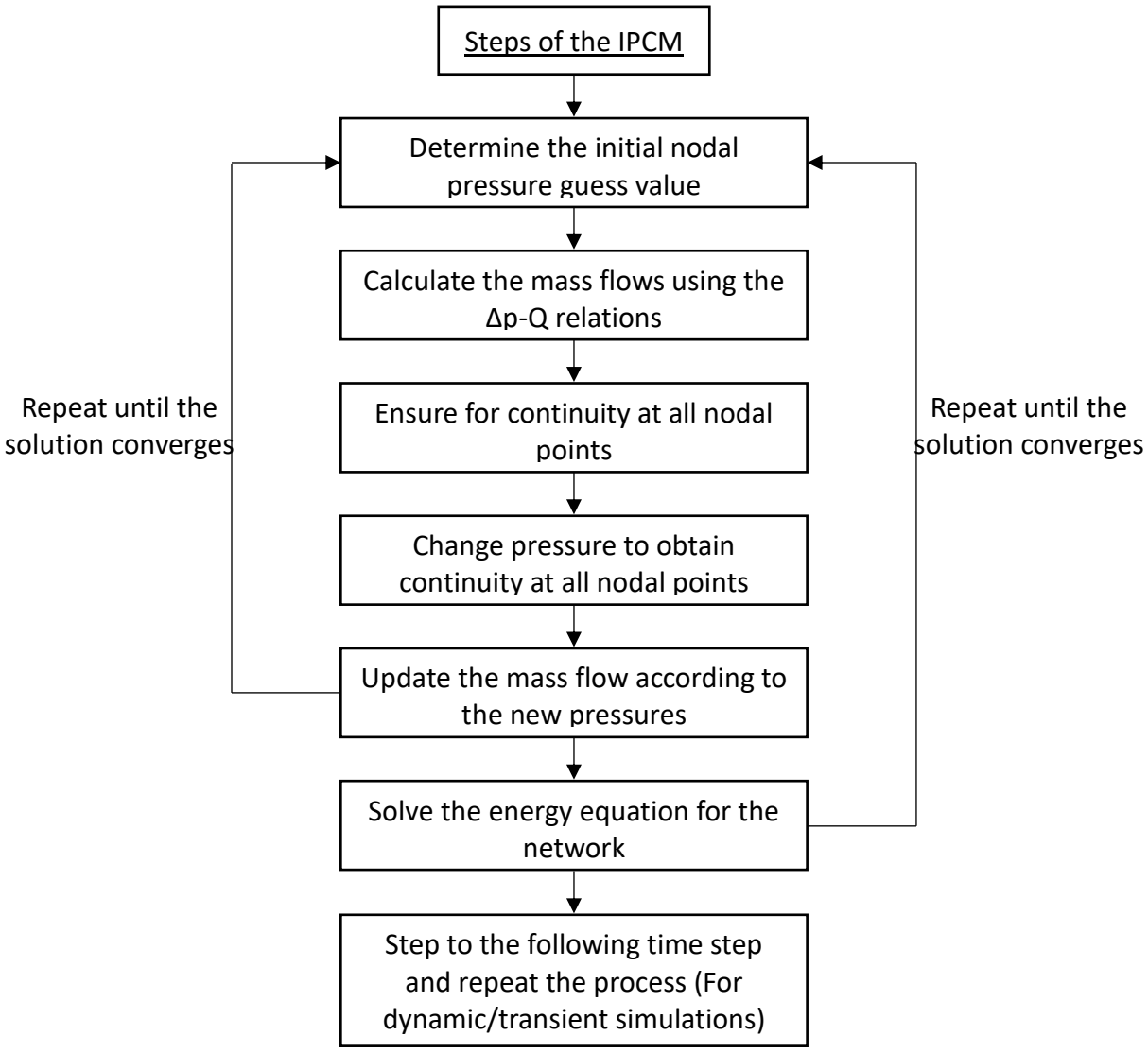

Figure 2.11: Diagram of the steps for the IPCM

Flownex uses a segregated solution algorithm which solves the governing equations as well as additional closure equations consecutively. This means that the user can manipulate aspects such as relaxation parameters, the number of iterations and convergence criteria of the solution to gain an accurate solution in less time or to make the solver more stable [11]. These aspects of the solver will be used as the network become larger and more complex.

2.2.1 Flownex governing equations

The general conservation equations used by Flownex are listed in this paragraph. It is important to note that these equations were derived only for one-dimensional problems since Flownex is a one-dimensional network solver [11].

1. Conservation of Mass:

$$V\frac{\partial \rho}{\partial t}+\sum \dot{m}_e-\sum \dot{m}_i=0 \tag{1.7}$$

The equation (1.7) gives us a general equation of mass conservation where the first term $V\frac{\partial \rho}{\partial t}$ denotes the rate of density change within a volume and the second and third term indicates the total mass flowing in and total mass flow out of the control volume.

2. Conservation of Momentum:

The differential equation of the conservation of momentum can be written as

$$\rho\frac{\partial V}{\partial t}+\rho V\frac{\partial V}{\partial x}=-\frac{\partial p}{\partial x}-\rho g\frac{\partial z}{\partial x}+\frac{\partial p_{0M}}{dx}-\frac{\partial p_{0L}}{dx} \tag{1.8}$$

where the first term on the left-hand side contains the rate of momentum accumulation and the second describes the rate of momentum flowing in and out of the control volume. The terms on the right-hand side of the equation describe the forces acting on the control volume, which is the net force of static pressure on the inlet and outlet, the net force due to gravity and the net force associated with machine work and pressure losses in contact with the wall. Equation (1.8) can also be written for compressible or incompressible fluids where the density is assumed to be relatively constant (does not change significantly due to a change in pressure) for incompressible and changing for compressible.

Incompressible flow (for a pipe with length L):

$$\rho L\frac{\partial V}{dt}+(p_{0e}-p_{0i})+\rho g(z_e-z_i)=\Delta p_{0M}-\Delta p_{0L} \tag{1.9}$$

Compressible flow (for a pipe with length L):

$$\rho L\frac{\partial V}{dt}+\frac{p}{p_0}(p_{0e}-p_{0i})+\rho g(z_e-z_i)=\Delta p_{0M}-\Delta p_{0L}-\frac{1}{2}\rho v^2\frac{1}{T_0}(T_{0e}-T_{0i}) \tag{1.10}$$

3. Conservation of Energy:

$$V\frac{\partial}{\partial t}(\rho h_0-p)+\sum \dot{m}_e(h_{0e}+gz_e)-\sum \dot{m}_i(h_{0i}+gz_i)=\dot{Q}-\dot{W} \tag{1.11}$$

The conservation of energy equation (1.11) is written in terms of the rate of change of total energy, the total energy flowing in and out of the system and the source terms which is the total heat added to the control volume and the work done by the control volume on its surroundings.

2.2.2 The implicit solution algorithm

It is important to note that the IPCM is an implicit solution algorithm. Methods such as the method of characteristic do exist for hyperbolic conservation laws. These methods form part of the explicit compressible methods, which is used as solution algorithms [12]. There are advantages and disadvantages to using implicit and explicit solution algorithms and these are summarized and expressed in Table 2.3 [11].

Table 2.3 Comparison between the explicit and implicit solution algorithm

	Advantages	**Disadvantages**
Implicit methods	• Unconditionally stable • Can solve networks with diverse types of fluids	• Difficult to implement • Potentially inaccurate when using long time steps • Potentially slow
Explicit methods	• Easy to implement • Accurate	• Strict time step limitation • Difficult to solve networks with diverse types of fluids

From a practical point of view, the implicit methods are much more stable than that of explicit methods. This means that for slow transient simulations, implicit methods are more computationally efficient and can produce more stable solutions under diverse conditions than that of explicit solutions [12].

2.2.3 Important components used in the modelling process

This chapter contains the Flownex components used to build the larger main components of the steam cycle. A description of each component is given by highlighting its use and applicability.

a) Pipe

The pipe component models flow through a conduit by including pipe geometry and losses such as friction or secondary losses. The component utilizes the mass flow rate to determine the pressure drop and uses the Darcy-weisbach formulation. Another important feature of the pipe element is that it calculates node volume from its geometry specification, thereby adding thermal inertia in the simulation model, which is unique to this component.

The pipe element also includes fluid acceleration, which enables to calculate waves and is able to detect chocked flow. The component is used in the project where flow through pipes occurs and where pressure drop modelling is of significance. Figure 2.12 shows an illustration of the component.

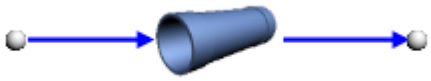

Figure 2.12: Pipe component in Flownex

b) Flow resistance element

The flow resistance is also a component used to model flow, but with a slightly simplified pressure drop modelling. This component is ideal for connecting two nodes without increasing the simulation time of the solver. The pressure drop is defined by a flow admittance and further control can be used by adjusting an opening. This enables the flow resistance element to be also used in control aspects such as simulating a control valve. The flow resistance element is shown in Figure 2.13.

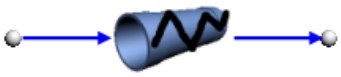

Figure 2.13: Flow resistance element in Flownex

c) General empirical relationship component

The general empirical loss component is yet another component to model pressure drop. It can be used to model the pressure drop through various components such as valves, heat exchanges, etc. The component uses the volume flow rate to determine the pressure drop. The component has been used in the project to specifically model the pressure drop that occurs over the main condensate inlet valve of the deaerator. The component is illustrated in Figure 2.14.

Figure 2.14: General empirical relationship component in Flownex

d) Two-phase tank

The two-phase tank essentially acts as a node in the Flownex Simulation Environment by allowing flows in and out of the component. The component specifically models two-phase flows where one can separate the flows by specifying a connection height: 0 is defined as liquid flow and 1 is defined as vapour flow. The component also contains a steady-state design option which is used for level calculations. If the two-phase tank models condensation, the steam mass flow is calculated based on the amount of heat transfer that occurs during condensation. The assumption for this

component is that complete and instantaneous mixing and thermal equilibrium occurs among its contents where the liquid fills from the bottom of the tank. The component is shown in Figure 2.15.

Figure 2.15: Two-phase tank component in Flownex

e) Composite heat transfer element

The composite heat transfer element is used to model heat transfer. This component models convection-conduction-convection over a flat plate. One can specify various layers of material for the component and it is can be used to model condensation in the feed-heater component. The composite heat transfer element is displayed in Figure 2.16.

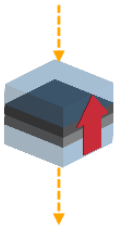

Figure 2.16: Composite heat transfer element in Flownex

f) Boundary condition

The boundary condition is used to specify various parameters, such as flow, pressure, temperature, etc. to a network. The condition can also be used to specify an inactive flow, such as the cascading inlet flow for a feed-heater. The boundary condition is shown in Figure 2.17.

Figure 2.17: Boundary condition component in Flownex

g) Script

The script component is used to define or manipulate any type of property available to the script in a C# environment. The script uses various classes and an example of using the script is by calculating various steam properties defined in Flownex. Simple and complex calculations can further be performed such as curve fit methods and calculating the total heat transfer between two components. The script component in displayed in Figure 2.18.

Figure 2.18: Scripting component in Flownex

h) Excel component

The excel component is used to import excel spreadsheets into Flownex. The project utilized this functionality by specifically using the component to define design input data for the main steam cycle components in an easy-to-use manner. The excel component is shown in Figure 2.19.

Figure 2.19: Excel component in Flownex

i) Simple turbine

The simple turbine models the flow through a turbine using various pressure drop and efficiency correlations. This component was specifically applied by implementing new correlations into the project's turbine component by manipulating current correlations through the use of a script. The simple turbine component is shown in Figure 2.19.

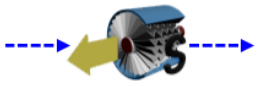

Figure 2.20: Simple turbine component in Flownex

2.2.4 Flownex typical network layout

The typical network layout is represented in Figure 2.21 where the network consists of elements in between nodes. Each flow network also consists of at least two boundary conditions where the first boundary condition indicates the inlet or *upstream* flow and the second boundary condition indicates the exit or *downstream* flow.

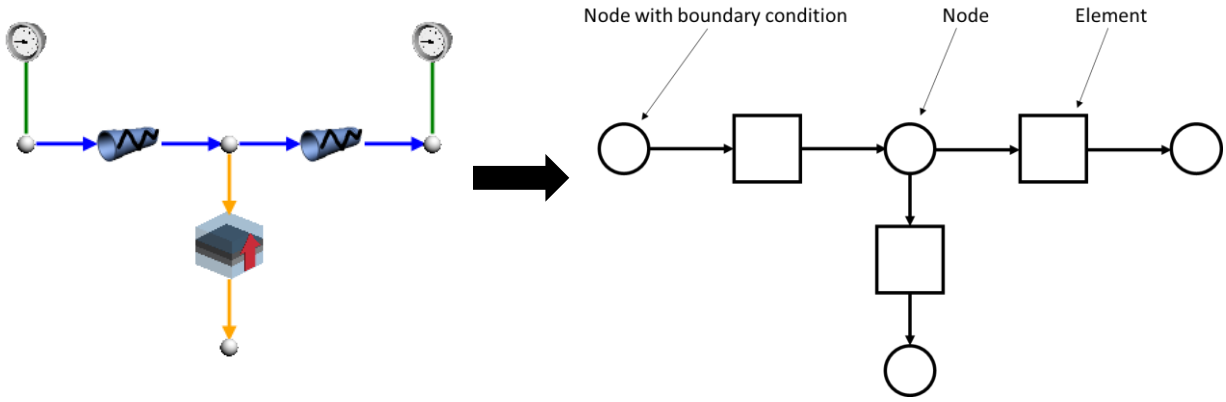

Figure 2.21: Typical Flownex network layout

2.2.5 Compound component

Flownex has the functionality of creating custom compound components which can be developed by the user. The purpose of the compound component is to include sub-networks into a larger network which makes the larger network more manageable [10]. Properties from the sub-network can also be added to the compound component making the compound component to behave itself just like a normal Flownex component. An example of using a compound component for a sub-network is shown in Figure 2.22.

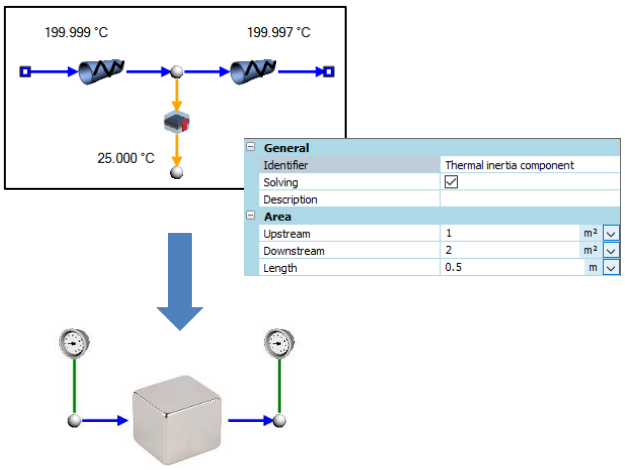

Figure 2.22: Example of a sub-network in a compound component as used in Flownex

The compound component is of particular interest for the project's purpose of integrating smaller networks into a larger integrated cycle. This will enable the user to add or remove main components from the network conveniently and specific inputs and outputs can also be displayed in the components property grid. The main advantage of the compound component is that it will make the integrated more manageable and it will look similar to a mass and energy balance diagram.

2.2.6 Steady-state vs dynamic modelling

The difference between steady state and dynamic modelling is that the coefficients in the governing equations do not change with time. This implies that the time term, seen in equation (1.12), is equal to zero for all three conservation equations.

$$\frac{\partial}{\partial t} = 0 \tag{1.12}$$

In the application of thermo-fluid analysis, the time term being zero implies that there is no accumulation of energy or mass in the system. Thus, the result for the system at time 1 seconds will be the same at time 50 seconds.

In Flownex the user can choose between solving the simulation network for a steady-state or transient scenario. During a steady-state scenario, the solver solves the governing equation time independent. Also, the steps of the IPCM, described in section 2.2.2, is followed up to just before the last step. For transient scenarios, the entire process of the IPCM is repeated after each time step. The size of the time step can be adjusted by the user, but caution should be taken as larger time steps may make the solver unstable.

2.3 Previous Dynamic models of thermal power plant cycles

Dynamic models of steam power stations have been done in the past for several reasons and applications. These applications vary from understanding the response from disturbances, start-up procedures, control aspects, and flexibility increase such as new innovations [13]. The range of applications for the dynamic models was also dependent on computer resources available, especially in the early 1990s and afore. Since then, computer resources have become much more efficient in that large simulations can be run for almost any type of application and scenario.

This chapter will focus on a literature study on previously developed dynamic models for thermal power plants. Papers that had the objective of modelling a network by using user-friendly components will be of specific interest.

2.3.1 Dynamic models of thermal power plant cycles.

A paper (1999) on the dynamic modelling of complete power plant systems is by Lu [14], in which the author described the simulation techniques involved in steady-state and dynamic modelling. The author further provided a model for a 677 MW coal- and gas-fired power station as a case study and the software of choice was MATLAB/SIMULINK. The purpose of the project was mainly to provide fault finding and operational and training guidance.

The model presented components in which the techniques, described in the paper, have been coded as functions in MATLAB and modules in SIMULINK. These component models were then used to create the network of the power station using a graphical user interface, shown in Figure 2.23. The model contained a detailed model of the boiler component but simplifications were made regarding the turbine models' extraction points. The components were presented in a user-friendly type manner for ease of input and output data. The author's paper further presented the reader with a good oversight to dynamic modelling in general.

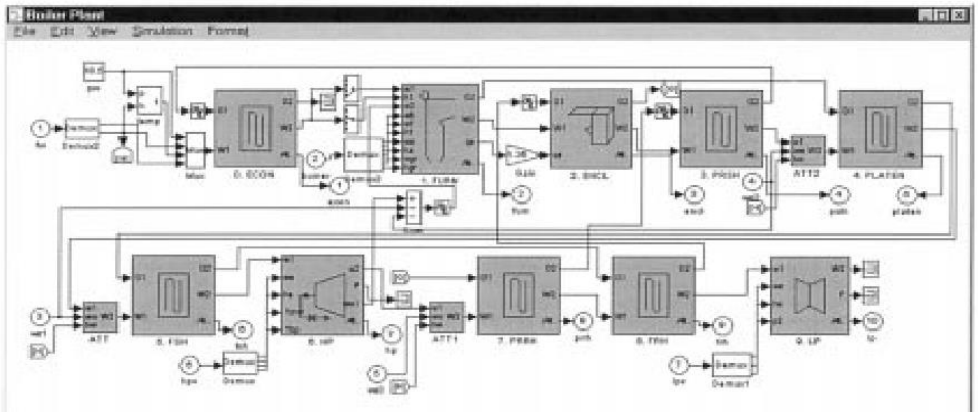

Figure 2.23: Boiler plant model of Lu [14], built in MATLAB and SIMULINK.

The model has been validated by step changing the main steam pressure set point, and a sudden change of the main steam valve opening. The dynamic responses seemed to be in line with what would happen in an actual power plant in terms of mass flows, water levels, and steam pressures. However, the dynamic model lacked proper verification to that of actual plant data.

A paper (2006) on system-based dynamic modelling of power plants was presented by Shirakawa [15] where the objective was to present a dynamic tool for control related purposes. The components had to be built in such a manner so that someone who is not a specialist in some of the more detailed modelling techniques will be able to use it, such as a design engineer.

The model contained object-oriented models which can be easily interlinked with each other to build the entire cycle. The plant model of a combined-cycle 265 MW power plant is shown in Figure 2.24. It can be seen from the figure that the main components are represented by the icons and the steam/water piping and gas ducting is represented by the vectors. This layout makes the model look like that which one would typically see on a plant system diagram.

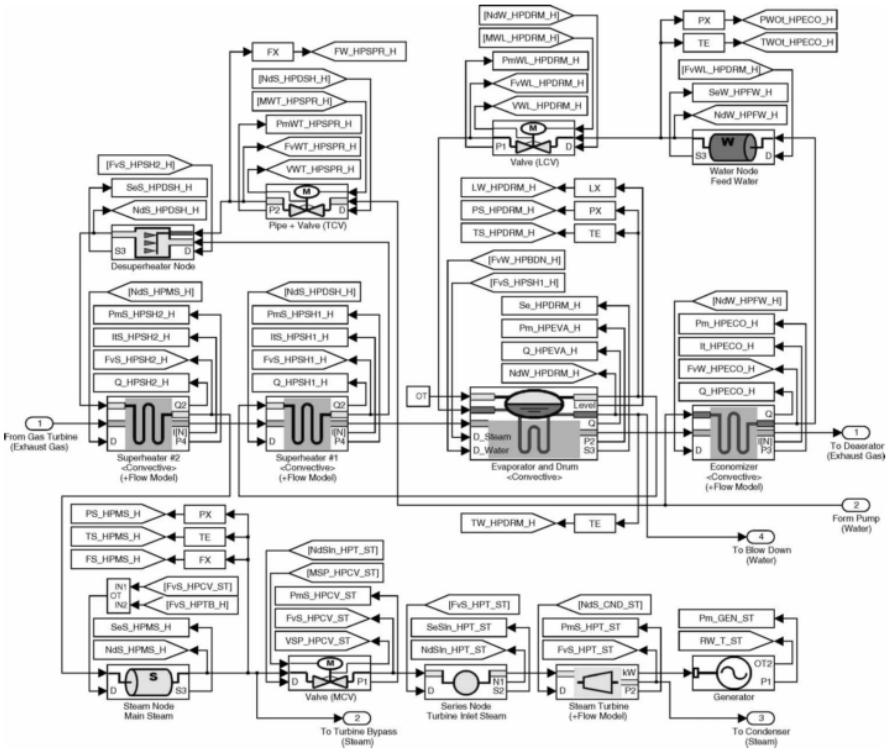

Figure 2.24: Plant model by Shirakawa [15] presented in MATLAB and SIMULINK

The model was verified to the data of a 340 MW combined cycle power station. Cold start-up conditions were used and results were compared with generator speed and output, turbine exhaust gas temperature and the fluid properties of the high-pressure steam. The simulation results, which is shown in Figure 2.25, compared well with that of actual plant data and proved that the model can be used for plant system and control design.

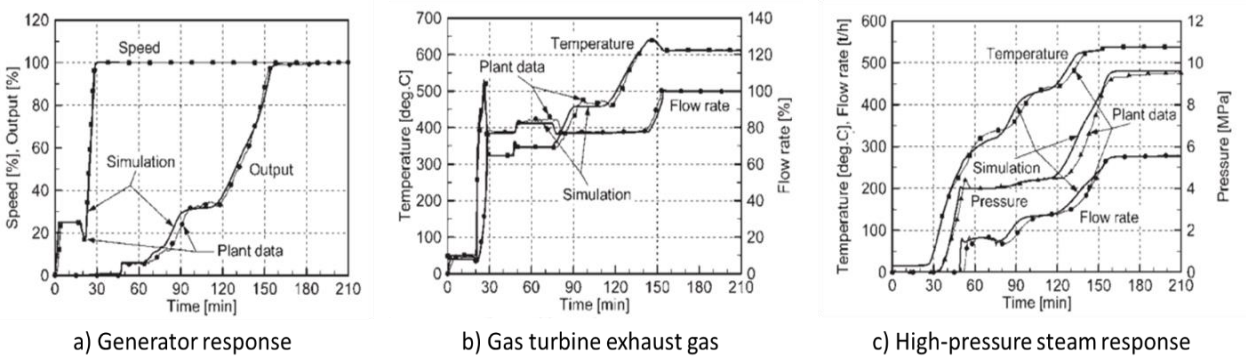

a) Generator response b) Gas turbine exhaust gas c) High-pressure steam response

Figure 2.25: Comparative results for simulation and plant data by Shirakawa's [15] plant model

Further developments (2007) on dynamic thermal models of power stations was done by Colonna et al. [16] and Van Putten et al. [17]. The model focused on a small simple Rankine cycle and the purpose was to develop a dynamic model to design and operate the power station during abnormal and off-design load conditions (which is critical for smaller power plants). Components were

developed using the simulation software SimECS where each component consisted of certain modules, which contained the physical relations and laws of conservation in the lumped parameters form. Some empirical correlations were also used, especially for heat transfer components.

The correctness of the modules was initially validated by comparison to available experimental data from a laboratory scale test setup (where the experimental data can be found on the internet). After a successful validation process for steady-state and dynamic results, the components were then used to create a model for a small 600 kW biomass fired steam power plant. The complete model with each key component is shown in Figure 2.26.

The full model of the biomass-fired steam power plant was initially validated by looking at steady-state results obtained from other trusted software with the same conditions. Off-design conditions for the biomass power plant were under consideration. The plant's off-design steady-state validation agreed with the experimental data. The dynamic validation was then done by step-wise changes to input values. Unfortunately, data from an actual plant case-study were not available. Instead, the model was only validated with consistency and compliance to what one would expect to see according to physical phenomena and showed good agreement.

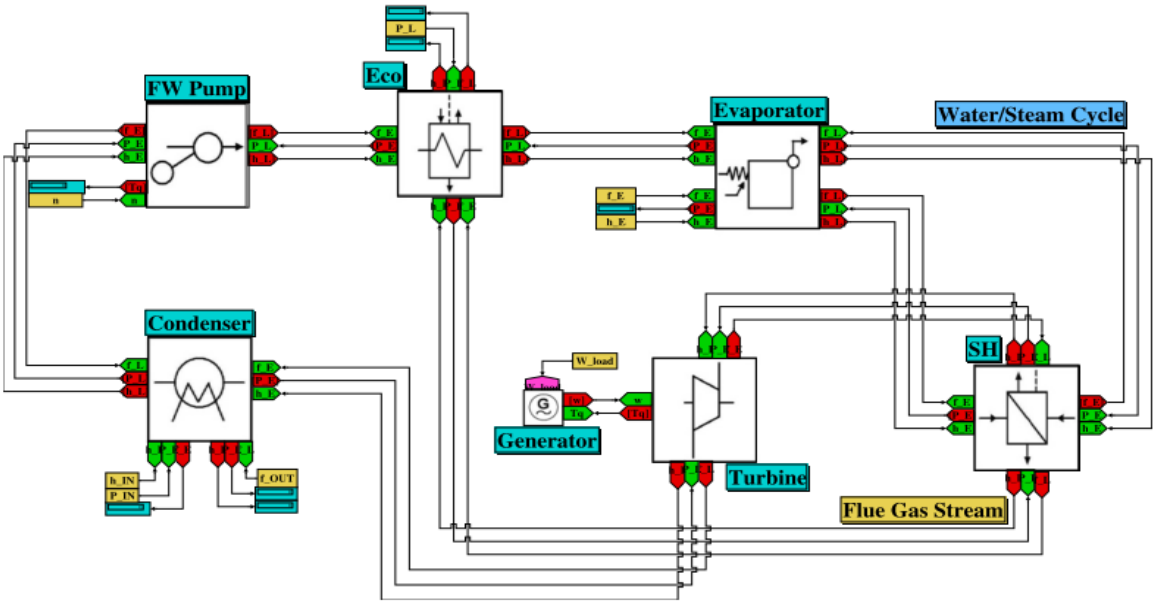

Figure 2.26 Biomass fired steam power plant process model on SimECS, by van Puten, H. et al. [17]

More recent advances in thermo-hydraulic power generation simulations (2011) is presented by Meinke et al. [18], in which the authors presented a coal-fired power plant using the existing well-known non-commercial library ThermoPower. The library consists of pre-defined models of the power station components programmed in the Modelica language [19]. The research was focussed on the start-up processes of a specific power station situation in Germany and looked at the stresses involved in thick-walled components during these processes.

The model contained the full water-/steam circuit, the combustion chamber of the boiler and the fresh air passage, all whilst including the components dynamic behaviour and different operating modes. Control schemes for the power station model were also included and worked in conjunction with the water-/steam circuit. The model has been extensively validated with plant data and showed very good agreement with minimal differences. Results of these validations can be seen in Figure 2.27, where the desired power output, boiler steam pressure outlet, temperatures of the inlet of the economizer and outlet of the evaporator and the net generator power is shown. The model could be used to simulate the different operating modes and successfully compare this with the occurring wear of the plant components.

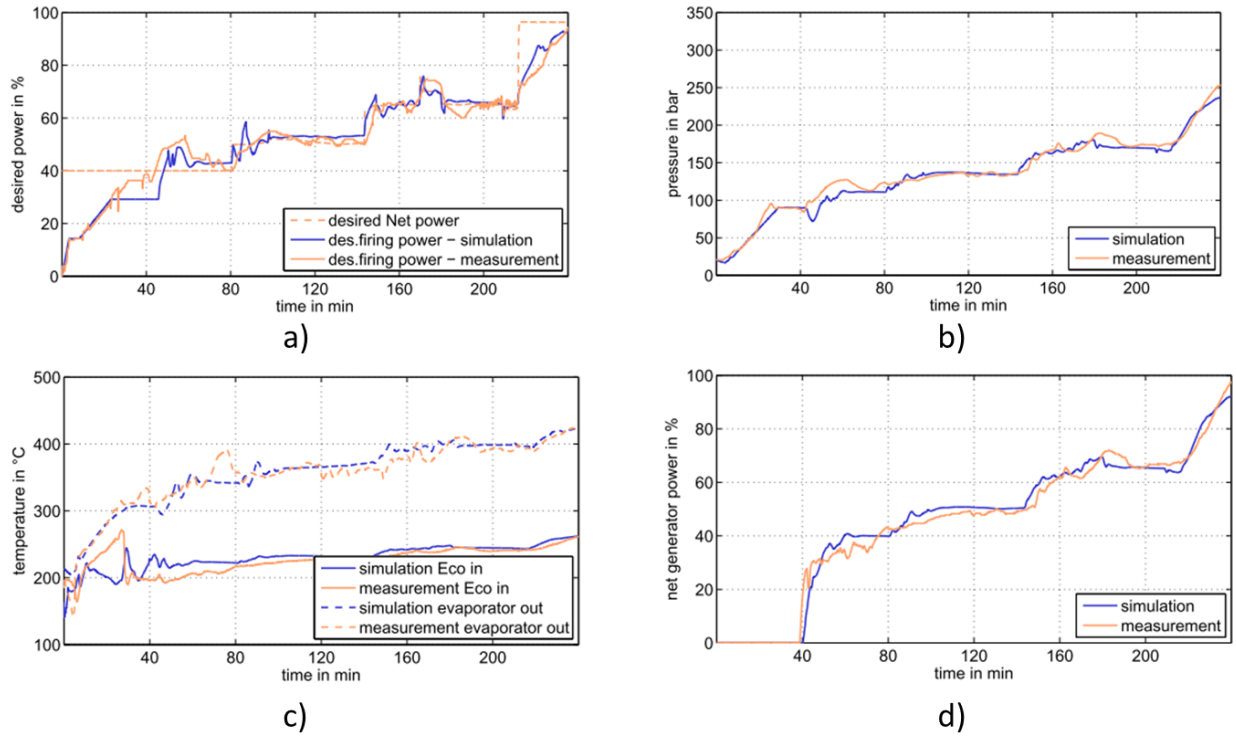

Figure 2.27: Desired power output (a), boiler steam pressure outlet (b), temperatures of the inlet of the economizer and outlet of the evaporator (c) and the net generator power (d) of the model by Meinke, S et al. [18]

Another model of a thermal power plant (2014) was developed by Oko et al. [20], in which the author modelled a 500 MW coal-fired subcritical power plant using the simulation software gPROMS. The purpose of the paper was to present a complete power plant mode, viz., the water-/steam cycle and flue gas cycle, which can operate at a wide range of operating conditions.

The complete simulation model is shown in Figure 2.28, where one can see the main component models of the cycle. The component models contained first principles modelling equations together with the physical properties of the working fluids, obtained from Multiflash® which is based on Peng-Robinson property package. The inputs required for the complete model were fuel burn rate,

governor stem valve position, excess air in furnace, attemperator water flow, condenser pressure, cooling water flow rate, feedwater valve setting and the back pass damper setting.

The validation of the model was firstly done by using steady-state results from existing plant data at various loads. This was, however, limited to the steam side due to unavailable data for the gas side. The results of the tests were promising with results within 5% relative error for low load (70%) operation. Dynamic model validation could not be performed due to a lack of open literature plant data. Step and ramp changes of the major input variables have, however, been performed and results agreed with the expected trends. The author concluded that for future modelling techniques, it is better to use ramp changes than step changes.

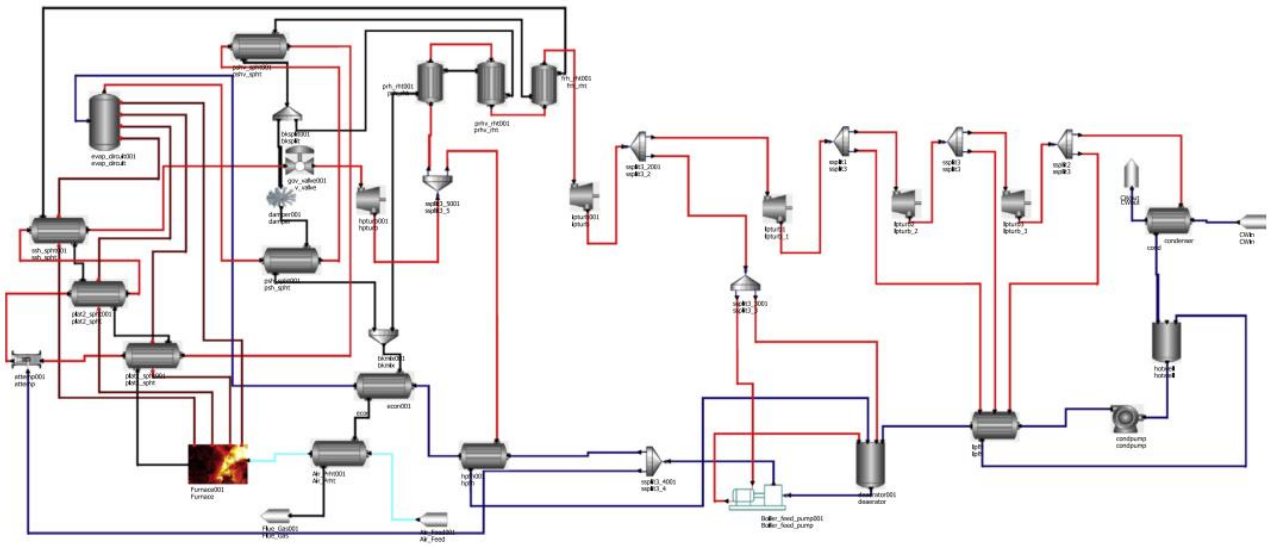

Figure 2.28: Oko et al.'s model of a complete power station using the gPROMS modelling software [20]

One of the most recent studies (2015) on dynamic simulation was done by Starkloff et al. [1], in that the authors developed and validated a model for a large coal-fired power station. The aim of the project was to develop a model to investigate operational flexibilities of a power station, such as off-design conditions. The model has been created by using the process simulation software APROS, which includes all the power plant components together with their control schemes. It is further shown that the simulation software, APROS, has a high reputation for capturing the real behaviour of dynamic processes in power plants [13].

The model simulated a large once-through hard coal-fired power plant, situated in Germany. The model was validated with real plant data and showed considerably favourable results. These results are shown in Figure 2.29 where the measured pressure of the high-pressure section of the steam generator and the mass flow of the steam generator have been compared to that of the model. The model further contained different firing levels and this made it possible to shut these different levels off, which differentiates this paper from the rest found in the literature of dynamic models.

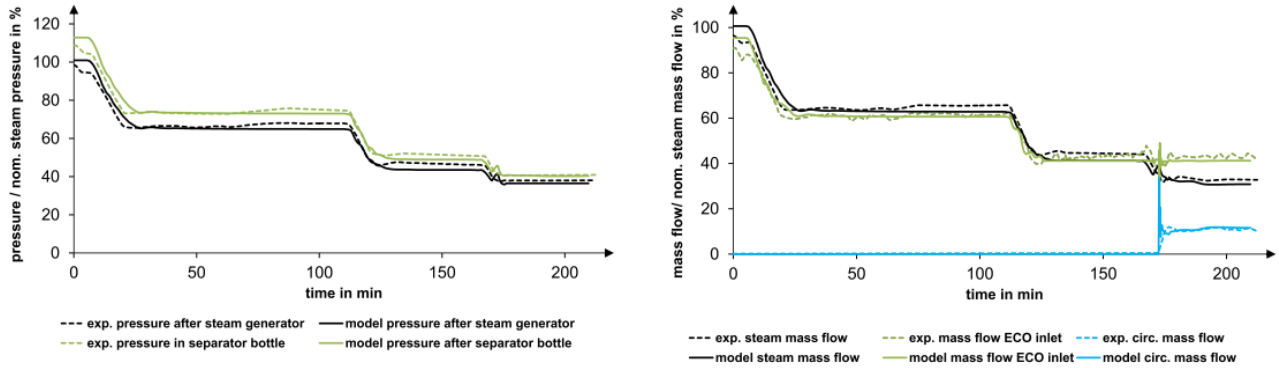

Figure 2.29 Comparison results for Starkloff et al. [1] dynamic model of a large coal-fired power station.

2.3.2 Conclusion on previous dynamic simulations

This now draws an end to the literature study on previous dynamic simulations. It is evident that research has been done on the topic of complete dynamic models of thermal power stations. However, shortcomings such as fully validated models and lack of detail on the steam side of the early models are present.

Only recent studies showed validated models of thermal power stations with more detail. Although the validation was done with more detail, there was still a lack on short transient scenario validation and it is only on these short transient scenarios where one can truly observe the effects of dynamic properties of the components. Most of the studies were performed at rates that would approach quasi-steady conditions, with the controller response being the main dynamic aspect. This opens a door to short off-design dynamic modelling of large thermal power stations, and the project will focus on beginning to fill the gap for short dynamic modelling that was left by the previous authors.

2.4 Plant data

Plant data was used in the study to define and determine the accuracy and fidelity of the developed component models. Three types of plant data were used in the study, namely:

- Heat balance data
- Acceptance test data
- Operational plant data

Each type of data was used in the models for a specific purpose. The following sections will briefly describe the type of data and finally conclude on how it was used in the models.

2.4.1 Heat balance data

Heat balance data is data that is usually supplied by the turbine original equipment manufacturer. The data is readily available and reliable in that it is used as checks and verification to acceptance test data. The data is also used to as reference data whenever components need to be replaced or when upgrades in the plant are required [2].

Heat balance data are given for the turbine steam cycle for different load cases, ranging from 100% down to 40%. These load cases give a good indication of the expected performance of the plant. The parameters that are used in the data include pressure, temperature, enthalpy and mass flow readings. These parameters are calculated by using various software where the component characteristics have been pre-defined. It is therefore important to note that heat balance data is not actual plant measurements, but rather predictions. It's level of accuracy is a function of the fidelity of the software and inputs used, which in some cases can be 50 years old. Therefore, it can only be used as verification to the model.

2.4.2 Acceptance test data

The purpose of acceptance test data is to verify the performance as predicted by the original equipment manufacturer. The tests are usually carried out in a few months where actual measurements are recorded from the station just after it was commissioned. These tests also occur in conjunction with the original equipment manager and ESKOM as to ensure that certain codes (such as the ASME Performance Test Code [21]) is followed. There is, however, no guarantee that all the standards are followed when the measurements are taken, but the data is however verified with heat balance data to add credibility. Normally acceptance tests are only done comprehensively at 100% load.

The following tolerances are to be considered for the acceptance test data, the conclusions were made by Neerputh in his study for appropriate steam turbine models [2]:

- Critical pressure measurements have a tolerance of ±0.1 % and non-critical pressure measurements ±0.25 %.
- The main steam flow is considered accurate within a tolerance of ±0.05 % and the extraction flows ±2 %.
- Temperature measurements are considered accurate within ±0.5 K.

It was further noted that truncation also plays a role in the accuracy of the measurements, especially with pressure measurements where 3-4 decimals places might be significant such as at the low-pressure turbine and feedwater heater extraction points.

2.4.3 Operational plant data

Operational plant data is data recorded as actual measurements from the plant daily. These measurements are then stored on servers and can be accessed via a distributed control system or third-party software like EtaPro, which is a performance and condition monitoring tool [22]. EtaPro was used as the data extraction tool for this project.

The extraction tool works by initially establishing which measurements are required. This can be done by identifying the measurements using a piping and instrumentation diagram and taking down the tags of the measurements of interest. The tags are usually presented in the following format where the description of the format is listed in Table 2.4 [23].

LEP4 RM00 F 003

Table 2.4: Measurement tag description

Value	Description
LEP4	Unit description: Unit 4
RM00	Line description: Main condensate line (This may vary depending on the standard used: AKZ or KKS)
F	Measurement description: Flowmeter
003	Measurement point: 3rd flow meter in the condensate line.

Once the tags have been identified, one can determine the date and interval at which the data should be extracted. Choosing the interval of the data should however be cautioned since the values given might not be the actual interval at which the data was recorded. The program populates between the measured data points constantly.

The data is extracted into an excel spreadsheet where it can be further processed and interpreted. The program is also able to export the description of the measured point as well as its engineering units, which is crucial especially for pressure measurements given in gauge pressure.

The tolerances associated with operational test data is much poorer than that of acceptance test data. Many of the plant measurements are not the same as the ones used in the plant acceptance tests and the instruments degrade over time. The resolution of these measurements can be seen by the step change in increments of recorded data. The following tolerances have therefore been assumed by considering the above factors.

- Critical pressure measurements have a tolerance of ±0.5 % and non-critical pressure measurements ±1 %.

- The main steam flow is considered accurate within a tolerance of ±0.1 % and the extraction flows ±5 %.
- Temperature measurements are considered accurate within ±1 K.

2.4.4 Conclusion on plant data and its implementation

Heat balance data is initially used to define the performance characteristics in the models, due to the data being easily accessible and interpreted. The data is used as design data and annotated by using the subscript D in the component models. Heat balance data is then used to verify the models as to ensure that the methods are correctly implemented.

Acceptance test data are measurements taken from the plant after the plant has been commissioned. The advantage of the acceptance test data is that it is measurements from components which have not been in service for a very long time, thus the measurements will be from components that are more ideal. Acceptance test data was used in the study to validate components as well as to validate the integrated model during steady-state operation for different loads.

Operational plant data is data which is actual measurements obtained per interval for a given date. It was used to validate the component models during transient operation. Consideration must be given to potential component ageing as well as unreliable data.

3. Closed feedwater heater component modelling

In chapter 2.1.6, it was explained that the feedwater heater has the function of heating up the feedwater before it enters the steam generator and this has a direct influence on the total efficiency of the cycle. The feedwater heater is also part of the regenerative section of the cycle.

This chapter will focus on the feedwater heater component with a short literature study on the workings and types of feedwater heaters, specifically focussing on the heaters found in the ESKOM fleet. The numerical modelling aspects, validation and verification studies and conclusions of the model will then be discussed at the end of the chapter. Finally, an overview of the various developed feedwater heater components will be given.

3.1 Theory and characteristics of feedwater heaters

3.1.1 Purpose

The feedwater heater works as a shell-and-tube heat exchanger and uses steam, extracted at various points in the turbine train, to heat up feedwater flowing through the tubes. By doing this, one can reduce the amount of heat (coal needed) required to maintain the evaporation rate, thus increasing the overall cycle efficiency. It also reduces the amount of heat lost to the environment due to the condenser. Thyese efficiency gains are however only applicable for a specific number of heaters, as explained in section 2.1.5 by the optimum point of regeneration.

The feedwater heater is placed in two sections of the feedwater line: termed the high-pressure (HP) and the low-pressure (LP) section. The HP section is located between the boiler feed pump and the boiler, and the LP section is located between the condenser pump and the deaerator. Refer to an illustration in Figure 2.5.

3.1.2 Types of feedwater heaters and their physical attributes

In the Eskom fleet, there are several types and sizes of feedwater heaters in operation each with a specific purpose and application. To create a model which is applicable to most heaters, it is important to generalise the feedwater heater under a specific set of categories.

A recent study done by Allie [4] investigated a thermal model for a feedwater heater and looked at the heaters from at least 6 different power stations in the ESKOM fleet. The author recommended that the heaters should be categorised per the following criteria:

- Tubesheet or header type
- Vertical or horizontal in orientation
- One, two or three zoned heat transfer
- Long or short drain cooling zone, if applicable

A description of each heater follows with a conclusion on how these categories will be implemented on the final heater.

Tubesheet or header type

The type of heater refers to how the tubes are connected to the outside vessel. The tubesheet and header type connections are shown in Figure 3.1 a) and b).

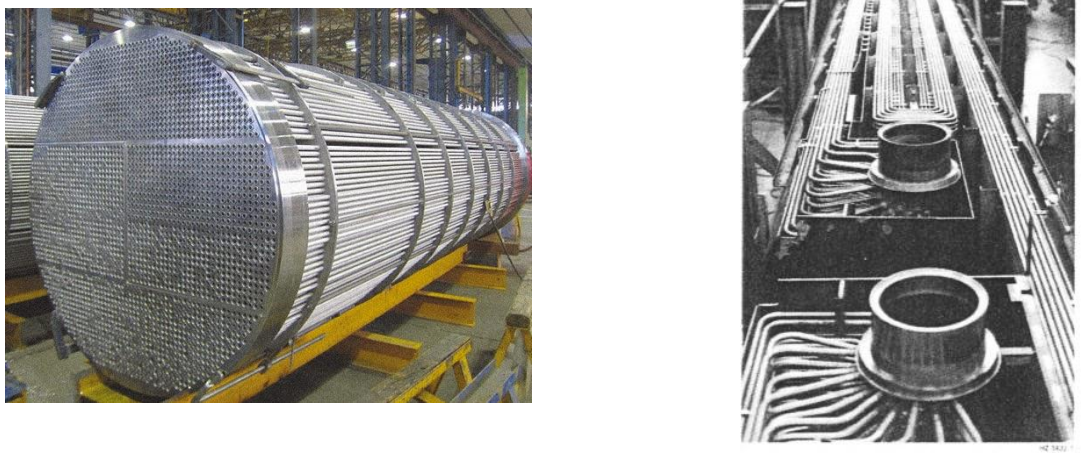

(a) (b)

Figure 3.1: Tubesheet (a) and header type (b) feedwater heaters [24], [25]

Tubesheet feedwater heaters consist of a tube plate situated at one end of the feedwater heater. These heaters consist of U-tubes where the ends of tubes are welded to the tubesheet. The tubesheet is further divided into two sections: the inlet/upstream section where the feedwater enters and the outlet/downstream section where the feedwater exits. The tubesheet is generally in the thickness of 10-25 mm [26], where thicker tubesheet is used at higher operating conditions.

For header type feedwater heaters, the tubes are welded to inlet and outlet headers (separate cylinders). These headers are situated perpendicular to the shell and are connected to the inlet and outlet pipes of the feedwater flow. Header type feedwater heaters are generally 10-20% the thickness of a tubesheet, resulting in lower maximum stresses and is therefore much more reliable under varying load conditions, but more expensive due to the close tube-to-nipple welds [25], [4].

Vertical or horizontal in orientation

The orientation of the heater is usually determined by the amount of space available and the structural constraints in terms of the thermal expansion experienced by the heater [4]. The orientation does not influence the heat transfer significantly, but a horizontal heater is more stable in terms of level control. A diagram for each orientation of heater is shown in Figure 3.2.

A term widely used for level control is liquid capacitance. The liquid capacitance is defined as the free volume per centimetre of the liquid level. For a horizontal feedwater heater, much more liquid is required to raise the level of say 1 cm compared to that of the vertical feedwater heater. The liquid capacitance is therefore large for the horizontal heater and smaller for vertical heaters. Thus, the higher the liquid capacitance for a heater, the better level control can be achieved.

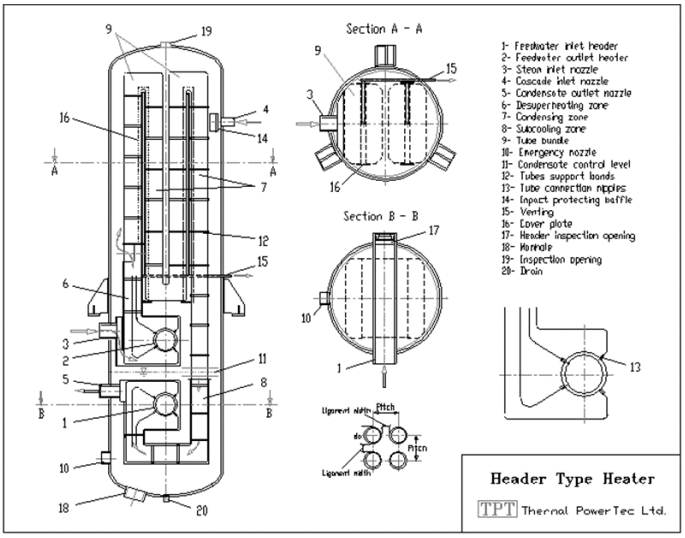

a)

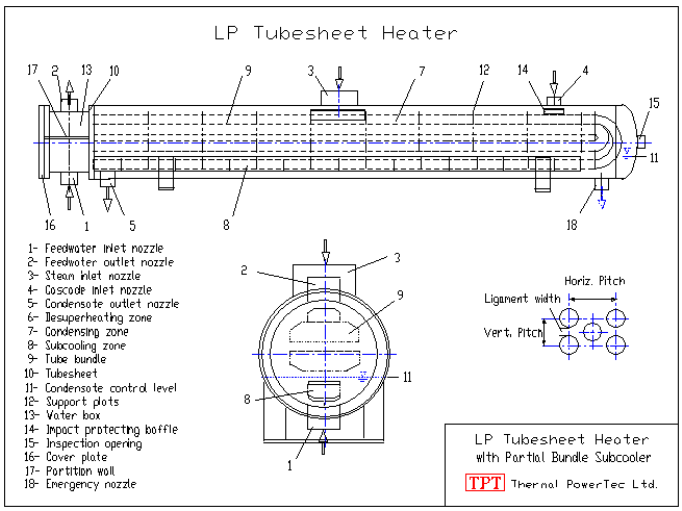

b)

Figure 3.2: a) Three-zoned closed vertical header type FWH, b) Three-zoned closed horizontal tubesheet FWH [27]

One, two or three zoned heat transfer

The three heat transfer zones in the heater consist of the desuperheating (DSH) zone, condensing (COND) zone and the drain cooling (DC) zone. The COND zone will always be present inside the heater since most of the heat transfer occurs in the zone, shown in the following chapter.

The heat transfer for the three zones can be illustrated by using a temperature to position curve shown in Figure 3.3. The steam enters the DSH zone at a superheated state at point 1, it then cools down to a saturated point 2, and condenses to the point 3. The steam is then subcooled below saturated liquid state and exits the heater at point 4. The feedwater enters the feedwater heater at the DC zone, point 5. The water is then heated up in the COND zone (6-7) and exits the heater at the DSH zone, point 8.

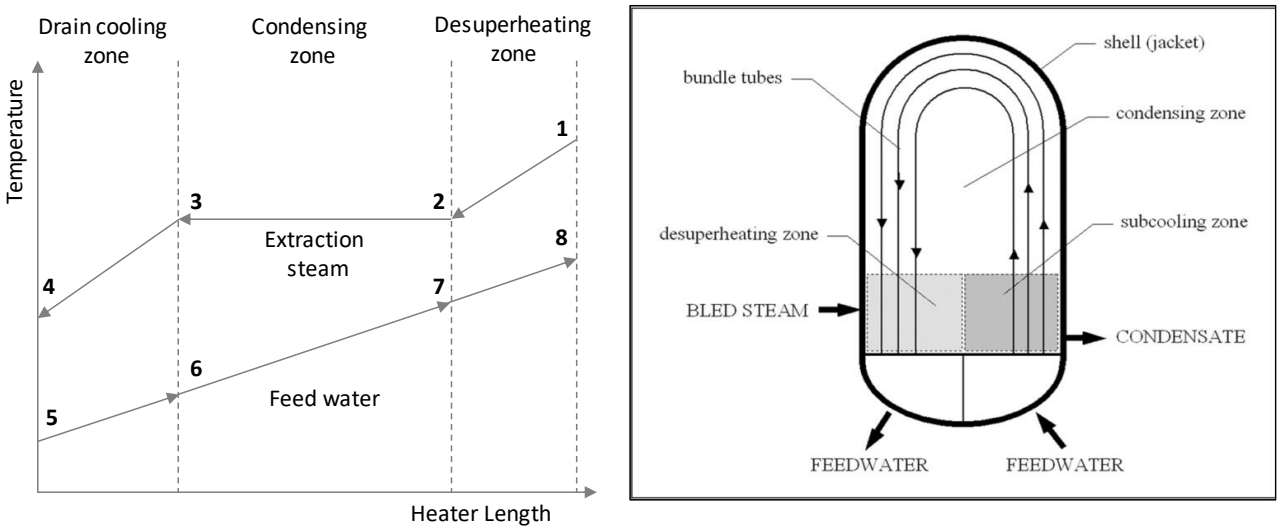

Figure 3.3: Temperature – length diagram and illustration of a three-zoned vertical two-pass feedwater heater [28]

The number of zones will largely depend on the design of the heater and the position of the heater in the power station network. If the steam, being bled from one of the turbines, enters the heater at a quality of below 1 then the feedwater heater will only consist of the COND zone and a DC zone. The DC zone is a separate zone separated by a metal plate called a shroud, see Figure 3.4 where only liquid drain is present. The DC zone is used to avoid flashing of the condensate, as this may happen if it cascades into a lower heater with a lower pressure. Flashing can also be avoided by using what is known as a flash tank [4].

Long or short drain cooling zone, if applicable

The drains cooler, which is responsible for removing the excess heat from the steam as it exits the COND zone, can be defined as either being long or short in length for a horizontal heater. A short DC zone does not span the entire length of the heater, but all the tubes flow through this zone. A long DC zone spans the entire length of the heater but is lower in height and thus not all the tubes

pass through this zone. This means that only some of the feedwater, as it enters the tube bundle, is in contact with the zone.

Table 3.1: Notable pros and cons between a short and long DC zone [29]

Long DC	Short DC
Liquid capacitance is higher due to the long DC zone's height being under the normal level. This translates to better level control.	Liquid capacitance is lower since the normal water level is under the height of the DC zone. Water level control is therefore more difficult.
Due to a higher capacitance, the long DC zone is more stable at off-design conditions.	The short DC zone makes use of the barometric effect to increase the level above the normal level inside the zone. At low loads where the pressure might drop inside the vessel, steam and liquid can mix in the DC zone and it will lose its effectiveness. Flashing of the steam can also occur downstream of the heater.
Due to the lower height of the long DC zone, the reheat effect (which is the effect of the superheating zone directly heating the liquid in the DC zone) is avoided.	The short DC zone is subject to this reheating effect due to the height of the shrouds being very close to the superheating zone.
More tubes are required for the long DC zone to obtain the same Terminal Temperature Difference, since not all the tubes run through the zone.	All the tubes run through the zone, therefore, fewer tubes are required to reach a certain Terminal Temperature Difference.

In Table 3.1, a summary of some of the most prominent advantages and disadvantages of both types of DC zones are given. It is evident that the long DC zone is more stable under certain off-design conditions with better level control and the short DC zone has better heat transfer performance due to all the tubes running through the zone.

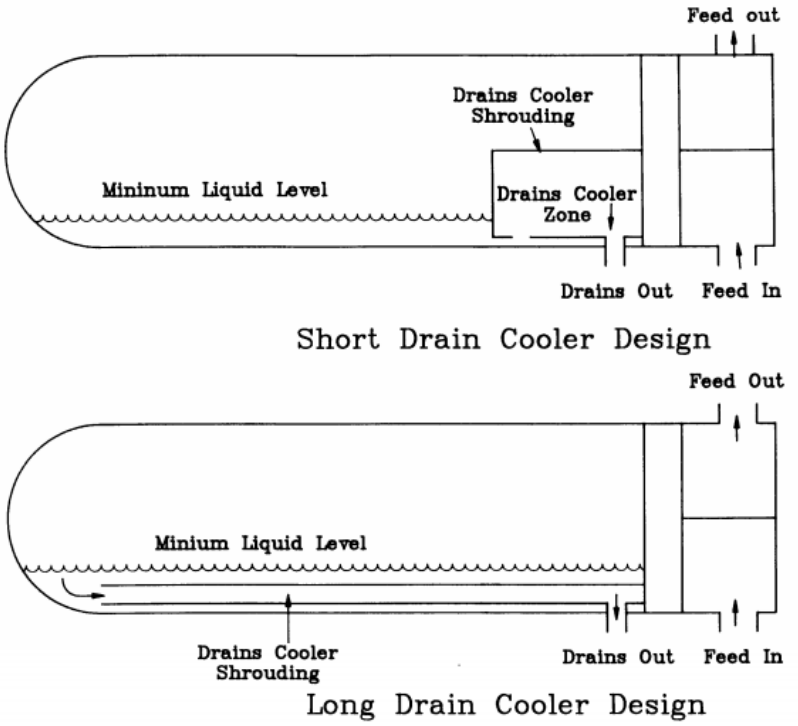

Figure 3.4: Diagram of a long and short drains cooler [29]

Conclusion on feedwater heater categories

The purpose of the feedwater heater model is to model the component so that it can be applied to most feedwater heaters in the ESKOM fleet. Generalizing the model is difficult since there are so many various configurations of the component in industry.

It is after careful consideration decided that the current model will be split into two main components: a horizontal model and a vertical model. Each of the models will be able to change type and if the type is tubesheet then the DC zone will be able to be chosen as either a shrouded drain cooler or a normal liquid level. These parameters will be used in the geometry calculations of the heater as to determine the correct liquid level capacitance, pipe lengths and liquid volumes.

3.1.3 Performance characteristics of feedwater heaters

The typical heat transfer distribution of the three heat transfer zones is shown in Figure 3.5, which displays the heat transfer distribution from 5 different heaters in a power station. It can clearly be seen that the COND zone contributes to most of the heat transfer for all the heaters in the power station.

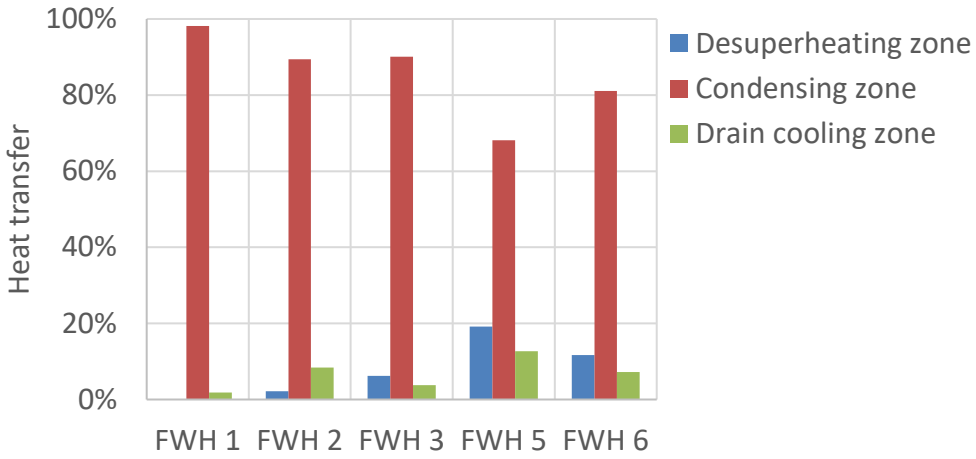

Figure 3.5: Typical heat transfer distribution of the three zones for different heaters in the feedwater heater train of a large coal-fired power station

A critical parameter which is used to rate the feedwater heater is the terminal temperature difference (TTD). This parameter is defined as

TTD = saturation temperature of extracted steam – exit feedwater temperature (2.1)

The TTD can be calculated for any type of heater since condensation occurs, which means the presence of a saturation temperature, in all types of heaters. Typical values of the TTD lie around 3°C or less and the parameter gives a good indication of the performance of the heater. Smaller values indicate that the heater is performing efficiently but requires larger heaters, whereas larger values indicate that the heater is underperforming [6]. A negative TTD is possible in the case of heaters with a DSH zone.

A parameter which is used for level control is the drain cooler approach (DCA). The DCA is defined as

DCA = inlet feedwater temperature – extraction steam outlet temperature (2.2)

The parameter is usually in the range of -12°C and an increase in the parameter gives an indication of a level decrease and the decrease of the DCA gives an indication for a level increase. Although the level can be measured by other means, such level indicating instruments, the DCA can give a rough indication to the level since it is coupled to the performance of the heater.

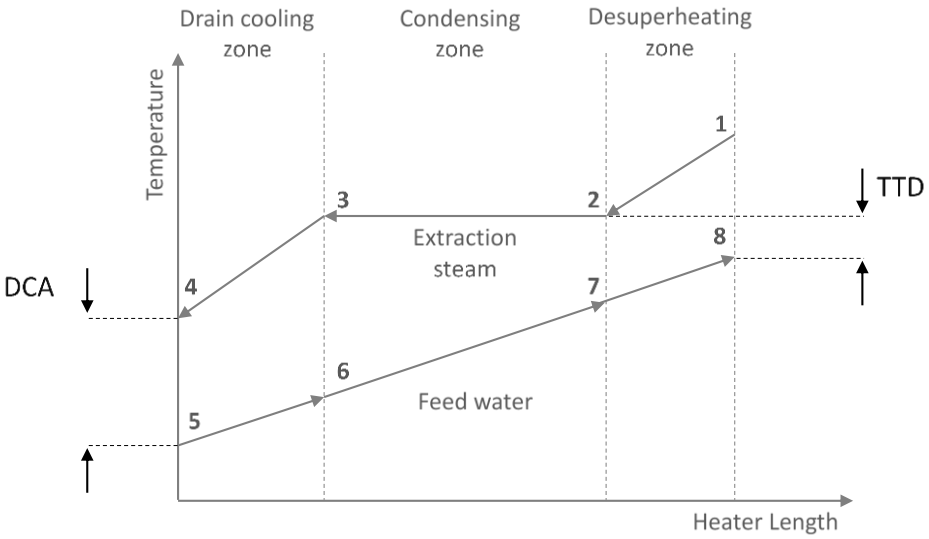

Figure 3.6: Heater performance indicators on a temperature to length diagram of a three-zoned heater

Factors which influence the TTD and DCA negatively [26]:

- Improper water level control (which affects the area of heat transfer)
- Disruptions in the extraction points, such as pressure drops or temperature changes
- Fouling, which is caused by unwanted material accumulating on the wall of the tubes and thus increasing its thermal resistance
- Tube plugging

3.1.4 Design methods for shell-and-tube heat exchangers

It was mentioned that feedwater heaters are essentially shell-and-tube heat exchangers where condensation heat transfer occurs over the tube bundle. Designing these heat exchangers can be difficult and various methods in literature can be followed to perform the design of shell-and-tube heat exchangers. The design essentially involves

- Geometry calculations,
- Heat transfer correlations and
- Pressure drop correlations.

Two typical problems which occur in heat exchanger design is the problem of rating the heat exchanger and sizing the heat exchangers [30]. The rating problem refers to determining the thermohydraulic performance of the heater for an already geometrically defined heater. The sizing problem is concerned with determining the actual dimensions of the heater where the performance of the heater is already known.

Two methods are widely used to address the two design problems which are the well-known Kern method and the Bell-Delaware method. The Kern method provides a simple method for calculating the heat transfer and pressure drop correlations but does not account for baffle to shell and tube to baffle leakage [31]. The bell-Delaware method considers the baffles in the heater and thus pressure drop correlations are seen to be more accurate. The Bell-Delaware method is the most widely accepted method to use and is more comprehensive in terms of rating and sizing the heat exchanger [30].

The feedwater heater will therefore use the Bell-Delaware method which will enable to compensate for the unknown design parameter such as the tubesheet thickness and the clearance between the tube bundle and shell.

3.2 Thermodynamic models of FWHs in literature

This section will include a short literature study on thermodynamic feedwater heater models found in literature. The review will be done based on three categories, viz. general models, area allocation and the influence of level on performance of heaters. Lastly, the Flownex model of M. Thakaso will be discussed in more detail since the current feedwater model uses this model as a basis.

3.2.1 General thermodynamic models

One of the first thermal models developed was by Koehler and Weber [29], in which the authors used PEPSE to analyse heater performance of feedwater heaters with long DC zones. PEPSE is essentially a steady-state tool for mass and energy balance modelling in which various “what if” studies can be performed to analyse various power plant components in terms of performance. The purpose of the study was to evaluate the performance of heaters, parameters such as the TTD and DCA, before the heaters get installed on site. This was done to ensure that the TTD and DCA guaranteed by the vendor, who planned to replace the heaters where more than 10% of the tubes were plugged, was met.

The model was further described in a study done by Weber and Minner [32] in which the study centred on using the PEPSE JW method and comparing that with the Modified Delaware Method. The model applied various heat transfer correlations, geometrical constraints and area calculations. A noteworthy assumption was made in the model which was that the steam leaving the DSH zone is at saturated conditions. Thus, all the steam gets efficiently cooled down to saturated conditions and no superheated steam enters the COND zone. The study showed the implementation of the PEPSE methodology for various heaters, especially heaters under low-load conditions.

Fernández, Valdés and Tristán [33] presented a thermal model for a feedwater heater in the application of a nuclear-powered power station. The model was specifically developed for when wet steam is extracted from the turbines with the aim of diagnostic purposes. This was done by including a moisture removal effectiveness factor to the steam properties entering the feedwater heater, since the steam properties are not always measured at the extraction lines. The model used the LMTD method as well as the NTU method to determine the various thermodynamic properties feedwater and steam flows.

The model contained the following assumptions:

- The overall heat transfer coefficient (HTC) throughout the heater is kept constant.
- Flow rates and specific heats of the fluids are constant.
- Heat losses are not regarded.
- An equal heat transfer surface is assumed on each tube pass.

The assumption of no heat loss and the overall HTC is kept constant throughout the heater will be incorporated into the current model.

A recent fully defined thermodynamic model was developed by Allie [4], in which the model can specifically be used to verify the performance of heaters when limited design data are presented. The model that was developed included at least four different HTC correlations where each correlation could be analysed, the model further incorporated an additional zone where the steam exiting the DSH zone does not take after the assumption that it exists at saturated conditions. The model works by requiring the general geometrical inputs from the heater and choosing the corresponding correlations for the user input data.

One of the major contributions of the model was the inclusion of sub-zones in the COND zone. The model splits the COND zone into two regions, i.e., the condensing **R** zone and the condensing **C** zone. The condensing **R** zone represents the zone where the feedwater flowing through the DC zone first enters the COND zone (this sub-zone is present in a long and short DC zone). The condensing **C** zone is where the feedwater enters the COND zone directly without any contact to the DC zone (this sub-zone is only present in a horizontal feedwater heater with a long DC zone). The COND zone was then split into a third subzone called the condensing **S** zone. This zone represents the steam which is not fully desuperheated in the DSH zone and enters the COND zone as superheated steam. A schematic of the subzone for a horizontal feedwater heater with a long DC zone is represented in Figure 3.7 where the flow diagram of the steam and feedwater through these zones are shown in Figure 3.8.

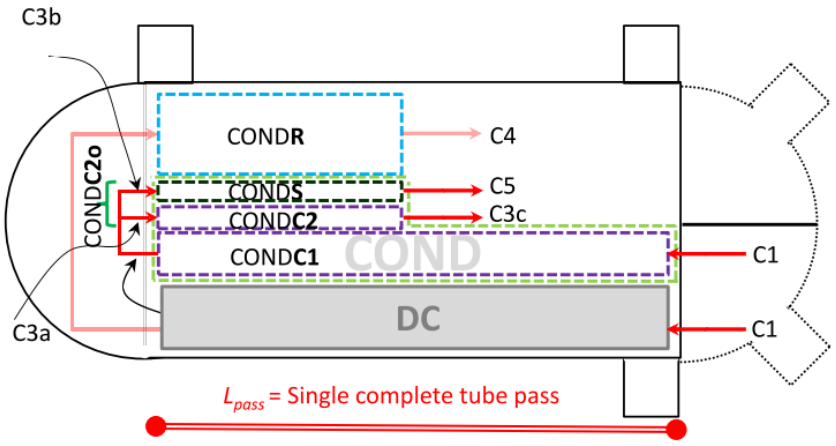

Figure 3.7: Schematic of the sub-zones of a horizontal feedwater heater with a long drain cooling zone [4]

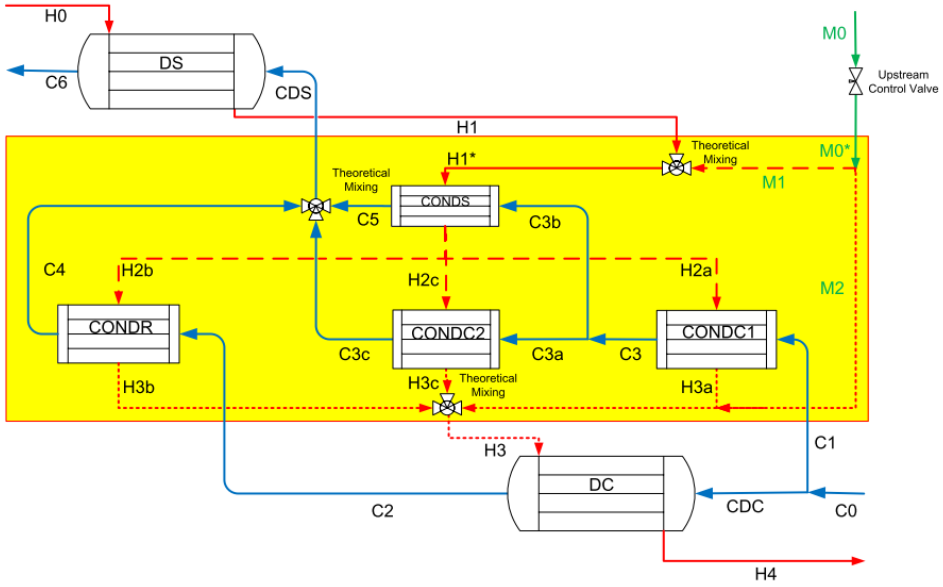

Figure 3.8: Flow diagram of the different zones in a horizontal feedwater heater with a long drain cooling zone [4]

It can be noted in Figure 3.7 and Figure 3.8 that the inclusion of a condensing **C1** and **C2** are also included in the model. This simply represents the two passes in the model and makes the area discretisation in the model easier.

The model was also extensively tested with a total of 30 feedwater heaters in operation. The results agreed well with the performance results given by various vendors. The study, however, did not include fouling and tube plugging in the modelling methodology. The model is further cumbersome in some respects to the time it takes to do the correlation permutations, since a complete run takes 1944 correlation permutations which result in about 1 hour of computation time. Software integration hurdles were also encountered during the study. The author's final concluding remarks were that the model is suitable to evaluate the performance characteristics for feedwater heaters supplied by vendors and the evaluation of existing heaters (clean and without tube plugging).

3.2.2 Area allocation

Area allocation refers to the total area required by each heat transfer zone. There can be a maximum of three zones, as noted in the previous section and the area is directly proportional to the amount of heat transfer in that zone. It is important to understand what the driving force behind the area allocation is, since the area of each zone changes depending on the specific conditions of the heater.

An investigation was done by Hussaini, et al. [34] in which the area for each zone's area in a closed feedwater heater is determined from heater performance data. A numerical model was set up for the heater and was tested together with a detailed calculation method using the LMTD approach. The numerical model is essentially a performance analysis of the heater where the total heat transfer area and inlet parameters of the flow are known. The numerical model is then used to determine the area allocation to each of the three zones and the outlet flows. The numerical model and the LMTD method agreed well when validated.

Three tests were then done to determine which parameters might have the largest influence on the area allocation of the heater. These tests included a change in the inlet temperature, flow rate and pressure of the steam. It was found that the area allocation was insensitive to any change in inlet temperature whereas the areas changed quite drastically due to a change in inlet pressure and steam mass flow. The results of the change in inlet pressure is shown in Figure 3.9. From the figure, one can see that as the pressure increase so thus the area for the subcooling zone. A pressure rise in the steam means that less area is needed to condense the fluid and thus the level will subsequently rise. The impact of the liquid level will be expounded on more in chapter 3.2.3.

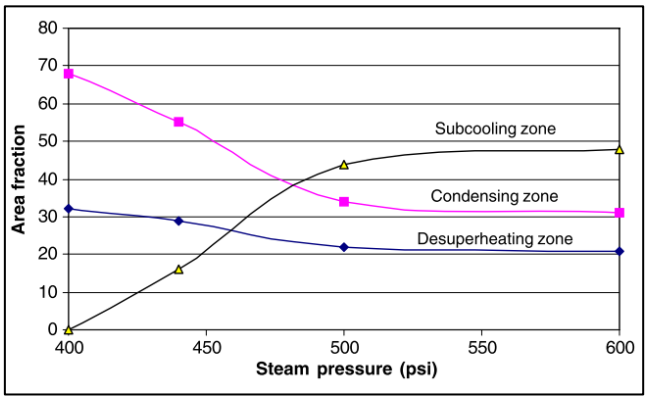

Figure 3.9: Change in zonal area allocation due to a change in steam pressure [34]

Another driving factor is the effect of fouling on the heater. Fouling refers to the accumulation of unwanted material on a surface which increases the resistance to effective heat transfer between the fluid flowing through the pipe and the steam flowing over the pipe. Research was done by M.A. Antar and S.M. Zubair [35] on the impact of fouling on the performance of a multi-zoned heater.

The authors used a similar numerical model approach to that of Hussaini et al., as described in previously in the section.

The study's findings were very much the same as Hussaini et al., in terms of the influencing flow parameters on the heat transfer area. For the fouling investigation, the authors considered two models, i.e. a simplified linear model and an exponential model. Both models resulted in an overall decrease in the HTC over time due to the accumulation of fouling. The authors then found that the decrease in HTC had the greatest impact on the COND zone, compared to that of the other two zones. The effect of fouling on the overall HTC is further shown in Figure 3.10.

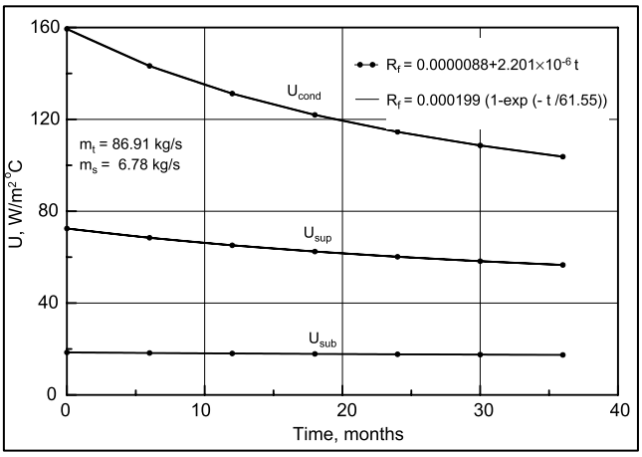

Figure 3.10: Effect of fouling on the overall HTC for the three zones of a feedwater heater [35]

3.2.3 Level and performance

The level and performance of a heater are very much interlinked. Only two zones are however affected by the level, which is the COND zone and the DC zone. This is because as the level rises the subcooling zone area increases and the COND zone area decreases. The increase and decrease of the areas influence the heat transfer performance as discussed in the previous section and ultimately affects the performance parameters of the heater.

Research has been done on horizontal heaters operating at low-level conditions since low-level conditions cause the DC zone to malfunction and lead to a decrease in heater economy. This happens because as the level drops below the diving port, the entrance region for the condensate to the DC zone, a mix of steam and water enters the zone. Consequently, the mixture has an adverse effect on the downstream pipes causing vibration and erosion [26]. The area of condensation is enlarged and the steam is no longer cooled below a subcooled state. This increases the DCA quite dramatically. The TTD is also decreased since the feedwater is now subject to a larger area of condensation heat transfer resulting in an increase in the outlet temperature of the feedwater.

J. Xu et al. [36] investigated the effects of varying conditions for feedwater heaters when looking at liquid level, especially low liquid level. A mathematical model of a feedwater heater was set up and incorporated the leaked steam-water mixture into the model's DSH zone heat transfer calculations.

J. Xu et al. proposed the following mathematical modelling technique to model the low-level phenomena appropriately and with reasonable accuracy. They firstly expressed the ratio between the steam area and the drain area is proportional to the mass flow of steam and drain. The formula derived for the cross-sectional area of the condensate is given as

$$S_h = \frac{\pi D_s^2}{8} - \left(\frac{D_s}{2} - h_w\right)\sqrt{\frac{1}{4}D_s^2 - \left(\frac{1}{2}D_s - h_w\right)^2} - \frac{1}{4}D_s^2 \sin^{-1}\left(\frac{D_s - 2h_w}{D_s}\right) \tag{2.3}$$

where D_s is the inner shell diameter and h_w is the water level inside the shell. The steam cross-sectional area under the diving port is given as

$$S_s = \frac{\pi D_s^2}{8} - \left(\frac{D_s}{2} - h_s\right)\sqrt{h_s\left(D_s - h_s\right)} - \frac{1}{4}D_s^2 \sin^{-1}\left(\frac{D_s - 2h_s}{D_s}\right) - S_h \tag{2.4}$$

where h_s is given as the diving port height. These areas are further illustrated in Figure 3.11 together with the annotations.

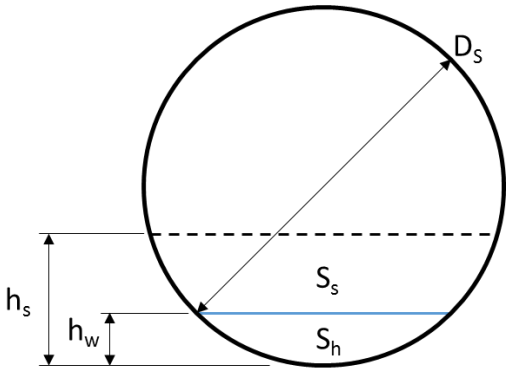

Figure 3.11 Cross-sectional area calculation according to Xu et al.

When the water level is above the diving port height, then the heat transfer equation is used for single phase heat transfer on the outside of the pipes. As soon as the height of the liquid drops below the diving port then steam starts to leak into the DC zone. The amount of steam that is leaked into the DC zone is therefore calculated by incorporating this area ratio and is given as

$$m_l = m_s \frac{S_s(v_l/v_s)}{S_s(v_l/v_s) + S_h} \tag{2.5}$$

where (v_l/v_s) is the ratio of the specific volume of liquid over steam. The authors then used the steam leakage to determine the heat transfer characteristics of the zone. The mathematical model

developed by J. Xu et al. is a model which can be applied to both three zoned HP heaters as well as two-zoned low-pressure heaters. The equations developed is also termed as universal and can be applied when calculating the effects of low level or just varying level in the feedwater heater.

The impact of varying conditions on feedwater heater was further investigated by S.M. Hossienalipour et al. [37]. The research focussed on investigating the effects of the varying level on the performance of the heater and used J. Xu et al.'s model, especially the calculation for the steam-water mixture entering into the DC zone, as their mathematical modelling approach.

The author's obtained what is known as a "knee" curve and is shown in Figure 3.12. This represents the DCA change as the level changes. One can see that the DCA dramatically increases at the point where steam starts entering the DC zone, which is at around 0.15 m. The model also correlates well with the experimental and test data. From the curve, one can determine a safe yet reliable level to deem as the normal level for the heater.

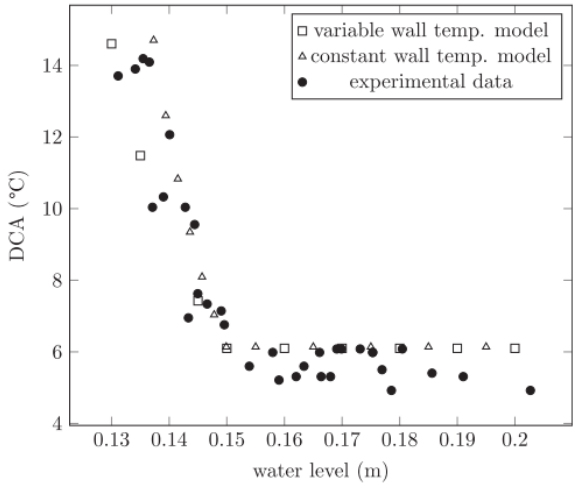

Figure 3.12: Effect on DCA as the level decreases in a horizontal high-pressure feedwater heater [37]

The low-level modelling is deemed as an abnormal condition and not an off-load condition. This condition will also only occur when the control system is not accurately calibrated or is not able to cope with fast-changing conditions. The phenomenon of low-level modelling will therefore not be included in the final feedwater heater model but can be further investigated in future research. The effect of the level on the overall heat transfer, when the level rises or when it drops will be included in the final feedwater heater model.

3.2.4 M. Thakaso's Flownex FWH model

Thakaso [5] recently developed a thermodynamic model of a feedwater heater by using Flownex. The model was implemented on a specific HP heater on one of the power station in the ESKOM fleet. The grey-box modelling technique is used in the model which consists of using first-principles

and correlations obtained from plant data. The model delivered credible results with regards to acceptance test data. Steady-state results showed that the energy and temperature distribution throughout the heat corresponded well with plant data and the transient behaviour of the model agreed to what one would expect from the heater. Comparison results for the average feedwater temperature during a load change from 80% to 100% is shown in Figure 3.13.

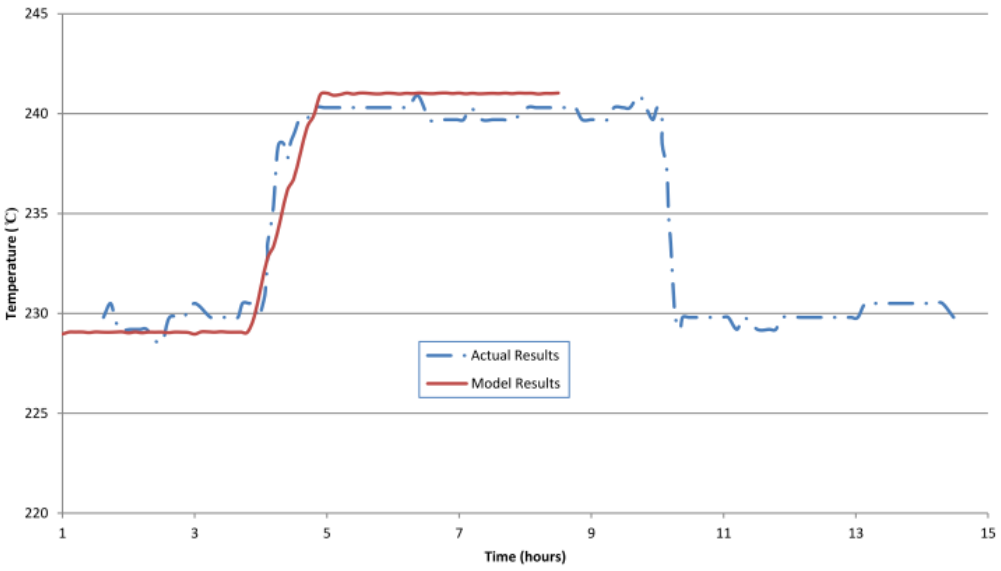

Figure 3.13: Average feedwater temperature during load changes [5]

The model contained heat transfer modelling for all three zones, thermal mass modelling and pressure drop modelling on the tube side. The following assumptions were made regarding the model:

- No pressure-drop over the shell side.
- The shell material is neglected for the simulation.
- Level control is possible in the model, but geometric changes to internals are not included.
- There is no heat lost to the atmosphere.
- The model is only calibrated for load conditions ranging from 40% to 100%. Lower load conditions can however be achieved by the model but results may not be accurate.
- All the steam from the superheated zone is cooled down to saturated conditions as it enters the COND zone.

The Flownex model is shown in Figure 3.14 with the red circle indicating the DSH zone, the orange circle indicating the COND zone and the green circle indicating the DC zone. The steam line in the model is the vertical network with the flow resistance components and the feedwater line is the horizontal network with the pipe components.

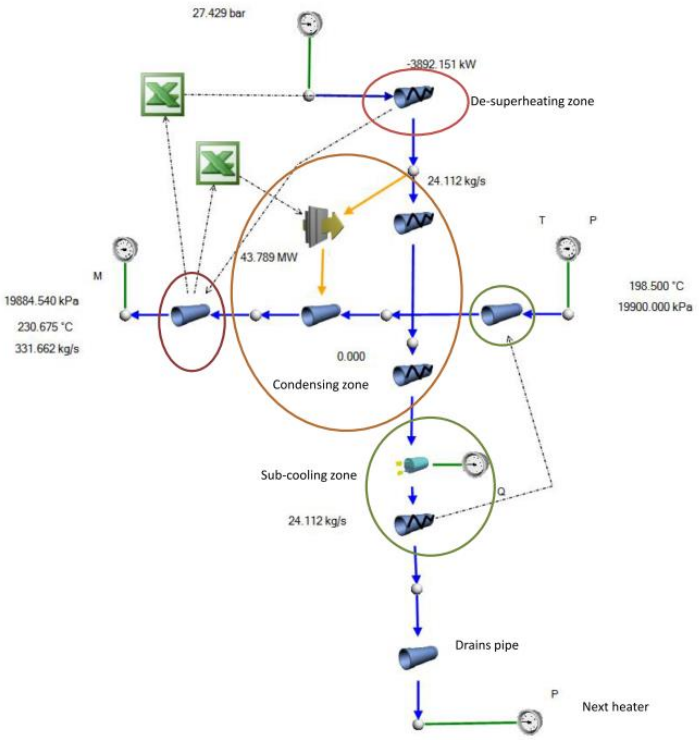

Figure 3.14: Flownex model of the FWH by M. Thakaso [5]

The DSH zone in the component is modelled by simply calculating the amount of heat needed to cool down the steam from inlet conditions to saturated steam conditions. The heat is then removed from the steam network and transferred to the feedwater outlet flow.

The COND zone is modelled by using high-level input and output design conditions. This is done by firstly determining the overall HTC from the design conditions for each load case. The overall HTC is then used to calculate a representative overall convective HTC, which is used in the Flownex component. Two assumptions are made for this calculation method:

- The inside and outside convective heat transfer area is taken to be 1 m^2.
- The inside and outside convective HTC is set to be equal to the representative overall convective HTC.

The overall HTC is driven by the mass flow of the feedwater which in turn is driven by the load case of the power station. A curve is fitted to represent the overall HTC in relation to the feedwater flow for a specific heater and implemented in the model using an excel spreadsheet.

The model was initially tested with steady-state plant data and yielded an outlet feedwater flow temperature error of less than 0.5% for all load cases. The bled steam outlet temperature showed the most significant error of 2.83% at a 40% load case scenario. A short-coming for the steady-state model was that the model did not run with ease of use, i.e. the designer, which solves certain

parameters in the Flownex network by using an iterative solving mechanism, had to be used to solve the network. The author recommends that further research needed to be done to make the network run without the use of the designer.

The model was then tested with transient plant data. The plant data involved a load change from 80% to 98% and the inlet and outlet temperatures of the feedwater of interest were recorded. The model was then run through the same conditions and the results showed relatively good agreement and are shown in Figure 3.13. Recommendations were made regarding the transient capabilities of the model and are listed below.

- The ratio between the inside and outside HTC should be investigated.
- An investigation should be done to include more thick-walled components in the feedwater heater component such as the tubesheet/header.
- Shell side pressure drop may have to be included since other heaters in the fleet indicated such phenomenon.

The final remarks by the author indicated that a robust methodology has been developed for modelling heaters with very little detailed component specifications, which was applied to a Flownex model. Further work is however required to model thermodynamic phenomena such as the effects due to the thermal inertia of thick-walled components. Work also needs to be done to test the model in an integrated network, i.e., by using the model in a feedwater heater train.

3.2.5 Conclusion on thermodynamic models

It is evident that a lot of studies have been done on the thermohydraulic modelling of feedwater heaters. These studies looked at improving the life-cycle of the heaters, area allocation of different zones under various conditions and abnormal conditions such as a low level.

Most of the heater models were developed by looking at determining the overall HTC from the heater's physical layout and steam flow properties. It is only recently that Thakaso's model looked at determining the effectiveness of heat transfer by looking at various design data. The model indicated very good validation results. This method requires little or no specific detail about the heater which makes it ideal to be implemented in the current model.

3.3 Feedwater heater component model

The chapter focusses on the current developed Flownex model of the feedwater heater. A model overview will be given following by, modelling methodologies, implementation of these methodologies and the verification and validation of the model. The final feedwater heater component model will then be presented with its conclusions and recommendations.

3.3.1 Model overview

The aim of the feedwater heater component model is to replicate the thermodynamic and hydraulic responses that are encountered in the actual feedwater heater component. The component was developed in the Flownex by following the various modelling methodologies described in the literature. The model further used Thakaso's [5] Flownex model, described in section 3.2.4, as a base model and progressed the model by addressing many of the shortcomings described by Thakaso. Table 3.2 represents an overview of Thakaso's Flownex model and the contributions made by the current model.

Table 3.2: Improvements and key attributes of Thakaso's Flownex feedwater heater model and the current Flownex feedwater heater model

M. Thakaso's Flownex model	Current Flownex model
The methodologies were only applied to a specific feedwater heater in an ESKOM power station	The model is a generalized model, i.e. can be implemented as an HP or LP heater.
The model contains all three heat transfer zone.	The model can be set to a one, two or three zoned heater.
The model only represented the level by a simple representation, i.e. with a cylindrical volume.	The model represents the level rise accurately; for that of a horizontal heater as well as that of a vertical heater.
The model included the thermal inertia due to the tube wall thickness and the liquid volume.	The thermal inertia of the tubes, liquid volume and the tubesheet are included in the model.
The model difficult to operate, the use of the designer is required to use the model.	The model operates as a compound component with user-friendly, plug-and-play capabilities.
	The model simulates the influence of the liquid level inside the shell on the heat exchange capabilities of the heater.
	Calibration of the model through the adjustment of the number of tubes plugged and fouling factor.
	I/O HTC ratio implemented

The feedwater heater model was further implemented in what is known as a compound component which is a custom build component in Flownex which consists of a smaller network. Three compound components were created for each different geometry specification, these types of geometries include

- A feedwater heater with no geometrical specifications
- A feedwater heater with a horizontal orientation

- A feedwater heater with a vertical orientation

The feedwater heater model contains a shell side in which the steam flows, and a tube side in which the feedwater flows. Heat is then transferred between the two sides through the tube wall due to the temperature difference between the tube and shell side. The feedwater heater model is shown in Figure 3.15. The model flow diagram is shown just below Figure 3.15 in Figure 3.16.

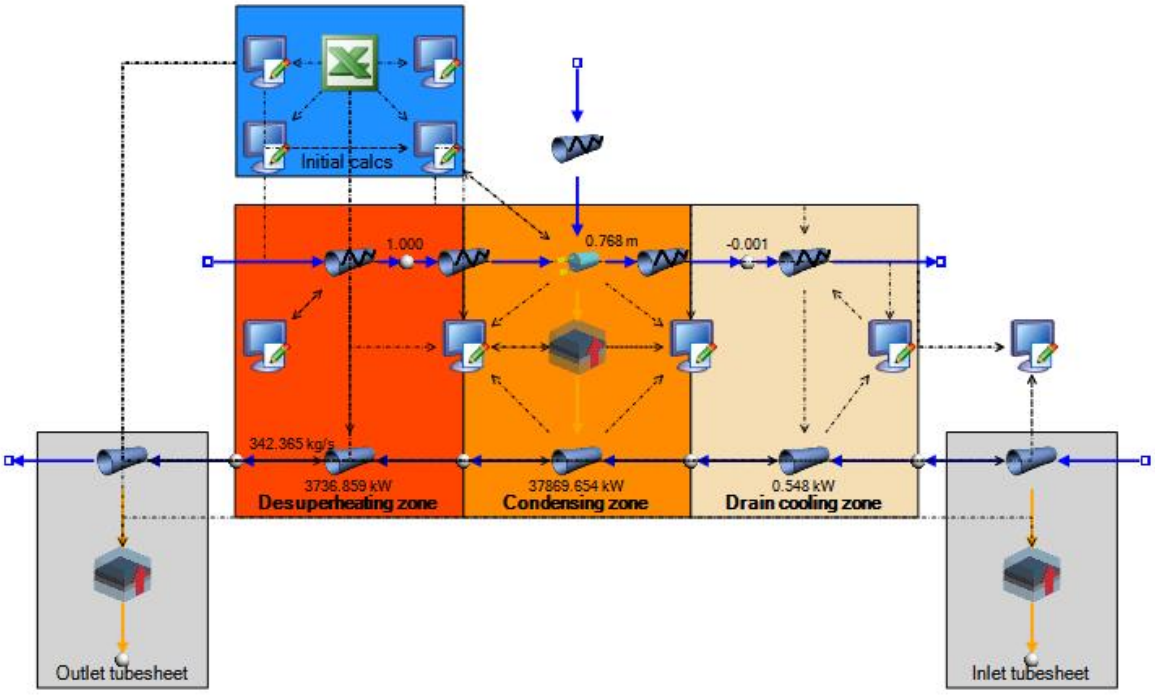

Figure 3.15: Detailed feedwater heater model in the Flownex

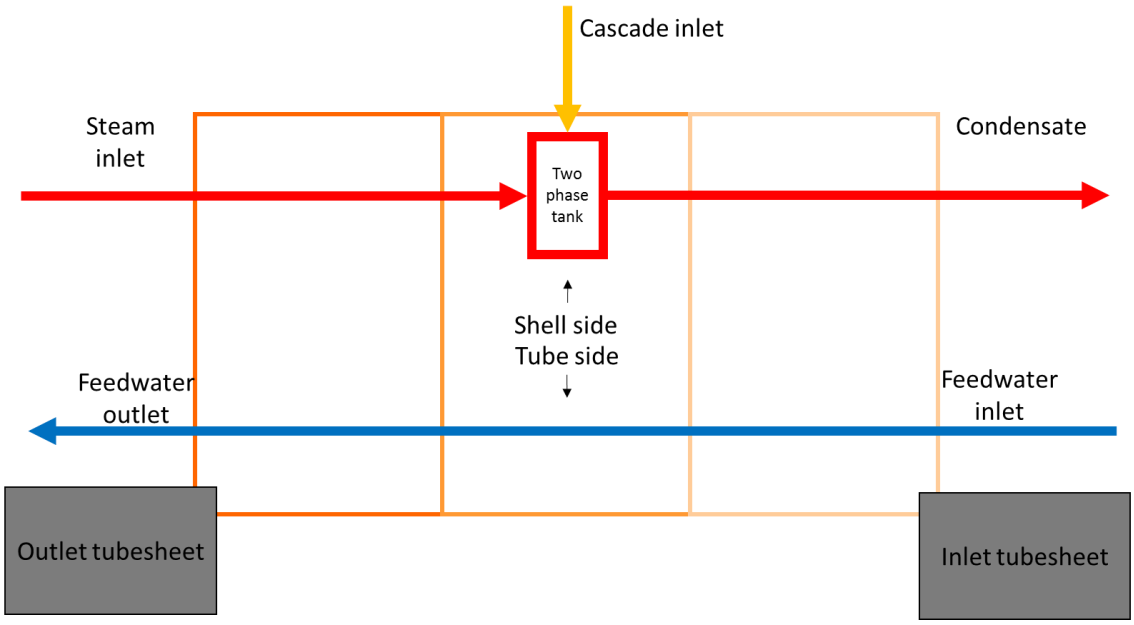

Figure 3.16: Network flow diagram of the feedwater heater model

3.3.2 Desuperheating zone

The desuperheating (DSH) zone's primary purpose is to cool the steam down from inlet conditions to saturated vapour state. The zone is designed as to not let the steam condense all the way in the zone, since the condensate might severely damage the zone's internal structure. Due to the design, some steam might enter the COND zone [4]. The model will however assume that the zone is effective in removing all the superheat from the steam, as is done in many other feedwater heater models.

The heat can be calculated by taking the difference between the inlet enthalpy and saturated vapour enthalpy and multiplying that by the amount of steam flow through the heater. The equation for the total heat transfer is given as

$$\dot{Q}_{DSH} = \dot{m}(h_1 - h_2) \tag{2.6}$$

where $\dot{Q}_{DSH}$ is the amount of heat transferred by the DSH zone [kW], $\dot{m}$ is the amount of bled steam (BS) [kg/s], h_1 the inlet enthalpy of the steam [kJ/kg] and h_2 the enthalpy of the steam at the saturated steam point [kJ/kg].

In the Flownex model, the heat transfer is calculated by using a script. The amount of heat transfer is transferred in this zone via a data transfer link from the shell side to the tube side. The tube side pipe further models the pressure drop of the feedwater as it flows through the tubes in this section. The script that is responsible for the DSH zone is shown in Figure 3.17.

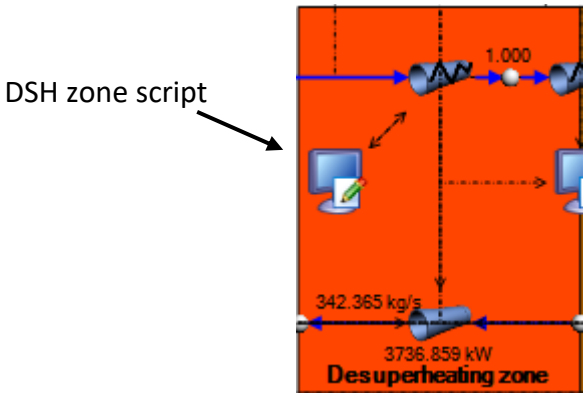

Figure 3.17: Desuperheating script, Flownex network

3.3.3 Condensing zone

The condensing (COND) zone is responsible for cooling the steam from a saturated steam phase to saturated liquid phase. Most of heat transfer occurs in this zone, consequently this zone is modelled with the greatest of detail.

The COND zone is modelled by using a two-phase tank connected to a pipe element through a composite heat transfer element. This element is essentially a convection, conduction, convection (CCC) heat transfer problem across a flat plate. The element uses properties from the material and fluid, flowing on the external sides, as inputs in calculating the total amount of heat transfer.

By knowing the material, the conduction properties can be easily obtained. The convection properties are however not that trivial to determine. The convection properties are mostly depended on specific fluid properties and the geometrical layout of the FWH. All of this must be considered to accurately calculate the HTC, especially for the outside where the tube layout and mode of condensation play a significant role.

The model takes a different approach to the normal method of determining the amount of heat transfer for the zone. It models the conduction heat transfer from a top-down approach by using design parameters to determine a representative overall HTC (UA). This eliminates very specific geometry and fluid flow inputs.

The coefficient is determined for each load case and a curve is fitted through the data by taking the feedwater mass flow as the load indicating parameter. The feedwater mass flow is chosen since it is directly coupled to the load of the entire cycle. The methodology for obtaining the representative HTC is further explained in Figure 3.18 and expounded on in the rest of the chapter.

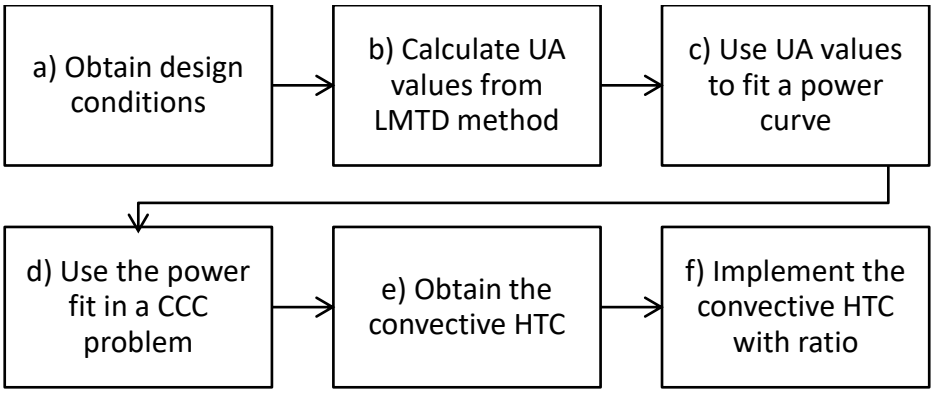

Figure 3.18: Methodology for determining the overall HTC

a) Obtain design conditions

The first step in the heat transfer calculations is to obtain the design inputs from a heat balance diagram or similar plant data. The inputs required from plant data are summarised in Table 3.3. A minimum of three inputs are required to fit the power fit curve.

Table 3.3: Input variables needed from plant data

Bled steam	Feedwater	Cascade
Mass flow	Mass flow	Mass flow
Inlet pressure	Outlet pressure	Inlet enthalpy
Inlet enthalpy	Outlet enthalpy	

b) Calculate the UA values from the LMTD method

The LMTD method is then used to determine the UA values for each load condition. The LMTD methods makes use of the inlet and outlet temperature, where these temperatures can be obtained from the design input data and are summarized in Table 3.4, with reference to Figure 3.6, the method states

$$\dot{Q}_{COND} = UA\frac{\Delta T_2 - \Delta T_1}{\ln\left(\frac{\Delta T_2}{\Delta T_1}\right)} \tag{2.7}$$

where $\Delta T_1 = T_2 - T_7$; $\Delta T_2 = T_3 - T_6$

For the feedwater temperatures, it is assumed that the pressure drop on the tube side is not large enough to make a remarkable difference. The temperatures can simply be calculated by using the properties of steam, as shown in Table 3.4.

Table 3.4: Condensing heat transfer temperature calculations

T_2	$T_2 = f(p_s, x=1)$
T_3	$T_3 = f(p_{i,s}, x=0)$
T_6	$T_6 = f(p_{i,fw}, h_6)$ where $h_6 = h_7 - \frac{\dot{Q}_{COND}}{m_{fw}}$

T_7	$T_7 = f(p_{i,fw}, h_7)$ where $h_7 = h_8 - \frac{\dot{Q}_{DSH}}{m_{fw}}$

It is important to note that if the heat contains cascade from a heater higher in the line, it must be included in the total COND heat transfer. Figure 3.19 illustrates how the heat transfer is calculated for the COND zone.

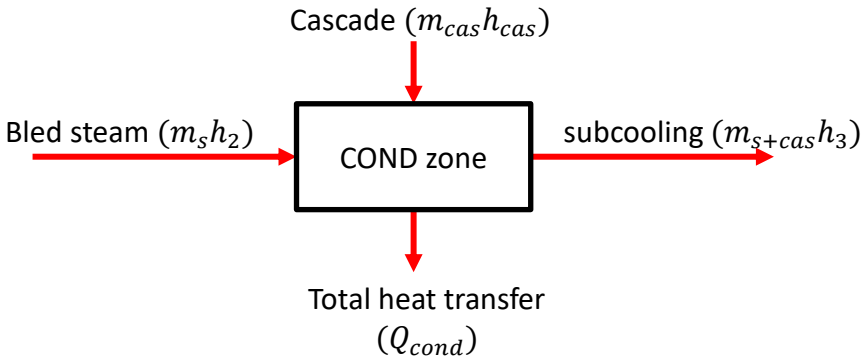

Figure 3.19: Condensing heat transfer

The cascade from the heater higher up in the line enters the FWH usually in the two-phase region. It is assumed that all the cascade flows directly into the heater, thus the heat transfer equation for the COND zone, by referring to Figure 3.19, is

$$\dot{m}_2 h_2 - \dot{Q}_{COND} + \dot{m}_{cas} h_{cas} = (\dot{m}_{s+cas}) h_3 \tag{2.8}$$

or

$$\dot{Q}_{COND} = \dot{m}_2 h_2 + \dot{m}_{cas} h_{cas} - (\dot{m}_{s+cas}) h_3 \tag{2.9}$$

The overall HTC can now be determined by using the calculated heat transfer and selected temperatures. The next step will be to plot a curve for each calculated overall HTC.

c) Use the UA values to fit a power curve

Each load condition now contains a specific UA value. To make this data applicable for all possible load changes, a power fit is fitted through the UA values. Thakaso [5], noted that the HTC on the tube side followed a power law form and thus a power fit was used to fit the data. The mass flow of the feedwater is used as the load indicating factor. An example of the power fit is shown in Figure 3.20. The curve fit method is shown in Appendix B.

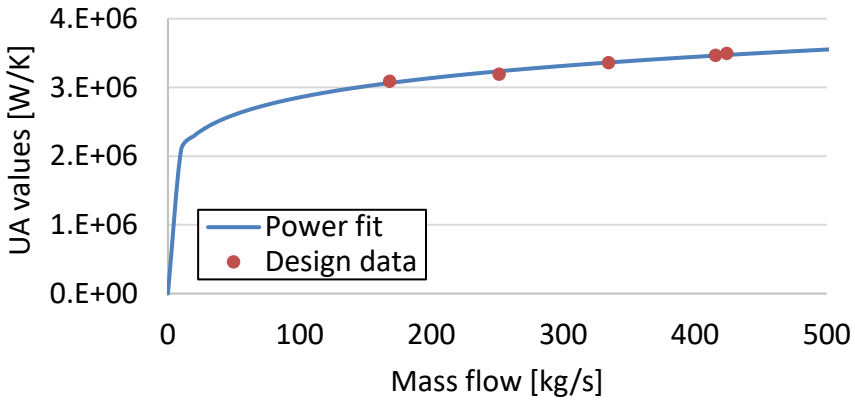

Figure 3.20: Example of a power fit curve for the overall HTC

d) Use the power fit in a CCC problem

The formulation for the CCC problem (ignoring the effects of fouling) is given as

$$UA = \frac{1}{\frac{1}{h_i A_i} + \frac{\Delta x}{kA} + \frac{1}{h_0 A_0}} \tag{2.10}$$

where the subscripts i, o refers to the inside and outside of the tube. The tube wall thickness Δx, the conductivity is k and A refers to the conduction area which is the average area between the inside and outside area. The convection HTC is also defined for each side as h. The parameters are further illustrated in Figure 3.21 for a flat plate.

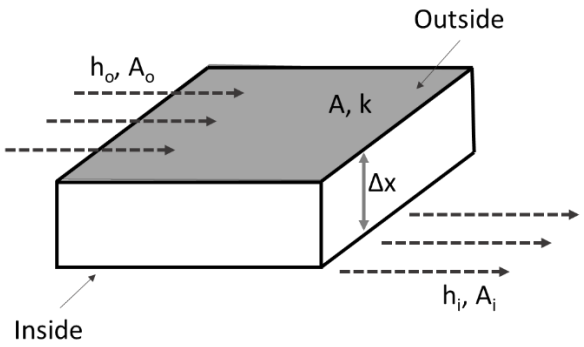

Figure 3.21: Variable illustration of the convection, conduction, convection problem

One can further define the problem by including fouling (R), which will specifically be used as a calibration for a heater that has been in service. A new UA value is therefore calculated.

$$\frac{1}{UA^*} = \frac{1}{UA} + \frac{R_{f,i}}{A_i} + \frac{R_{f,o}}{A_o} \tag{2.11}$$

e) Obtain the convective HTC

The next step is to ensure that the UA curve can be applied to the composite heat transfer element in Flownex. Unfortunately, Flownex does not contain an input for the UA value and the value must therefore be formulated back into a value which can be used in the Flownex component. A sensible value which can be used is the inside convective HTC.

In order to write equation (2.10) in terms of the inside convective HTC one first need to define the outside convective HTC, which can be done by defining a convective HTC ratio R_h as

$$R_h = \frac{h_i}{h_0} \tag{2.12}$$

The ratio can now be applied in equation (2.10), where the fitted UA^* in equation (2.13) is applied and the area of each convective side is included in the convective HTC.

$$h = \frac{1 + \frac{1}{R_h}}{UA^* + \frac{\Delta x}{kA}} \tag{2.13}$$

The convective HTC ratio is determined through a rough estimation of what the inside and outside heat transfer would be. This is done by using the Dittus-Boelter equation and the Nusselt integral approach over multiple pipes. Only a rough estimation is necessary since the amount of heat transfer is only dependent on the UA curve that was fitted with the design data. The ratio is only required to be somewhat accurate since it plays a role in the transients of the pipe wall. The Dittus-Boelter equation in respect to the inside HTC is given as [38]

$$Nu_D = 0.0243 \cdot \mathrm{Re}^{4/5} \cdot \mathrm{Pr}^{0.4} \tag{2.14}$$

The Nusselt integral approach for a single horizontal pipe is given as [39]

$$h_o = 0.729 \left[\frac{g \rho_l (\rho_l - \rho_g) h_{lg}^* k_l^3}{\mu_l (T_{sat} - T_w) D} \right]^{0.25} \tag{2.15}$$

where this equation is adjusted for a vertical heater with vertical pipe as

$$\frac{h_{vert}}{h_{horiz}} = 1.29 \left(\frac{D}{L} \right)^{0.25} \tag{2.16}$$

This overall HTC can then be split back into the inside and outside convective HTC using the ratio (h_r) to be implemented into Flownex. Uncertainties are however associated with these correlations.

It was reported by Allie [4] that uncertainties as high as 25% can be experience for the Dittus-Boelter correlations and uncertainties as high as 33% for the Nusselt integral approach.

f) Implementation into Flownex

Implementing the above methodology into Flownex was done by using scripting. Three different scripts were used where two of the scripts are run at the initial steady-state of the simulation and the third script is run during the transient behaviour of the simulation.

The first script (script A in Figure 3.22) uses inputs from the excel sheet and calculates the power fit curves using non-linear regression. The second script (Script B in Figure 3.22) continually calculates the overall convective HTC using the power fit. This script uses the feedwater mass flow to determine the inside HTC and from there determines the overall convective HTC using the convective HTC ratio, which is calculated in the third script (Script C in Figure 3.22). It is important to note that script B and Script C is run during a transient scenario since the inputs to these scripts change throughout the simulation. A mesh independence study for the heat transfer element was done and is shown in Appendix C.

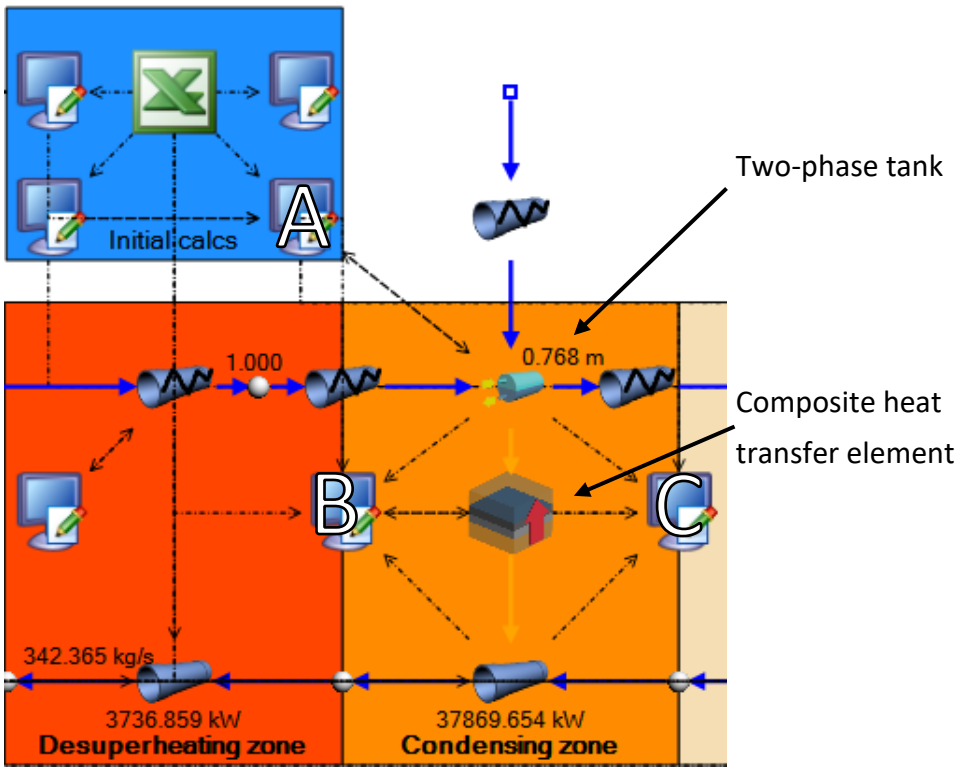

Figure 3.22: Condensing scripts, Flownex network

The inputs dialog for the composite heat transfer element is shown in Figure 2.1, where it can be noted that the convection area, upstream and downstream, is set to 1 m^2. The reason being that the convection HTC in equation (2.13) already includes the area as derived in equation (2.13).

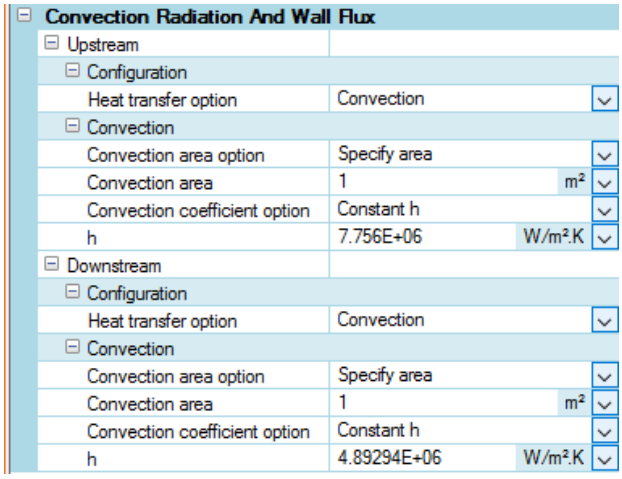

Figure 3.23: Inputs dialog for the condensing zone's composite heat transfer element

The final input required is the tube properties. A sample tube material is used, which is carbon steel AISI 1010. This material must be specified since the overall transient results of the heater is affected by the tube material.

3.3.4 Drains cooling zone

The drains cooling (DC) zone cools the fluid down even further, below saturated liquid point. This zone, as indicated in beginning of this chapter, does not contribute a considerable amount of heat transfer to the total system and was modelled accordingly.

The heat transfer for the zone was initially calculated by using a linear approximation between the highest operating point and the lowest operating point as shown in equation (2.17). The temperature distribution curve for the feedwater heater is shown in Figure 3.24 where the feedwater outlet temperature and condensate outlet temperature is compared with design data.

$$\dot{Q}_{DSC} = \frac{\dot{Q}_{D,\max load} - \dot{Q}_{D,\min load}}{\dot{m}_{D,\max load} - \dot{m}_{D,\min load}} \cdot \dot{m}_{current} \tag{2.17}$$

The temperature distribution curve shows that the feedwater leaving the vessel corresponds well to the design data. However, the extraction steam flowing out of the heater as condensate do not agree well with the design data at design conditions. This means that there is room for improvement to the linear approximation for heat transferred in the DC zone.

A better approximation for the calculation of heat transfer in the DC zone is a second order polynomial. This was applied to all load cases. The results are also shown in Figure 3.24, where one can see that the feedwater outlet temperature has not changed by much and the condensate temperature leaving the heater corresponds well with the design data, especially at low load conditions. The method used in finding the second order polynomial is shown in Appendix B.

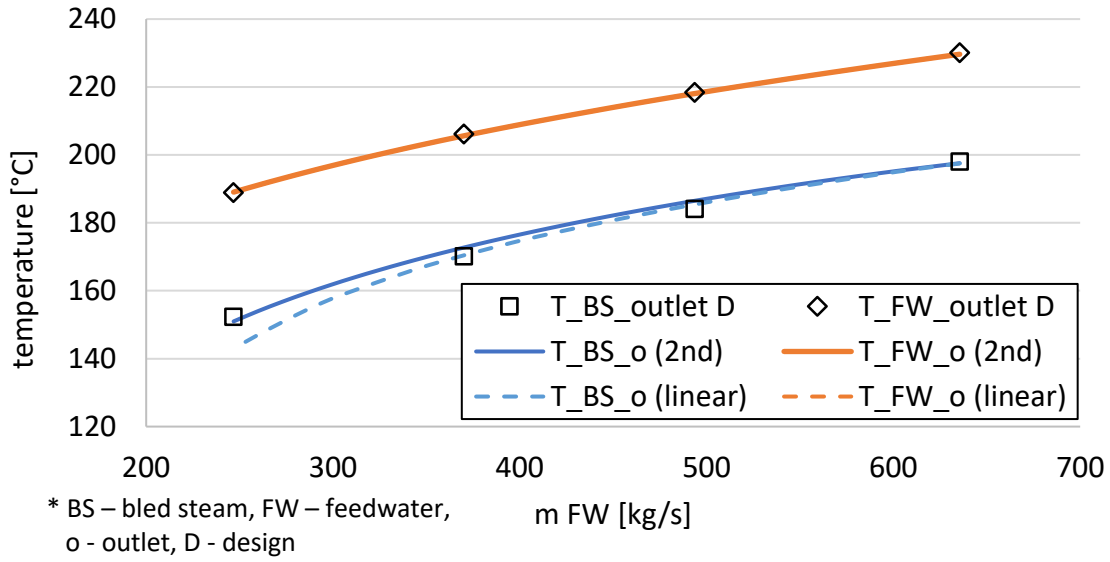

Figure 3.24: Temperature distribution curve, DC zone's heat exchange with a linear approach and polynomial approach

3.3.5 Accurate level representation

Geometrical aspects inside a heater play a significant role in the control and performance of a heater [37]. The effects of level variations fall under the transient capabilities of a heater since the level is assumed to be at normal level during steady-state conditions.

The initial step in modelling the geometry of the heater is to classify the heater as either horizontal or vertical. It is further important to identify the design method from which assumptions and calculations for the geometry will be made. The model uses the Bell-Delaware method since the method is the most comprehensive and widely accepted method for sizing a shell-and-tube heat exchanger [30].

Another crucial step is the implementation of the geometry into the Flownex. This will dictate the final calculation since the overall purpose is to present the feedwater heater geometry in the SE. Flownex used the two-phase tank to represent the level. The two-phase tank is essentially a node with a volume and calculates the level inside the volume based on the fluid quality at the specific pressure [40]. The two-phase tank can specify the geometry of the vessel in two ways:

- Simple specification, i.e. the input of a shell volume and diameter or height.
- Specific specification, i.e. the input of the shell geometry using a table.

The specific specification, using an input table, is employed in the current model since the geometry will required more detail than just the volume and diameter of the shell. This option builds the geometry with the inputs of a constant horizontal cross-sectional area and a height for each increment. It essentially builds frustums (the remaining portion of a pyramid with equal sides when

the upper part has been cut off) on top of each other to form the vessel shape. A simplified illustration of such a geometry is shown in Figure 3.25. The initial Area is defined as 0 m^2, which indicates the starting area.

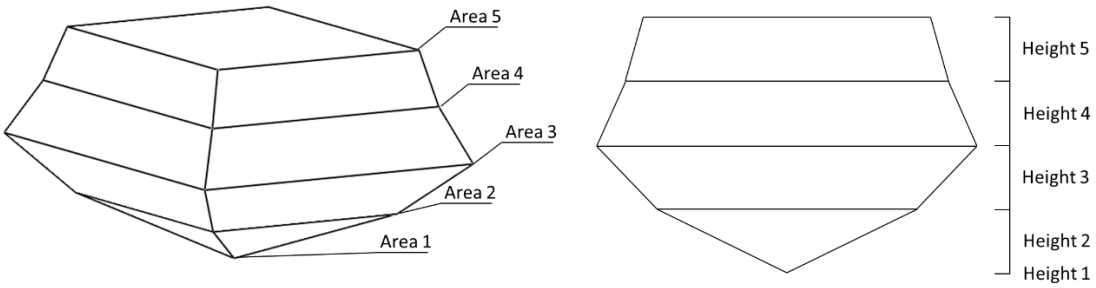

Figure 3.25: Example of a frustum build geometry in the two-phase tank

Modelling the geometrical aspects of the **horizontal heater** is more complex due to the nonlinear rise in level. The level will increase drastically at the bottom of the shell due to the low liquid capacitance and will increase less drastically at near the half way mark of the shell due to the high liquid level capacitance. The existence of the pipes and free volume around the pipes, as well as the shape of the DC zone further complicates matters.

The following assumptions are made to model the horizontal heater geometry of the shell:

1. Only factors which have a major effect on the liquid capacitance will be modelled (This includes the number of tubes, outer diameter of the tubes, layout of the tubes, DC zone geometry and clearances between the tube bundles and shell).
2. All initial geometrical calculations, such as the number of pipes and bundle to shell clearance, will be modelled in accordance to the Bell-Delaware method.
3. A total number of 40 increments will be used to model the bottom part of the shell and the upper part will only be modelled by using 1 increment.

The implementation of the shell geometry followed a four-step process:

a) Obtain the input parameters:

The initial step in obtaining the frustum build is to acquire the input parameter. These input parameters are summarized in Table 3.5.

Table 3.5: Input parameters for horizontal feedwater heater geometry

Property	Description	Engineering unit
N_{passes}	Number of tube passes	[-]
L_{ti}	Tube length	[m]
D_s	Inner shell diameter	[m]

L_{design}	Design level	[m]
d	Outer tube diameter	[m]
L_t	Tube wall thickness	[m]
N_{tubes}	Total number of tubes	[-]
L_{DC}	Drain cooling length	[0-1]
H_{DC}	Height of drain cooler	[0-1]
L_{bb}	Bundle to shell clearance	[m]
L_{ts}	Tubesheet thickness	[m]
P_L	Pitch layout	[0,1]
P_t	Tube pitch	[m]

Most of these parameters can be obtained from plant data or drawings of the component. The user is however able to only input some of the parameters and use equations described by the Bell-Delaware method to calculate the rest. The following equations are used if the specified parameters are not found within the plant data [30].

The **number of tubes**:

$$N_{tubes} = \frac{CTP(D_s - L_{bb})^2}{CL(P_t)^2} \tag{2.18}$$

where CTP is the tube pass constant and is given as 0.93, 0.9 and 0.85 for 1, 2 and 3 tube passes irrespectively. CL is the layout constant given as 0.87 for a tube layout of 30° and 60° and 1.0 for a tube layout of 45° and 90°. The tube pitch layout is shown in Figure 3.40.

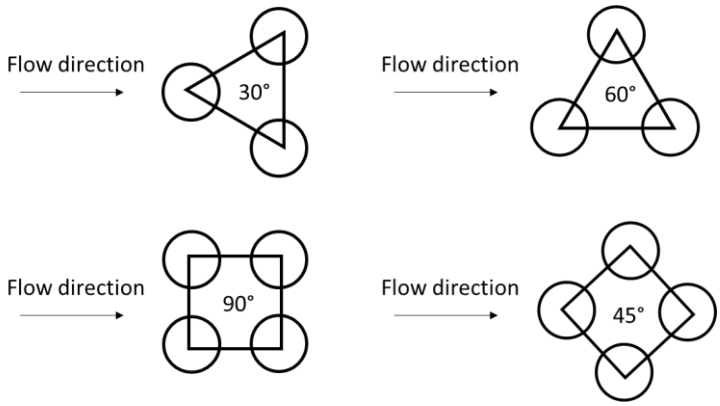

Figure 3.26: Tube pitch layout configuration

The **Bundle to shell clearance:**

$$L_{bb} = 12.0 + 0.005 \cdot D_s \tag{2.19}$$

where the inside shell diameter is used in unit millimetres.

The **Outside tube limit diameter:**

$$D_{otl} = D_s - L_{bb} \tag{2.20}$$

The **Tubesheet thickness:**

$$L_{ts} = 0.1 \cdot D_s \tag{2.21}$$

b) Determine the volume of the vessel per increment

The volume of the shell per increment is calculated by using the equation for a partially filled cylinder with the inclusion of the endcap. The endcap, which is approximated as a half sphere is included in the second part of the calculations. The volume for such a cylinder is illustrated in Figure 3.27 and derived in equation (2.22).

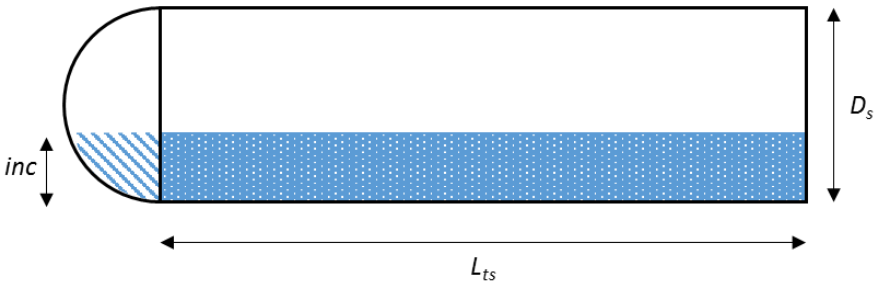

Figure 3.27: Volume of a partially filled cylinder with an endcap

$$Vol = L_{ti} \cdot D_s \cdot \left(\frac{2 \cdot \cos^{-1}(z) - \sin(2 \cdot \cos^{-1}(z))}{8} \right) + \frac{\left[\pi \cdot inc^2 \left(\frac{D_s}{2} \right) - \pi \frac{inc^3}{3} \right]}{2} \tag{2.22}$$

where

$$z = \left(1 - \frac{2 \cdot inc}{D_s} \right) \tag{2.23}$$

and where inc is defined as the current level of the vessel. Since the volume is split up into various frustums, this calculation is done for each incremental level. The number of increments was chosen as 40 for the first half of the vessel and one increment for the second half of the vessel.

Only one increment for the top half of the vessel has been implemented since high-level conditions, that is when the level is usually past the half-way point of the vessel, emergency stop valves at the turbine extraction lines will close off. This is to prevent any condensate from entering back into the extraction lines and entering the turbine which can cause damage to the turbine blades [41].

c) Determine the free volume of the vessel per increment

The free volume is defined as the volume in which the liquid/steam can flow. The free volume is represented in Figure 3.28 as the blue diagonal lines and dotted area. By adding these two areas, one can determine the free volume at each incremental level.

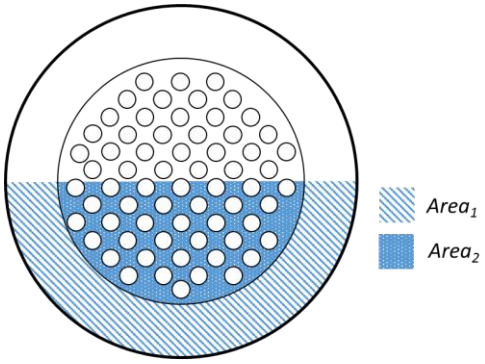

Figure 3.28: Free volume cross-sectional representation

$Area_1$ can be calculated as

$$Area_1 = Vol - Vol_{bundle} \tag{2.24}$$

where $Vol_{bundle,increment}$ is simply calculated by using equation (2.22), but instead of using the inside diameter of the shell, we use the outside tube limit diameter calculated in equation (2.20).

can be calculated as

$$Area_2 = Vol_{bundle} \cdot \left(1 - \frac{N_{tubes} \cdot d^2}{D_{otl}{}^2}\right) \tag{2.25}$$

where the second part of the equation refers to the percentage of area open for a specific number of tubes with a diameter d and in an area with diameter D_{otl}. The free volume per increment can thus be calculated by using equation (2.26).

$$Vol_{free} = Area_1 + Area_2 \tag{2.26}$$

d) Use the free volume to calculate the area of each frustum

The calculated free volume is now used as the volume for each consecutive frustum. The volume for a frustum is formulated in equation (2.27) where $Area_1$ and $Area_2$ now refers to the bottom and top area of the frustum as shown in Figure 3.29.

$$Vol_{frustum} = \frac{inc}{3}\left(Area_1 + Area_2 + \sqrt{Area_1 \cdot Area_2}\right) \tag{2.27}$$

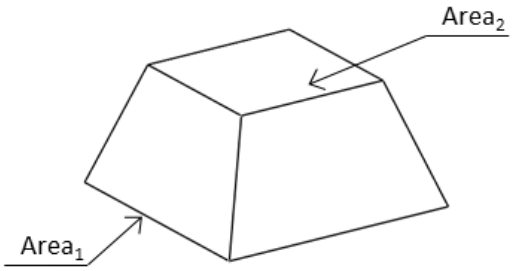

Figure 3.29: Frustum area allocation

The calculation process starts by initially guessing $Area_1$. Equation (2.27) is then rewritten and used to calculate $Area_2$, where the process repeats itself for each increment. It was however noted that the areas calculated created a variance in results for the areas shown in Figure 3.30 a). This variance was caused by the initial guess value.

By choosing a better initial area this variance can be minimized. The same problem occurred just after the DC zone's shroud, when the liquid volume increases suddenly. Again, an initial guess value was chosen at the point where the DC zone ended and the variance could be eliminated. The guess values were automatically guessed in the scripting environment in Flownex by roughly running through several guess values and choosing the one with the least amount of variance.

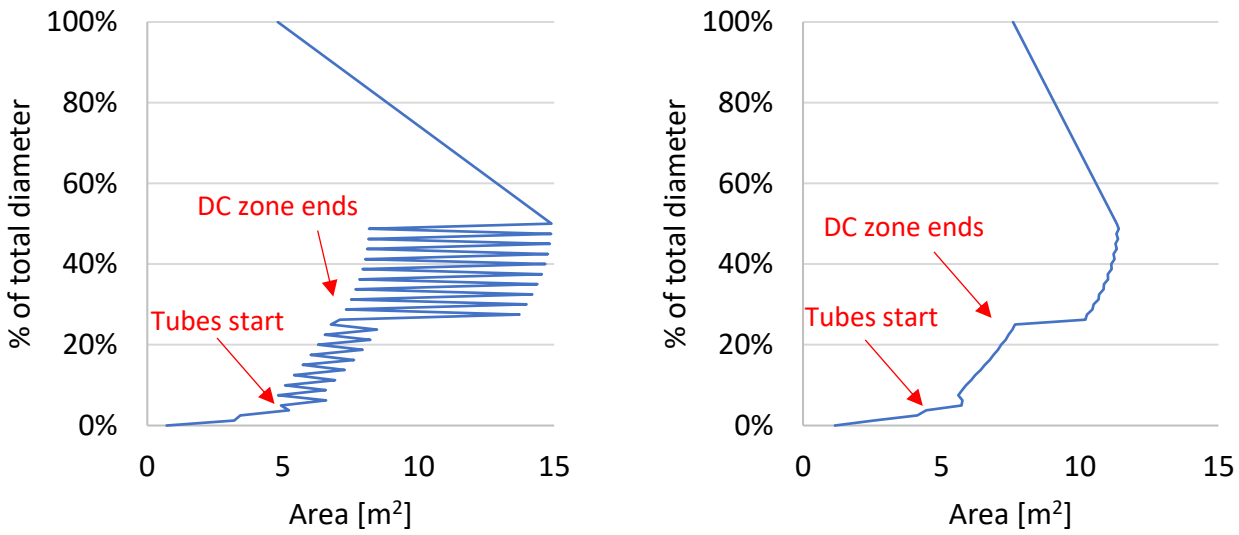

Figure 3.30: Cross-sectional area of each frustum for a build starting with an uncalibrated starting area (a), with a calibrated starting area (b).

It should be mentioned that by guessing two of the areas the results might have a small offset error but it will not influence the results significantly. Another method of smoothing the curve is by

choosing a larger amount of increments, but validation for the methodology, seen in Appendix A, proved to show that accurate results is obtained by using the optimized initial guess areas.

The **vertical heater**'s geometry has been modelled in similarly to that of the horizontal heater, in that a set of frustums was also used to build the geometry in Flownex. The difference comes in with the determination of the free volume per level increment since the level change in the heater, tubesheet or header type stays linear. This is because the liquid capacitance does not change at various levels for the vertical heater.

3.3.6 Level control

The need for an appropriate level control is essential for a feedwater heater in terms of its performance and longevity of its life cycle [37]. It was described in section 3.2.2 and 3.2.3 that the level change influences the heat transfer performance of the heater. Also, if the water level drops below the diving port of a horizontal heater, as seen in Figure 3.4, steam enters the DC zone and downstream pipes causing vibration and erosion.

The level inside the feedwater heater is usually controlled through a valve sitting at condensate return. Very seldom would one find a control valve positioned at the steam inlet since this valve then changes the pressure inside the shell, which has dramatic effects on the steam inside the shell since the saturation conditions then suddenly change. Having a control valve at the condensate return only influences the water level and thus better control can be achieved [42].

The water level is controlled by opening and closing this condensate return valve. The current Flownex model incorporates level control by allowing the level to be monitored. A control valve can thus be placed just after the model which can interact with the level.

The Flownex element that models the level is the two-phase tank. The level is coupled with the quality inside the vessel which is specified by the user beforehand. The two-phase tank is then coupled with a downstream element (which can be the control valve or a pipe opening or even a pump) where the opening of that element is adjusted to ensure a mass balance inside the tank. During steady-state conditions, this value is adjusted using an iterative "designer" feature, whilst during transient conditions this value is free to be adjusted via control valve inputs from a controller.

During **steady-state** conditions, the quality is required for the two-phase tank. The quality specified is then used by the Flownex element to calculate a corresponding level. The level calculation is done by determining the volume fraction of liquid to steam inside the tank [11]. Specifying the quality can however be a bit misleading in the sense that the quality is not a direct indication to the level. Additional calculations were therefore done to enable the user to input the level directly. The

calculations are done in a script component (Script A in Figure 3.22). The calculation method is shown below.

The initial step in calculating the quality from the level is by obtaining the level from the user. Once the level is obtained from the user the specific frustum where the level is situated can be determined. This is done by taking the height of the level and evaluating the height of each frustum, where the calculation process for the frustums are shown in section 3.3.5. The method is further illustrated in Figure 3.31 below.

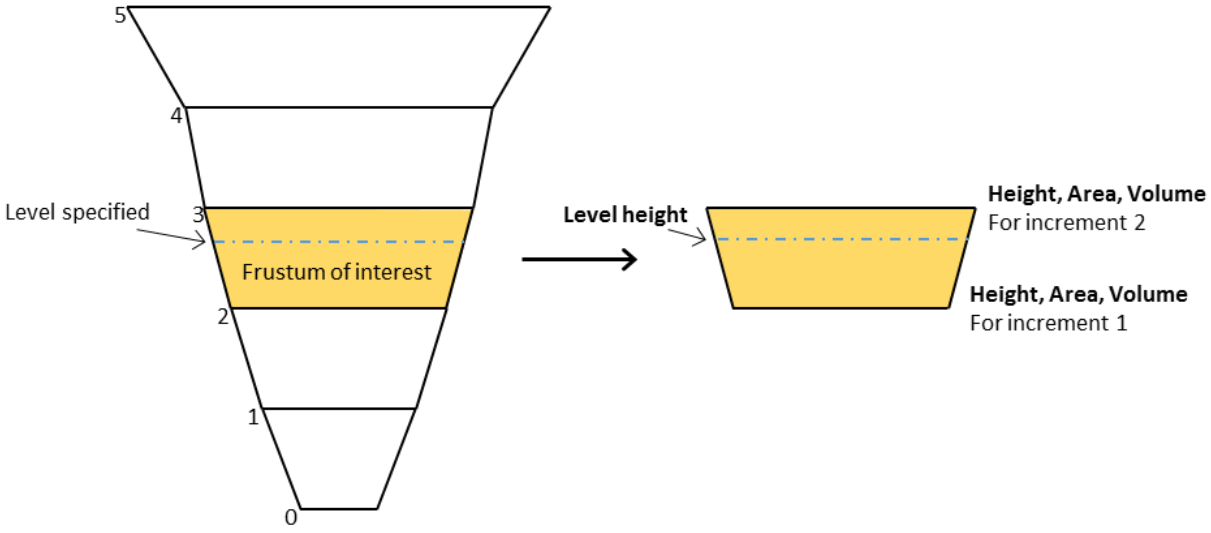

Figure 3.31: Diagram to show the calculation method for determining the quality from the level in the two-phase tank

Once the frustum where the fluid level lies has been identified the properties of that frustum can then be obtained; which includes the bottom and top height, area and volume from the bottom up. These properties are accordingly used to determine the properties of the partial frustum, the frustum which splits the original frustum into two due to the water level (as indicated in Figure 3.32).

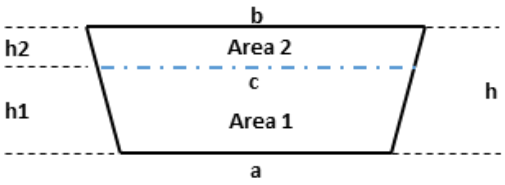

Figure 3.32: Specific frustum parameter allocation

The volume of the partial frustum is calculated as

$$V1 = \frac{h1}{3}(a^2 + c^2 + \sqrt{a^2 c^2}) \tag{2.28}$$

where c is the length of the area on which the level lies. To determine the value of c, one can use the following sets of equations

$$Area1 = \frac{a+c}{2} \cdot h1 \tag{2.29}$$

$$Area\,2 = \frac{c+b}{2} \cdot h2 \tag{2.30}$$

$$Area = \frac{a+b}{2} \cdot h \tag{2.31}$$

Therefore by rewriting the equations into one and rearranging we get

$$c = \frac{a \cdot h - a \cdot h2 + b \cdot h - b \cdot h1}{h1 + h2} \tag{2.32}$$

The variable *c* represents the cross sectional length or width of the partial frustum shown in Figure 3.32. By calculating c, the volume of the partially filled frustum can now be calculated. Since the volume up to the partial frustum is known, the volume under the level height can be calculated. The quality can consequently be calculated by using the mass of the liquid and the volume. The calculation process for the quality is shown below.

$$x = \frac{M_{gas}}{M_{gas} + M_{liquid}} \tag{2.33}$$

where

$$M_l = \frac{V}{v} \text{ and } M_g = \frac{V_{total} - V_{liquid}}{v_{gas}}$$

The calculated quality is then used in the two-phase tank element. The calculation method however requires the Flownex model to run twice in steady-state since the first run calculates the quality from the inputs and the second run the two-phase tank calculates the corresponding level from the calculates quality.

During **transient conditions**, the level is controlled by using the outlet valve or pump as in the case with low-pressure heaters. When a transient scenario is initialised the level stays constant since the mass flow in the network is in equilibrium and as soon as conditions start to change, such as the inlet steam pressure or the feedwater flow, the level will start to change. Control over the valve can then be initialized to the valve's opening or pump's speed to control the amount of mass flow through the element as to ensure a constant level. A typical scenario is illustrated in Figure 3.33 where the valve is represented by a flow resistance component and the PID component is used to control the opening of the element.

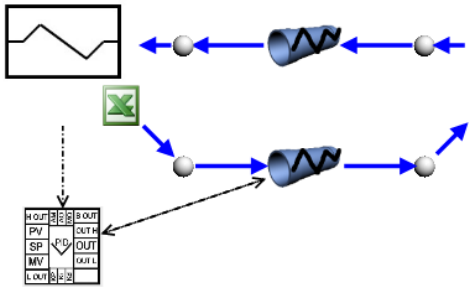

Figure 3.33: Flownex network illustrating transient control for the feedwater heater level

3.3.7 Influence of level on the performance

The water level influences the area allocated for heat transfer in both horizontal and vertical heaters. This reduction or increase in area has a direct effect on the heat transfer performance of the heater. Hossienalipour et al. [37] implemented the effect of the rising level on performance by taking the ratio of submerged tubes to the amount of unsubmerged tubes and implementing that to the overall HTC. The implementation method is as follows

$$U_m = \frac{U_{sub}A_{sub} + U_0 A_0}{A_{sub} + A_0} \tag{2.34}$$

where the subscripts *m* denotes the mean, *sub* denotes submerged *0* is not submerged. This method considers geometrical constraints but assumes a uniform distribution of tubes. A similar method is followed in the current Flownex model where the convective heat transfer area in the COND zone is multiplied by a ratio. This ratio is defined as the current water level over the total height of the vessel as shown in equation (2.35).

$$R_{Level} = \frac{L - L_{bb}}{h_{vessel} - 2 \times L_{bb}} \tag{2.35}$$

The ratio is implemented by multiplying the outside and inside convective area, assumed to be 1 m^2 in steady-state conditions, with the ratio. This ratio only changes during transient scenarios since the level specified by the user during steady-state conditions is assumed as the normal level. It also incorporates the bundle to shell clearance since the tubes only become submerged once the liquid level rises above the clearance. For a vertical heater the clearance is not incorporated for the influence of the level on the performance of the heater.

3.3.8 Tube plugging

Tube plugging is a procedure which is undertaken as tubes fail due to corrosion or erosion. As more and more tubes are plugged, less effective heat transfer area is available for the heater to function efficiently. Tube plugging is implemented into the current Flownex model like that of the level where a ratio is defined for the tubes plugged to the total amount of the tubes, given in equation

$$R_{tp} = \frac{N_{tp}}{N_{tubes}} \tag{2.36}$$

The ratio is then multiplied by the convective HTC inside and outside area. The ratio is applied during steady-state as well as transient scenarios for the heater. It should be mentioned that fewer tubes result in higher flow inside the remaining tubes, which increases the convective HTC. This is not considered in the model, but could be added by using a scaling law and Dittus-boelter eq.

3.3.9 Thermal inertia

One of the main objectives of the thesis is to provide a methodology for modelling transient effects for the power station components in the Flownex. To model these transient effects, one must first identify which factors will have transient behaviour. Also, refer to section 2.2.6 for a detailed description for the difference between steady-state and transient simulations.

Factors which will lead to transient effects for a feedwater heater are:

- Liquid water in the heater, i.e., in the tubes as well as in the shell.
- Thick walled components
- Condensate liquid level

The **liquid water in the tubes** and the shell is modelled in Flownex through the already defined conservation equations and appropriate definition of the pipes geometry. By taking the transient term, equation (1.12), into consideration Flownex models the transient effects of the water.

The **volume of the DC zone** is not included in the shell geometry as per calculation stipulated in section 3.3.5. To account for the volume, it is added to the DC zone's flow resistance component as a simple volume. It is calculated by using the current free geometry of the shell and the specified size of the DC zone by the user, shown in equation.

$$V_{DC} = V_{free} \cdot (DC_L \cdot DC_H) \tag{2.37}$$

The properties window for the DC zone's flow resistance is shown in Figure 3.34.

⊟ Discretization and Differencing Schemes		
Number of increments	1	
Discretization scheme	Central difference	
⊟ Volume and Inertia		
Volume	3.00411	m³
⊟ Operational Inputs		
Opening	1	
Heat Transfer		
Heat option	Fixed heat transfer	
Heat input	-0.548433	kW

Figure 3.34: DC zone's flow resistance element's property window indicating heat calculated and volume

The thick-walled components in the feedwater heater include the tube walls and the tubesheet. The **tube walls** are already included in the model through the COND zone's composite heat transfer element where the thickness in element direction is specified as the thickness of the tube wall. It is assumed that most of the tubes go through the COND zone [34], thus only these tubes will contribute to the model's thermal inertia.

The tube walls were discretized into four increments where the upstream conduction area is the outer tube area and the downstream area is the inside tube area. The thickness is taken as the tube wall thickness.

The **tubesheet** is modelled in Flownex by using a node connected to a pipe through a composite heat transfer element. Two separate configurations are built in the model as to accommodate the upstream and downstream tubesheet. The configuration is shown in the detailed Flownex model in Figure 3.15, and a simplified configuration of implementing thermal inertia into the Flownex is shown in Figure 3.35. Mesh independence for the composite heat transfer element was also done and is shown in Appendix C.

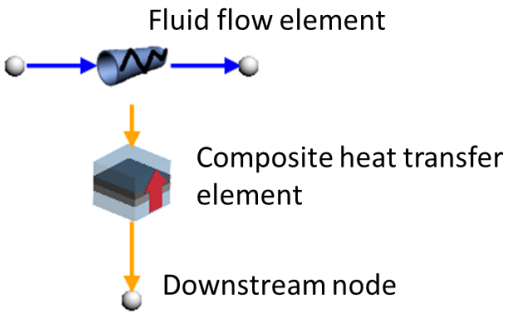

Figure 3.35: Thermal inertia in the Flownex

Modelling the tubesheet requires knowledge on how heat is transferred through the component. As the feedwater flows through the tubes heat is transferred as convection between the feedwater and tube inner wall. Conduction occurs between the tube wall and the tubesheet. Between the tubes, conduction also occurs around the tube wall with a radius of about half the tube pitch into

the tubesheet. At the outer bundle tubes, conduction occurs between the tube walls and the outer surface of the tubesheet. A simplified drawing is shown in Figure 3.36 of the tubesheet and the direction and point of the conduction heat transfer.

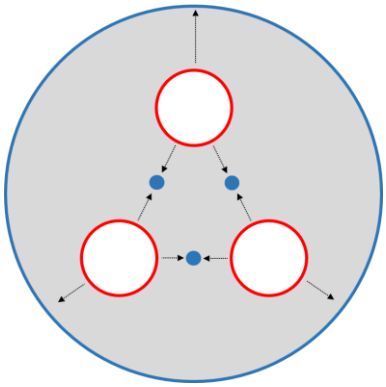

Figure 3.36: Simplified drawing of tubesheet heat transfer

To model the heat transfer in Flownex further simplification is required. The composite heat transfer element uses a flat plate as a model base, thus one is required to specify the up- and downstream areas and the thickness in element direction. Refer to Figure 3.21 for such a specific flat plate problem. The upstream area is calculated by taking the inside area of the tubes in contact with the tubesheet given as

$$A_{ts,upstream} = \pi \times d \times L_{ts} \times N_{tubes} \tag{2.38}$$

The total downstream area was calculated by taking the entire solid frontal area of the tubesheet, which is the frontal area minus the area occupied by the tubes, into account. This area is then divided by the number of tubes and a new radius is calculated. A new circle is essentially formed around each tube where the circle presents the downstream area's diameter as illustrated in Figure 3.37.

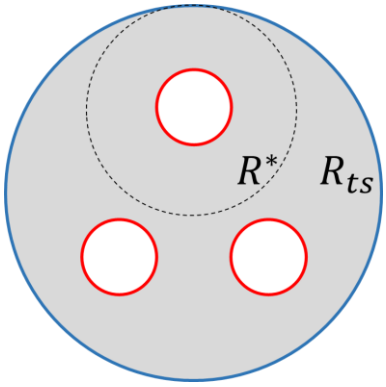

Figure 3.37: Downstream area's circle for the tubesheet calculations

The following calculation process was made to determine the new diameter. R_{ts} represents the tubesheet radius and R^* the new downstream area's radius. The tubesheet's area, which is the grey area in Figure 3.37, is calculated as

$$A_{ts} = \frac{\pi \cdot R_{ts}^{\ 2}}{2} - N_{tubes} \cdot \pi \cdot \left(\frac{d}{2}\right)^2 \tag{2.39}$$

The total area of the tubesheet is divided by two since only half of the tubesheet is accounted for in each case. The total area of the tubesheet can also be written in terms of R^* as

$$A_{ts} = N_{tubes} \cdot \left[\pi \cdot (R^*)^2 - \pi \cdot \left(\frac{d}{2}\right)^2\right] \tag{2.40}$$

Both equations can be set equal and the downstream area's radius simplifies to

$$R^* = \sqrt{\frac{R_{ts}}{2 \cdot N_{tubes}}} \tag{2.41}$$

Finally, the tubesheet downstream area can be calculated as

$$A_{ts,downstream} = 2 \cdot \pi \cdot R^* \cdot L_{ts} \tag{2.42}$$

and thickness in element direction is calculated by simply subtracting downstream area's radius from the tube's inside radius.

The inlet and outlet tubesheet was implemented in the Flownex network of the heater. The implementation consisted of a basic pipe, composite heat transfer element and a node. The inlet tubesheet was added to the inlet of the tube-side of the heater and the outlet to the outlet of the tube-side of the heater, as shown in Figure 3.15. The inside convection heat transfer is modelled by using the Dittus-Boelter correlation. The tubesheet networks and parameters are shown in Figure 3.38.

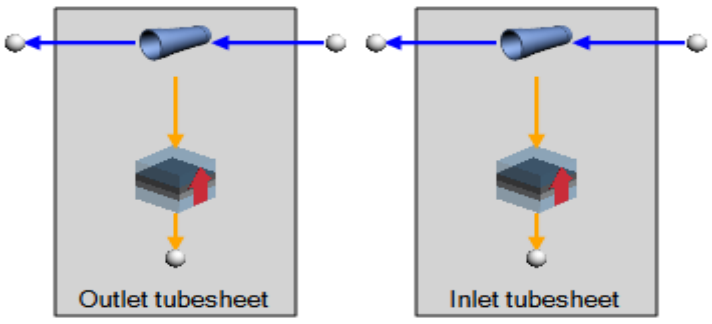

Figure 3.38: Inlet and outlet tubesheet networks with parameter settings

During steady-state operation, the downstream nodes are the same temperature as the upstream pipes. Once a transient scenario is run where the upstream pipes change temperature the downstream nodes will slowly catch up to the temperature of the pipes depending on the size and thickness of the tubesheet specified.

3.4 Verification and Validation of the model

3.4.1 Performance verification and validation

Performance verification and validation for the models were done by using heat balance data and acceptance test data. The data was taken from Kriel powerstation. Heat balance data was initially used to verify the correctness of the models and thereafter the acceptance test data to the validate the accuracy of the models.

Two heaters were modelled in the study, namely an HP heater and a LP heater. Both heaters were chosen where condensate from a heater upstream cascaded into the heater. This is to ensure that all the performance characteristics of the heater models are tested. The two networks are shown Figure 3.39.

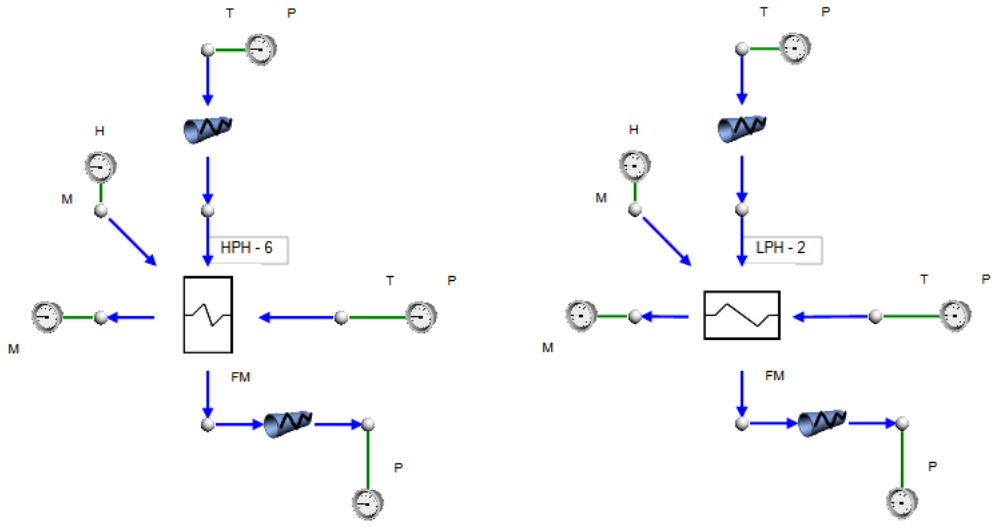

Figure 3.39: HP and LP heater Flownex network

The networks were set up by using heat balance data as design input data. Boundary conditions were used at the inlet and outlet bled-steam and feedwater flow lines. A boundary condition was also used at the cascade inlet of both heaters. These boundary conditions then represented the conditions of the plant data and the models were run for four different load cases.

Verification of the models was done by using heat balance data as boundary conditions. The verification process is to test the accuracy of the models and to ensure that all the methods implemented are correct in the models. Results for the outlet temperatures are shown in Figure 3.40 and the outlet mass flow of the condensate is shown in Figure 3.41.

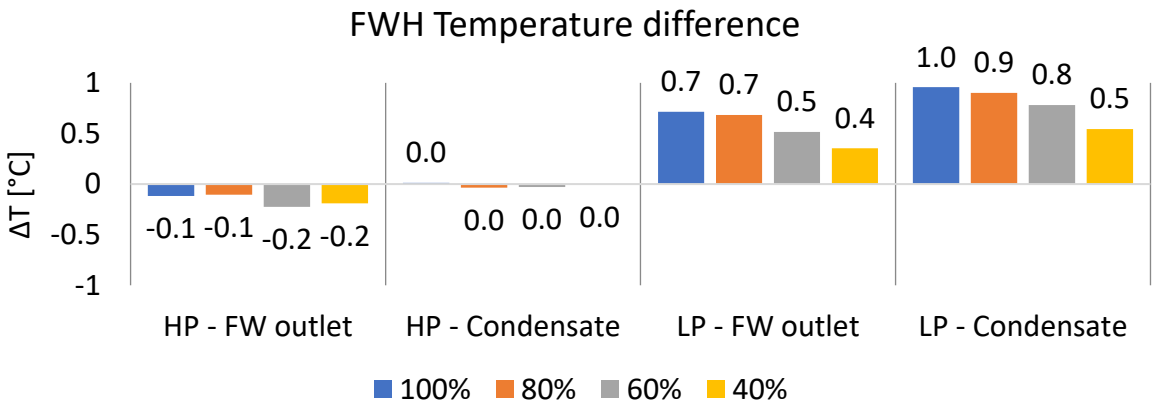

Figure 3.40: HP and LP heater verification for feedwater outlet and condensate temperatures

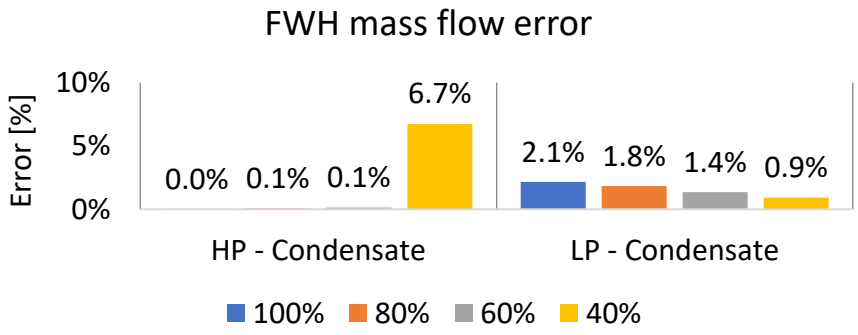

Figure 3.41: HP and LP heater verification for condensate mass flows

The temperature differences are within 1 °C, and the Condensate flow rates are also well below 5%. The only mass flow error that is above average is the 40% load case for the HP heater. The higher error at the low load is however due to very low flow rates which are encountered at this load, resulting in inaccuracy of the flow measurement.

Validation for both models in Figure 3.39 was done using plant acceptance test data for the boundary conditions. The inputs for both the HP and low-pressure heater were that of the heat balance. The same network was set up as with the verification process for the heat balance data.

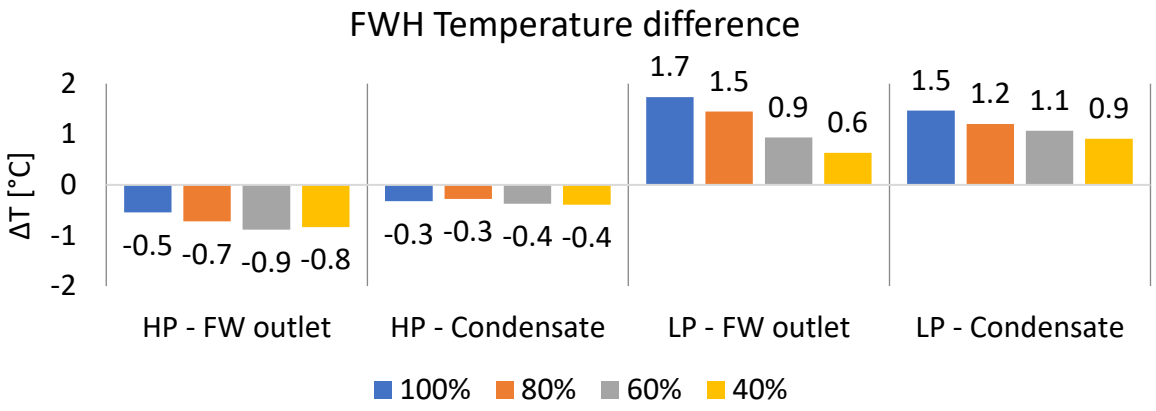

Figure 3.42: HP and LP heater validation for feedwater outlet and condensate temperatures

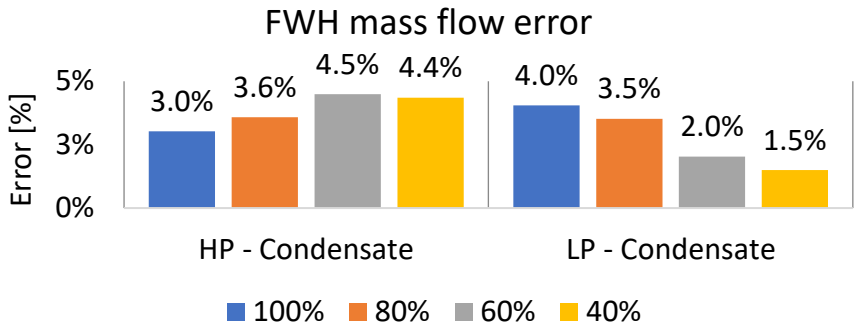

Figure 3.43: HP and LP heater validation for bled steam outlet flow

The temperature and mass flow results for the HP heater are well within the tolerances as specified in 2.4.4. The mass flows for the low-pressure heater also falls within the tolerances, but it is likely that the mass flows were calculated in the acceptance test data and not measured. The low-pressure feedwater outlet temperatures are slightly off by 1 °C, but still correlates well when considering that heat balance data was used as input to the models.

3.4.2 Geometrical level validation

The geometry of the heater was validated by comparing the level change of the heater to that of a 3D CAD model of an actual heater. The validation was specifically done for the horizontal heater since the vertical heater's level change is linear. The purpose of the validation was to indicate if the approach of modelling the volume as a set of frustums stacked on each other is valid.

The 3D CAD model was set up by extracting the free volume of the shell, representing the shell side volume in which water can flow. By doing this one can measure the volume of the liquid inside the shell. The Flownex model is set up by using the table specification. The volume of liquid in the shell can then be obtained from the results in Flownex.

Both models were set up using the same geometrical parameters. Five cases were then run where a parameter was changed in each case as to ensure that the Flownex model captures all geometrical aspects of the heater. The parameters of each case are listed in Table 3.6.

Table 3.6: Geometrical validation parameters for horizontal feedwater heater

Geometrical Parameters	Case 1	Case 2	Case 3	Case 4	Case 5
Shell					
Diameter [m]:	2	2	2	2	1.6
Bundle to shell clearance [m]:	0.25	0.25	0.25	0.25	0.025
Tubes					
Length [m]:	10	10	10	10	8
Diameter [m]:	0.03	0.03	0.03	0.03	0.05
Pitch [m]:	0.06	0.06	0.03	0.06	0.1
Drain cooling zone					
Height [0-1]:	0	1	0.5	0.5	0.5
Length [0-1]:	0	0.25	0.5	0.25	0.3

The 3D CAD model of case number 3 is shown in Figure 3.44 as illustration. One can see that the inside of the volume is represented as a solid and the tubes and DC zone as empty.

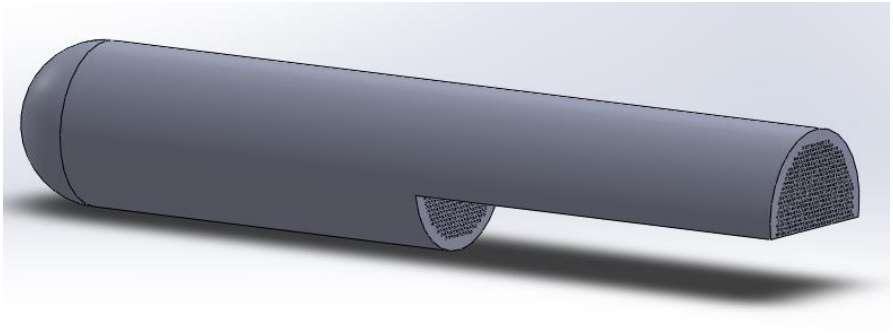

Figure 3.44: 3D CAD model of a horizontal feedwater heater with a short drain cooler

The measurements of both models were taken by changing the level incrementally within the heater. This was done in the CAD model by cutting the part from the model which lies above the incremental level and then measuring the volume of the solid that is left. The error between the Flownex model and the 3D CAD model were then compared.

It is important to mention that the volume of each increment was taken as the volume over the entire volume of the shell. This normalized the volume as to present the data from a total volume perspective. The total volume perspective is important because a large error at the starting increments of the shell will not have a significant impact on the heaters performance due to the little amount of liquid in those starting increments. Results for Case 5 is shown in Figure 3.45; the other case results are shown in Appendix D.

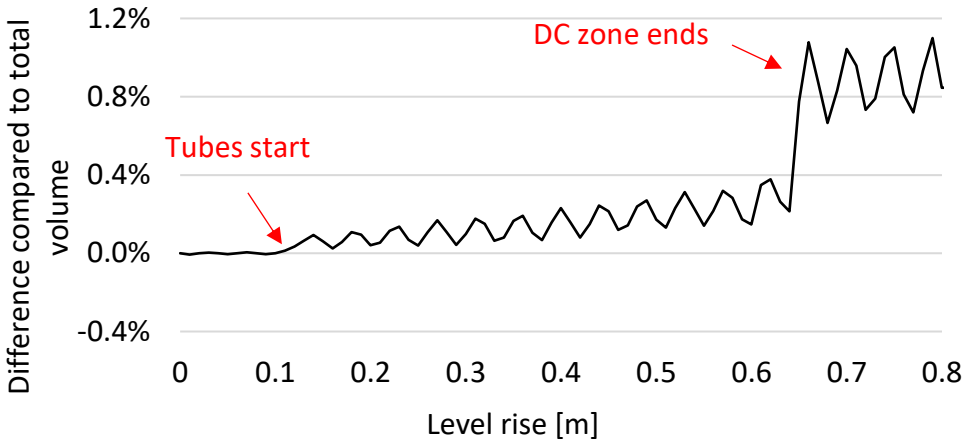

Figure 3.45: Volume comparison between horizontal Flownex feedwater heater model and 3D CAD model

From initial inspection, one can see that the error between the Flownex model and the 3D CAD model is below 1.5 %. This already shows that the methodology of presenting the model in Flownex as frustums stacked upon each other will result in a fairly accurate representation of the actual geometry of a feedwater heater.

One can further see that the error fluctuates at the point where the tubes start. This is because the tubes represented in the Flownex model is worked out as a percentage of volume and thus presents a continues decline or increase whereas the 3D CAD model contains discreet tubes which will cause the increase or decrease in volume to vary.

The final observation is that the error is suddenly stepped up where the DC zone stops. It was mentioned in the methodology section where the calculation of the frustum volume that the area just after the DC zone ends is guessed as to ensure that the rest of the area transitions continues. The step up in error is therefore attributed to the guessed value.

3.4.3 Transient characteristics – Convective HTC ratio

The inside and outside HTC ratio (R_h) refers to the ratio between the inside and outside tube wall's convective HTC. This ratio was first specified in the calculation of the overall HTC in equation (2.13) . The ratio is calculated via a script component using the Dittus-Boelter relationship for inside convective HTC and the Nusselt integral approach for the outside HTC.

There are however uncertainties associated with these correlations as noted by Nazier [4]. But the effect of the ratio is only experienced during transient scenarios since the steady-state calculation process essentially ensures that the amount of heat transfer stays constant regardless of the ratio.

A case study was done to understand the sensitivity and importance of the model due to the ratio under various transient conditions. These varying conditions involved changing the *Biot number*, which is a dimensionless parameter used to determine the temperature drop inside a solid relative to the temperature drop experienced by the solid's surface and the fluid [43]. An alternative way of describing the *Biot number* is that it gives an indication to what the heat transfer rate limiting process is, referring between conduction or convection. The *Biot number* is defined as

$$Bi = \frac{hL_c}{k} \tag{2.43}$$

where h refers to the convective HTC, L_c the characteristic length and k the thermal conductivity.

Looking again at the formulation for the *Biot number*, the following two assumptions can be made:

- A large *Biot number* will indicate that conduction heat transfer will be the limiting process since the conduction heat transfer rate through the material will be slow.
- A small *Biot number* will indicate the convection heat transfer will be the limiting process since the convection heat transfer rate on the surface of the material will be slow.

Following these points, a Flownex model has been set up with the feedwater heater to test the effect of the HTC ratio on the transient results of the model due to varying the *Biot number*. The Flownex model is the conduction zone of the feedwater heater model. The model is shown in Figure 3.46.

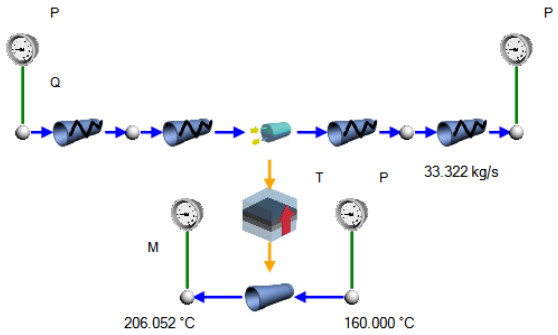

Figure 3.46: Feedwater heater condensing model to test transient results due to varying R_h values

The model was run by changing the inlet feedwater temperature from 180 °C to 160 °C. The time it took for the outlet temperature of the feedwater to drop by 3 °C was then recorded. The choice of range for the Bi number and ratio was based on a calculated Bi number and ratio of a heater in service. The results are shown in Figure 3.47.

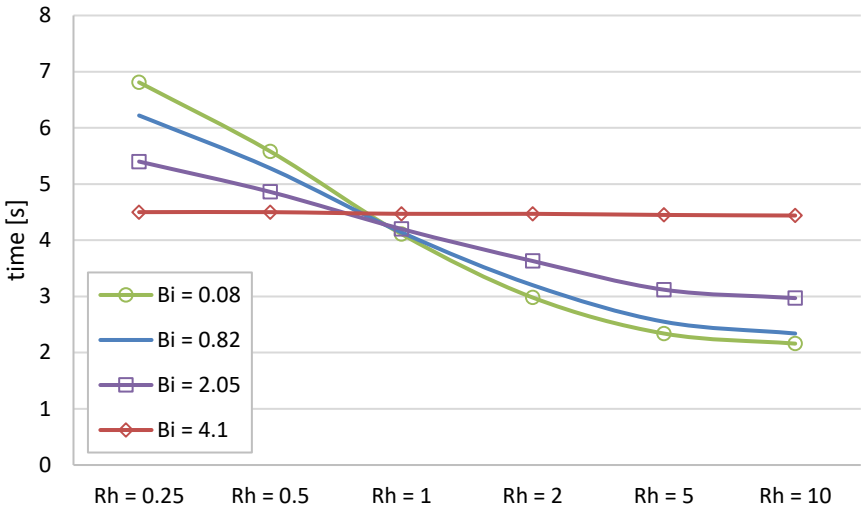

Figure 3.47: Effect of HTC ratio on heater transient performance due to different Biot numbers

The first noteworthy observation that can be made from the Figure 3.47 is that at a very high Biot number the effects of the ratio on the transient effects of the heater is negligible. In contrast, when the Biot number is small the effects of changing the ratio is much larger. Also, with a heat transfer ratio of 1 the Biot number does not influence that transient results of the heater.

These results correspond with the definition of the Biot number in that at high Biot numbers conduction will be the rate limiting process and at low Biot numbers convection will be the rate limiting process.

The practical implication of this is that the ratio of the outside and inside HTC will impact the heater depending on the thickness of the tubes and flow conditions. This means that the heater in the high-pressure train might experience more of an influence from the ratio than a heater in the low-pressure train.

To further illustrate the practical implication of the ratio, the ratio was calculated for different heaters on a power station. The Biot number is also calculated to show the conditions of the heater. The calculated results are shown in Figure 3.48.

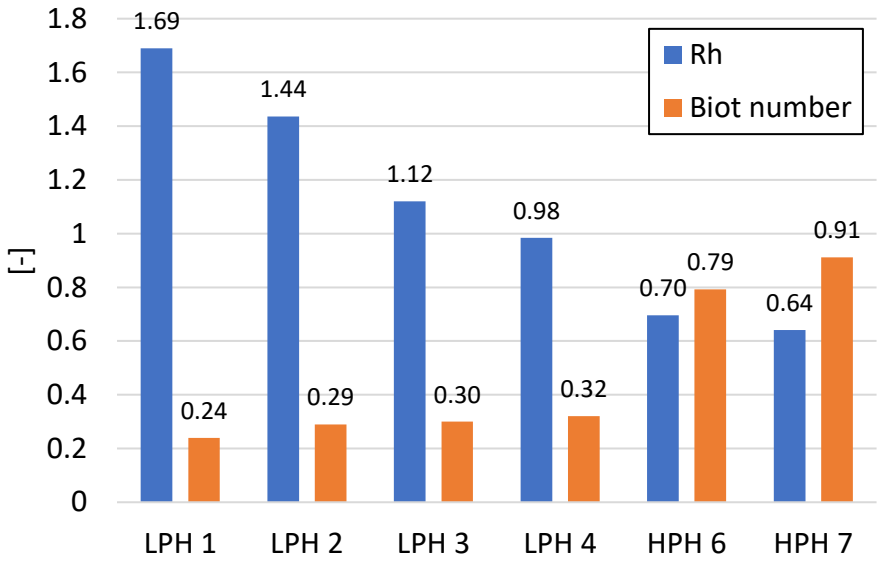

Figure 3.48: Heat transfer ratio and biot number for different heaters in a powerstation at full load

The following points, based from Figure 3.47, should be considered for interpreting the Figure 3.48.

- The HTC ratio will not influence the transient results as much for a high Biot number (Bi >= 1) than a smaller Biot number (Bi < = 0.5).
- The transient effects for a R_h of 1 will be the same for all Biot numbers.
- The Biot number gives an indication to the heat rate limiting process.

From Figure 3.48 one can initially see that the HTC ratio does vary for different heaters as well as the Biot number. Low-pressure heater 1 shows a low Biot number and a HTC ratio above 1, thus the transient results will be effected by the ratio. HP heater 7 shows a Biot number closer to 1, thus the HTC ratio calculated will not influence the transient results as for heater 1.

3.4.4 Conclusion on verification and validation

Verification and validation of the feedwater heater model could be done on the heater's performance, geometrical representation and transient capabilities. It could specifically be shown that using heat balance design data, the heater showed very good results when the temperature measurements was compared to that of acceptance test data.

A case study was done on the effect of the convective HTC ratio for the condensing zone. The study revealed the sensitivity of the ratio to the model's short transient behaviour. The study could also show that LP heaters will be less sensitive to the convective HTC compared to HP heaters.

3.5 Final FWH components in Flownex

The final feedwater heater component model has been packaged in Flownex as an easy-to used high fidelity model. The model is accessible from the Flownex components library. The model works by simply dragging and dropping the component into a drawing page. The user is then required to specify the design inputs for the model in the Excel spreadsheet and steady-state behaviour options. The component will run if correctly specified, displaying results in either the component's property window or inside the compound component. The chapter will further elaborate on the final feedwater heater component.

3.5.1 Component "family"

A compound component was created for three different configurations of heater models. These configurations are for a heater with

- no geometrical specifications,
- vertical geometrical specifications and
- horizontal geometrical specifications.

The three configurations shown in Figure 3.49, where the nodal descriptions are given for the vertical heater.

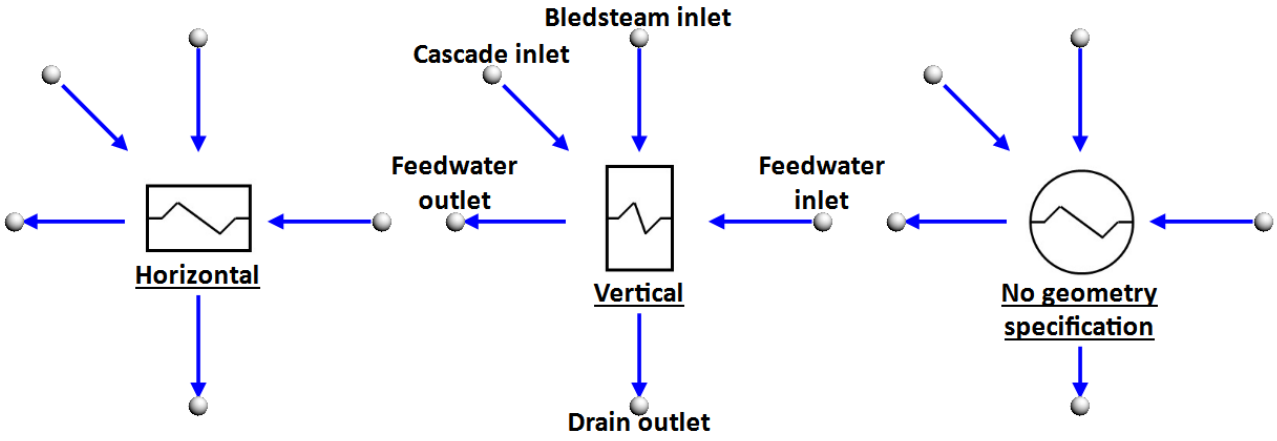

Figure 3.49: Three configurations for the final feedwater heater model component

3.5.2 User inputs

The user inputs are specified by using the Excel table for design inputs and the property window inputs for operational inputs. Both performance and operational inputs will be described in the heater without geometrical specifications, and geometrical specifications will be described in the horizontal and vertical heater sections.

Heater without geometrical specifications

These inputs are essentially the design performance inputs for each heater. The inputs for the heater are shown in Figure 3.50.

Feedwater heater (Unspecified)

The feedwater heater component utilizes bled steam from the steam turbines to heat up the feedwater in the cycle.

DESIGN INPUTS:

Load Condition	P_BS_inlet [kPa]	P_FW_outlet [kPa]	H_BS_inlet [kJ/kg]	H_BS_outlet [kJ/kg]	H_FW_outlet [kJ/kg]	m_BS [kg/s]	m_FW [kg/s]	m_Cas [kg/s]	h_Cas_in [kJ/kg]
1	418.6	1334	2956.9	611.7	601.3	17.78	342.365	0	0
2	417.9	1333	2954.4	611.5	601.3	17.73	341.092	0	0
3	334.3	1132	2959.2	577.4	572.9	13.299	269.256	0	0
4	252.5	934	2974.4	536.7	535.7	9.201	201.425	0	0
5	199.2	813	2970.4	504.1	505.4	6.901	160.179	0	0
6	0	0	0	0	0	0	0	0	0

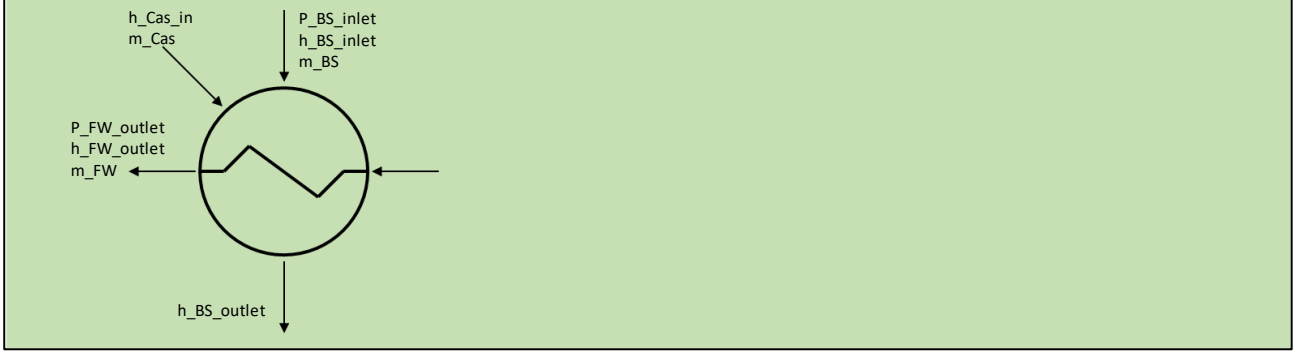

Figure 3.50: Excel input table for heater with no geometrical specifications

The user is required to input a minimum of three load conditions and up to six load conditions. These conditions can be obtained from any type of data, but it is advised to use heat balance data due to its availability and credibility. Furthermore, if the heater does not contain any cascade then the inputs for the cascade must be set to zero as in the case of Figure 3.50.

The operational inputs for the heater is specified by using the compound components property window. The inputs that can be initially specified is the steady-state control options for the two-phase tank. The steady-state solving solves the scripts and excel tables are used in the initial design phase of the heater. The steady-state solving should be 0 when a transient scenario is run. The inputs further contain an elevation property which specifies an elevation for all nodes and tanks inside the component collectively.

The heater with no geometrical specification does contain a volume and level but is specified as an arbitrary size, ie., 10 m^2. Lastly, inputs for the tube losses can be specified which include the tube roughness, tubes plugged and fouling resistance. These inputs are shown in Figure 3.51.

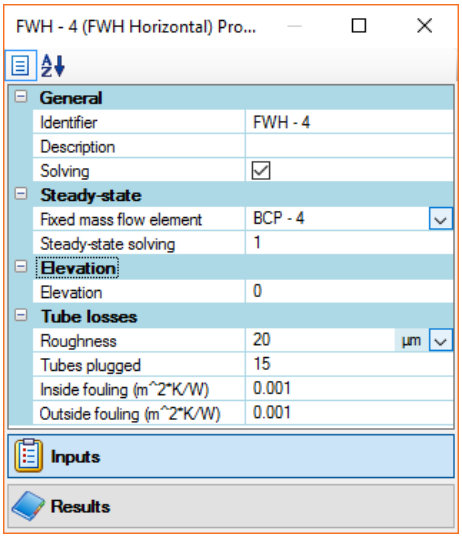

Figure 3.51: Feedwater heater component inputs via the property window

Horizontal heater

The horizontal heater contains inputs specific to that of a horizontal heater. These inputs are shown in Figure 3.52. The description drawings of the heaters are shown in the subsequent figures, Figure 3.53 and Figure 3.54.

SHELL GEOMETRY:				
Type:	0 [0;1]	Header: 0; Tubesheet: 1		
Tube passes (N_passes):	2 [-]	2 passes if tubesheet is selected		
Tube length (L_ti):	10 [m]			
Inner shell diameter (D_s):	2 [m]			
Design level	0.5 [m]			
TUBE GEOMETRY:				
Outer tube diameter (d):	0.03 [m]			
Tube wall thickness (L_t):	0.0025 [m]			
Tubes per bundle (N_tubes):	354 [-]	0 if unkown		
DC ZONE:				
Length (DC_L):	0.5 [0-1]	DC zone configurations:	Full submersion:	Length: 0; Height: 0
Height (DC_H):	0.5 [0-1]		Partial bundle:	Length: 0-0.5, Height: 0-0.5
			Full length:	Length: 1, Height: 0-0.5
ADDITIONAL INPUT PARAMETERS:				
Bundle to shell clearance (L_bb):	0.25 [m]	Formula, if not specified:	L_bb = 12.0 + 0.005*D_s (mm)	
Tubesheet thickness (L_ts):	0.2 [m]	Formula, if not specified:	L_ts = 0.1*D_s (mm)	
Pitch Layout (P_L):	0 [0,1]	0 = Square, 1 = Triangular		
Tube pitch (P_T):	0.05 [m]			

Figure 3.52: Geometrical Excel inputs for the horizontal feedwater heater component

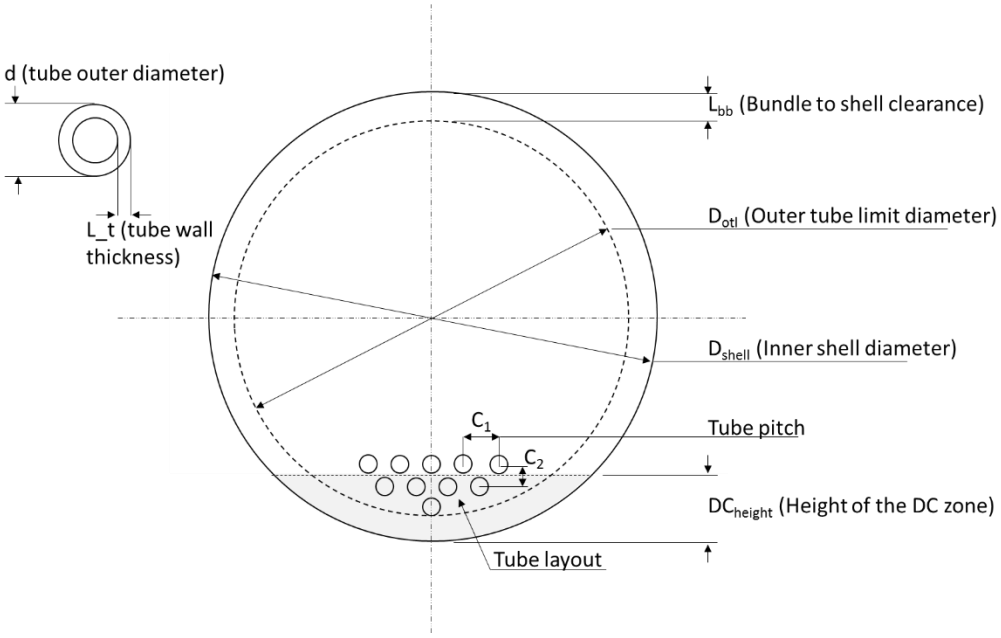

Figure 3.53: Diagram of a cross sectional area of a horizontal FWH

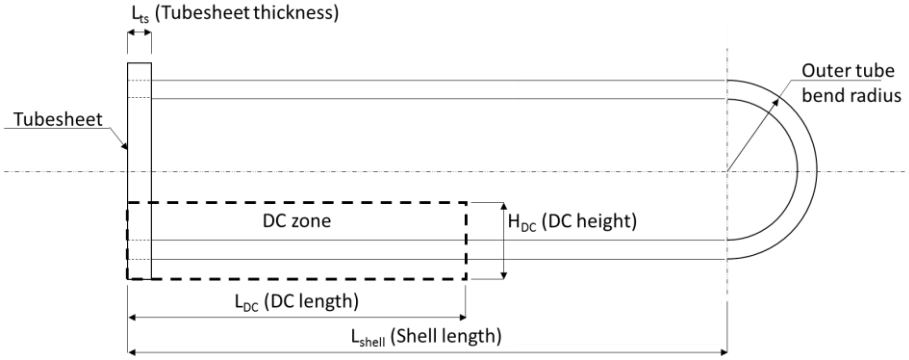

Figure 3.54: Diagram of the side view of a tubesheet type horizontal FWH

The shell geometry inputs define the shell shape and its attributes. The user is first able to define the type of shell, i.e., header or tubesheet. It is noteworthy that if a tubesheet is selected then the number of tube passes must be set to 2. The tube length is defined as the length from the tubesheet to the outer tube bend. The design level is assigned to the heater as the normal level. Any change from this level will result in an increase or decrease in heat transfer for the COND zone.

The tube geometry defines the tubes inside the shell. The tubes are defined first by the outer tube diameter. The tube wall thickness is then given where the inner tube diameter is automatically calculated. The number of tubes must also be specified.

The DC zone must thereafter be specified. The zone is specified by a percentage of height, which is defined as 0 being no DC zone to 1 where the DC zone extends to half way up the heater.

Final additional inputs can be given by the user which is to further define the heater's geometry. The bundle to shell clearance can be defined or if unknown the calculation can be made by taking shell diameter into account. The formula for the bundle to shell clearance is given as

$$L_{bb} = 12.0 + 0.005 \cdot D_s \tag{2.44}$$

where D_s refers to the inner shell diameter given in units millimetre [26]. The tubesheet can also be calculated by again taking the inner shell diameter into account in millimetres as

$$L_{ts} = 0.1 \cdot D_s \tag{2.45}$$

The final two parameters that can be specified is the tube layout and the tube pitch which is illustrated in Figure 3.53. The property window for the horizontal heater is the same as for the heater with no geometrical specification, shown in Figure 3.51.

Vertical heater

The vertical heater is similarly specified as in the case with the horizontal heater but with minor differences. The Excel input sheet for the vertical heater is shown in Figure 3.55.

SHELL GEOMETRY:			
Type:	0 [0;1]	Header: 0; Tubesheet: 1	
Tube passes (N_passes):	2 [-]	2 passes if tubesheet is selected	
Tube length (L_ti):	10 [m]		
Inner shell diameter (D_s):	2 [m]		
Design level	0.5 [m]		
TUBE GEOMETRY:			
Outer tube diameter (d):	0.03 [m]		
Tube wall thickness (L_t):	0.0025 [m]		
Tubes per bundle (N_tubes):	354 [-]	0 if unknown	
ADDITIONAL INPUT PARAMETERS:			
Bundle to shell clearance (L_bb):	0.25 [m]	Formula, if not specified:	L_bb = 12.0 + 0.005*D_s (mm)
Tubesheet thickness (L_ts):	0.2 [m]	Formula, if not specified:	L_ts = 0.1*D_s (mm)
Tube layout (P_L)	1 [0,1]	0 = Square, 1 = Triangular	
Tube Pitch (P_T)	0.05 [m]		

Figure 3.55: Geometrical Excel inputs for the vertical feedwater heater component

The user is initially required to input the type of heater. This activates or deactivates the thermal inertia due to the tubesheet in the heater. The amount of tube passes can then be specified, two tube passes if the heater is of tubesheet type.

All the other inputs are specified as in the horizontal heater's specifications. One can note that the vertical heater does not contain a specification for the DC zone since the level inside the heater acts as the DC zone.

3.5.3 User results

The heater component displays results in two ways: component results in the property window and detailed results in the component network itself. Critical results for the component is shown in Figure 3.56. The component results indicate the heat transfer of each zone, mass flows of the various inlets and outlets, pressure drop over the tube side, performance parameters and the level for the vessel. The ability for the component to display the level enables one to accurately control the component through a control loop.

Detailed results can be obtained by double-clicking on the compound component. This will open the component's internal network where each Flownex element can be inspected.

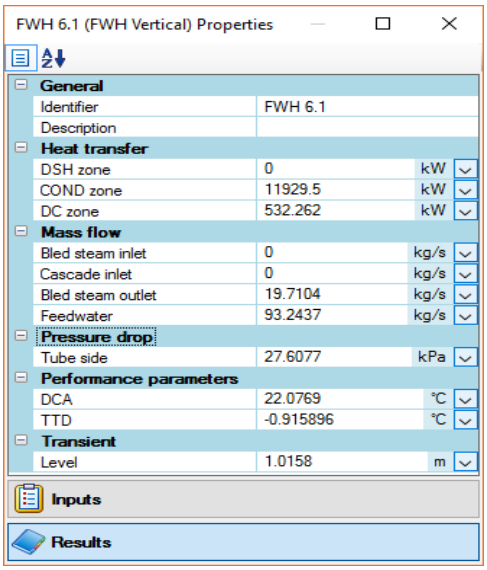

Figure 3.56: Feedwater heater component results

The component results are the same for all heater components.

3.5.4 Limitations

The feedwater component model have been modelled with the following limitations:

- No pressure drop occurs over the shell side of the heater
- Baffles are not included in the geometrical calculations
- The header type heater only includes straight tube passes, whereas an actual header type heater contains a more complex tube pass arrangement as seen in Figure 3.2 a).
- Tube plugging does account for increased flow velocities in the tubes but the heat transfer is not directly influenced due to the increase in velocity. Instead, the heat transfer is affected by changing the total area of heat transfer.
- The vertical heater does not contain a shrouded DC zone

4. Turbine component modelling

Axial turbines are used to convert the energy stored into the steam into rotational work. This chapter will primarily focus on modelling the turbine component in the Flownex. It will begin by giving a brief overview of the theory behind the turbine and then a literature study on previous dynamic models. It will then be explained how the current turbine model was modelled in the Flownex and validation and verification done on the model. Finally, the component family will be described of the turbine component.

4.1 Theory and characteristics of steam turbines

In chapter 2.1.4 an introduction was given to the axial steam turbine. It was described that the conversation of the energy in the steam to shaft work occurs primarily in two phases, i.e., the conversion of potential energy to kinetic energy through the fixed blades and then the conversion of kinetic energy into shaft work through the rotating blades.

The development of steam turbines has come a long way, with some of the first prototypes built in 120 BC by a Greek inventor Hero of Alexandria [6]. Since then, various configurations have been developed where the two most prominent steam turbine types are the

- Impulse and
- Reaction turbines.

The impulse turbine works where the steam in the fixed blades is expanded completely or to the point of the following stage. The steam then enters the rotating blades where the cross-sectional area remains constant thus the pressure remains constant. The absolute velocity however drops as the steam does work to rotate the blades and turn the shaft.

The reaction turbine works in an equivalent manner as the impulse turbine, where the difference comes in with the rotating blades. As the steam enters the fixed blades, it expands and the absolute velocity of the steam increases. The cross-sectional area of the rotary blades are not constant and therefore the expansion process continues in the rotary blades. An example was given by Neerputh [2] which explained the reaction force that occurs to the rotary blades of the turbine. Neerputh explained that the reaction force felt by the blades is the same way as one would experience by holding a hose-pipe in the air with high-pressure water coming out at the end. Both types of turbine stages are shown in Figure 4.1.

Further calculations can be done through the knowledge of the turbine geometry through velocity and blade triangles. These calculations include the amount of work, velocity and efficiency per stage.

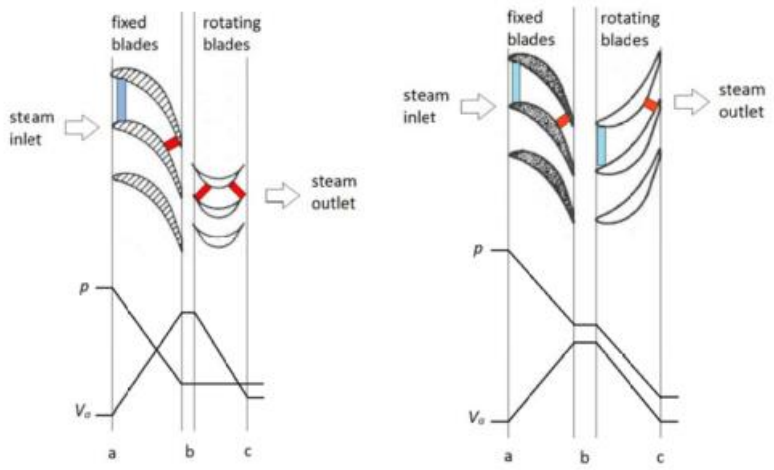

(a) (b)

Figure 4.1: a) Diagram of an impulse turbine stage, b) diagram of a reaction turbine stage [2]

The rest of the chapter will focus on the steam and what forces affect the steam as it is sent through the turbine.

4.1.1 Steam path

The turbine component is situated between the boiler and the condenser. As the superheated steam exits the boiler, it is expanded through the turbines as dry steam and exits the turbine at an expanded yet dry state (in the ideal case). Thereafter the steam is sent to the condenser to cool the steam back into a subcooled state to be pumped through the system. The steam path for the turbine is illustrated in Figure 4.2.

As the steam enters the turbine, it's pressure energy is converted into velocity as it flows through the stationary blades. It is the stationary blades which act as the nozzle for the steam. The velocity is then converted into rotational work as the steam hits the rotational blades. The path of the steam also increases in cross-sectional area over the length of the turbine due to the steam increasing in specific volume as the pressure drops after each stage.

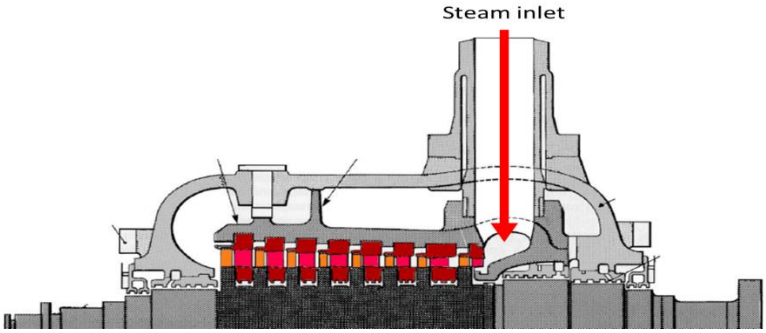

Figure 4.2: Steam path through a high-pressure turbine [41]

It is noteworthy that as the steam flows through the turbine, it gets in contact with the shaft, blades, inner, and outer casing. This implies that temperature differences between the casing and the steam should be considered, especially at start-up conditions where the difference in temperature is significant [44]. This effect will contribute to the transient inertia of the component and will be included in the final turbine component model.

4.1.2 Flow energy in the steam

The flow energy of the steam in the is attributed to the high pressure and temperature of the steam. One can relate it to steam being exhausted from a container at high pressure. If the pressure inside the vessel is increased the velocity of the steam will also increase, if choking does not occur in the outlet nozzle.

The stationary blades provide the mechanism for increasing the velocity of the steam inside the turbine. The task is then to design the rotating blades to capture the energy of the high velocity steam. Choking can occur in the stationary blades but also in the rotating blades for a reaction turbine since the reaction turbine's rotating blades are also a form of a nozzle [45].

The amount of energy from the steam can be calculated by using velocity diagrams. These velocity diagrams depend on the type of turbine, blade angles, blade speed and the steam flow velocity. The total energy can be calculated quite accurately if the velocity triangles is correctly defined. Typical velocity triangles for a turbine stage is shown in Figure 4.3.

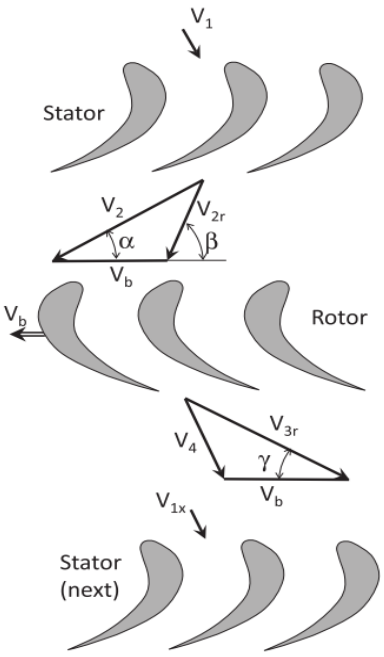

Figure 4.3: Velocity triangles for a typical turbine stage [45]

4.2 Turbine models in literature

The turbine component is in itself a very complex piece of machinery and can become even more complex when modelling the component. Two general methods can be applied when modelling a turbine, empirically based of through detailed CFD analysis [45]. Since detailed CFD analysis requires the knowledge of exact geometrical attributes of the turbine, it is considered out of the scope for the project.

4.2.1 Pressure drop models

Empirically based methods are generally derived from analysis of velocity triangles. These methods are applied to calculate the pressure drop through the turbine as well as the efficiency of the turbine. The advantage of using empirically base methods is that the methods require very little input data to model the turbine. The accuracy is however affected but due to recent developments, these methods have become significantly more accurate [46], [45].

A recent study was done by Neerputh [2], in which the author investigated the applicability as well as accuracy of some of the most popular methods for predicting the pressure drop and efficiency of the turbine. The pressure drop correlations investigated were Stodola's ellipse law, Schegliaiev's model, the general empirical law and the constant flow co-efficient.

Each of the methods were applied to a Flownex model and it was found by the author that the general empirical law and Stodola's law in the volume form produced the best results in terms of mass flow and pressure drop. An interesting find by Fuls [46] in a study to enhance the original Ellipse showed the that the Ellipse law, which Neerputh [2] found as being one of the most accurate, is very comparative to the pressure drop law used to model pipe flow. The equation however ignores compressibility effects and thus is not able to model choking conditions, which may occur at off-design conditions.

Alternative to correlations, one can model the turbine stage by using nozzle theory. It was discussed in 4.1.1 that the steam flows through a nozzle at the stationary blades of the turbine. Thereafter the work is extracted via the rotary blades. In the case of a reaction turbine, the rotary blades act as a nozzle as well. One can therefore use nozzle analogy to model the pressure drop through the stationary blades and use velocity triangles to calculate the work through the rotary blades.

Research was done by Fuls [45] for the stage-by-stage modelling of steam turbines by using nozzle theory. A Flownex model was set up by using a restrictor with loss coefficient to model a nozzle. The component further contains two coefficients, a "loss" and "contraction" coefficient which was set appropriately to comply with the nozzle theory set by the author. The model was compared to the

results of a test case done by the Advisory Group of Aerospace Research and Development (AGARD). The group tested a well calibrated gas turbine where exact measurements between stages could be made. Fuls further validated the model with an IP and LP steam turbine of a 600MW subcritical power station. For both cases, the Flownex model agreed well with both test cases and off-design conditions also showed very good agreement. Fuls concluded that the model can be used as a validation case for empirical models, especially when specific plant data for specific scenarios are not available.

We come now to the most recent developments for empirical correlations which is the method present by Fuls [46] on the enhancement of Stodola's ellipse law for determining the pressure drop of a turbine segment. This law is an enhancement over the original ellipse law correlated by Stodola in 1900 [47] by extending the equation by Cooke and Traupel. The law can operate by using design conditions without the knowledge of exact geometrical details regarding the turbine, which can often be very difficult to obtain.

Stodola's ellipse law was originally obtained by observing the pressure ratio of the inlet and outlet conditions with changing mass flow of a turbine. The shape of the curve was seen to be elliptical and the equation in the volume form is given as

$$\dot{m}_{EL} = \dot{m}_D \frac{p_i}{p_{i,D}} \sqrt{\frac{T_{i,D}}{T_i}} \cdot \frac{\sqrt{1-\left(\frac{p_e}{p_i}\right)^2}}{\sqrt{1-\left(\frac{p_{e,D}}{p_{i,D}}\right)^2}} \tag{3.1}$$

where D denotes the design conditions. This law is widely used in turbine models and has been verified to produce reasonable results under normal operating conditions. These operating conditions include:

- Turbines with a large amount of stages.
- Turbines with a relatively small pressure drop between stages.

Fuls however stated that whenever these normal conditions are not met, the ellipse law becomes inaccurate. Fuls illustrated this by plotting the law with a nozzle with a high pressure drop, as shown in Figure 4.4. It can additionally be seen from the figure that when there is choking, which does occur in turbines operating at abnormal conditions, the ellipse law does not incorporate it.

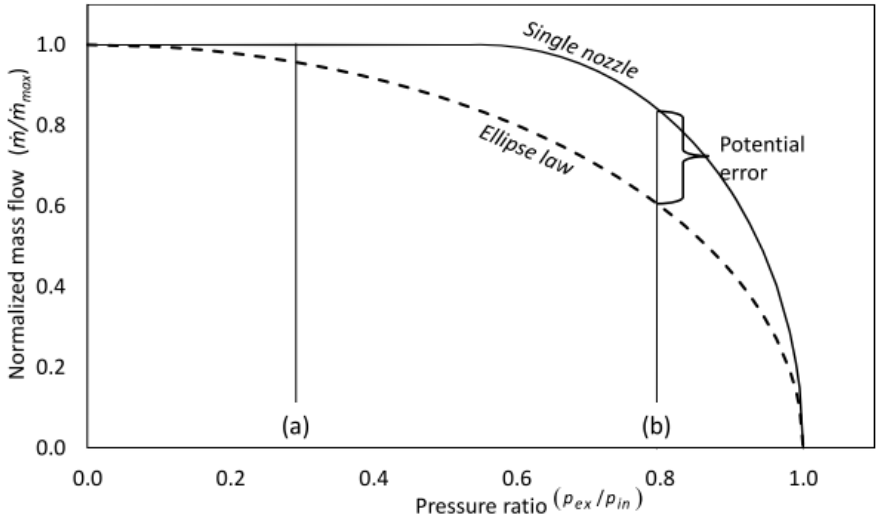

Figure 4.4: Error between Ellipse law and single nozzle for a turbine with a high pressure drop [46]

Fuls then derived a semi-ellipse law, which substitutes the exponent of the Ellipse law with an empirical number α and incorporated the pressure ratio r with the critical pressure ratio r^*. The semi-ellipse law in the volume form is presented as

$$m_{SE} = m_D \sqrt{\frac{p_{0,i} \cdot v_{i,D}}{v_i \cdot p_{0,i,D}}} \cdot \frac{\sqrt{1-\left(\frac{r-r^*}{1-r^*}\right)^{\alpha}}}{\sqrt{1-\left(\frac{r_D-r^*}{1-r^*}\right)^{\alpha}}} \tag{3.2}$$

Fuls further provided methods in which the critical pressure ratio exponent α and the critical pressure ratio $r*$ can be determined by using design data and some knowledge about the turbines geometrical layout. The validation results for the semi-ellipse law is shown in Figure 4.5, where the exit pressure of the last stage of an IP turbine. The ellipse law and the semi-ellipse law was compared to the results of a nozzle model. The new semi-ellipse law developed by Fuls delivers more credible results than that of the original ellipse law, especially under off-design conditions.

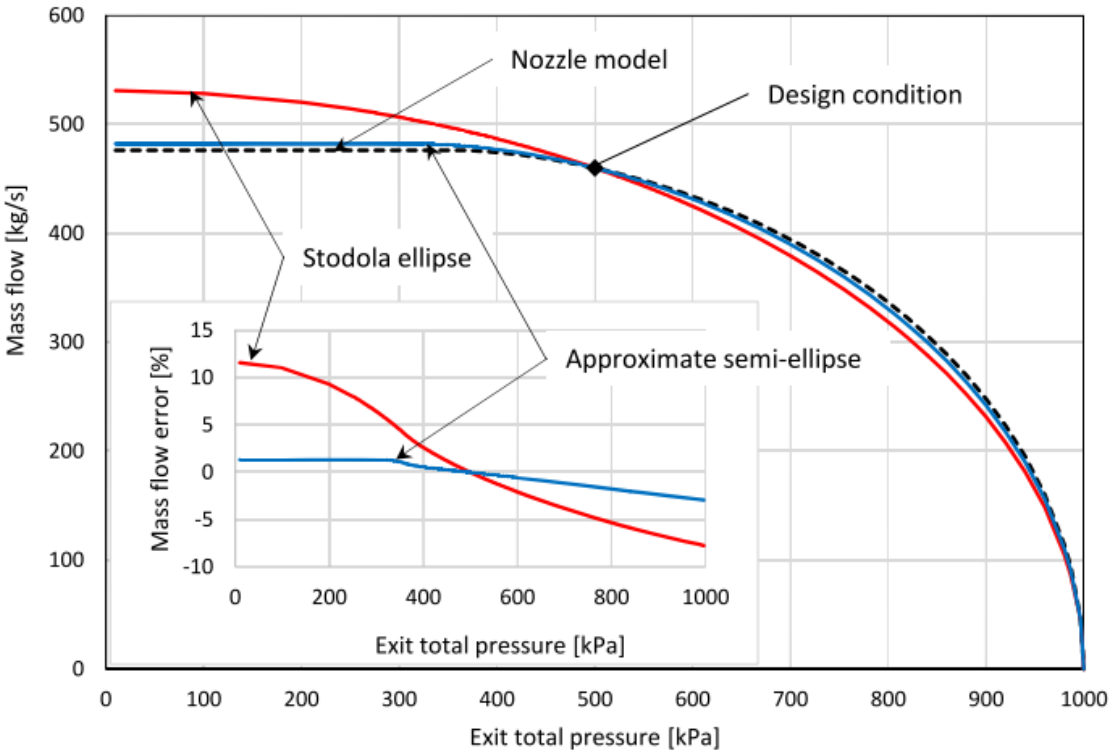

Figure 4.5: Validation results for the newly developed semi-ellipse law compared to a nozzle model and Stodola's ellipse law [46]

4.2.2 Efficiency models

The axial steam turbine's efficiency is defined as the total work with the turbine over the ideal work of the turbine. The actual work performed by the turbine considers losses which occur. These losses are defined as either interior or exterior losses.

Examples of interior losses are losses due to friction between the steam and the blades and or casing, viscous forces of the fluid flowing over the profile of the blade thus increasing its entropy, moving blade losses which occurs due to the rotation of the blades where the steam entering the stage is not at an optimum angle, etc. Examples of exterior losses are mechanical losses due to turbine bearings, shaft sealing losses where steam escapes from the outer shaft glands, heat losses due to conductivity and radiation from the casing, etc.

Neerputh [2] did a comprehensive study on various efficiency models for the implementation into Flownex. The following models were investigated.

- Spencer, Cotton and Cannon
- Method employed in the PEPSE code
- Ray method
- Darie method

The author tested all 4 methods analytically and compared the results with acceptance test data from three power stations. The tests were run for three load cases from each power station. The results showed an overall good correlation between the applied efficiency models and acceptance test data. The Ray method showed the overall least error and this method was therefore implemented in the current Flownex model. The results for the four methods are shown in Figure 4.6.

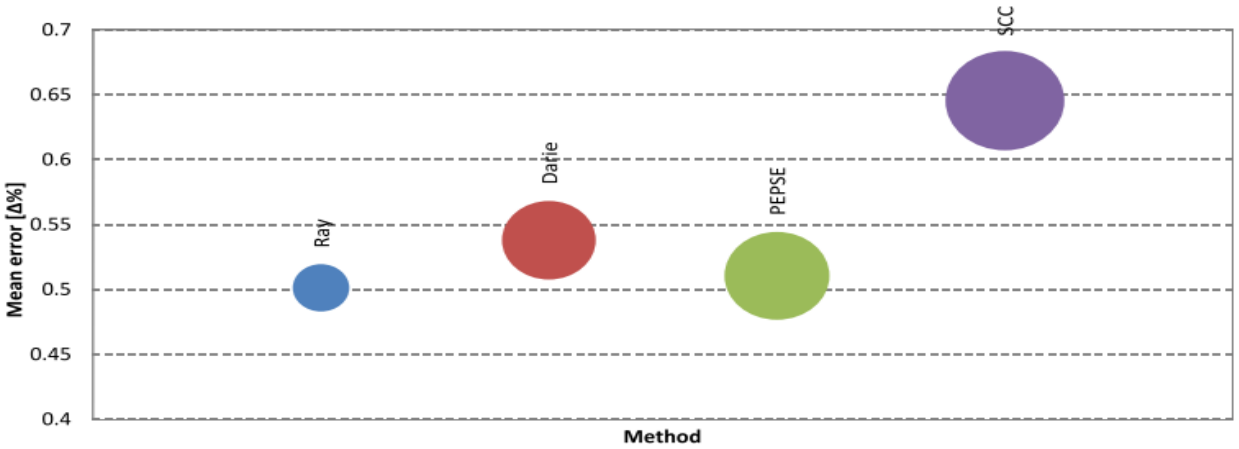

Figure 4.6: Standard deviation and the mean error for the four efficiency methods [2]

Ray's method is a semi-empirical one to predict the off-design efficiency which is described by taking the ratio of the blade tip speed (turbine shaft speed N) and the theoretical steam velocity (isentropic enthalpy drop Δh_s). The method by Ray [48] is presented in equation (3.3).

$$\eta = \eta_D - \beta \left(\frac{N / \sqrt{\Delta h_s}}{N_D / \sqrt{\Delta h_{sD}}} - 1 \right)^2 \tag{3.3}$$

The coefficient β is defined as 1 for an impulse turbine and 2 for a reaction type turbine. The equation can now be used in the Flownex model given the inputs for the isentropic enthalpy drop, shaft rotating speed and design efficiency.

4.2.3 Conclusion

A literature study was done on two methods for modelling the turbine's pressure drop and efficiency, which is the semi-ellipse law by Fuls [46] and Ray's method [48]. Both methods stem from a study done by Neerputh [2] in which various pressure drop and efficiency correlations were looked at and tested. The study concluded that the two methods were the most accurate, whilst using very little design input data. These two methods will thus be used in the current model.

4.3 Turbine component model

The axial steam turbine is modelled in Flownex by using the simple turbine component. This component models the steam flowing through a turbine without the use of a chart. The pressure flow is modelled by using the semi-ellipse law described by Fuls and the power by Ray's semi-empirical method. The final attributes of the model are listed

Table 4.1: Final turbine component attributes

Attribute	Attribute application
Pressure drop:	Semi-ellipse law
Efficiency:	Ray's semi-empirical method
Thermal inertia:	Shaft and casing
Rotational inertia:	Shaft
Application:	High, intermediate and low-pressure turbines
Extraction:	Multiple extractions

The final Flownex component is shown in Figure 4.7 and the network flow diagram is shown in Figure 4.8.

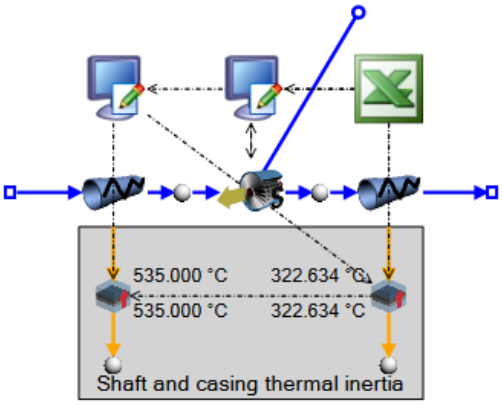

Figure 4.7: Detailed turbine model in the Flownex

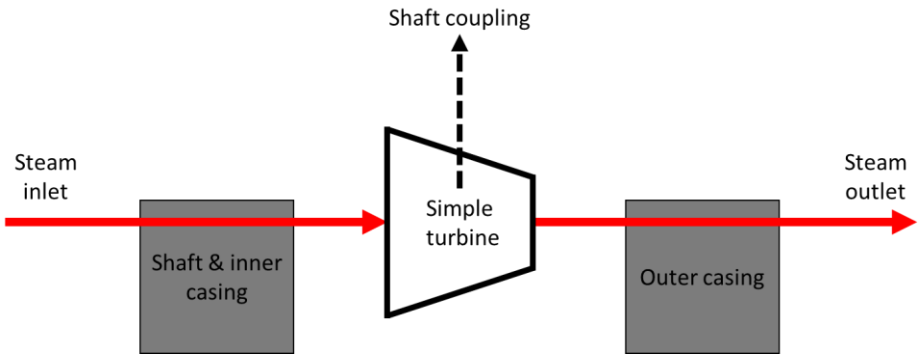

Figure 4.8: Network flow diagram of the turbine model

4.3.1 Pressure drop modelling

The pressure drop over the turbine is modelled by implementing the semi-empirical method as described by Fuls in section 4.2.1. It was shown that the method produces more favourable results than the original Stodola's ellipse law. The method also uses minimum design and geometrical input data and works well under off-design conditions.

Implementing the law into Flownex is not as trivial as simply choosing the law from the already defined simple turbine component's property library since the law is not included in the list. The law was therefore implemented by using the script component where a three step methodology process was followed.

a) Mass flow determination according to the semi-ellipse law

The initial step in implementing the semi-ellipse law is to determine the mass flow going through the turbine segment according to the law. The semi-ellipse law is given in the volume from in equation (3.2).

The law requires design inputs which is specified by the user through the Excel input table. These inputs are classified per segment. The law also requires operational parameters which are all obtained from inside the simple turbine component in the Flownex model. Table 4.2 gives a summary of the inputs used per turbine segment.

Table 4.2: Design and operational inputs for the Flownex turbine component model

Design inputs	Operational inputs
Mass flow [kg/s]	Upstream pressure [kPa]
Upstream pressure [kPa]	Upstream enthalpy [kJ/kg]
Upstream enthalpy [kJ/kg]	Downstream pressure [kPa]
Downstream pressure [kPa]	Pressure drop [kPa]
Alpha exponent	Fluid density [kg/m^3]
Critical pressure ratio	Speed [rpm]
Design efficiency	
Beta - efficiency	
Speed [rpm]	

b) Calculation of the loss coefficient through the calculated mass flow

The next step in the implementation process is to set the simple turbine to calculate the same mass flow as determined for the semi-ellipse law given the same boundary conditions. The simple turbine contains four empirically based laws which can be used to determine the pressure drop over the

element [11]. The empirical loss coefficient loss option has been chosen due to simplicity in equation from. The law is given as

$$\Delta p_0 = C_k \rho^{\beta} \dot{Q}^{\alpha} \tag{3.4}$$

where Δp_0 is the total pressure drop [Pa], C_k is the loss coefficient, ρ is the mean density [kg/m^3] and Q is the volume flow rate [m^3/s]. The coefficient β and α is given as 1 and 2 respectively according to Flownex [11]. The equation can be rewritten in terms of the mass flow and the given coefficients as

$$\Delta p_0 = C_k \rho \left(\frac{\dot{m}}{\rho} \right)^2 \tag{3.5}$$

or

$$C_k = \frac{\Delta p_0 \cdot \rho}{\dot{m}^2} \tag{3.6}$$

The loss coefficient can therefore be calculated by using the inputs from the simple turbine and the mass flow calculated from the semi-ellipse law. These calculations are done iteratively until convergence is reached. The model is further able to model choking by fixing the mass flow once the critical pressure ratio is reached.

c) Implementation of the loss coefficient into the simple turbine

The last step is to implement the calculated loss coefficient in the simple turbine. This is done by transferring the coefficient via a data transfer link to the turbine. This value is transferred after each iteration as to ensure convergence as stated in the previous paragraph. The property input window for the simple turbine is shown in Figure 4.9.

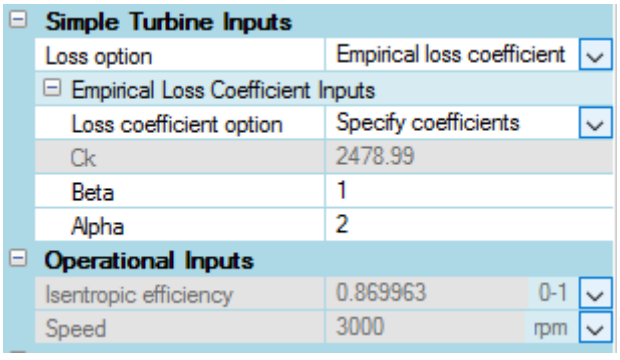

Figure 4.9: Simple turbine inputs window

4.3.2 Efficiency modelling

The efficiency implementation of the turbine is simply done by calculating the efficiency using Ray's semi-empirical model given in equation (3.3). The design inputs are obtained from the Excel input table, which include the design speed, design efficiency and design isentropic enthalpy drop (calculated via script using the input enthalpy and outlet isentropic enthalpy shown in equation (3.7)). The operational inputs are obtained from the simple turbine itself, which include the turbine speed and isentropic enthalpy drop (again using equation (3.7)).

$$\Delta h_s = h_1 - h_2 \text{, where } h_2 = f(p_2, s_1) \tag{3.7}$$

The efficiency calculated is then sent to the simple turbine as an input via a data transfer link. The calculation process also occurs iteratively as equation (3.3) requires iterative inputs from the Flownex as discussed in the above paragraph.

4.3.3 Shaft coupling and speed

As noted in literature, the turbine component compromises of stationary blades and rotary blades where the rotary blades are connected to a rotating shaft. The rotation shaft can be quite thick in diameter (between 0.3 and 0.7m in diameter) as to withstand the forces involved. Due to the sheer size of the shaft, rotational inertia plays a key role in the dynamic behaviour of the turbine.

The shaft was therefore modelled in the Flownex by using what is known as a shaft component. The shaft component is a component which models the effects of rotational inertia by being connected to a component with a specific speed, as in this case the simple turbine. The connection is made by a shaft coupling link. The typical setup of the connection is shown in Figure 4.10.

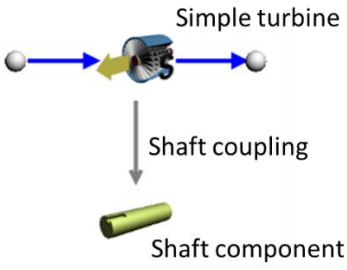

Figure 4.10: Turbine and shaft coupling

The only user input which is required is the rotational inertia of the shaft which is given as kg.m^2. This is calculated by using geometry specification of the shaft. In the current Flownex turbine component the rotation inertia is calculated by using the shaft's mass, radius. The equation for rotational inertia of a shaft is given in equation (3.8).

$$I = m \cdot R^2 \tag{3.8}$$

The methodology for implementing the shaft in the turbine's compound component is by using a shaft coupling and what is known as a port exposer. The port exposer exposes the coupling to the compound component so that a shaft can be connected to the network inside the compound component. The port exposer is shown in Figure 4.7 as the blue circle at the top centre of the figure. The rotational inertia is also calculated by a script in the compound component and the user can connect the inertia with a data transfer link to the shaft outside the turbine compound component. A typical network setup is shown in Figure 4.11.

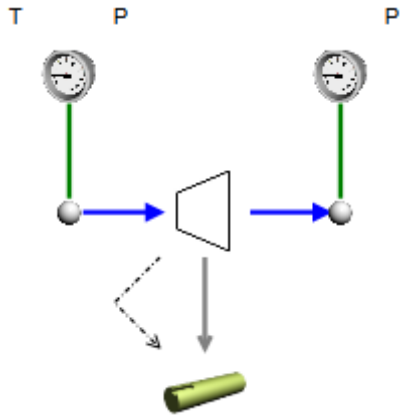

Figure 4.11: Turbine compound component shaft coupling

4.3.4 Thermal inertia

It was mentioned in the steam flow section of the turbine (section 4.1.1) that as the steam flows through the turbine, it gets in contact with the shaft, blades, inner -, and outer casing. Due to the contact, some thermal inertia will be experienced by the steam if large temperature differences are present between the components and the steam. This has therefore been included in the model.

Owing to the complex geometry of the turbine, simplifications have been made to model the dynamic effect of the transient inertia. The following simplifications are made:

- Only the shaft and inner casing will be modelled since these components will have the largest effect on thermal inertia.
- The components have been modelled by only using mass and contact surface area.
- Contact surface area is greatly simplified.
- Radiation heat transfer is neglected.

Flownex makes use of a CCC heat transfer component called a composite heat transfer element to model most heat transfer problems. Modelling thermal inertia of a specific mass is done by connecting a node to a pipe through a composite heat transfer element. During steady-state

operation both the pipe and the node will be at the same temperature. During transient operation, the two elements' temperature will differ depending on the conditions of the fluid flowing in the tube and the difference over time is determined by the geometry and heat transfer effectivity specified by the composite heat transfer element. The thermal inertia setup is shown in Figure 3.35.

The shaft is modelled by taking the outer surface of the shaft as the cross-sectional area upstream. The inner area is taken up to the centreline of the shaft, which ends up being infinitely small. The length of heat transfer is specified by the radius of the shaft. If one were to display the geometry generated by the composite heat transfer coefficient, it would come out to be wedge as shown in Figure 4.12.

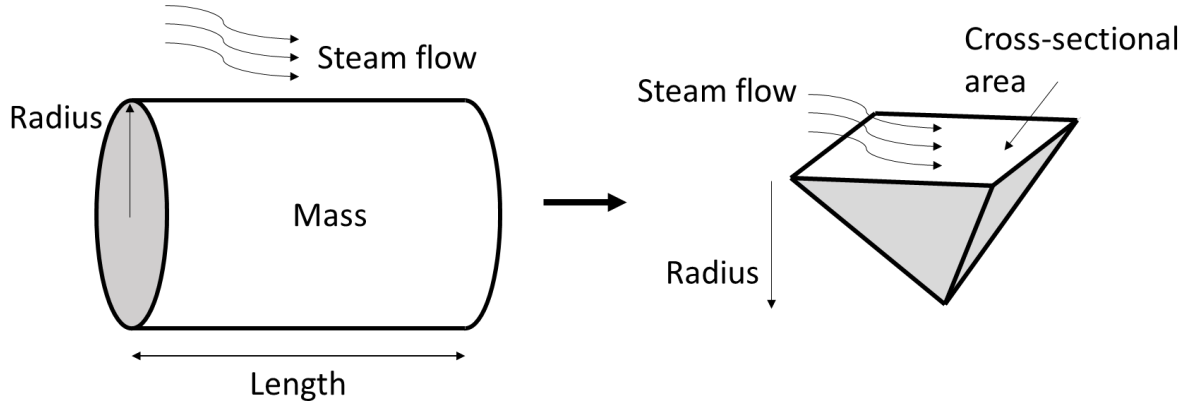

Figure 4.12: Shaft geometry in the Flownex

Design specification for the shaft was already made by the radius and mass through the calculation of thermal inertia. The model used these design inputs to calculate the shaft's outer surface area by using the shaft's density which is relatively constant, assuming that the shaft is a solid shaft. Equation (3.9) is used to calculate the outer surface of the shaft.

$$A_{st} = \frac{2 \cdot m_{st}}{\rho_{st} \cdot r_{st}} \tag{3.9}$$

where the subscript s refers to the shaft's properties.

The outer casing is modelled in the Flownex as a flat plate. The effective inside and outside area is assumed to be the same and the area is calculated from the average radius of the inner casing defined by the design inputs. The thickness of the casing is also a design input. Mesh independence for the heat transfer element was also done and is shown in Appendix C.

It should be noted that it is assumed the shaft sees the inlet temperature, and the casing the outlet temperature. This is a significant simplification since the actual shaft and casing sees a distributed temperature as the steam flows through the turbine.

4.3.5 Multiple extractions

The turbine compound component represents a turbine segment, i.e., the stages of the turbine between the inlet and outlet or first extraction point. If one were to model a turbine with one or two extraction points then two or three of the components will have to be placed next to each other where some of the inputs are shared between the components.

It was after consideration decided to rather create one compound component which contains multiple turbine components as to accommodate for the multiple extraction points. This meant that calculations can be made regarding the inputs shared and fewer input data is ultimately required. Figure 4.13 shows the Flownex network setup for the turbine compound component with 2 extraction ports. Script components were used to do the calculations and data transfer links to transfer inputs between elements.

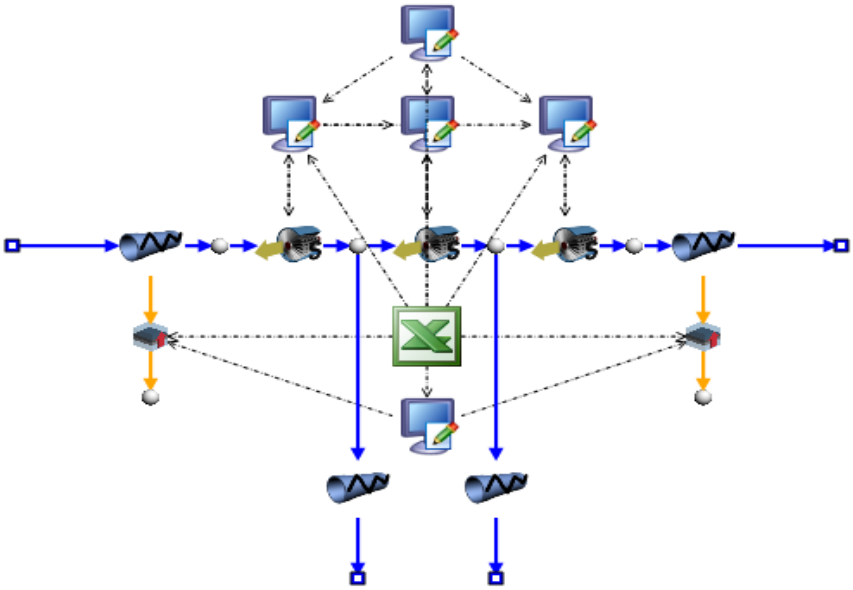

Figure 4.13: Flownex network setup of a turbine component with multiple extraction ports

The inputs required for one turbine component was summarized in Table 4.2. The shared inputs between the two consecutive turbine segments are shown in Table 4.3.

Table 4.3: Shared design inputs for turbine component with multiple extractions

Design inputs	**Description**
Mass flow [kg/s]:	Mass flow of first segment minus the extraction flow
Upstream pressure [kPa]:	Downstream pressure of the first segment
Upstream enthalpy [kJ/kg]:	Enthalpy at extraction
Downstream pressure [kPa]:	Downstream pressure

4.4 Validation and verification of the model

4.4.1 Pressured drop

The pressure drop over the turbine component was validated by comparing the results to the pre-defined ellipse law and the results obtained by Fuls in Figure 4.5. Two networks were set up in the Flownex where the turbine compound component and the normal Flownex simple turbine component with the same boundary conditions were compared. The semi-ellipse law, as given in equation (3.2), was implemented in the first network whereas the ellipse law, specified by equation (3.1), was used in the second network.

The simulation was run by specifying to pressure boundary conditions at either end of each network and lowering the downstream pressure as the simulation progressed. Mass flow results were then recorded for both networks and plotted in Figure 4.14.

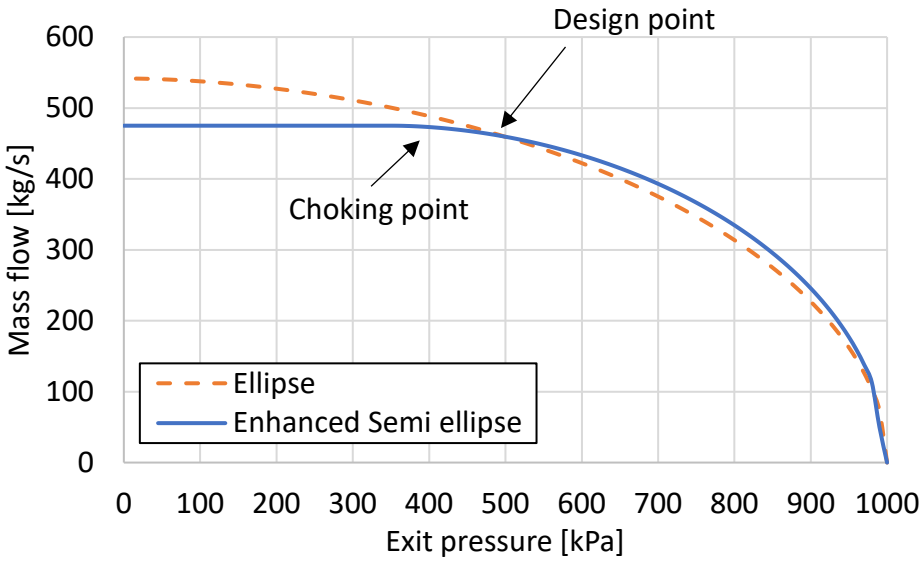

Figure 4.14: Pressure drop validation for the Flownex model of the turbine

The mass flow results shown in the figure correlate well with what is seen in Figure 4.5. Especially when looking at the comparison between the semi-ellipse law and the normal Ellipse law and after the point where choking occurs. This means that the implementation of the semi-ellipse law is done correctly and further test can be performed by the model.

4.4.2 Thermal inertia

Validating the thermal inertia for the model can be difficult and even though plant data is available, finding transient data which are solely attributed to thermal inertia of the shaft and outer casing is

not trivial. The model was instead tested to show the effects of the thermal inertia on the total results of the turbine model.

A simulation was run where the size of the shaft and casing were changed for a specific transient scenario. The transient scenario involved setting the shaft and casing's initial temperature to 25 °C and then recording the time it takes for the outlet steam temperature to raise by 0.3 °C. The benchmark inputs for the sizing of the shaft and casing is shown in Table 4.4.

Table 4.4: Design inputs for benchmark thermal inertia validation case

Design input	Value
Mass	12330.75 [kg]
Radius	0.5 [m]
Thickness	0.05 [m]
Time	1008.2 [s]

The design inputs were changed in by varying each input separately. The results are plotted in Figure 4.15.

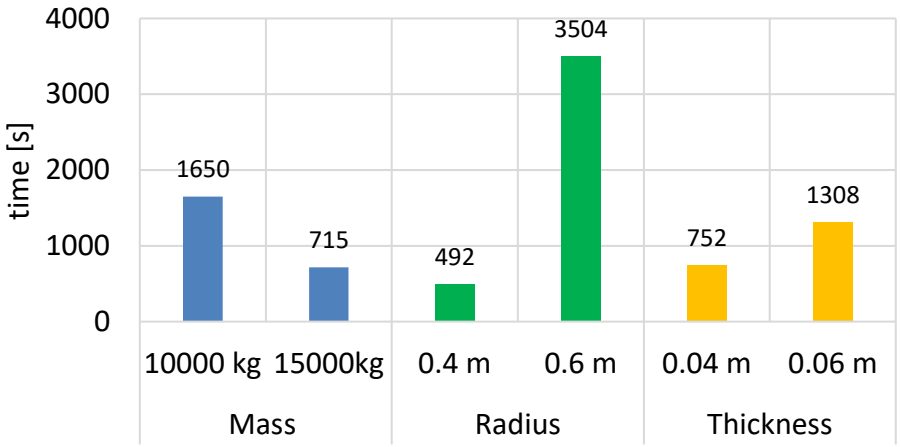

Figure 4.15: Design parameter study for thermal inertia results of the turbine component

From the results, it can initially be seen that the effects of changing geometry specifications of the shaft and casing do influence the model dynamically. By changing the mass to a larger mass, the time decreases which is contrary to what one would expect. This is due to the manner on how the area is calculated by equation (3.9) where a larger mass will equate to a larger heat transfer area.

The increase in radius of the shaft translates to a longer conduction path to the centre of the shaft, which will increase the time of heat transfer as seen in the figure. The thickness of the outer casing will also contribute to a longer conduction path which translates to an increase in time.

One can now conclude that the turbine model is able to capture the behaviour of transient inertia. Simplifications have however been made and these assumptions should be considered when specifying the design inputs.

4.4.3 Rotational inertia

The turbine model can model the effects of rotational inertia due to a shaft's rotational speed. This however does not include the effects of the gearbox on the shaft. A simulation was set up to study the response of the model to the methodology applied in section 4.3.3 due to the rotating shaft.

The simulation involved running the turbine at a specific speed and then suddenly dropping the inlet pressure of the turbine fr.67 bar to 1 bar. Something which is generally encountered with a turbine trip [41]. The model network is set up to that of a typical boiler feed pump turbine and boiler feed pump where the two components is connected with a shaft. There is generally a gearbox to reduce the speed from the turbine to the pump but for simplification was not included in the network. The network setup is shown in Figure 4.16.

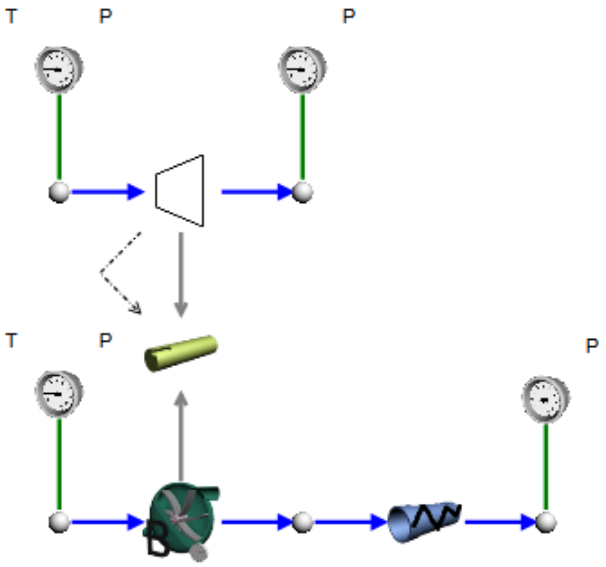

Figure 4.16: Network setup for studying the behaviour of the rotational inertia for the turbine's rotating shaft

The model was run for three different thicknesses of the shaft and the reduction in speed was recorded for the shaft over time. The results are shown in Figure 4.17.

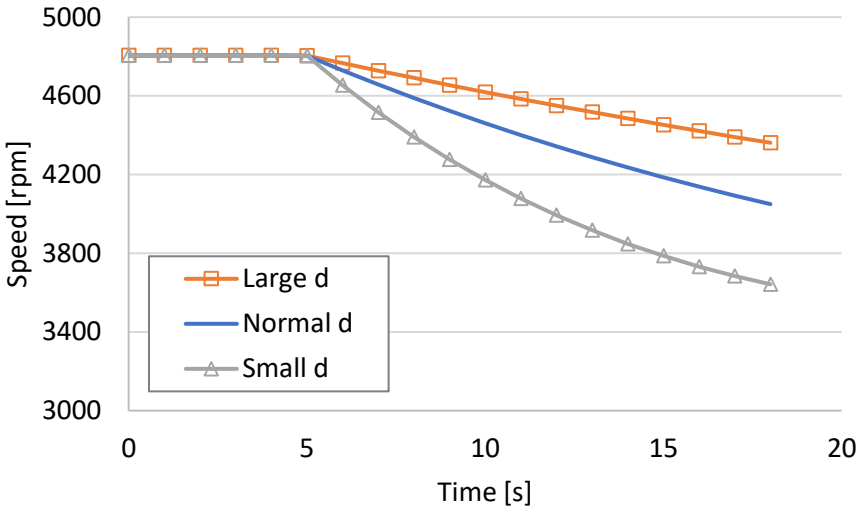

Figure 4.17: Effect of changing the diameter of the shaft on the rotating speed during transient operation

It can be seen by changing the diameter of the shaft the time it takes for the shaft to slow down is affected. The larger diameter results in a larger rotational inertia which means that the shaft will take longer to slow down whereas a smaller diameter will result in the opposite which is observed in the Figure 4.17.

4.4.4 Conclusion on verification and validation

Verification and validation could be done for the turbine model regarding the turbine's pressure drop and transient capabilities due to the shaft and casing. The results for the pressure drop of the turbine was compared to the results which was produces by Stodola's Ellipse law and the comparison agreed to that of Fuls.

Transient capabilities of the shaft's thermal/rotational inertia and the shaft's thermal inertia could clearly be shown. The analysis included changing main parameters and the effects of changing these parameters could clearly be seen during short transient scenarios.

4.5 Final turbine components in Flownex

4.5.1 Component "family" (Multiple extractions)

The final turbine component model contains three types of turbine configurations:

- Turbine with no extraction points
- Turbine with one extraction point
- Turbine with two extraction points.

The component family for the turbine is shown in Figure 4.18.

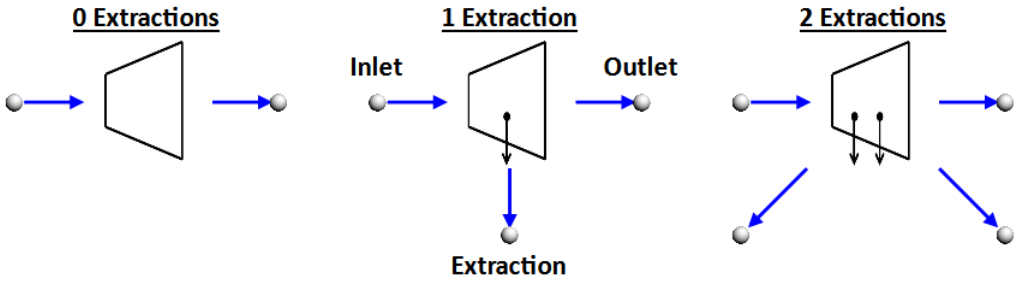

Figure 4.18: Three configurations for the final turbine model component

4.5.2 User inputs

The turbine component only contains design inputs. These inputs are specified by using an Excel spreadsheet inside the component. One should however ensure that the component connects to the correct Excel spreadsheet as incorrect reference is usually the source of most errors. The Excel spreadsheet for the turbine component with one extraction is shown in Figure 4.19.

Turbine The turbine uses the energy stored in the steam and converts this into shaft work			
Fluid property inputs:	**Value**	**Unit**	**Component schematic**
M_flow	397.12	kg/s	M_flow P_upstream h_upstream P_downstream
P_upstream	3125	kPa	
h_upstream	3488.37	kJ/kg	
P_downstream	418	kPa	
Turbine segment:	**Value**	**Unit**	**Pressure drop equation**
Critical p-exponent (α)	2.05	-	$\dot{m} = \dot{m}_D \sqrt{\frac{p_{0in} \cdot v_{in,D}}{v_{in} \cdot p_{0in,D}}} \sqrt{\frac{1-\left(\frac{r-r^*}{1-r^*}\right)^{\alpha}}{1-\left(\frac{r_D-r^*}{1-r^*}\right)^{\alpha}}}$
Critical p-ratio (r^*)	0.54	-	
Reaction (β = 2), Impuls (β = 1)	1	-	
efficiency (η_D)	0.87	-	
Turbine physical parameters:	**Value**	**Unit**	**Efficiency drop equation**
Speed	3000	rpm	$\eta = \eta_D - \beta \left[\frac{N/\sqrt{\Delta h_{s,D}}}{N_D/\sqrt{\Delta h_s}} - 1\right]^2$
Shaft radius	0.4	m	
Shaft weight	2000	kg	
Outer casing thickness	0.05	m	
Outer casing radius	0.7	m	

Figure 4.19: Design inputs for the turbine component model with no extraction points

Design inputs for the fluid properties can initially be specified. These inputs are used for both the pressure drop and efficiency correlations. The turbine segment is then defined which contain inputs for the coefficients of the pressure drop and efficiency equation. Lastly the inputs can be specified for the turbine's physical parameters. These inputs are used for defining the turbine casing's thermal inertia and shaft's rotational inertia.

For a turbine with one extraction point, the turbine segment inputs are defined for each segment. Also, fluid properties are defined for the extraction point as well. The fluid properties of the complete turbine section are shown in Figure 4.20.

M_flow	397.12	kg/s
P_upstream	3125	kPa
h_upstream	3488.37	kJ/kg
P_downstream	418	kPa
M_extraction	15	kg/s
P_extraction	1796	kPa
h_extraction	3321.5	kPa

Figure 4.20: Fluid property inputs for turbine component model with one extraction point

The fluid properties for a turbine component with two extractions are shown in Figure 4.21.

M_flow	402.63	kg/s
P_upstream	3229	kPa
h_upstream	3476.1	kJ/kg
P_downstream	441	kPa
M_extraction 1	20.405	kg/s
P_extraction 1	1805	kPa
h_extraction 1	3318.6	kJ/kg
M_extraction 2	37.499	kg/s
P_extraction 2	948	kPa
h_extraction 2	3135	kJ/kg

Figure 4.21: Fluid property inputs for turbine component model with two extraction points

4.5.3 Results

Results for the turbine component are displayed either as component results or detailed results. The component results are displayed in the properties window where the results are given per turbine segment. Detailed results are obtained by double clicking on the component, which displays the component network where each element can be inspected. The component results for a turbine with two extractions points are shown in Figure 4.22.

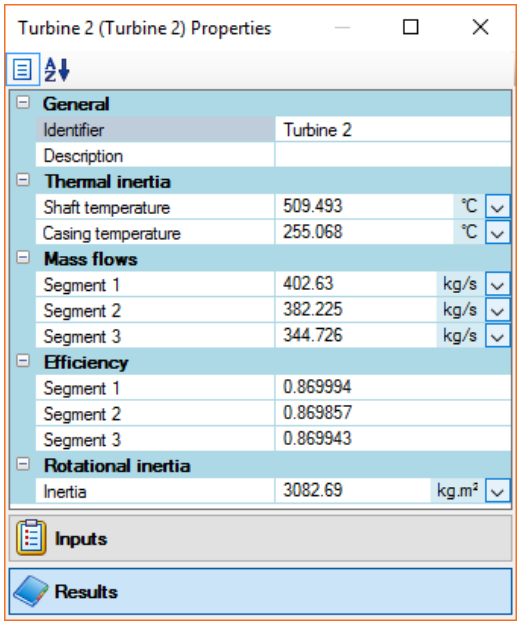

Figure 4.22: Turbine component model with two extractions results

Results are given for the thermal inertia, which includes the temperatures of the shaft and outer casing. Mass flow and efficiency of each segment and the rotational inertia for the entire turbine component is also given.

4.5.4 Application

The component works by placing the component from the Flownex library into the drawing page. From here the right connections can be made to the component, as seen in Figure 4.23. It is initially required to specify the turbine component's design inputs. This is done through the Excel table, explained in the user inputs section. Extraction lines can now also be connected with heaters in the network.

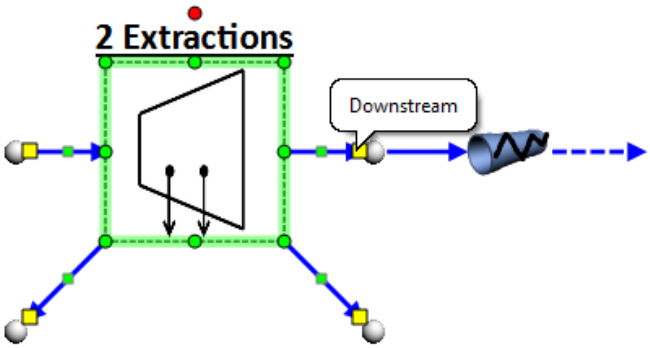

Figure 4.23: Turbine component application

4.5.5 Limitations

The turbine component has been modelled with the following limitations:

- Ray's method requires the knowledge of the isentropic enthalpy drop, which requires certain fluid properties which can be difficult in Flownex, especially in earlier versions of the software.
- Only the shaft and inner casing's thermal inertia has been modelled; assuming, the shaft sees the inlet temperature of the steam and the inner casing sees the outlet temperature of the steam.
- The turbine's rotational inertia requires the knowledge of the turbine segment's weight.

5. Deaerator component modelling

5.1 Theory and characteristics of the deaerator

The deaerator is essentially an open-type feedwater heater where various fluids are mixed and heat is transferred in between the fluid. The deaerator also acts as a deaeration device to remove any gasses which might be trapped in the condensate and bled-steam of the powerstation. It is important to note that the deaeration occurs not only to remove the air but rather to remove unwanted gasses, called non-condensable gasses (NCG), trapped in the air. These gasses can vary from Oxygen, Nitrogen, Carbon Dioxide and Ammonia Dioxide and the causes of the gasses are wide spread where the most prominent cause is corrosion inside the tubes [3].

The deaeration process works based on two common scientific principles. The first principle is based on Henry's law, which states that the amount of gas in the solution is directly related to the partial pressure of the gas over the solution. Thus, at a constant temperature if one were to decrease the partial pressure (hypothetical pressure of the gas if the volume only contained that specific amount of gas) the amount of gas would also decrease. The second principle is that of temperature where if the temperature of the solution increases to saturated state, then the amount of gas trapped in the solution would decrease [41].

Looking from a practical stance, the process of the deaeration inside the heater occurs by firstly decreasing the pressure of the condensate entering the vessel and secondly increasing the temperature to saturated conditions by mixing it directly with bled-steam from the turbine. This now releases the NCGs from the water where the gases are released into the atmosphere via a vent.

Two types of deaerators are currently employed by the ESKOM fleet: the spray-tray type and the spray-scrubber type [3]. A brief description of each follows.

5.1.1 Spray-tray deaerator

A Spray-tray deaerator consists of two stages where each stage is designed to remove the corrosive gasses found in the feedwater. The first stage is where most of the deaeration occurs [49]. The feedwater enters the spray-tray deaerator at the top and is sprayed via nozzles into the upcoming steam. The feedwater is heated to just below the saturated steam temperature and moves toward the next stage.

In the second stage, the feedwater flows uniformly through the trays in thin films. The steam enters at the bottom of the tray where it condenses from stage two to stage one and partly exists at the top vent with most of the corrosive gasses. The condensed steam together with the gas-free

feedwater collects at the bottom and falls into a storage tank below. This process is illustrated in Figure 5.1 below.

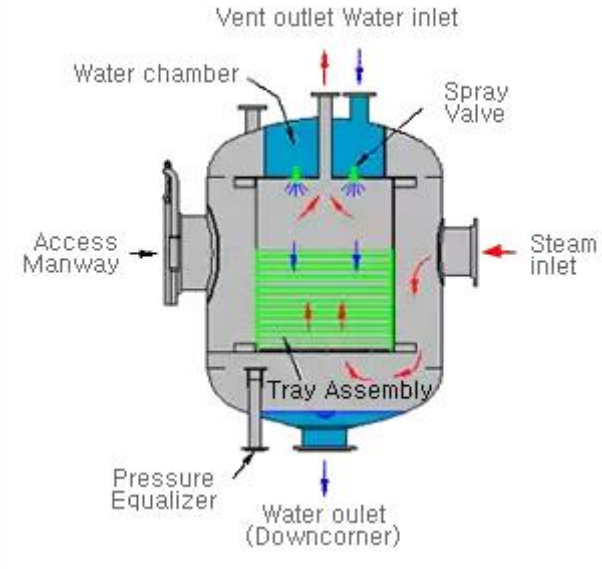

Figure 5.1 Spray-Tray type deaerator [50]

5.1.2 Spray-scrubber deaerator

The spray-scrubber type deaerator (also known as a stork type deaerator) works in the very same way as the spray-tray type deaerator, the only difference is that the tray section is replaced with what is called a scrubber section. The feedwater enters the spray-scrubber deaerator at the top where the feedwater is atomized via specially designed valves. These valves are specially arranged not to spray against the outer surface of the spray chamber [51]. The atomized feedwater is mixed with the upcoming steam where most of the corrosive gasses are extracted, as with the spray-tray type.

The feedwater is then briskly mixed with the oxygen free steam and sent through scrubbers where the remaining gasses are released from the feedwater. It is the violent action of the water/steam mixture through the scrubbers that release the remaining gasses from the water. The scrubbers are efficiently designed to remove these gasses in a way as to not induce any chatter or vibration inside the chamber [51]. An illustration of the spray-scrubber type deaerator are shown in Figure 5.2.

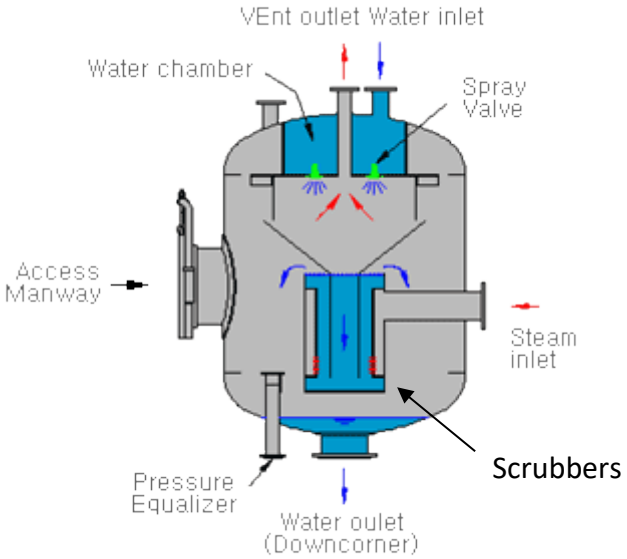

Figure 5.2: Spray-scrubber type deaerator (modified from source) [50]

5.2 Deaerator models in literature

As stated in the previous chapter, the deaerator is an open feedwater heater where condensate, steam and cascading condensate mix. From first principles, one can view the deaerator as simply an energy balance where fluids mix and exchange heat. Very little losses occur in the system simply because the fluids are directly in contact with each other whereas in a closed feedwater heater, losses like fouling and tube plugging decrease the heat transfer capabilities of the heater.

One can model the deaerator by taking a control volume around the deaerator and looking at all the fluids entering and exiting the control volume. A depiction of the deaerator control volume is shown in Figure 5.3. The fluids entering the deaerator are the main condensate, return condensate and bled-steam. The fluids exiting the deaerator are the vent steam and the deaerated water/ feedwater.

The mass balance over the deaerator can be written as:

$$m_{mc} + m_{bs} + m_{rc} = m_{vs} + m_{FW} \tag{4.1}$$

The energy balance over the deaerator can be written as:

$$m_{mc}h_{mc} + m_{bs}h_{bs} + m_{rc}h_{rc} = m_{vs}h_{vs} + m_{FW}h_{FW} \tag{4.2}$$

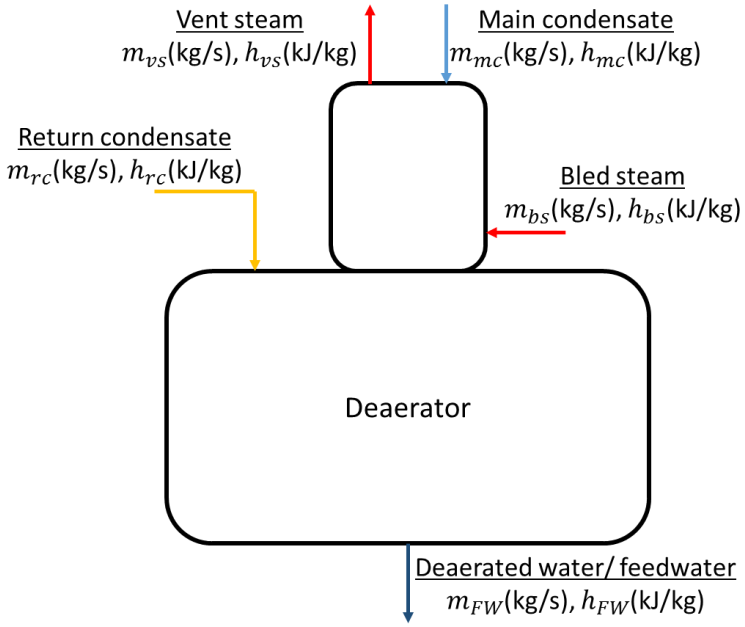

Figure 5.3: Deaerator control diagram for mass and energy balance [3] (modified)

5.2.1 R. Banda's deaerator model

Recent developments on the deaerator modelling was done b R. Banda [3], in which the deaerator was modelled by taking energy and mass conservation into account as well as determining the amount deaeration that takes place from the process. The model consisted of an analytical model and a Flownex model.

The purpose of the **analytical model** was to determine the mass flow and thermodynamic properties of the five streams entering and leaving the deaerator as shown in Figure 5.3. The model was also used to determine the amount of oxygen in the feedwater exiting the vessel.

Mass and energy balance conservation equations was used to determine the properties for the bulk system. These conservation equations are given in equation (4.1) and (4.2). Momentum conservation was used to determine the pressure drop over the vent pipe.

To determine the amount of oxygen in the outlet of the feedwater the model made use of the continuity equation for oxygen diffusion from a spherical droplet. The assumption for the model is mainly that all the deaeration takes place in the preheater section, which is the section where the droplets are in contact with the rising steam. This simplifies the model considerably since the intricate geometry of the tray or scrubber section is required if the assumption is not made. The oxygen continuity equation in its integrated from is shown in equation (4.3).

$$\omega_{O2}(t) = \omega_{O2,i} \cdot e^{\left(-6\frac{Sh \cdot D_{O2,mc}}{D_{32}^2} \cdot t_{mt}\right)} \tag{4.3}$$

where ω_{O2} is the concentration of oxygen in parts per billion. The inputs for equation (4.3) are summarized in Table 5.1.

Table 5.1: Input parameters to R. Banda's analytical model of the deaerator

Input	Description
$\omega_{O2.in}$	Inlet concentration of oxygen
$D_{O2.mc}$	Diffusivity of oxygen in water
D_2	Droplet diameter
t_{mt}	Time available for mass transfer
Sh	Sherwood number

Each of the parameters input parameters for equation (4.3) are then determined through a various relations and methods. These methods are however dependent to the type of spray nozzle, where the author looked at a pressure swirl simplex atomizer due to its feasibility in terms of the project's constraints.

The model further contained a section called the pre-calculations section which is used to determine unknown parameters such as the nozzle discharge diameter and the vent steam pipe pressure loss coefficient. The inputs required for the pre-calculations section are those of a 100% load case and are used to calibrate the model.

The model was validated using plant acceptance test data from Kriel power station. Some pre-processing of the data had to be done since not all the measurements were directly taken at the inlets and outlets of the deaerator. The thermal-hydraulic validation of the model showed good agreement with plant data with an average error of 0.128% and a range of between 0% and 1.81%.

Unfortunately, plant acceptance test data did not show any information regarding the oxygen content for the feedwater. The model therefore had to be tested with similar work done by Sharma et al. [52]. The validation was however only qualitative since raw data could not be obtained from Sharma et al.'s work. The results from the validation were satisfactory and all deviations could be explained.

Flownex model

We now move on to the more important section of the literature review which is the section on R. Banda's Flownex model. The Flownex model is the numerical modelling approach to the deaerator. The main components of the model were the general empirical relationship, the flow resistance element and the two-phase tank. The Flownex deaerator model is shown in Figure 5.4 with the description of each element indicated in the figure.

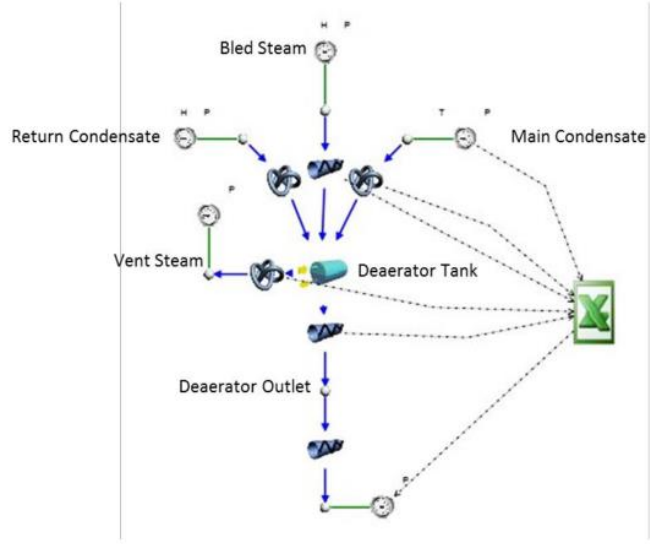

Figure 5.4: R. Banda's Flownex network of the deaerator [3]

The model has been developed by considering the main components which will have a significant effect on the thermos-hydraulic properties of the cycle. Each of the main components are described below.

Main condensate inlet nozzle

The main condensate inlet nozzle has been modelled using a general empirical relationship element. The inputs for the component has been set: β as 1, α as 2 and C_k (loss coefficient) as a function for the appropriate pressure drop. The current model used an excel spreadsheet to determine the appropriate loss coefficient and varies it depending the load condition.

Bled steam inlet

The bled-steam inlet has been modelled using the flow resistance component set to a flow admittance of 0.01. The component has also been set to disregard any density variations in the steam.

Return condensate inlet and vent steam exit

The return condensate inlet and vent steam exit have both been set to use a general empirical relationship element with the same inputs as that of the main condensate inlet nozzle. The difference is that the loss coefficient is set to a calculated constant.

Feedwater outlet

The feedwater outlet is modelled as two flow resistance elements where the first flow resistance is only there for solving purposes and the second as the “fixed mass flow” element. The flow admittance of the second flow resistance is essentially used to simulate the boiler feed pump during

operation. During a transient scenario, the “fixed mass flow” option is switched off which enables the flow to vary depending on the conditions.

Excel spreadsheet

The Excel spreadsheet is used to solve the continuity equation for oxygen diffusion from a spherical droplet as described in equation (4.3). It also serves the purpose of changing the loss coefficient for the main condensate nozzle inlet general empirical relationship element.

Deaerator tank

The deaerator tank was modelled by using the two-phase tank component. The geometry of the two-phase tank was specified using the component’s simple volume specification where a volume and diameter was used. Also, the component was specified to only release steam at the vent outlet and liquid water at the feedwater outlet.

Oxygen gas

The oxygen concentration was modelled in the Flownex component by using the trace elements function. The trace elements represent elements in a fluid with a concentration of below 100 ppm in the Flownex. It was however noted by the author that one cannot see the oxygen as suspended particles in the fluid but using this approach was the most sensible and convenient.

The Flownex model was validated by using the analytical model’s results. The model was initially calibrated at a 100% load case, where a curve was fitted for the main condensate inlet nozzle’s loss coefficient. Results for the model are shown in Figure 5.5. The thermal-hydraulic results show good agreement with plant acceptance test data with errors ranging from 0.02% to 0.67%. The author attributed the errors to rounding off and steam property interpolation errors. Also, the author mentioned that the pressure inside the vessel is slightly lower than that of the bled-steam pressure causing differences in the total mass flow. The oxygen concentration showed a larger error of up to 27.17% but the author made it clear that the high percentage is attributed to comparing very small values. The values were then compared by rather taking difference which resulted in a better comparison.

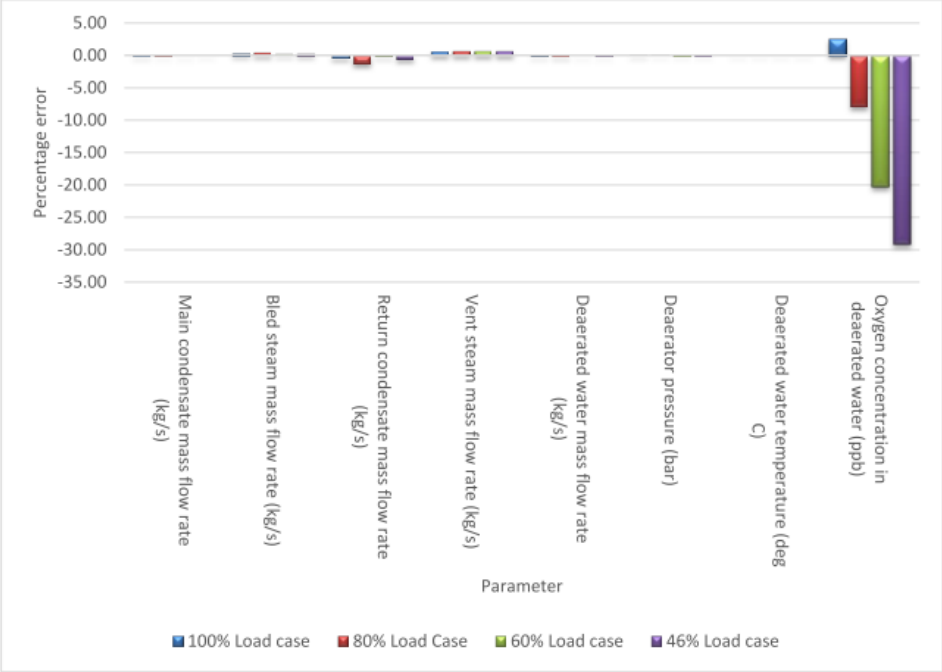

Figure 5.5: R. Banda's Flownex model of deaerator's results for various load cases [3]

5.2.2 Conclusion on literature study of previous models

It was sufficient for the scope of the component to only review that which was done by R. Banda. An analytical model as well as numerical model on Flownex was developed where both the models showed overall satisfactory results. A lot of work went into the determination of the oxygen content at the feedwater but it was noted that it is highly dependent on the specific geometry of the nozzle. This makes it difficult to implement this on a more generalized model and will therefore not be implemented in the current model. The methodology of the Flownex model will however be implemented in the current model.

5.3 DA component model

5.3.1 Model overview

The aim of the Deaerator model is model the thermodynamic behaviour of the component as one would see on the power station. The methodology presented by R. Banda's showed to be a realistic and relatively simple methodology to model a deaerator in the Flownex, where the validated thermodynamic results showed good agreement with plant acceptance test data. It was for this reason that the current model will use the same methodology.

It should however be noted that the current model will be implemented as a generalized model and will therefore not include the oxygen determination for the feedwater outlet stream. The vent

steam outlet will also not be included in the current model. From the results of Banda's model, the vent steam mass flow for a specific 600 MW power station was in the range of 0.332 kg/s. This is not a significant amount compared to the mass flows of the other flows and one also needs to know the specific valve geometry as to model the vent steam outlet, which is not always known to the user. Table 5.2 shows an overview of the current model compared to that of R. Banda's model.

Table 5.2: Improvements and key attributes of Banda's Flownex deaerator model and the current Flownex deaerator model

R. Banda's Flownex model	Current Flownex model
Model the vent steam	Vent steam not modelled
Pressure drop over main condensate inlet valve calibrated for a specific heater	Pressure drop over main condensate inlet valve automatically calibrated for various load cases.
Oxygen determination for the feedwater outlet stream	Oxygen content not determined for feedwater outlet stream
Water level indication in deaerator tank	Water level indication in deaerator tank
	Component packaged

The current deaerator model is shown in Figure 5.6 where the flow diagram of the heater is shown in Figure 5.6. The network is built in that the main condensate, return condensate and bled-steam flows into the deaerator tank/ two-phase tank and feedwater flows out of the tank. The calculation area includes calculations for the valve pressure drop and inputs to the geometry of the tank.

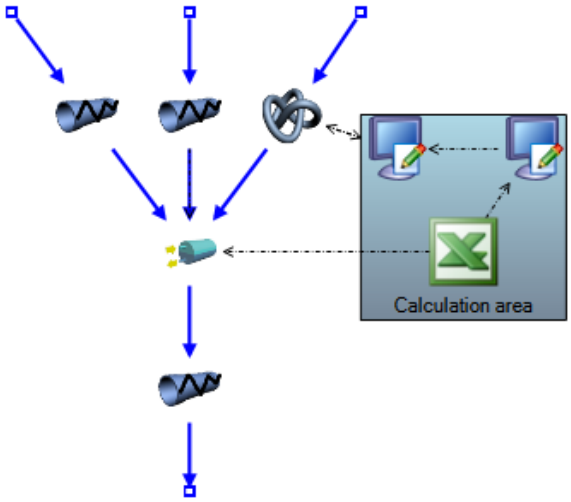

Figure 5.6: Detailed deaerator model in the Flownex

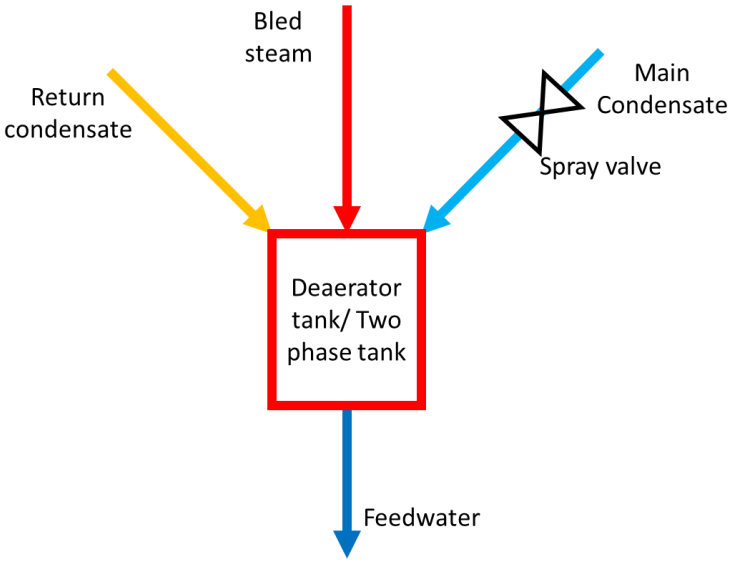

Figure 5.7: Network flow diagram of the deaerator model

5.3.2 Main condensate spray nozzle modelling

There are various types of spray nozzles with unique flow characteristics. Some have spring-loaded parts that causes it to self-adjust as the flow changes. One therefore needs to represent this empirically.

The main condensate spray nozzle has been modelled by using the variable geometry valve methodology of Banda [3] where a curve has been fit to the general empirical relationship's loss coefficient. This method gives a variable pressure over the valve depending the load conditions.

The method was however altered to make the process more automatic in that the user is only required to put in data for various load cases and the curve is then automatically generated by the script component. The curve that was fitted by Banda is shown in Figure 5.8 and the equation for the graph in equation (4.4).

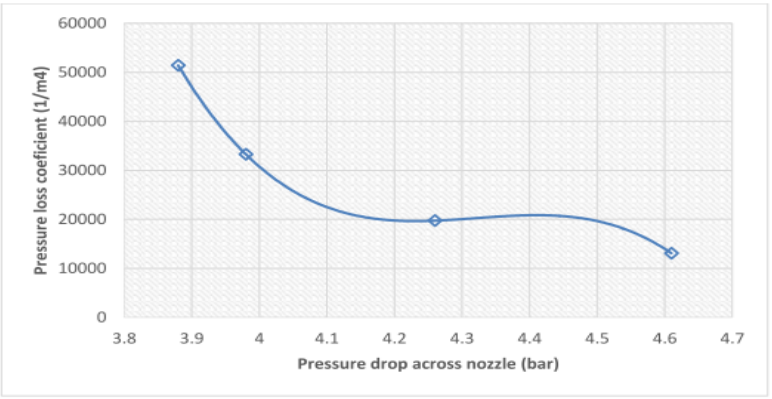

Figure 5.8: R. Banda's pressure loss coefficient variation for the nozzle pressure drop

$$C_k = -416416.321545 \cdot \Delta P^3 + 5397591.36223 \cdot \Delta P^2 - 23311137.0325 \cdot \Delta P + 33564487.0541 \quad (4.4)$$

Generating a curve from a third order polynomial by using raw data is quite an extensive exercise and a simpler method would be to generate a linear curve. Load condition properties were therefore compared and it was observed that the pressure drop and mass flow through the main condensate valve displayed a linear trend for the various load conditions. A typical trend from a power station is shown in Figure 5.9 where the equation for the line is shown on the figure.

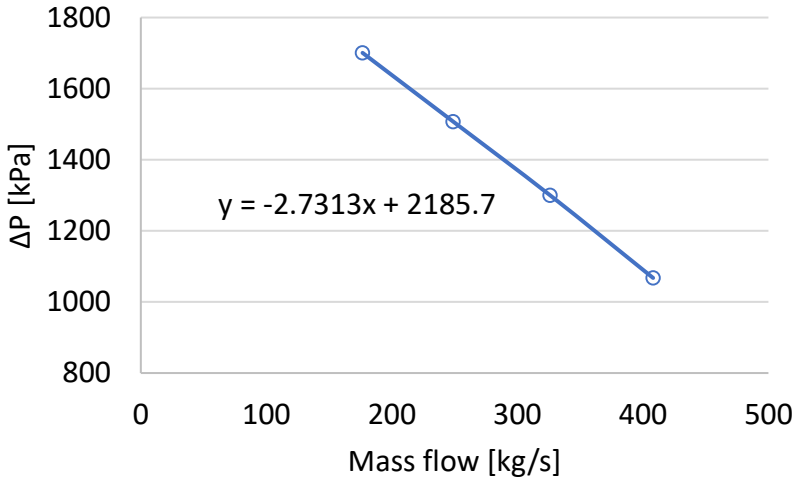

Figure 5.9: Trend line for the pressure drop vs mass flow of the deaerator main condensate valve

The following methodology has been implemented to generate the curve from load condition input data.

a) Obtain input data

Input data is initially obtained where a minimum of three and a maximum of six load conditions are required. The mass flow through the main condensate valve and the pressure drop over the valve is required. The input data can be obtained from any source, i.e. heat balance, acceptance or operational plant data, but the general method would be to use heat balance data. Refer to section 2.4 for a literature review on the various types of plant data and its credibility.

b) Generate coefficients for the linear curve

The next step in the methodology is to generate the linear curve through the data. This is done by the least squares method and is summarized in Appendix B.

c) Use the coefficients to generate a loss coefficient for the appropriate pressure drop

The last step of the implementation process is to use the coefficients to obtain a specific pressure drop for the given mass flow. The mass flow is obtained from general empirical relationship and used as an input to the script. The script then calculates the pressure drop from the mass flow by

using the linear equation defined by the coefficient calculated in the second step. By knowing the pressure drop the loss coefficient can be calculated by using equation (4.5), which is the rewritten from of the general empirical relationship's equation.

$$C_k = \frac{\Delta p}{\rho^{\alpha} \dot{Q}^{\beta}} \tag{4.5}$$

where α is 1 and β is 2.

The three steps methodology is split into an Excel spreadsheet and two scripts. These components are shown in Figure 5.10 with the allocated steps from the methodology shown in the figure. It should also be mentioned that script 3 is the only script that runs during a transient scenario and data is transferred after each iteration.

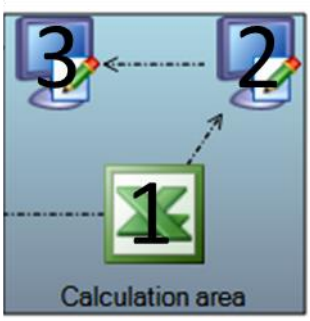

Figure 5.10: Calculation process for the main condensate valve pressure drop

5.4 Validation and verification of the model

5.4.1 Heat balance verification (Lethabo)

The component was initially verified by using the heat balance data with which the component was initially defined. The simulation was set up by using the inputs from the heat balance to define the pressure drop valve and the boundary conditions. The following conditions in Table 5.3 was used.

Table 5.3: Boundary conditions for deaerator model verification

Boundary condition	**Load case**			
	100 %	**80 %**	**60 %**	**40 %**
m_{MC} [kg/s]	408.16	325.905	248.756	176.661
Δp [kPa]	1067.5	1300.4	1507.5	1700.6
T_{MC} [°C]	128.7	122.3	114.3	104
p_{BS} [bar]	6.524	5.23	3.96	2.605
h_{BS} [kJ/kg]	3061.7	3068.7	3061.3	2999.1

m_{RC} [kg/s]	72.989	55.068	38.337	24.441
h_{RC} [kJ/kg]	725.8	680	629.2	135.9

Each load case was then run by specifying a parameter table in the Flownex. The main results, which include the feedwater outlet flow and temperature and the pressure drop over the valve, was then recorded and plotted together with heat balance results in Figure 5.11.

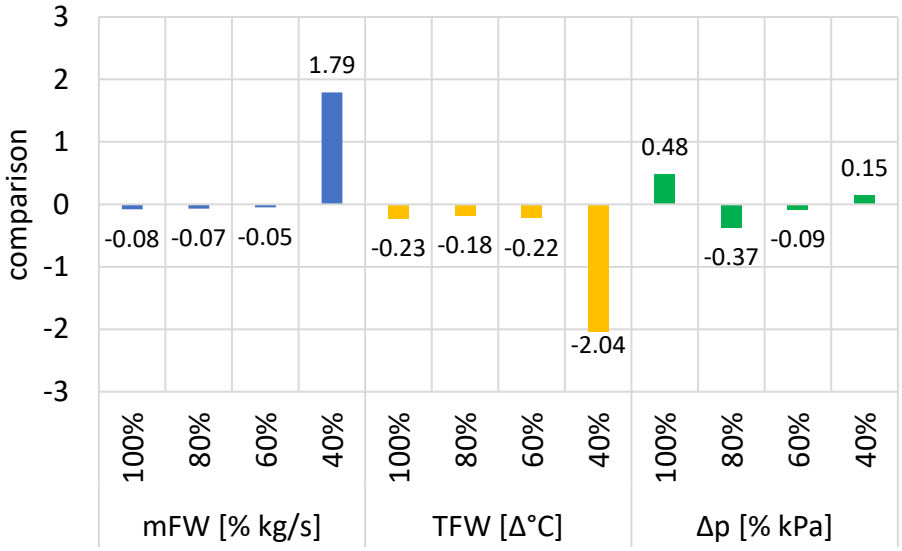

Figure 5.11: Heat balance verification for the Flownex deaerator component

Mass flow results from the heat balance verification show satisfactory results where the largest error is at the 40% load case. This is because at the lower loads lower flow rates are encountered, thus a small difference will result in a larger percentage. Also, flow measurement devices work almost entirely from a pressure drop – thus a small pressure drop results in less accurate flow measurements. The temperature results are also satisfactory where the largest temperature difference is at the 40% load case. Pressure drop results show very good agreement with heat balance data which indicates that the linear trend is a suitable method for modelling the valve.

The model showed overall reliable results and the solving time of the deaerator model was minimal and without any complications. Confidence in the model is now established and further validation can be done.

5.4.2 Validation through plant acceptance test data

The same methodology was followed as in the verification of the deaerator model. The only difference is that the boundary conditions are defined by plant acceptance test data and the valve pressure drop is still defined by heat balance data (known as design data). The main results were then compared using plant acceptance test data. The boundary conditions are shown in table.

Boundary condition	Load case			
	100 %	**80 %**	**60 %**	**40 %**
m_{MC} [kg/s]	408.16	325.905	248.756	176.661
Δp [kPa]	1067.5	1300.4	1507.5	1700.6
T_{MC} [°C]	128.7	122.3	114.3	104
p_{BS} [bar]	6.524	5.23	3.96	2.605
h_{BS} [kJ/kg]	3061.7	3068.7	3061.3	2999.1
m_{RC} [kg/s]	72.989	55.068	38.337	24.441
h_{RC} [kJ/kg]	725.8	680	629.2	135.9

The simulation was again run using the new boundary conditions as specified. Results for the Feedwater mass flow and temperature for different load cases are shown in Figure 5.12.

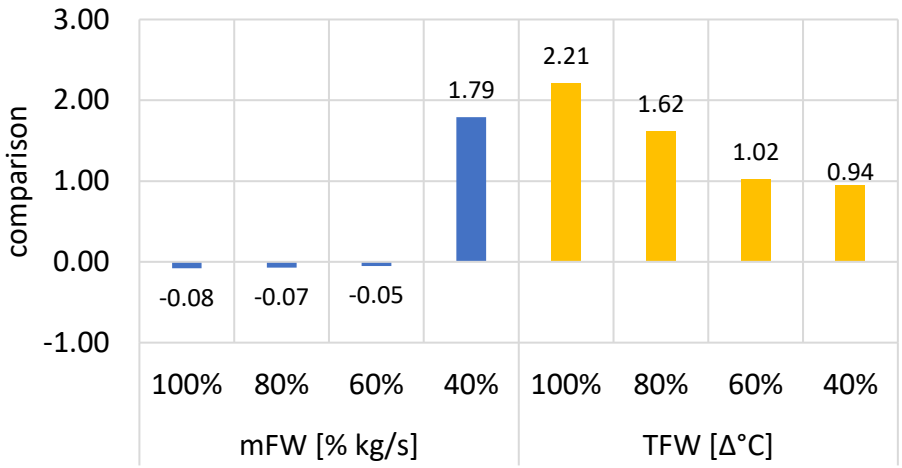

Figure 5.12: Plant acceptance test data validation for the Flownex deaerator component

Results for both the mass flow and temperature are shown do be well in the tolerance range as specified in section 2.4.2 for plant acceptance test data. The temperature results are slightly higher than that of the plant acceptance test data. A plausible cause is that the heater assumes no heat loss to the environment and thus the outlet temperature will be higher compared to the actual deaerator component.

5.4.3 Conclusion on verification and validation

The deaerator model has been verified through heat balance data and validated by using plant acceptance data. Both studies showed overall satisfactory results and the differences in results

could be explained. By also testing the model for various load conditions, it can be concluded that the model has a high degree of fidelity.

5.5 Final DA component in Flownex

The deaerator component was finally packaged into a usable compound component which contains user inputs, calculation methods and results. The final deaerator component is shown in Figure 5.13.

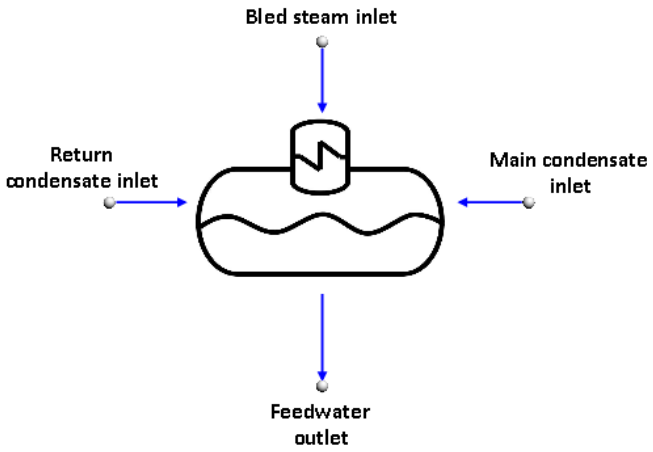

Figure 5.13:Final Deaerator compound component in the Flownex

5.5.1 User inputs

The Deaerator component contains two sets of inputs which are the main condensate spray nozzle's pressure drop characteristics and the geometry of the vessel. It should be mentioned that the geometry assumes a horizontal cylinder and ignores the upper tank. The Excel input table for the component is shown in Figure 5.14.

Deaerator

An open feedwater heater with the purpose of removing any excess gasses trapped in the feedwater.

Condensate design mass flow:

Load condition	Mass flow [kg/s]	Delta P [kPa]
1	450	180
2	464.96	150
3	365.93	120
4	281.5	100
5	0	0
6	0	0

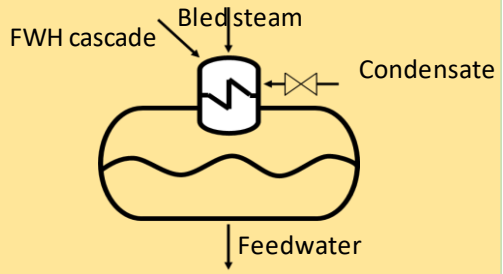

Geometrical specifications:

Volume:	200	m^3
Diameter	4.5	m

Figure 5.14: Excel input table for the deaerator Flownex component

The main condensate valve pressure drop design parameters include the mass flow and pressure drop for a minimum of three load cases and a maximum of six load cases. The geometrical inputs define a horizontal tank geometry with a volume and a diameter. The inputs are summarized in table.

Table 5.4: Excel input design parameters for the deaerator tank

Input parameter	Description	Engineering unit
m_{MC}	Main condensate mass flow	Kg/s
Δp	Valve pressure drop	kPa
Volume	Vessel volume	m^3
Diameter	Vessel diameter	m

The component further contains non-design inputs specified in the property window. The inputs are the fixed mass flow element which refers to the two-phase tank's steady-state control options and the normal level of the vessel/tank. These inputs are shown Figure 5.15.

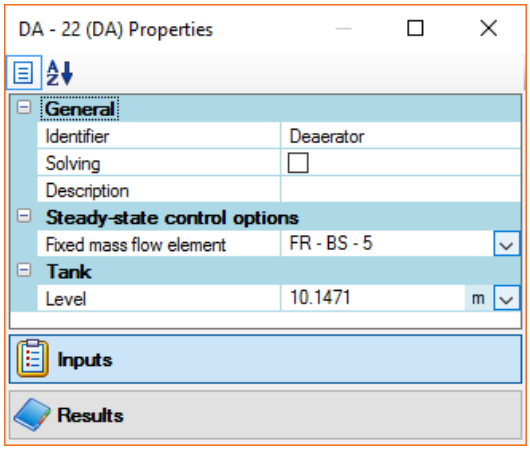

Figure 5.15: Non-design input for the Flownex deaerator component

5.5.2 Results

The most important results for the component is displayed in the component's property window. The results are the main mass flows, vessel inside pressure and the current level inside the vessel. These results are shown in Figure 5.16.

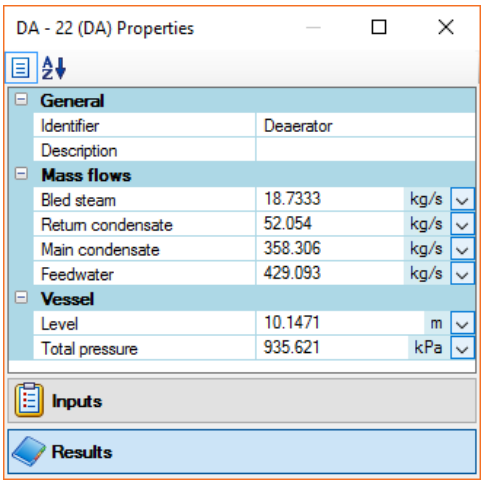

Figure 5.16: Results for the Flownex deaerator component.

More detailed results can simply be obtained by double clicking on the compound component which will display the detailed network. Once there the user will be able to click on each individual Flownex element for a comprehensive list of inputs and results.

5.5.3 Application

The component works by initially placing the compound component from the Flownex library into the drawing page. The next step is to connect all links of the component to the surrounding network. The link connection is shown in Figure 5.17. The next step is to define a outlet

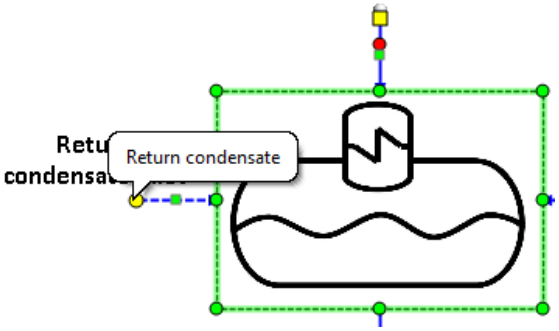

Figure 5.17: Link connection for the Flownex deaerator component

Once the component is connected, the design inputs must be defined. This is done by specifying it in the provided Excel spreadsheet. It is important that the spreadsheet should allocated in the correct directory under the project tasks folder and the Excel spreadsheet has been executed correctly. Flownex tends to not always keep track of Excel changes thus it falls on the user to ensure that all design parameters are correctly specified for the component.

If the component is connected to the right inputs and outputs and the design parameters has been specified then the component will run. Further problems or errors are usually allocated to the incorrect definition of physics for the component.

6. Component integration

6.1 Low-pressure heater train

The Low-Pressure train for Lethabo power station consists of three LP feedwater heaters. Each heater is mounted horizontally and is of tubesheet type. The feedwater heater network configuration is displayed in Figure 6.1 as one would find in the cycle.

Feedwater enters the low-pressure heater train at Low-pressure heater (LP-H) 1, flows through LP-H 2 and exits at LP-H 3. LP-H 3 receives extraction steam from the IP turbine. LP-H 2 and 3 both receive extraction steam from LP-H 1 and 2. LP-H 3 cascades condensate to LP-H 2 and LP-H 2 cascades condensate into LP-H 1. All the condensate essentially collects in LP-H 1 and is thereafter pumped back into the feedwater line.

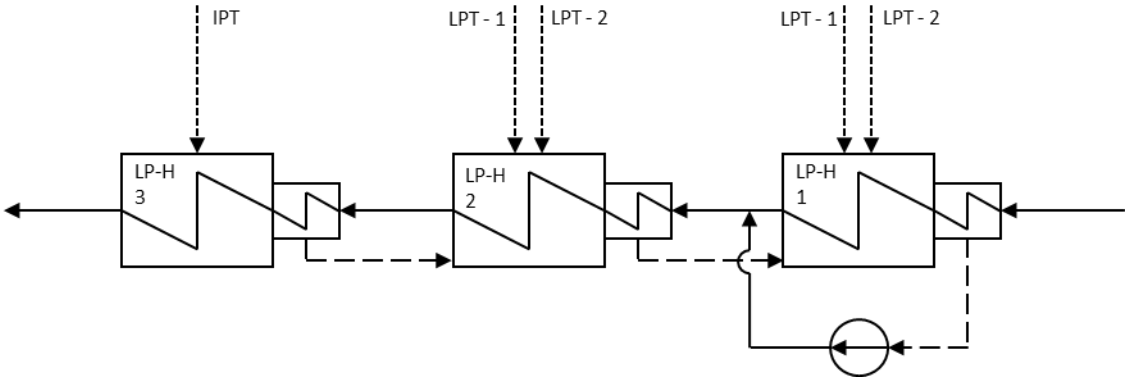

Figure 6.1: Low-pressure heater train for power station 1

6.1.1 Flownex network

The LP-H component model was used in Flownex to build the LP heater train. Each component's inputs were specified with plant and heat & energy balance data. The components were interconnected by using flow resistance components with a flow admittance set to 100. This will not induce a noticeable pressure drop but enables the network to be analysed at various points and makes it more manageable. The flow resistance components were also used as valves at the condensate drain's pipe where the opening is used as valve's opening. The pump at LP-H 1 is a design component where its head is designed for the pressure rise required. The Flownex network is shown in Figure 6.2, where one can see that it looks like the diagram shown in Figure 6.1 with each boundary numbered in red.

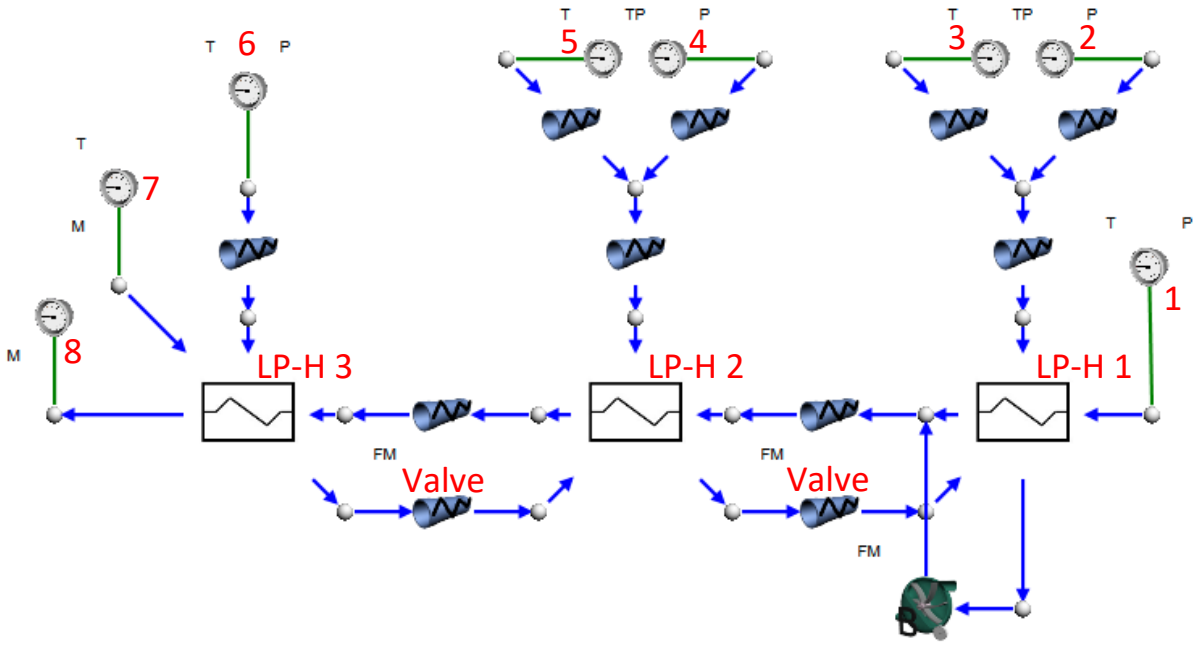

Figure 6.2: Low-pressure heater train network in Flownex

6.1.2 Steady-state scenario

Boundary values for the network were set up to include three load cases. The operational plant data were obtained from using EtaPRO™ (full description in section 2.4). The boundary values are summarized in Table 6.1, where the feedwater flow is defined as the outlet flow.

Table 6.1: Boundary values for the low-pressure heater train of power plant 01

Boundary	Description	Property	400 MW	500 MW	600 MW
1	Feedwater	P [kPa]	828.51	890	1110
		T [°C]	38.77	41.851	45.801
2	Extraction	P [kPa]	30.61	36.854	40
		T [°C]	77.59	77.818	78.103
3	Extraction	P [kPa]	30.81	37.05	40
		T [°C]	77.59	77.818	78.103
4	Extraction	P [kPa]	92.1	112.675	133.766
		T [°C]	142.53	142.61	142.035
5	Extraction	P [kPa]	93.103	113.456	136.953
		T [°C]	142.53	142.61	142.035
6	Extraction	P [kPa]	286.17	332.556	386.562
		T [°C]	211.03	211.044	210.298
7	Cascade	M [kg/s]	0	0	0
		T [°C]	25	25	25
8	Feedwater	M [kg/s]	251.57	342.773	425.801

The model was tested for each load case. Critical result parameters were then compared. Each LP-heater was also calibrated by adjusting the number of tubes plugged and fouling factor to correlate with the operational plant data. The parameter used to calibrate each LP-heater component was the condensate outlet temperature and the calibration load was 500 MW. The results are shown in Figure 6.3.

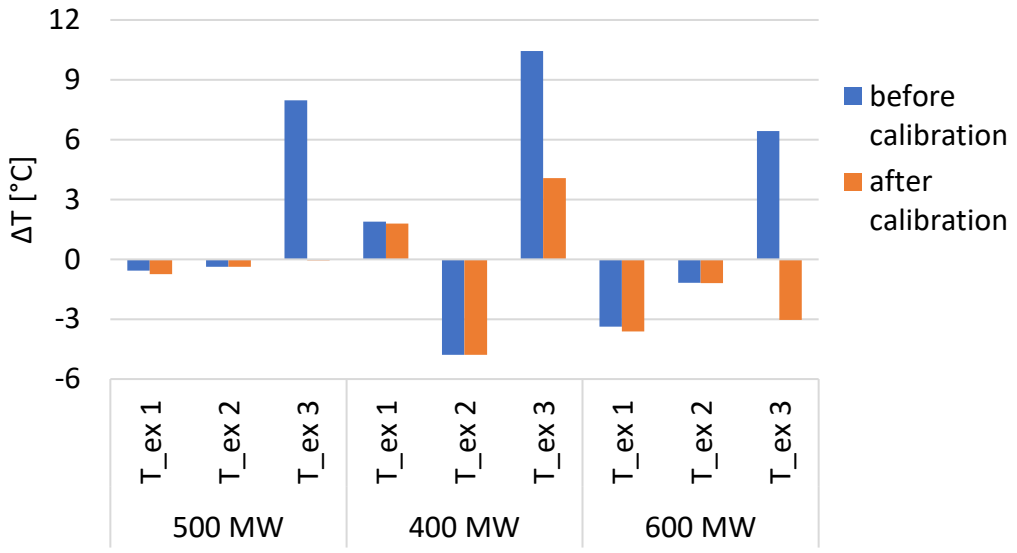

Figure 6.3: Steady-state temperature results for the low-pressure heater train of Lethabo power station at different loads

From initial inspection, one can see the temperature results for the first two heaters correlate relatively well with plant data before calibration. However, the exit temperature for heater three seems to overshoot for all three load cases. This is mostly due to the heater's design data being ideal heat balance data. After calibrating of the final heater for the 500 MW case, one can see a notable difference in results where temperature differences are seen under 4 °C for all three load cases.

The drain outlet mass flow was also compared to that of the plant data. The mass flow measurement is taken just before the condensate drain pump of heater one. The parameter's importance lies in the fact that the amount of bled-steam is proportional to the heat transfer of the feedwater heater since the parameter is determined by the two-phase tank.

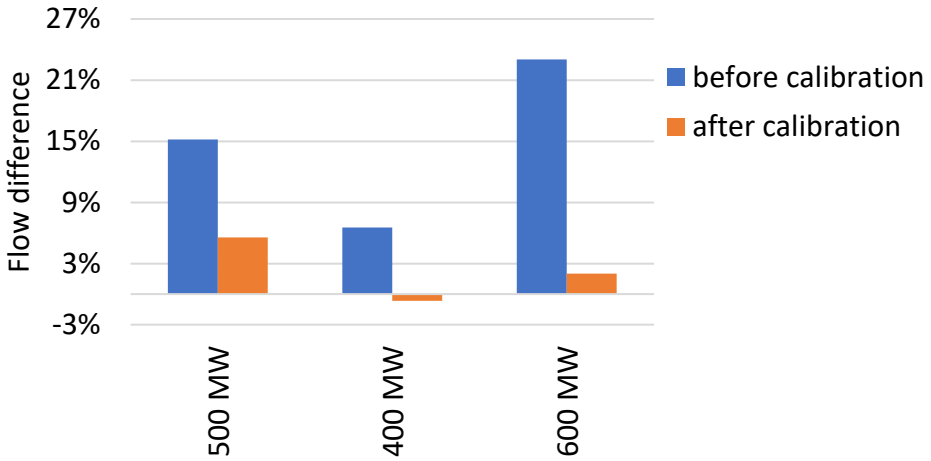

Figure 6.4: Steady-state drain outlet flow results for the low-pressure heater train of Lethabo power station at different loads

The bled-steam results from the low-pressure train before calibration show that more steam is extracted by the feedwater heaters than that indicated by the plant data. This correlates with what one would expect as more efficient heaters are able to handle more steam. After calibration, the model shows good agreeance with plant data, considering a mass flow measurement tolerance of 2%, where the error is 5% and under.

6.1.3 Transient scenario

A transient validation case was done on the low-pressure feedwater heater component where it was tested in an integrated heater train. The test was done to show that the heater can model an actual heater in service by using minimal design input data and at off-design transient conditions. The same network setup was used as in the steady-state scenario.

The off-design scenario was a sudden turbine trip. The scenario involved closing the bled-steam valves suddenly at the time of the trip and running the rest of the boundary conditions from plant data.

Inputting the power plant data into the Flownex in time-dependent increments was unfortunately not available and a script had to be developed to input the data in the boundary conditions of the model. The network setup is shown in Figure 6.5.

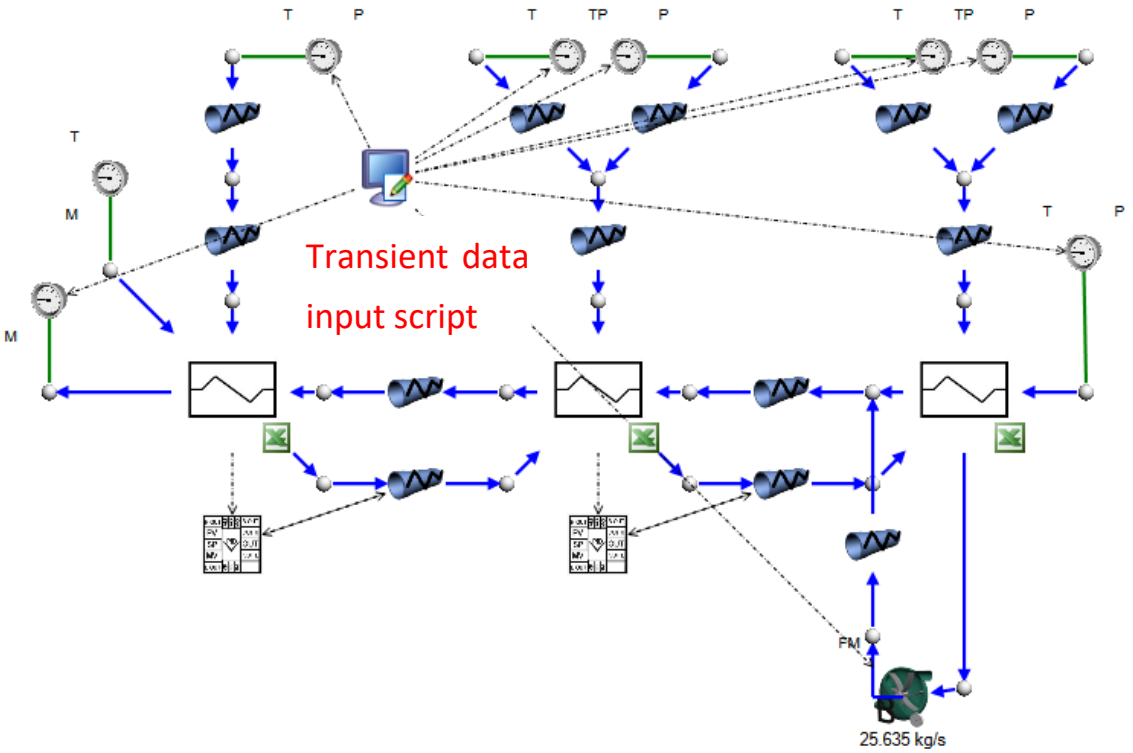

Figure 6.5: Transient network setup for the low-pressure heater train of Lethabo power station

The network setup included PID (Proportional, derivative and integral) components which have been roughly tuned to keep the level of the low-pressure feedwater heaters constant. One can also see that the boundary conditions are connected via data transfer links to the transient data input script. The simulation was run and the outlet condensate temperature of each heater was recorded. The recorded results are shown in Figure 6.6.

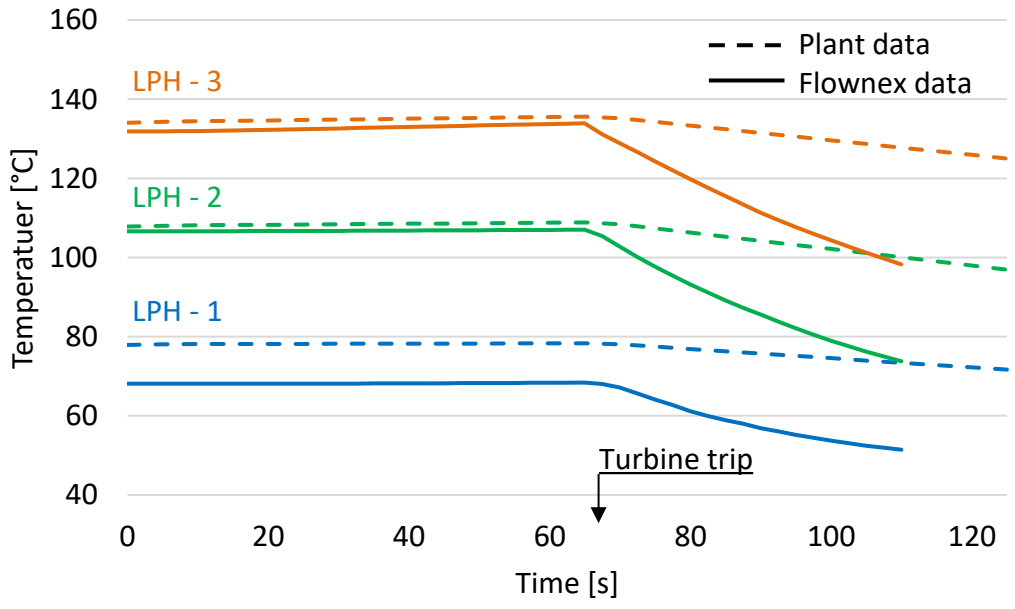

Figure 6.6: Transient results for low-pressure heater train with a sudden bled steam valve close

Initially, it can be observed that for low-pressure heater 2 and 3 the plant and Flownex data correlate well for the first 65 seconds. However, the first heater underperformed with condensate outlet temperatures 10 °C below the plant data. In the design, process heaters are sometimes over-designed as to still deliver the performance required in the cycle after fouling and tube plugging [30]. This might explain the discrepancy in the results for low-pressure heater 1.

The turbine trip event occurred at approximately 65 seconds. The bled-steam valves closed linearly at this time and it took 2-3 seconds for the valves to fully close. The results show that the condensate outlet temperatures of each heater in the Flownex model drops suddenly. This quick drop is not observed in the measured plant data. A second study was done where the time for the bled-steam valves to close was extended to 10-20 seconds. The results are shown in Figure 6.7.

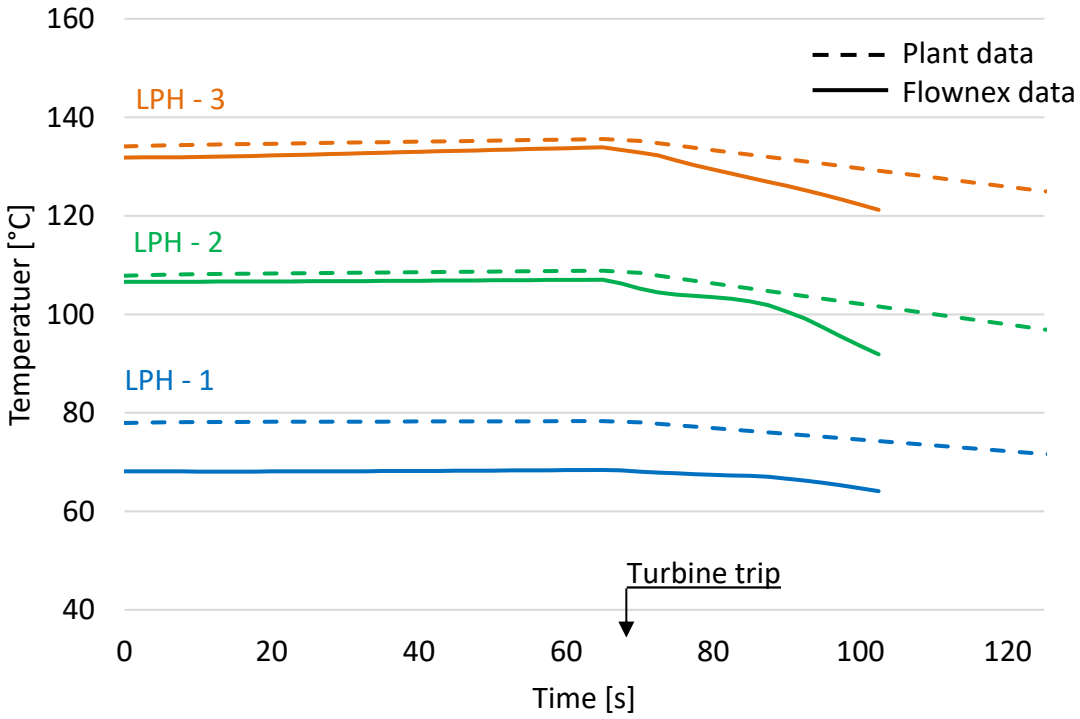

Figure 6.7: Transient results for low pressure heater train with a slow bled steam valve close

The results due to the slower bled-steam valve close seem to be more in line with what is seen on the plant data. Currently the valve's opening close linearly, but this will not reduce the mass flow linearly as per the flow element's quadratic equation. Further studies can be done to ensure that the mass flow through the bled-steam's valves reduces linearly which might result in a better comparison to what is seen in plant data.

6.2 High-pressure heater train

The High-Pressure heater train for Lethabo power station consists of two identical pairs of HP feedwater heaters. Each heater is mounted vertically and is of header type. The feedwater configuration is displayed in Figure 6.8.

The High-Pressure heater train consists of two heater banks or pairs, heater 5 and 6. Each bank is replicated and thus the feedwater stream is split into two streams flowing through each heater bank. Steam is extracted from the HP and IP turbines to the heaters. HP heater 6 cascades its condensed steam into heater 5 and heater 5 cascades the steam back to the deaerator or feedwater tank.

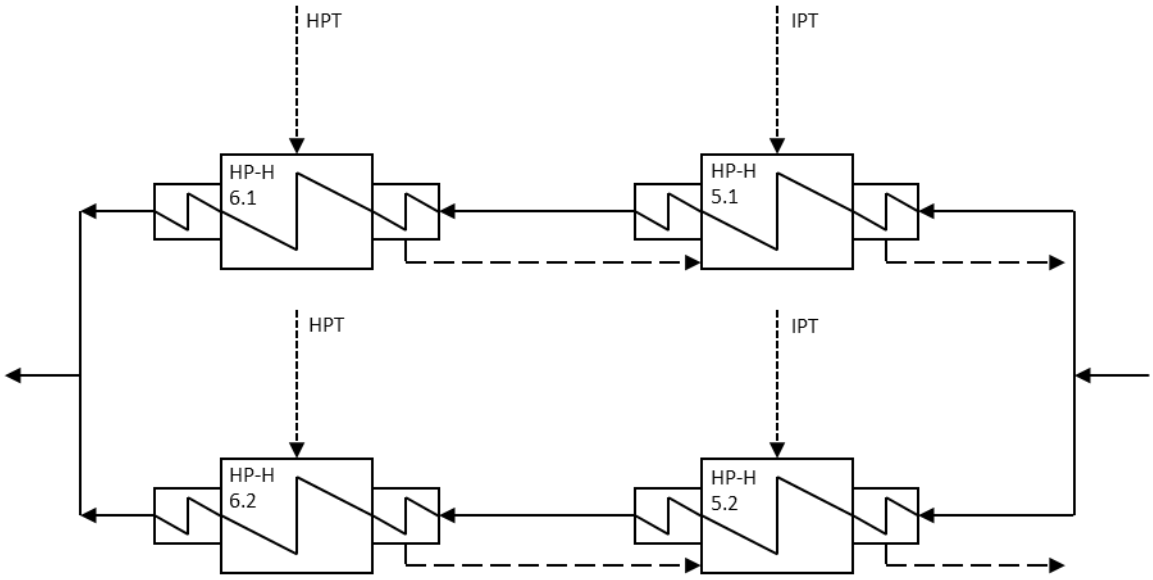

Figure 6.8: High-pressure heater train for power station 1

6.2.1 Flownex network

The high-pressure heater bank was modelled in the Flownex by using the HP feedwater heater component. Lethabo power station was used as a case study where the high-pressure heater bank consists of two pairs of vertical header type heaters. Heat and energy balance data and one or two geometrical drawings were used as input specifications for the heaters. The high-pressure heater bank Flownex model is shown in Figure 6.9.

The feedwater enters the train at boundary conditions number 1, thereafter it splits into two streams flowing through the heaters and returns into the same stream at boundary condition number 6. Extraction steam enters the heaters at boundary conditions number 3 and 4. The bled-steam then drains either into the downstream heater or to boundary conditions number 2. Boundary conditions number 5 are the cascade inlet flows for the heaters number 5 and 6.

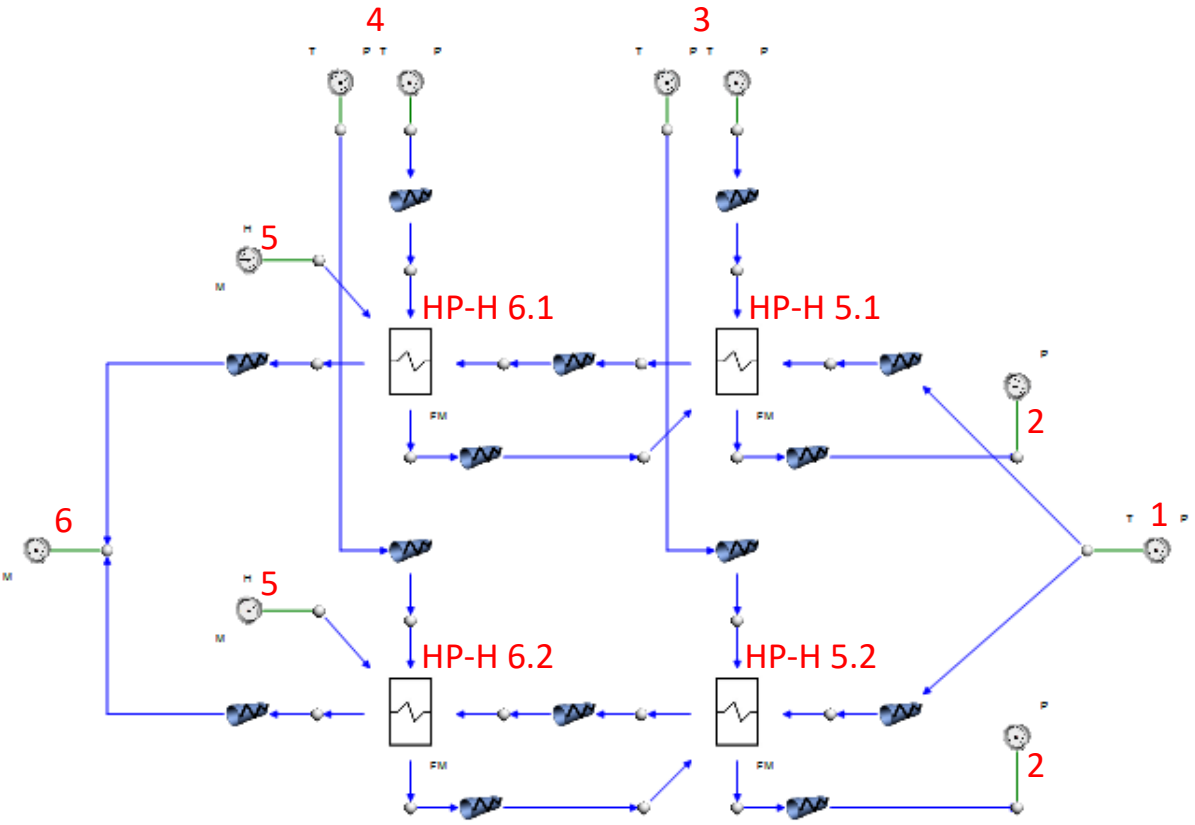

Figure 6.9 High-pressure heater train network in Flownex

6.2.2 Steady-state scenario

A similar steady-state scenario was run on the high-pressure heater network as for the low-pressure heater network. Load data was obtained from EtaPRO™ and the heaters were calibrated after initial testing. Boundary conditions are shown in Table 6.2.

Table 6.2: Boundary values for the high-pressure heater train of power plant 01

Boundary	Description	Property	400 MW	500 MW	600 MW
1	Feedwater	P [kPa]	828.51	890	1110
		T [°C]	38.77	41.851	45.801
2	Extraction	P [kPa]	30.61	36.854	40
		T [°C]	77.59	77.818	78.103
3	Extraction	P [kPa]	30.81	37.05	40
		T [°C]	77.59	77.818	78.103
4	Extraction	P [kPa]	92.1	112.675	133.766
		T [°C]	142.53	142.61	142.035
5	Extraction	P [kPa]	93.103	113.456	136.953
		T [°C]	142.53	142.61	142.035
6	Extraction	P [kPa]	286.17	332.556	386.562

		T [°C]	211.03	211.044	210.298
7	Cascade	M [kPa]	0	0	0
		T [°C]	25	25	25
8	Feedwater	M [kg/s]	-251.57	-342.773	-425.801

Recorded results for the high-pressure heater train included the feedwater outlet temperatures for each heater and the heater condensate outlet mass flow. The temperature and mass flow results are summarized in Figure 6.10 and Figure 6.11 respectively.

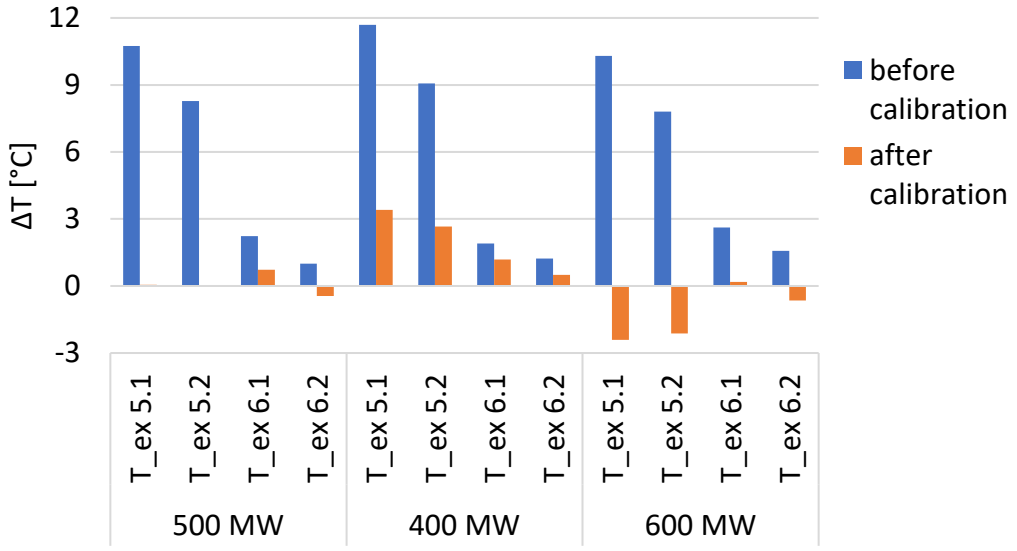

Figure 6.10: Steady-state temperature results for the high-pressure heater train of Lethabo power station at different loads

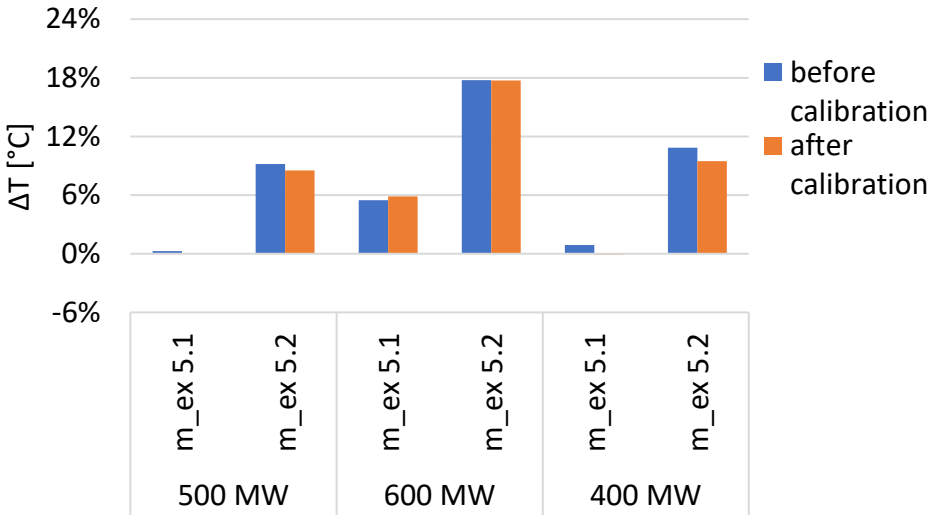

Figure 6.11: Steady-state bled steam mass flow results for the high-pressure heater train of Lethabo power station at different loads

From the temperature results in Figure 6.10 one can see that the heaters overperform before calibration but after calibration, results at all three load cases agree well with operational plant data.

Mass flow results in Figure 6.11 agree well for the first bank, i.e. heater 5.1 and 6.1 for all load cases. The results for the other heater bank (heater 5.2 and 6.2) do not agree as well with plant data. A possible cause for the difference is that the exact flow distribution through the heaters for the extraction steam is not known. Instead, a duplicate boundary condition with the same inputs as for heater bank 1 was set up.

6.3 Full cycle integration

Full cycle integration was done on the three components. The purpose of the integration was to illustrate that the components can work on a full cycle whilst using minimal design input data. Also, the components were tested at various load conditions to show that the components have a high degree of fidelity.

6.3.1 Model description

Kriel power station was used as a test case, where the heat balance diagram was used as a blueprint for the network setup. The network contained the main components of the steam cycle and some auxiliary components. The complete network consisted of the following components summarized in Table 6.3. It should be noted that the HP heater train is split into two identical banks, but is assumed to be one train in the model.

Table 6.3: Components of the full component integration

Type	Component	Quantity	Fluid
Main	Turbine with no extraction	1	High-pressure steam
	Turbine with 2 extractions	3	Intermediate and low-pressure steam
	Low-pressure heater	4	Condensate, bled steam
	Deaerator	1	Condensate, bled steam, feedwater
	High-pressure heater	2	Feedwater, bled steam
	Boiler feed pump	1	Feedwater
Auxiliary	Condensate pump	2	Condensate
	Throttle valve	1	High-pressure steam
	Valve	4	Condensate, feedwater
	Boundary conditions	12	-
	Various pipes	31	Condensate, bled steam, feedwater

The network diagram of the complete cycle is shown in Figure 6.12. It should be noted that in the current integrated model, the boiler, condenser and condenser feed pump is set as boundary conditions since it is outside the scope of the project. These boundary conditions are shown in Figure

6.13. Also, zero boundary conditions have been set to the feedwater heaters that do not contain any cascade from an upstream heater.

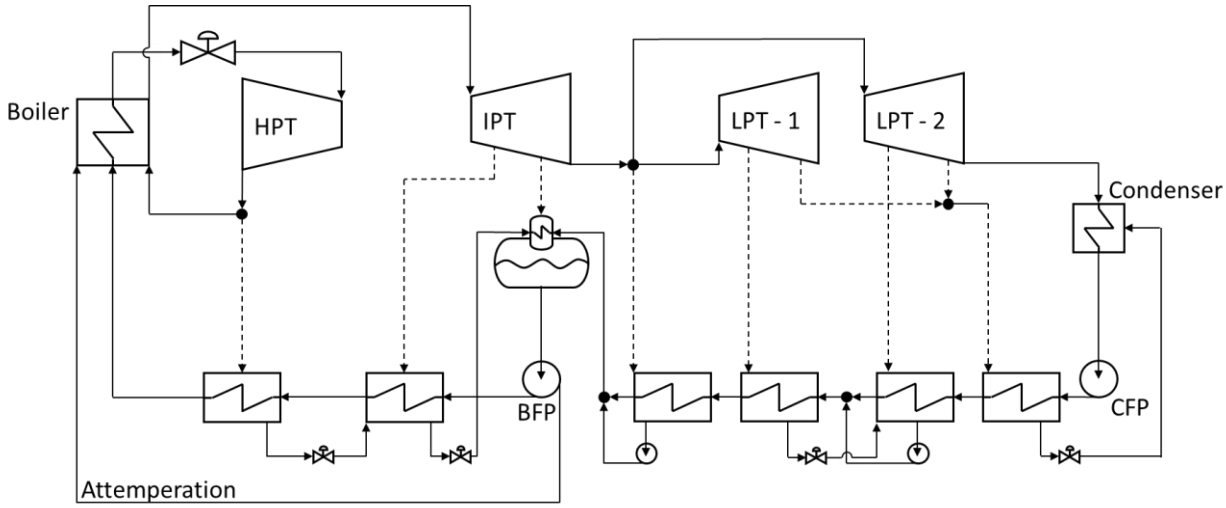

Figure 6.12: Network diagram of complete cycle integration

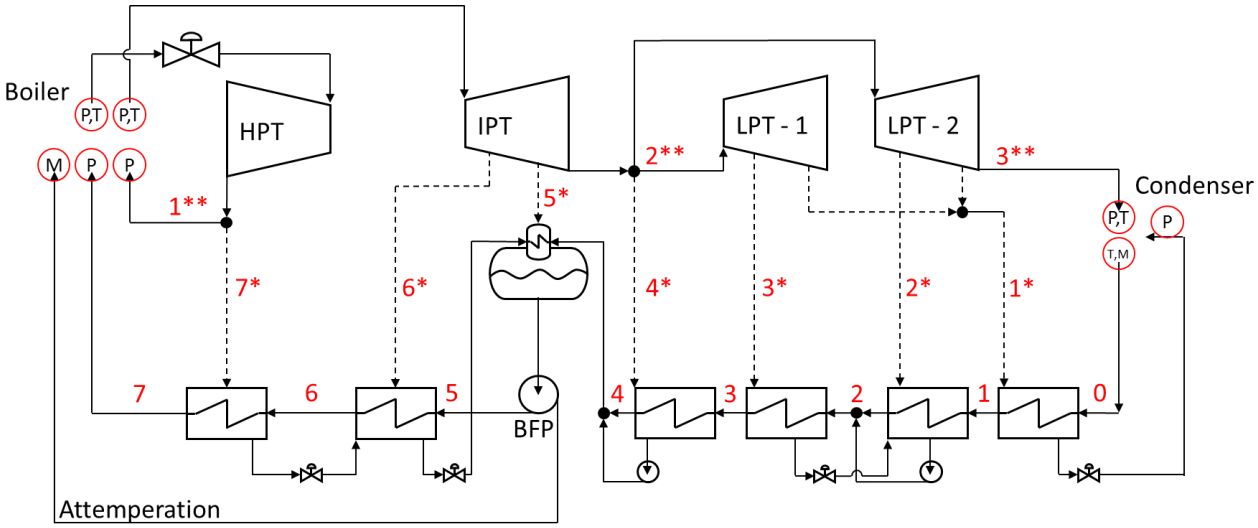

Figure 6.13: Network of integrated cycle with boundary conditions

The network consisted of two main streams, i.e., the condensate/feedwater stream and the main steam stream. These two networks are then interconnected through extraction points. The extraction points are shown as dotted lines in both Figure 6.12 and Figure 6.13.

The boundary conditions set for the main steam stream were inlet pressure and temperature conditions and outlet pressure conditions. The condensate/feedwater contains inlet mass flow and temperature conditions and an outlet pressure condition.

An additional auxiliary component was added to the full cycle, which was the throttle valve at the inlet of the main turbine. This component was developed by Fuls [53] and the purpose is to model the control valve found in front of the main steam turbine.

This throttle valve component is used in the network to control the amount of steam flowing through the network. The input required is the design mass flow and a percentage operating mass flow is then specified which determines the opening and closing of the valve. The valve is modelled by using the well-known flow resistance component. The Flownex network of the control valve is shown in Figure 6.14.

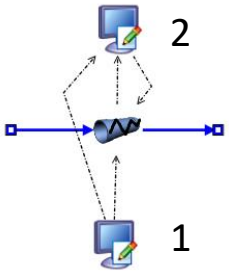

Figure 6.14: Control valve Flownex network

The bottom script in Figure 6.14 sets the component to model the pressure drop as specified during design conditions, whilst the valve is fully open. The second script determines the mass flow based on the user's specified throttle ratio.

The model in Flownex is shown in Figure 6.15. Most of the components were connected by the flow resistance elements where the element's flow resistance was set not induce a pressure drop. Through these components, the network becomes more manageable and the various measurement points can be done. One can also observe that the networks look very similar to that of the flow diagram in Figure 6.12.

It should be reiterated that the network integration was done to test component integration and to show that that the components can operate under various load conditions. The final integrated Flownex network contained the following assumptions and limitations:

- Only steady-state scenarios were run, thus eliminating the need for a complex control system.
- No shafts were connected to the network, as this is only needed for transient behaviour of the cycle.
- Main boundary conditions set up for the boiler and condenser as explained above.
- Turbine component's efficiency set to a rough estimation of actual plant data of the turbine efficiencies were not available.
- The attemperation steam was taken after boiler feed pump wherein actual plant conditions the steam is bled from between the pump's stages. This can be done by splitting the pump into two separate pump stages but complications with regards to the modelling of two pumps after the boiler were encountered.

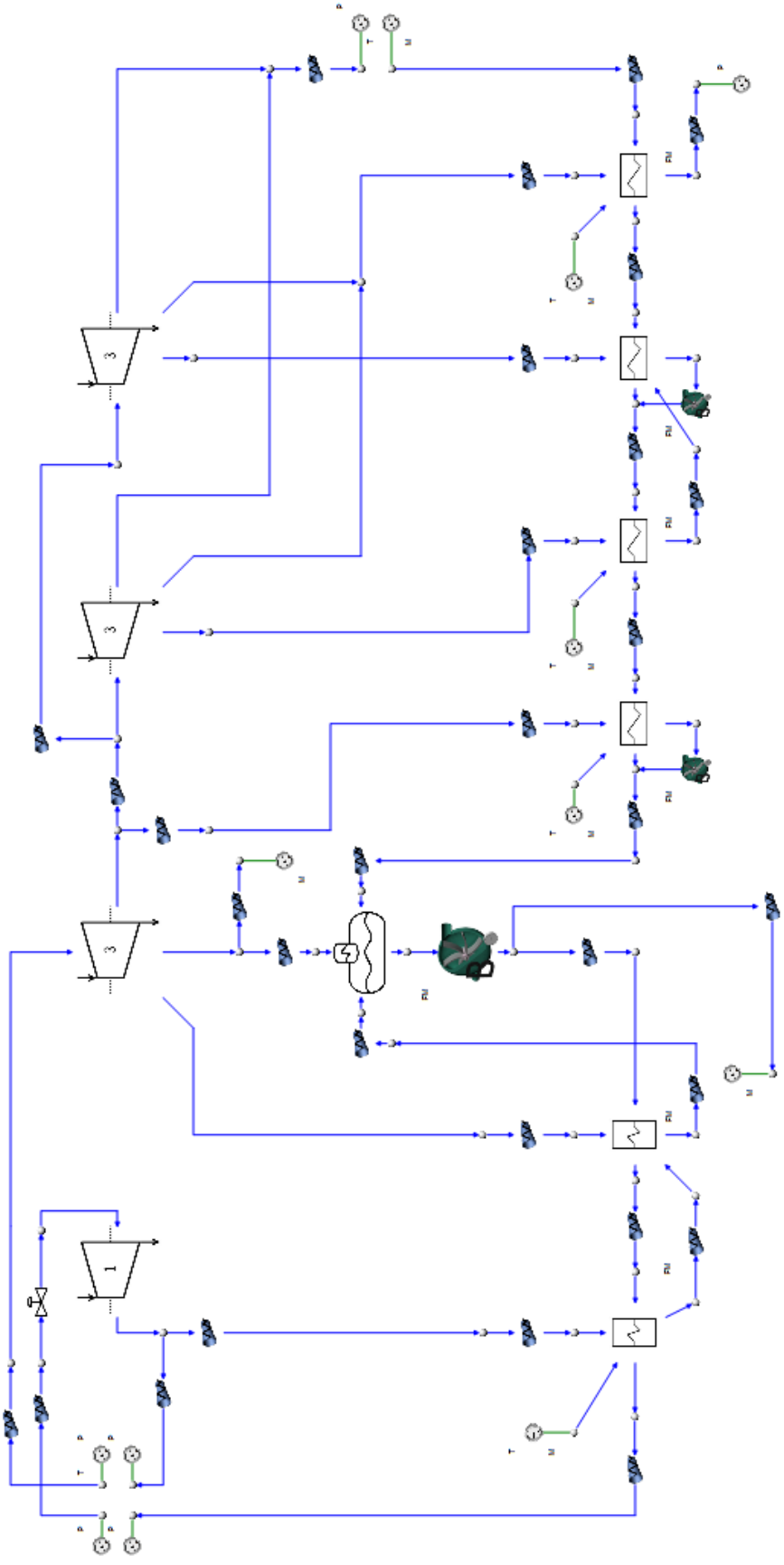

Figure 6.15: Integrated cycle in the Flownex

6.3.2 Model results and discussion

The network's main measurements were taken, as indicated in Figure 6.13, for the four different load cases and compared to plant acceptance test data.

The condensate and feedwater temperature results are shown in Figure 6.16 and the steam temperatures are shown in Figure 6.17. The maximum difference in temperature is indicated at the top of each measurement point in the graphs.

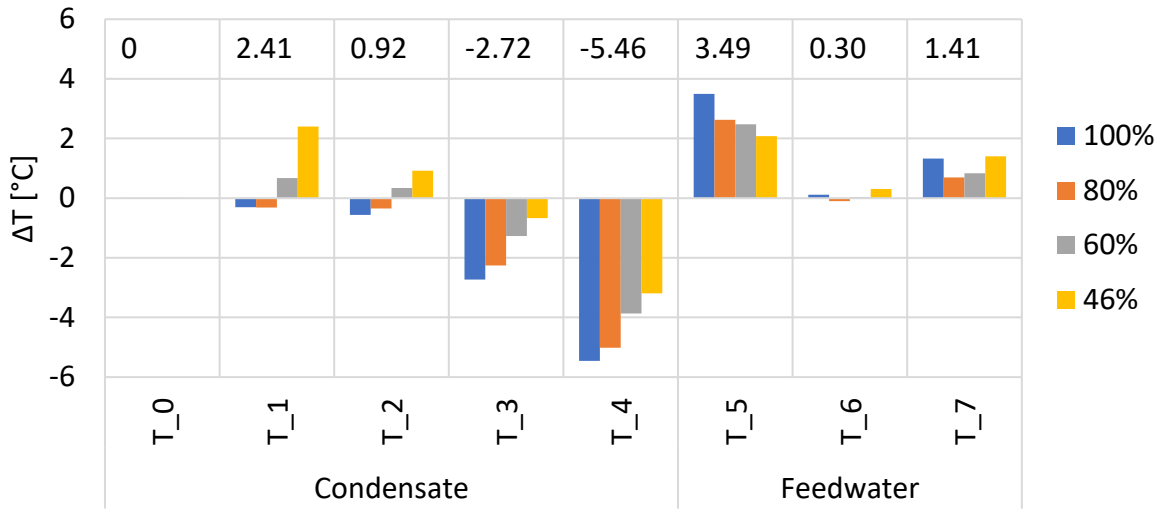

Figure 6.16: Full integrated cycle condensate and feedwater temperature results

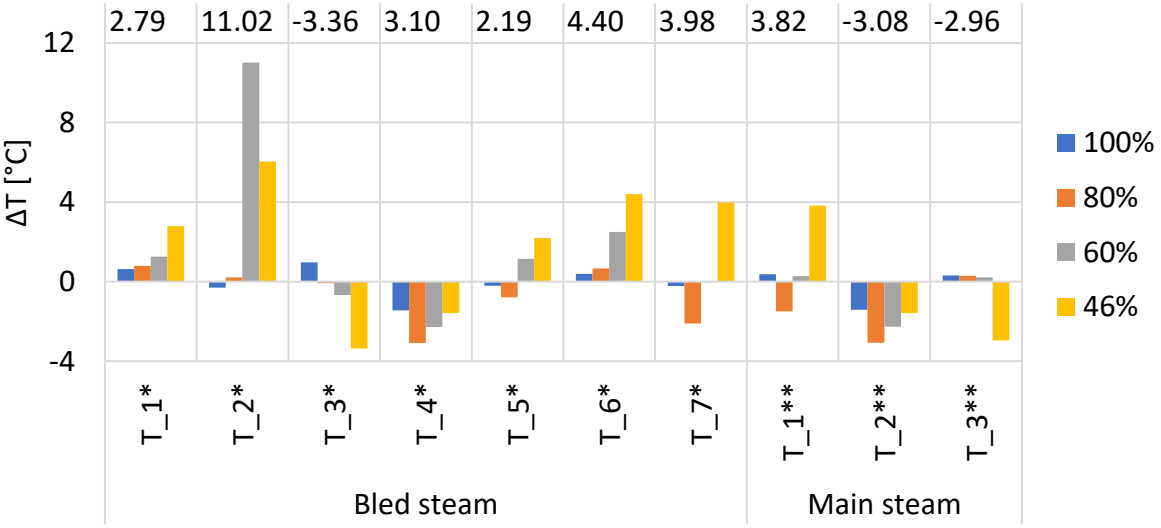

Figure 6.17: Full integrated cycle steam temperature results

From initial inspection, one can see that the feedwater and temperature results are all under 6°C. The steam temperatures are all under 5°C, except for the temperature measurement at measurement point 2* for 60% load case, which is at the first extraction point of the LP turbine.

The main flow results compared to plant acceptance test data is shown in Figure 6.18 and Figure 6.19. The maximum percentage difference of each measurement for the different loads is again showed at the top of the graph.

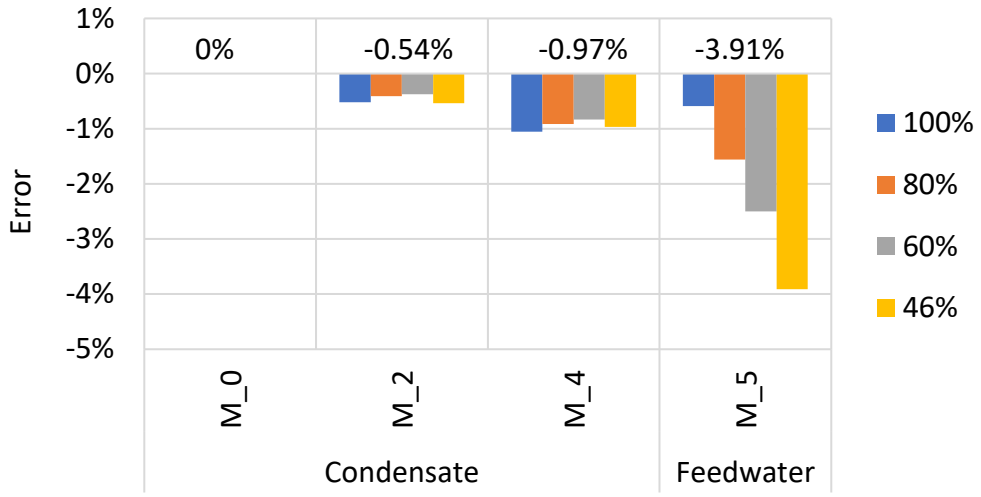

Figure 6.18: Full integrated cycle condensate and feedwater flow results

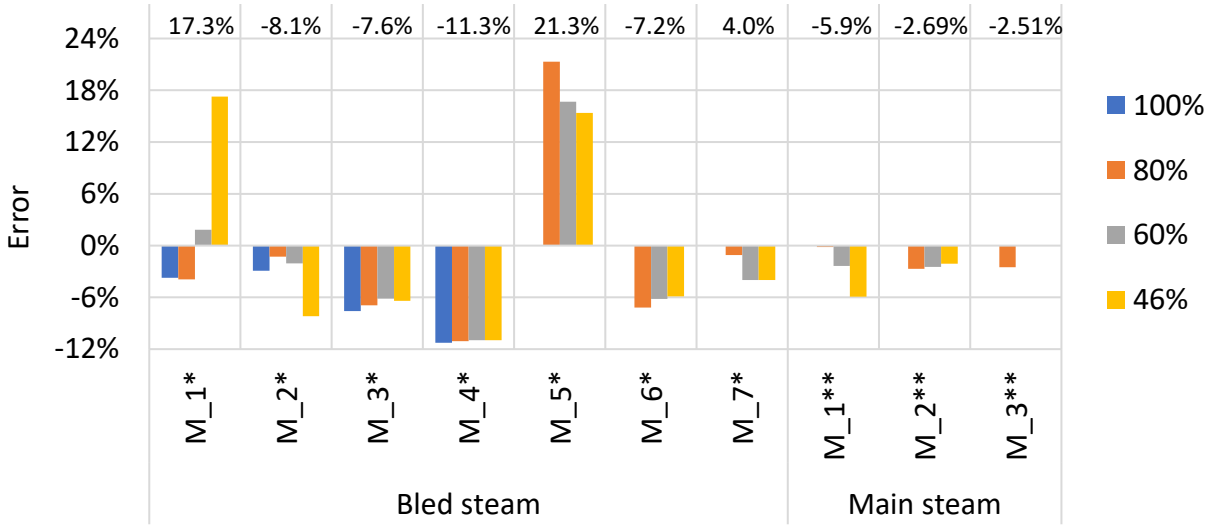

Figure 6.19: Full integrated cycle steam flow results

The condensate and feedwater mass flows are all under 4%, with the highest being the mass flow after the deaerator. The main steam mass flows, designated as M**, are for all load cases under 6%. The bled-steam mass flows differ quite significantly but if one were to look at the amount of bled-steam compared to the main steam flow, the difference is not that significant.

The steam pressure results are shown in Figure 6.20 where the maximum pressure difference is again shown at the top of the figure for each measurement point.

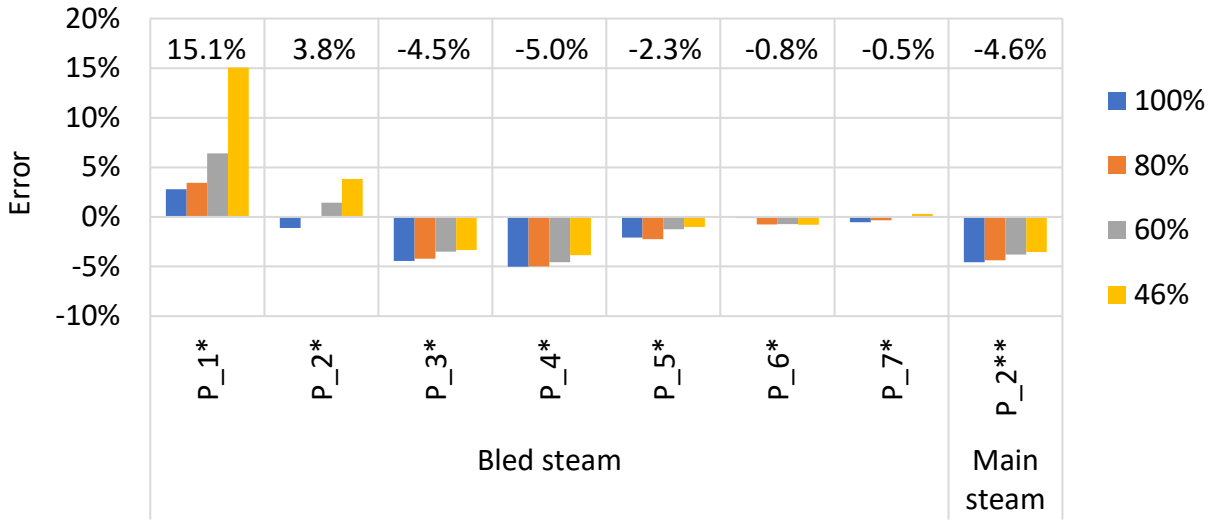

Figure 6.20: Full integrated cycle steam pressure results

One can see from the figure that most of the pressure differences all fall under 5% difference. It is only the pressure difference of bled-steam point 1 at the low-pressure turbine which is above the norm. By considering the amount of mass flow for this extraction point at the lowest load, the difference is not significant.

7. Project conclusions and recommendations

7.1 Project's conclusions

The purpose of the study was to develop the components for a high-fidelity transient engineering simulator of a large coal-fired power station, which consisted of the feedwater heater, deaerator and the turbine. The component models were developed using the following design requirements:

- Use and enhance existing methodologies for modelling power plant components.
- Develop the models using minimal design inputs.
- Include transient behaviour into the models such as level change, thermal inertia and rotational inertia.
- Package the components for further use, with the aim of cycle integration.
- Integration of the models in a complete power station cycle with validation using plant data.

The four points mentioned, were achieved for all three components. Each component was developed by using minimal design inputs and results from various verification and validation studies compare well with plant data. The components could also be fully integrated into a complete cycle. The components showed a high degree of fidelity when operating in the cycle and off-design conditions could also be tested.

Following is a brief conclusion of each component while the full cycle integration is expounded on in the last section.

7.1.1 Feedwater heater

A Feedwater heater component has been developed in Flownex. The model is a generalized model and can be applied to most of the ESKOM feedwater heaters. The heater model has been packaged into three high-level components: a heater with no geometrical specifications, with vertical specifications and with horizontal specifications.

The heater models all three heat transfer zones with the major assumption that steam exits the DSH zone at saturated conditions. The heater furthermore models the COND zone by employing plant performance data and correlates the amount of heat transfer with feedwater mass flow by using the overall HTC. This enables the heater to model the heat transfer with minimal design input data accurately, which is valuable especially when very little information is available for the heater in service.

Transient effects due to thick metal components such as pipe walls and the tubesheet are also included in the model. This enabled a case study to be done where the various pipe and flow configurations using the Biot number could be analysed. The study showed that uncertainties associated with the convective HTC during transient scenarios play a larger role with high-pressure heaters than for low-pressure heaters.

A comprehensive methodology for the liquid level inside the heater was developed with the aim of modelling the level change using minimal input data. The methodology proved to be successful when results were compared to a simplified feedwater heater 3D CAD model.

The model was finally validated with plant data. Results show good agreement, especially considering that the heater was defined using heat balance data and tested with plant acceptance test data. Results also show very good agreement with main temperature measurement differences under 2 °C. Steam mass flow, which is determined by the model, showed an error of under 5 % for all load cases.

7.1.2 Turbine

A Flownex model for the turbine component was developed which can be applied to impulse or reaction type turbines. The turbine also accommodates multiple extraction lines, which enables it to be used in a Rankine cycle with regeneration.

The pressure drop of the component is modelled by using Fuls' semi-ellipse law [54], which is an improvement to the original Stodola's ellipse law, especially at off-design conditions. The pressure drop is also modelled by using very little design input data but with a good degree of accuracy, especially under off-design conditions.

The efficiency of the model is modelled by using Ray's method, which includes design conditions and operational conditions. It could be shown in the literature study that Ray's method shows better results compared to three other common efficiency methods and thus it was chosen to be used in the current model.

Transient characteristics, thermal inertia due to shaft and casing and rotational inertia due to the shaft of the component could also be shown at various conditions. These conditions specifically included short transient scenarios, which was one of the main outcomes from the literature study.

7.1.3 Deaerator

A deaerator component model has been developed in Flownex. The model contains all the inlet and outlet flows, except for the vent outlet since the loss of flow through the vent will not influence the overall cycle results significantly.

The model can simulate the pressure drop over the main condensate inlet valve using design data. This now enables the model to be used as a generalized model in the power station network.

The model was set up using heat balance data and validated using plant data where mass flow and temperature results correlated within plant measurement tolerances. The model was finally packaged into an easy to use compound component with the focus on integration.

7.1.4 Component integration

Component integration has been done using the three packaged components.

Integration was initially done for the low-pressure heater by developing a low-pressure heater train. The heaters were set up using design heat balance data and plant drawings and results were compared using operational plant data. Initial temperature results showed that the heaters overperformed and after calibration, the main temperature differences were under 4°C.

The low-pressure heater models were set up for the same power station to test a short transient scenario; the scenario involved a turbine trip. The model's results initially compared well with plant data, and after the turbine trip temperatures seemed to fall quicker than that of the plant data. The closing speed of the extraction steam valves was decreased and results after the turbine trip showed a better comparison with plant data.

The high-pressure heater train was also modelled using the same methodology and power station. Steady-state results for the train could be obtained and after calibration, main temperature results were within 4°C at various load cases.

The three components were finally integrated into a complete cycle which consisted of an HP, IP and LP turbines, four LP and two HP heaters, and a deaerator component. Built-in Flownex components and a custom throttle valve component (developed by Fuls [46]) were used to model the various pumps and valves. The boundary conditions of the network consisted of the boiler, condenser and condenser feed pump components.

Steady-state results from the integrated network showed good agreement with plant data where main condensate and feedwater temperature differences were under 6°C for all load cases. Main

mass flow results were under 6% for all load cases. These results therefore indicate that the components were successfully integrated and of high-fidelity.

7.2 Project's recommendations

The following recommendations are proposed for the project concerning future work:

- A better geometrical representation can be achieved for specifically the header type feedwater heater.
- The turbine component's pressure drop law contains a critical pressure ratio and critical pressure ratio exponent which can be implemented by using methods presented by Fuls [46].
- A better defined short transient scenario for the low-pressure heater train can be used as validation.
- The complete integrated network can be combined with a control network to model the network during a transient scenario.
- Shaft components can be connected to the turbine train in the interconnected network.
- Boiler and condenser components can finally be used to replace the boundary components in the network to make the network a fully integrated power station cycle.

8. Bibliography

[1] R. Starkloff, F. Alobaid, k. Karner, B. Epple, M. Schmitz and F. Boehm, "Development and validation of a dynamic simulation model for a large coal-fired power plant," *Applied Thermal Engineering,* no. 91, pp. 496-506, 2015.

[2] R. Neerputh, "Development of appropriate steam turbine models in Flownex," Cape Town, 2014.

[3] R. B. Banda, "Modelling of the deaerator system in Flownex," Cape Town, 2015.

[4] M. N. Allie, "Thermal Modelling of Feedwater Heaters," Cape Town, 2016.

[5] M. Thakaso, "Development of a Performance-based High Pressure Feed-water Heater Model for Flownex SE," Cape Town, 2014.

[6] P. K. Nag, Power plant Engineering, New-Delhi: Tata McGraw-Hill Education, 2008.

[7] A. Rossouw, "Boiler system modelling using Flownex ®," Cape Town, 2015.

[8] K. Rayaprolu, Boilers for power and process, CRC press, 2009.

[9] A. T. Sayers, Hydraulic and Compressible flow Turbomachines, Cape Town: Mcgraw Hill Book Co Ltd, 1990.

[10] "Flownex General User Manual," Flownex SE, 2015.

[11] "Flownex Theory Manual," Flownex SE, 2015.

[12] A. J. Kriel, "Pressure formulation and adaptive control of numerical algorithms for transient flow in pipes," Potchefstroom, 2012.

[13] F. Alobaid, M. Nicolas, S. Ralf, L. Thomas, H. Christian and E. Bernd, "Progress in dynamic simulation of thermal power plants," *Progress in Energy and Combustion Science,* vol. I, no. 59, pp. 79-162, 2016.

[14] S. Lu, "Dynamic modelling and simulation power plant systems," *Proc Instn Mech Engrs part A,* no. 213, pp. 1-6, 1999.

[15] M. Shirakawa, "Development of a thermal power plant simulation tool based on object orientation," *Power and Energy,* vol. 220, no. 6, pp. 517-524, 2006.

[16] P. Colonna and H. van Putten, "Dynamic modeling of steam power cycles. Part I - Modeling paradigm and validation," *Applied thermal engineering,* no. 27, pp. 467-480, 2007.

[17] H. van Putten and P. Colonna, "Dynamic modeling of steam power cycles: Parrt II - Simulation of a small simple Rankine cycle system," *Applied thermal engineering,* no. 27, pp. 2566-2582, 2007.

[18] S. Meinke, F. Gottelt, M. Müller and E. Hassel, "Modeling of Coal-Fired Power Units with ThermoPower gocussing on Start-Up process," Germany, 2011.

[19] F. Casella and A. Leva, "Modelling of thermo-hydraulic power generation processes using Modelica," Italy, 2006.

[20] E. Oko and M. Wang, "Dynamic modelling, validation and analysis of coal-fired subcritical power plant," *Fuel,* no. 135, pp. 292-300, 2014.

[21] "ASME PTC 6: Steam Turbine Performance Codes," ASME, New York, 2004.

[22] "EtaPro," GP Strategies, 2017. [Online]. Available: http://www.etapro.com. [Accessed 31 October 2017].

[23] "Generic Plant Breakdown," ESKOM, 1998.

[24] "Seamless steel pipe," 2014. [Online]. Available: https://goo.gl/vGvNNe. [Accessed 24 February 2017].

[25] M. Youssef and S. C. Techn, "Header type feedwater heaters as retrofits for cycling units," in *Power-Gen Europe*, Paris, 1993.

[26] Standards for Closed Feedwater Heaters, Ohio: Heat Exchange Institue inc., 2009.

[27] M. Youssef, "Feedwater Heaters, Coolers," [Online]. Available: http://goo.gl/IT2N2l. [Accessed 5 March 2016].

[28] T. Barszcz and P. Czop, "Presentation of a virtual power plant environment and its application with combined first-principle and data-driven models intended for the diagnostics of a power plant – Part 1," *Simulation,* vol. II, no. 88, pp. 139-166, 2011.

[29] D. Koehler and G. Weber, "Using PEPSE to analyse feedwater heaters with long drain coolers," Commonwealth edison company, 1990.

[30] P. M. Subba rao, Design Fundementals of Shell-and-Tube Heat Exchangers, iitdelhi.

[31] Y. K. Shweta, S. B. Jagadish and M. B. Manjunath, "Analysis Comparing performance of a Conventional Shell and Tube Heat Exchanger using Kern, Bell and Bell Delaware Method," *International Journal of Research in Engineering and Technology,* vol. III, no. 3, 2014.

[32] G. Weber and G. L. Minner, "Using the PEPSE JW method to evaluate the deisgn performance of a feedwater heater with a short drain cooler," Commonwealth edison company, 1994.

[33] M. Á. Fernández, L. d. P. Valdés and C. A. Tristán c, "Thermal analysis of closed feedwater heaters in nuclear power plants," *Applied thermal of closed feedwater heaters in nuclear power plants,* vol. 68, no. 1-2, pp. 45-58, 2014.

[34] I. S. Hussaini, S. M. Zubair and M. A. Antar, "Area allocation in multi-zone feedwater heaters," *Energy Conversion & Management,* no. 48, pp. 568-575, 2007.

[35] M. A. Antar and S. M. Zubair, "The impact of fouling on performance evaluation of multi-zone feedwater heaters," *Applied Thermal Engineering,* vol. I, no. 27, pp. 2505-2513, 2007.

[36] J.-q. Xu, T. Yang, Y.-y. Sun, K.-y. Zhou and Y.-f. Shi, "Research on varying condition characteristic of feedwater heater considering liquid level," *Applied Thermal Engineering,* no. 67, pp. 179-189, 2014.

[37] S. M. Hossienalipour, S. M. Karbalaee and H. Fathiannasab, "Development of a model to evaluate the water level impact on drain cooling in horizontal high pressure feedwater heaters," *Applied Thermal Engineering,* no. 110, pp. 590-600, 2017.

[38] J. F. Heiss and J. Coull, "Nomograph of Dittus-Boelter Equation for heating and cooling liquids," *Industrial and chemical engineering,* no. 43, pp. 1226-1229, 1951.

[39] J. R. Thome, Engineering Data Book III, Lausanne: Faculty of Engineering Science and Technology, 2006.

[40] F. SE, "Flownex Library Manual," 2015.

[41] ESKOM, "Lethabo plant modules".

[42] L. C. Smith, "Succeed with condensate control," Chemical processing, 2008.

[43] F. P. Incropera, D. P. Dewitt, T. L. Bergman and A. S. Lavine, Principles of Heat and Mass Transfer, Singapore: John Wiley & Sons, 2013.

[44] M. Banaszkiewicz, "Steam turbines start-ups," *Transactions of the institute of fluid-flow machinery,* vol. I, no. 126, pp. 169-198, 2014.

[45] W. F. Fuls, "Accurate stage-by-stage modelling of axial turbines using an appropriate nozzle analogy with minimal geometric data," *Applied Thermal Engineering,* no. 116, pp. 134-146, 2017.

[46] W. F. Fuls, "Enhancement to the traditional ellipse law for more accurate modelling of a turbine with a finite number of stages," Cape Town, 2016.

[47] A. Stodola, Steam and Gas Turbines, New york: Peter Smith, 1945.

[48] A. Ray, "Dynamic modelling of power plant turbines for controller design," 1979.

[49] ECODYNE, "Spray-Tray," ECODYNE LIMITED, [Online]. Available: https://goo.gl/SXnw9Z. [Accessed 15 May 2016].

[50] "Spray & Tray type Deaerator," KOREA ENERGY INDUSTRIES, LTD., [Online]. Available: http://goo.gl/aM7l6U. [Accessed 15 May 2016].

[51] ECODYNE, "Spray-Scrubber," ECODYNE LIMITED, [Online]. Available: https://goo.gl/B5g4dG. [Accessed 15 May 2016].

[52] K. V. Sharma, K. V. Suryanarayana, P. K. Sarma, V. Dharma Rao and T. Subramanyam, "Oxygen stripping in deaerator feed water: condensation on spray droplets," *Heat and Mass Transfer,* vol. 46, no. 6, pp. 665-673, 2010.

[53] W. F. Fuls, "Simple Rankine Cycle Components," Cape Town, 2017.

[54] D. W. Fuls, "Enhancement to the traditional ellipse law for more accurate modelling of a turbine with a finite number of stages," Cape Town, 2016.

[55] L. Jestin, M. Fawkes, B. Maccoll and M. Koko, "Eskom Power Plant Engineering Institute (EPPEI), 5 - years research strategic plan," 2014.

[56] K. Krüger, M. Rode and R. Franke, "Optimal control for fast boiler start-up based on a nonlinear model and considering the thermal stress on thick-walled components," in *Conference on Control Applications*, Mexico City, 2001.

[57] K. J. Åström and R. D. Bell, "Drum-boiler dynamics," *Automatica,* no. 36, pp. 363-378, 2000.

[58] F. Alobaid, R. Starkloff, S. Pfeiffer, K. Karner, B. Epple and H.-G. Kim, "A comparative study of different dynamic process simulation codes for combined cycle power plants - Part A: loads and off-design operation," *Fuel,* vol. I, no. 153, pp. 692-706, 2015.

Appendix A. Mathcad verification

Appendix A contains the Mathcad code used to define the scripts in the Flownex models. The Mathcad calculations can be used as verification to the scripting components in the feed-heater and turbine components.

1. Closed feedwater heater

1. Performance characteristics

Load condition inputs:

$LC :=$

	0	1	2	3	4	5	6	7	8	9
0	1	1915	$2.05 \cdot 10^4$	3344	725.8	914.1	17.737	247.567	18.758	935.2
1	2	1526	$1.95 \cdot 10^4$	3350.9	680	873.9	13.94	198.412	13.94	884.1
2	3	1156	$1.87 \cdot 10^4$	3342.2	629.2	824	10.069	149.56	10.069	824.9
3	4	808.1	$1.8 \cdot 10^4$	3267.6	572	757.6	6.53	104.348	6.53	752
4	5	0	0	0	0	0	0	0	0	0
5	6	0	0	0	0	0	0	0	0	0

Unit conversion:

$i := \mathbf{0} .. \mathbf{5}$

$p_{BS.inlet_i} := LC_{i,\mathbf{1}} \cdot kPa$

$p_{FW.outlet_i} := LC_{i,\mathbf{2}} \cdot kPa$

$h_{BS.inlet_i} := LC_{i,\mathbf{3}} \cdot \frac{kJ}{kg}$

$h_{BS.outlet_i} := LC_{i,\mathbf{4}} \cdot \frac{kJ}{kg}$

$h_{FW.outlet_i} := LC_{i,\mathbf{5}} \cdot \frac{kJ}{kg}$

$m_{BS_i} := LC_{i,\mathbf{6}} \cdot \frac{kg}{s}$

$m_{FW_i} := LC_{i,\mathbf{7}} \cdot \frac{kg}{s}$

$m_{CAS_i} := LC_{i,\mathbf{8}} \cdot \frac{kg}{s}$

$h_{CAS.inlet_i} := LC_{i,\mathbf{9}} \cdot \frac{kJ}{kg}$

Heat transfer calculation for each zone:

$$Q_{DC_i} := \begin{cases} \left(m_{BS_i} + m_{CAS_i}\right) \cdot \left(h_{steam}\left(p_{BS.inlet_i}, "", "", \mathbf{0}, ""\right) - h_{BS.outlet_i}\right) & \text{if } p_{BS.inlet_i} > \mathbf{0} \\ (\mathbf{0} kW) & \text{if } p_{BS.inlet_i} = \mathbf{0} \end{cases} = \blacksquare$$

$$Q_{DSH_i} := \begin{cases} m_{BS_i} \cdot \left(h_{BS.inlet_i} - h_{steam}\left(p_{BS.inlet_i}, "", "", \mathbf{1}, ""\right)\right) & \text{if } p_{BS.inlet_i} > \mathbf{0} \\ (\mathbf{0} kW) & \text{if } p_{BS.inlet_i} = \mathbf{0} \end{cases} = \ldots$$

$$Q_{COND_i} := \begin{cases} m_{BS_i} \cdot h_{steam}\left(p_{BS.inlet_i}, "", "", \mathbf{1}, ""\right) \ldots & \text{if } p_{BS.inlet_i} > \mathbf{0} = \ldots \\ + -\left[\left(m_{BS_i} + m_{CAS_i}\right) \cdot h_{steam}\left(p_{BS.inlet_i}, "", "", \mathbf{0}, ""\right) + m_{CAS_i} \cdot h_{CAS.inlet_i}\right] & \\ (\mathbf{0} kW) \quad \text{if } p_{BS.inlet_i} = \mathbf{0} & \end{cases}$$

$$Q_{DSH} = \begin{pmatrix} \mathbf{9694.298} \\ \mathbf{7797.767} \\ \mathbf{5636.358} \\ \mathbf{3257.726} \\ \mathbf{0} \\ \mathbf{0} \end{pmatrix} \cdot kW \quad Q_{COND} = \begin{pmatrix} \mathbf{34364.901} \\ \mathbf{27584.954} \\ \mathbf{20393.832} \\ \mathbf{13549.838} \\ \mathbf{0} \\ \mathbf{0} \end{pmatrix} \cdot kW \quad Q_{DC} = \begin{pmatrix} \mathbf{6307.635} \\ \mathbf{4694.778} \\ \mathbf{3258.965} \\ \mathbf{1970.104} \\ \mathbf{0} \\ \mathbf{0} \end{pmatrix} \cdot kW$$

Temperature calculations at various points:

$$h_{7.FW} := h_{FW.outlet} - \frac{Q_{DSH}}{m_{FW} + \mathbf{0.000001}\,\frac{kg}{s}}$$

$$h_{6.FW} := h_{7.FW} - \frac{Q_{COND}}{m_{FW} + \mathbf{0.000001}\,\frac{kg}{s}}$$

$$T_{2_i} := \begin{cases} T_{steam}\left(p_{BS.inlet_i}, "", h_{steam}\left(p_{BS.inlet_i}, "", "", \mathbf{1}, ""\right), ""\right) & \text{if } p_{BS.inlet_i} > \mathbf{0} = \blacksquare \\ \mathbf{0}\ ^\circ C \quad \text{if } p_{BS.inlet_i} = \mathbf{0} & \end{cases}$$

$$T_{3_i} := \begin{cases} T_{steam}\left(p_{BS.inlet_i}, "", h_{steam}\left(p_{BS.inlet_i}, "", "", \mathbf{0}, ""\right), ""\right) & \text{if } p_{BS.inlet_i} > \mathbf{0} = \blacksquare \\ \mathbf{0}\ ^\circ C \quad \text{if } p_{BS.inlet_i} = \mathbf{0} & \end{cases}$$

$$T_{6_i} := \begin{cases} T_{steam}\left(p_{FW.outlet_i}, "", h_{6.FW_i}, ""\right) & \text{if } p_{BS.inlet_i} > \mathbf{0} = \blacksquare \\ \mathbf{0}\ ^\circ C \quad \text{if } p_{BS.inlet_i} = \mathbf{0} & \end{cases}$$

$$T_{7_i} := \begin{cases} T_{steam}\left(p_{FW.outlet_i}, "", h_{7.FW_i}, ""\right) & \text{if } p_{BS.inlet_i} > \mathbf{0} = \blacksquare \\ \mathbf{0}\ ^\circ C \quad \text{if } p_{BS.inlet_i} = \mathbf{0} & \end{cases}$$

Overall heat transfer coefficient:

$$UA_i := \begin{cases} \dfrac{Q_{COND_i}}{\left[\dfrac{\left(T2_i - T7_i\right) - \left(T3_i - T6_i\right)}{ln\left[\dfrac{\left(T2_i - T7_i\right)}{\left(T3_i - T6_i\right)}\right]}\right]} & \text{if } p_{BS.inlet_i} > 0 \\ 0 & \text{if } p_{BS.inlet_i} = 0 \end{cases} = \ldots \qquad UA = \begin{pmatrix} 1.856 \times 10^6 \\ 1.733 \times 10^6 \\ 1.56 \times 10^6 \\ 1.394 \times 10^6 \\ 0 \\ 0 \end{pmatrix} \cdot \frac{W}{K}$$

Unit conversion:

$$UA := \frac{UA}{\frac{W}{K}} \qquad m_{FW} := \frac{m_{FW}}{\frac{kg}{s}}$$

Mathcad built in non-linear regression:

$$f\left(m_{FW}, a, b\right) := a \cdot {m_{FW}}^b$$

$$dfda\left(m_{FW}, a, b\right) := \frac{d}{da}\left(a \cdot {m_{FW}}^b\right)$$

$$dfdb\left(m_{FW}, a, b\right) := \frac{d}{db}\left(a \cdot {m_{FW}}^b\right)$$

$$FF\left(m_{FW}, test\right) := \begin{pmatrix} f\left(m_{FW}, test_0, test_1\right) \\ dfda\left(m_{FW}, test_0, test_1\right) \\ dfdb\left(m_{FW}, test_0, test_1\right) \end{pmatrix}$$

$$test := \begin{pmatrix} 1 \\ 0.1 \end{pmatrix}$$

$$\begin{pmatrix} a \\ b \end{pmatrix} := \begin{cases} \begin{pmatrix} UA_0 \\ 0 \end{pmatrix} & \text{if } UA_1 > UA_0 \wedge UA_2 > UA_1 \\ genfit\left(m_{FW}, UA, test, FF\right) & \text{if } UA_1 < UA_0 \vee UA_2 < UA_1 \end{cases}$$

Coefficients:

$a = 292173.441$
$b = 0.336$

New overall heat transfer coefficient:

$$UA_t := a \cdot \left(m_{FW_0}\right)^b \cdot \frac{W}{K} = 1.859 \times 10^6 \cdot \frac{W}{K}$$

Inside heat transfer coefficient:

$Re_i := 42454.2$ *Reynolds number*

$Pr_i := 2.38563$ *Prandlt number*

$K_f := 0.671933 \frac{W}{m \cdot K}$ *Thermal conductivity of fluid*

$Nu_i := 0.0243 Re_i^{0.8} \cdot Pr_i^{0.4} = 173.374$ *Dittus boelter equation for fluid being heated*

$h_i := Nu_i \cdot \frac{K_f}{d} = 3883.191 \cdot \frac{W}{m^2 \cdot K}$ *In the FNX model - uses outside diameter of tube wall*

Outside heat transfer coefficient:

$\rho_L := 969.64 \frac{kg}{m^3}$ *Liquid density*

$\rho_v := 0.333233 \frac{kg}{m^3}$ *Vapour density*

$h_{VG} := 2299.46 \frac{kJ}{kg}$ *Enthalpy of evaporation*

$c_p := 4.187 \frac{kJ}{kg \cdot K}$

$T_{sat} := 145.24\ °C$ *Saturation temperature inside vessel*

$T_w := 139.929\ °C$ *Wall temperature*

$\mu := 0.00018889 \frac{kg}{m \cdot s}$ *Fluid viscosity*

$h_o := 0.728 \left[\frac{\rho_L \cdot (\rho_L - \rho_v) \cdot g \cdot h_{VG} \cdot K_f^3}{d \cdot \mu \cdot (T_{sat} - T_w)} \right]^{\frac{1}{4}} = 15651.422 \cdot \frac{W}{m^2 \cdot K}$ *Nusselt approach for a single tube*

Heat transfer coefficient ratio:

$R_h := \frac{h_o}{h_i} = 4.031$

Overall heat transfer coefficient by including fouling:

$UA' := \left[\frac{1}{UA} + \left(\frac{R_i}{A_t} + \frac{R_o}{A_t} \right) \right]^{-1} = 1.355 \times 10^6 \cdot \frac{W}{K}$

Convective heat transfer coefficient, determined by curve and includes fouling:

$$hA := \frac{\left(\frac{1}{R_h} + 1\right)}{\frac{1}{UA'} - \frac{L_t}{K_t \cdot A_t}} = 1.696 \times 10^6 \cdot \frac{W}{K}$$

2. Horizontal heater geometry

Shell geometry inputs:

$Type := 1$	*0 = Header, 1 = Tubesheet*
$N_{passes} := 2$	*Number of tube passes*
$L_{ti} := 10m$	*Length per tube pass*
$D_s := 2m$	*Shell diameter*
$L_{design} := 0.1m$	*Design level*

Tube inputs:

$d := 0.03m$	*Outer tube diameter*
$L_t := 0.001m$	*Tube wall thickness*
$N_{tubes} := 0$	*Number of tubes per bundle*
$N_{plugged} := 0$	*Number of tubes plugged*
$P_L := 1$	*0 = Square 1 = Triangular*

Drain cooling zone inputs:

$DC_L := 0.5$	*DC length percentage*
$DC_H := 0.5$	*DC height percentage*

Additional input parameters:

$L_{bb} := 0.25m$	*Bundle to shell clearance*
$L_{ts} := 0.16m$	*Tubesheet thickness*
$P_T := 0.05m$	*Tube pitch*
$K_t := 50 \frac{W}{m \cdot K}$	*Material thermal conductivity*
$A_t := 10000m^2$	*Material area*
$R_i := 0.001 \frac{m^2 \cdot K}{W}$	*Inside fouling factor*
$R_o := 0.001 \frac{m^2 \cdot K}{W}$	*Outside fouling factor*

Outside bundle diameter:

$$D_{otl} := D_s - 2 \cdot L_{bb} = 1.5\,m$$

Tube bend radius:

$$r_{tube} := \frac{\pi \cdot D_{otl}}{2} = 2.356\,m$$

Tube length by zone:

$$L_{DC} := L_{ti} \cdot DC_L = 5\,m$$
$$L_{DSH} := 0.25 \cdot L_{ti} = 2.5\,m$$
$$L_{COND} := L_{ti} \cdot N_{passes} - L_{DC} - L_{DSH} + r_{tube} = 14.856\,m$$

Inner tube diameter:

$$d_i := d - 2 \cdot L_t = 0.028\,m$$

Calculation if number of tubes are not given:

$$CTP := \begin{cases} 0.93 & \text{if } N_{passes} = 1 \\ 0.9 & \text{if } N_{passes} = 2 \\ 0.85 & \text{if } N_{passes} = 3 \end{cases}$$

$$CL := \begin{cases} 1 & \text{if } P_L = 0 \\ 0.87 & \text{if } P_L = 1 \end{cases}$$

$$N_{tubes} := \begin{cases} N_{tubes} & = 1299 \\ trunc\left(\frac{CTP}{CL} \cdot \frac{\pi \cdot D_s^{\,2}}{4 \cdot P_T^{\,2}}\right) & \text{if } N_{tubes} = 0 \end{cases}$$

Tubesheet thickness if tubesheet is present:

$$CHT_{thickness} := \sqrt{\frac{\left(\frac{D_s - 2 \cdot L_{bb}}{2}\right)^2}{N_{tubes}}} - \frac{d_i}{2} = 0.00681\,m$$

Initial horizontal geometry calculations:

$n := 40$ *Number of increments*

$i := 0 .. n$

$d_{bundle} := D_s - 2 \cdot L_{bb}$ *Total tube bundle diameter*

$inc_i := i \cdot \frac{D_s}{2 \cdot n}$ *Incremental length*

$H_{inc} := inc_n - inc_{n-1}$ *Height per increment*

$DC_{inc} :=$ for $k \in 0 .. n$ $= 40$ *Increment where DC zone ends*

  $x = k$

  break if $inc_k > DC_H \cdot D_s + 0.000001m$

out $= x$

Volume calculation function – inputs level and calculates volume underneath:

$$Vol(Length, Diam, increment) := Length\, Diam^2 \left[\frac{2 \cdot acos\left(1 - \frac{2 \cdot increment}{Diam}\right) - sin\left[2 \cdot \left(acos\left(1 - \frac{2 \cdot increment}{Diam}\right)\right)\right]}{8} \right] \ldots + \frac{\left[\pi \cdot increment^2 \cdot \left(\frac{Diam}{2}\right) - \pi \cdot \frac{increment^3}{3}\right]}{2}$$

Volume calculation of the bundle by using the function for a heater with a drain cooling zone and without:

$Vol_{increment_i} :=$

$out = Vol\left[\left(1 - DC_L\right) \cdot L_{ti}, D_s, inc_i\right]$ if $inc_i \le \left(DC_H \cdot D_s\right)$

$out = Vol\left(L_{ti}, D_s, inc_i\right) - Vol\left(DC_L \cdot L_{ti}, D_s, DC_H \cdot D_s\right)$ if $inc_i > \left(DC_H \cdot D_s\right)$

Volume calculation of the area between the shell and the bundle:

$Vol_{bundle.increment_i} :=$

$out = Vol\left[\left(1 - DC_L\right) \cdot L_{ti}, d_{bundle}, \left(inc_i - L_{bb}\right)\right]$ if $inc_i \le \left(DC_H \cdot D_s\right)$

$out = Vol\left[L_{ti}, d_{bundle}, \left(inc_i - L_{bb}\right)\right] - Vol\left(DC_L \cdot L_{ti}, d_{bundle}, DC_H \cdot d_{bundle}\right)$ if $inc_i > \left(DC_H \cdot D_s\right)$

$out = 0$ if $inc_i - L_{bb} < 0$

Free volume calculation:

$Vol_{Free_i} :=$

$out = Vol_{increment_i}$ if $inc_i < L_{bb}$

$out = \left(Vol_{increment_i} - Vol_{bundle.increment_i}\right) + \left[Vol_{bundle.increment_i}\left(1 - \frac{N_{tubes} \cdot d^2}{D_{otl}^2}\right)\right]$ if $inc_i \ge L_{bb}$

Calculation process to determine each area of each consecutive frustum:

$Area_0 := 0.71m^2$ *Initial area, this is the driven factor which...*
determines the smoothness of the curve.

$(j := 1 .. DC_{inc} - 1)$ *Runs the iterations only up to the DC height*

$Freevol_j := Vol_{Free_j} - Vol_{Free_{j-1}}$

$$Area_j := -\frac{Area_{j-1} \cdot H_{inc} - 6 \cdot Freevol_j + \sqrt{3} \cdot H_{inc} \cdot \sqrt{-\frac{(Area_{j-1})^2 \cdot H_{inc} - 4 \cdot Area_{j-1} \cdot Freevol_j}{H_{inc}}}}{2 \cdot H_{inc}}$$

Frustum areas just after the drain cooling zone:

$Area_{DC_{inc}} := 7.1m^2$ *Runs the iterations from the DC height to half-way mark of the shell*

$j := \begin{cases} DC_{inc} + 1 .. n & \text{if } DC_{inc} < n \\ n & \text{otherwise} \end{cases}$ *If the DC height is up to the half-way mark, then...*

the second part will only calculate the last area

$Freevol_j := Vol_{Free_j} - Vol_{Free_{j-1}}$

$$Area_j := -\frac{Area_{j-1} \cdot H_{inc} - 6 \cdot Freevol_j + \sqrt{3} \cdot H_{inc} \cdot \sqrt{-\frac{(Area_{j-1})^2 \cdot H_{inc} - 4 \cdot Area_{j-1} \cdot Freevol_j}{H_{inc}}}}{2 \cdot H_{inc}}$$

Calculation of the last area, which uses the last half of the shell volume:

$$Freevol := \left(\pi \cdot \frac{D_s^2}{8} \cdot L_{ti} + \frac{1}{3} \cdot \pi \cdot \frac{D_s^3}{8}\right) - \left(\frac{N_{tubes} \cdot d^2}{D_{otl}^2}\right) \cdot \left(\pi \cdot \frac{d_{bundle}^2}{8} \cdot L_{ti} + \frac{1}{3} \cdot \pi \cdot \frac{d_{bundle}^3}{8}\right)$$

$$Area_{n+1} := -\frac{Area_n \cdot \frac{D_s}{2} - 6 \cdot Freevol + \sqrt{3} \cdot \frac{D_s}{2} \cdot \sqrt{-\frac{(Area_n)^2 \cdot \frac{D_s}{2} - 4 \cdot Area_n \cdot Freevol}{\frac{D_s}{2}}}}{2 \cdot \frac{D_s}{2}}$$

$inc_{n+1} := D_s$

3. Vertical heater geometry

Shell geometry inputs:

$Type := 0$ *0 = Header, 1 = Tubesheet*

$N_{passes} := 3$ *Number of tube passes*

$L_{ti} := 8.85m$ *Length per tube pass*

$D_s := 1.75m$ *Shell diameter*

$L_{design} := 1m$ *Design level*

Tube geometry inputs:

$d := 0.025m$ *Outer tube diameter*

$L_t := 0.0022m$ *Tube wall thickness*

$N_{tubes} := 345$ *Number of tubes per bundle*

$N_{plugged} := 0$ *Number of tubes plugged*

$P_L := 0$ *0 = Square, 1 = Triangular*

Additional input parameters:

$L_{bb} := 0.25m$ *Bundle to shell clearance*

$L_{ts} := 0.16m$ *Tubesheet thickness*

$P_T := 0.05m$ *Tube pitch*

Outside bundle diameter:

$$D_{otl} := D_s - 2 \cdot L_{bb} = 1.25\,m$$

Tube bend radius:

$$r_{tube} := \frac{\pi \cdot D_{otl}}{2} = 1.963\,m$$

Tube length per zone:

$$L_{DC} := L_{ti} \cdot 0.25 = 2.212\,m$$

$$L_{DSH} := 0.25 \cdot L_{ti} = 2.212\,m$$

$$L_{COND} := L_{ti} \cdot N_{passes} - L_{DC} - L_{DSH} + r_{tube} = 24.088\,m$$

Inner tube diameter:

$$d_i := d - 2 \cdot L_t = 0.021\,m$$

Calculations for the number of tubes if not given:

$$CTP := \begin{cases} 0.93 & \text{if } N_{passes} = 1 \\ 0.9 & \text{if } N_{passes} = 2 \\ 0.85 & \text{if } N_{passes} = 3 \end{cases}$$

$$CL := \begin{cases} 1 & \text{if } P_L = 0 \\ 0.87 & \text{if } P_L = 1 \end{cases}$$

$$N_{tubes} := \begin{cases} N_{tubes} & = 345 \\ trunc\left(\frac{CTP}{CL} \cdot \frac{\pi \cdot D_s^2}{4 \cdot P_T^2}\right) & \text{if } N_{tubes} = 0 \end{cases}$$

Initial vertical geometry calculations:

$n := 40$ *Number of increments*

$i := 0 .. n$

$d_{bundle} := D_s - 2 \cdot L_{bb} = 1.25\,m$ *Total tube bundle diameter*

$inc_i := i \cdot \frac{L_{ti}}{2 \cdot n}$ *Incremental length*

$FreeVol := \frac{\pi}{4} \cdot d_{bundle}^2 - \frac{\pi}{4} \cdot d^2 \cdot N_{tubes} \cdot N_{passes} = 0.719\,m^2$ *Calculation of the free volume in the vertical heater*

$Area_i := FreeVol$

$Area_{n+1} := 0.00000 m^2$ *Sets the last area to 0*

4. Level calculations

Initial calculations:

$D_{level} := 0.5m$ *Design level*

$p := 416.992kPa$ *Current saturation pressure*

$V_t := 12.524m^3$ *Tank volume*

$$v_g := \frac{1}{\rho_{steam}\left(p, "", "", h_{steam}(p, "", "", 1, "") , ""\right)} = 0.445 \frac{m^3}{kg}$$

$$v_l := \frac{1}{\rho_{steam}\left(p, "", "", h_{steam}(p, "", "", 0, "") , ""\right)} = 0.001 \frac{m^3}{kg}$$

Liquid volume calculations:

$h_{initial} := D_{level}$ *Level set point (given by user)*

$i_L :=$ for $i \in 0..n$ $= 21$ *Determines the increment where the level sits*
  increment $= i$ if $h_{initial} < inc_i$
  break if $h_{initial} < inc_i$
increment

$h_{inc1} := inc_{i_L - 1} = 0.5\,m$

$h_{inc2} := inc_{i_L} = 0.525\,m$

$A_{inc1} := Area_{i_L - 1} = 6.757\,m^2$

$A_{inc2} := Area_{i_L} = 6.647\,m^2$

$V_{inc1} := Vol_{Free_{i_L - 1}} = 2.861 \cdot m^3$

$V_{inc2} := Vol_{Free_{i_L}} = 3.029 \cdot m^3$

$h_{tot} := 0.02m$ *Incremental height*

$h_1 := h_{initial} - h_{inc1} = 0\,m$

$h_2 := h_{inc2} - h_{initial} = 0.025\,m$

$a := \sqrt{A_{inc1}} = 2.599\,m$

$b := \sqrt{A_{inc2}} = 2.578\,m$

$$c := \frac{a \cdot h_{tot} - a \cdot h_2 + b \cdot h_{tot} - b \cdot h_1}{h_1 + h_2} = 1.543\,m$$

$$V_1 := \frac{h_1}{3} \cdot \left(a^2 + c^2 + \sqrt{a^2 \cdot c^2}\right)$$ *Volume of a frustum*

$V_1 := V_1 + V_{inc1}$ *Adds the calculated volume to the total value at the previous increme*

$V_1 = 2.8612 \cdot m^3$

$V_l := V_1 = 2.861 \cdot m^3$

Quality calculations:

$$M_l := \frac{V_l}{v_l} = 2636.594\,kg$$

$$M_g := \frac{V_t - V_l}{v_g} = 21.732\,kg$$

$$x := \frac{M_g}{M_g + M_l}$$ *Mass fraction*

$x = 0.00817$ *Quality used in two-phase tank*

2. Turbine component

1. Pressure drop and efficiency calculations

Design inputs:

$m_D := 415.662 \frac{kg}{s}$ *mass flow*

$p_{i.D} := 16100 kPa$ *Upstream pressure*

$h_{i.D} := 3324.8 \frac{kJ}{kg}$ *Upstream enthalpy*

$p_{e.D} := 3549 kPa$ *Downstream pressure*

$r_{c.D} := 0.1$ *Critical pressure ratio*

$\alpha := 2.05$ *Pressure ratio exponent*

$\beta := 2$ *Efficiency coefficient*

$\eta_D := 0.87$ *Turbine segment efficiency*

$N_D := 3000$ *Shaft rotating speed*

Flownex operational inputs:

$p_i := 16423.5 kPa$ *Upstream pressure*

$h_i := 3322.1 \frac{kJ}{kg}$ *Upstream enthalpy*

$p_e := 2014.3 kPa$ *Downstream pressure*

$\Delta P := p_i - p_e = 14409.2 \cdot kPa$ *Pressure drop*

$\rho := 30.355 \frac{kg}{m^3}$ *Fluid density (average)*

$N := 3000$ *Speed*

Pressure drop:

$r_D := \frac{p_{e.D}}{p_{i.D}} = 0.22$

$r := \frac{p_e}{p_i} = 0.123$

Density:

$$\rho_{i.D} := \rho_{steam}(p_{i.D}, "", "", h_{i.D}, "") = 51.035 \frac{kg}{m^3}$$

$$\rho_i := \rho_{steam}(p_i, "", "", h_i, "") = 52.171 \frac{kg}{m^3}$$

Mass flow:

$$m_{SE} = m_D \cdot \sqrt{\frac{\rho_i \cdot p_i}{\rho_{i.D} \cdot p_{i.D}}} \cdot \sqrt{\frac{1 - \left(\frac{r - r_{c.D}}{1 - r_{c.D}}\right)^{\alpha}}{1 - \left(\frac{r_D - r_{c.D}}{1 - r_{c.D}}\right)^{\alpha}}} = 427.826$$

Ck pressure drop value:

$$Ck := \left| \frac{\Delta P \cdot \rho}{m^2} \right| = 2389.656 \frac{1}{m^4}$$

Efficiency calculations:

$$s_{i.D} := s_{steam}(p_{i.D}, "", "", "", h_{i.D}) = 6.337 \cdot \frac{kJ}{kg \cdot K}$$

$$s_i := s_{steam}(p_i, "", "", "", h_i) = 6.326 \cdot \frac{kJ}{kg \cdot K}$$

$$h_{e.D} := h_{steam}(p_{e.D}, "", "", "", s_{i.D}) = 2919.155 \cdot \frac{kJ}{kg}$$

$$h_e := h_{steam}(p_e, "", "", "", s_i) = 2793.361 \cdot \frac{kJ}{kg}$$

$$\eta := \eta_D - \beta \cdot \left[\frac{N \cdot \sqrt{(h_{i.D} - h_{e.D})}}{N \cdot \sqrt{(h_i - h_e)}} - 1 \right]^2 = 0.839$$

2. Turbine casing calculations

Geometrical inputs:

$r_{shaft} := 0.5m$	*Shaft radius*
$m_{shaft} := 12330.8kg$	*Shaft mass*
$\rho_{shaft} := 7284 \frac{kg}{m^3}$	*Density of shaft*
$r_{casing} := 0.7m$	*Casing outside radius*
$th_{casing} := 0.04m$	*Casing wall thickness*

Calculations:

$L_{shaft} := \frac{m_{shaft}}{\rho_{shaft} \cdot \pi \cdot r_{shaft}^{2}} = 2.155\,m$ *Shaft length*

$A_{shaft} := 2 \cdot \pi \cdot r_{shaft} \cdot L_{shaft} = 6.771\,m^{2}$ *Shaft outside area*

$A_{casing.i} := 2 \cdot \pi \cdot \left(r_{casing} - th_{casing}\right) \cdot L_{shaft} = 8.938\,m^{2}$ *Inside area*

$A_{casing.o} := 2 \cdot \pi \cdot r_{casing} \cdot L_{shaft} = 9.48\,m^{2}$ *Outside area*

$A_{flow} := \pi \cdot \left(r_{casing} - th_{casing}\right)^{2} - \pi \cdot r_{shaft}^{2} = 0.583\,m^{2}$

$I_{shaft} := m_{shaft} \cdot r_{shaft}^{2} = 3082.7\,m^{2} \cdot kg$ *Rotational inertia*

Appendix B. Curve fit methods

Appendix B contains the curve algebra for the curve fit methods used in the deaerator and the feedwater heater component. (Least squares method (Deaerator valve pressure drop)

1. Least squares method (Deaerator valve pressure drop)

Data points in form of $(x_1, y_1); (x_2, y_2); \ldots (x_n, y_n)$ is given. It is required to fit a line through the points and a method for doing this is by using the least squares method. The first step is to calculate the mean values of both x - and y - values.

$$\bar{X} = \frac{\sum_{i=1}^{n} x_i}{n} \tag{1.1}$$

$$\bar{Y} = \frac{\sum_{i=1}^{n} y_i}{n} \tag{1.2}$$

The slope can now be determined by using the following formula:

$$m = \frac{\sum_{i=1}^{n} \left(x_i - \bar{X}\right) \cdot \left(y_i - \bar{Y}\right)}{\sum_{i=1}^{n} \left(x_i - \bar{Y}\right)^2} \tag{1.3}$$

The line is plotted with a load indication factor, in this case the mass flow. This results in the line going through the origin, thus the line constant equates to 0. The equation for the line therefore is written as

$$y = m \cdot x \tag{1.4}$$

2. Power fit (feedwater heater, condensing zone)

The feedwater heater's performance characteristics uses a power fit curve to define the data. The data is given as mass flow (x coordinates) and overall heat transfer coefficient (y coordinates). The power fit function is described in equation (2.1). The objective is to determine the coefficients a and b which will satisfy the data points given.

$$UA = a \cdot m^b \tag{2.1}$$

An approach is to take the natural logarithm of each side of equation (2.1), which then results in

$$\begin{aligned}\ln(UA) &= \ln(a \cdot m^b) \\ \ln(UA) &= \ln(a) + b \cdot \ln(m)\end{aligned} \tag{2.2}$$

Which is in the form of a linear equation $y = c + m \cdot x$. The least squares method can now be applied to the equation to determine the coefficients c and m as described in the previous paragraph and ultimately the coefficients a and b for the power fit by using the natural logarithm of the linear coefficients.

3. Second order polynomial (feedwater heater, drain cooling zone)

A second order polynomial curve fit is used in plotting the drain cooling zone's heat transfer performance. The method uses matrix calculations to fit the second order polynomial. Initially, data points is given in the form of $(x_1, y_1);(x_2, y_2);\ldots(x_n, y_n)$ where the mass flow is x and the total amount of heat transfer is y for the zone. The second order polynomial equation is given in equation (3.1).

$$y = a_2 \cdot x^2 + a_1 \cdot x + a_0 \tag{3.1}$$

The coefficients of the polynomial are determined by using linear algebra. This is done by first writing the data points in the following matrix equation

$$\begin{bmatrix} n & \sum_{i=1}^{n} x_i & \sum_{i=1}^{n} x_i^2 \\ \sum_{i=1}^{n} x_i & \sum_{i=1}^{n} x_i^2 & \sum_{i=1}^{n} x_i^3 \\ \sum_{i=1}^{n} x_i^2 & \sum_{i=1}^{n} x_i^3 & \sum_{i=1}^{n} x_i^4 \end{bmatrix} \begin{bmatrix} a_0 \\ a_1 \\ a_2 \end{bmatrix} = \begin{bmatrix} \sum_{i=1}^{n} y_i \\ \sum_{i=1}^{n} y_i \cdot x_i \\ \sum_{i=1}^{n} y_i \cdot x_i^2 \end{bmatrix} \tag{3.2}$$

which is in the form of $Ma = b$. This form represents a set of linear equations derived from the polynomial residual function. One can now find the inverse of matrix M and multiply it with matrix b to find the coefficients a.

$$a = M^{-1} b \tag{3.3}$$

Appendix C. Mesh independence studies

Appendix C contains the incremental and node independence studies used for modelling heat transfer. The importance of these studies is to model the heat transfer as accurately as possible whilst using the least amount of computational resources.

The thick-walled components are modelled by using the composite heat transfer element. This element models the heat transfer by using the well-known CCC problem. Convection is modelled by using multiple increments specified by the pipe element, and conduction by multiple node elements in the composite heat transfer element. The discretization for heat transfer in the composite heat transfer element is shown in Figure C-1.

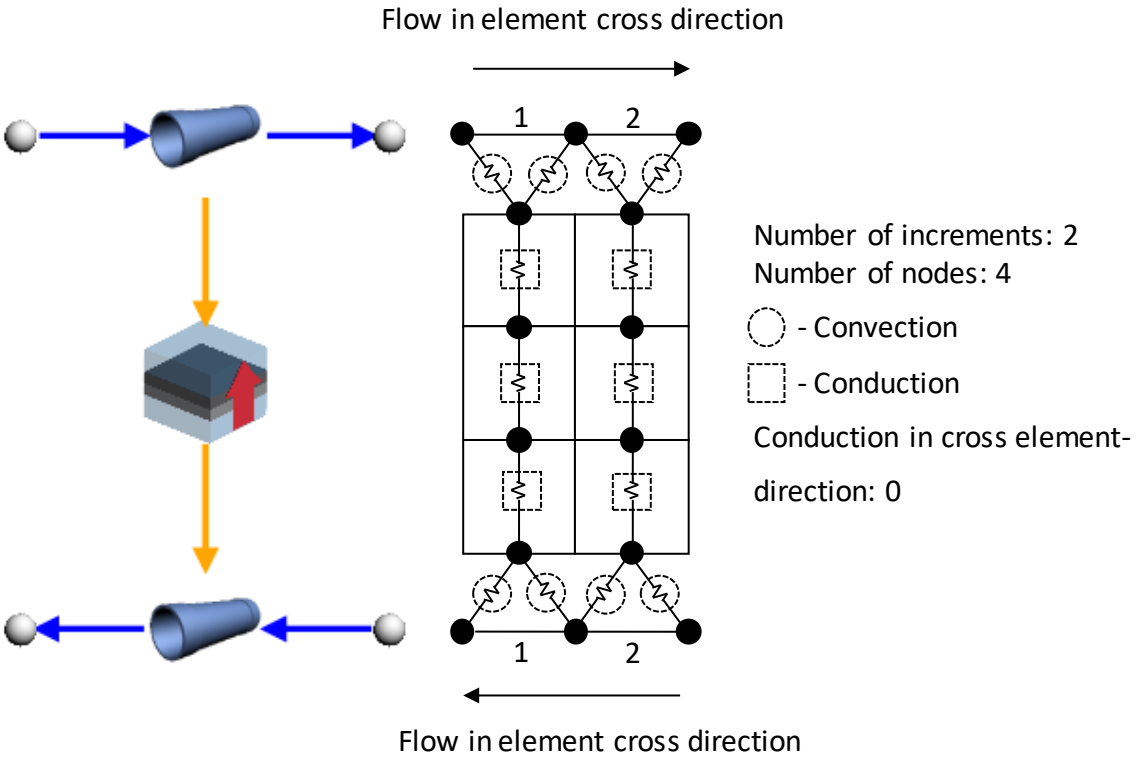

Figure C-1: Composite heat transfer element discretization

The example in the figure shows a network where the pipe element has been divided into two increments and the heat transfer element into 4 nodes. The number of nodes must not be lower than 2, which implies that no conduction occurs and the network will not solve.

Incremental or node independence refers to the point where increasing the number of increments does not influence the results to a significant degree. The independence studies is therefore done for each heat transfer element in the feedwater heater and the turbine models.

1. Feedwater heater component's condensing zone

The condensing zone of the feedwater heater is modelled by using a two-phase connected to a pipe through a composite heat transfer element.

The number of increments for the pipe element was tested by looking at the amount of conduction heat transfer by the zone. The number of increments were increased from one up to 15. It was noticed that the solving time of the model increased by 1 second during the study. The recorded results are shown in Figure C-2. The number of nodes were tested by suddenly dropping the inlet feedwater temperature of the heater and recording the time it takes for the outlet to drop by a few degrees. These results are also displayed on Figure C-2.

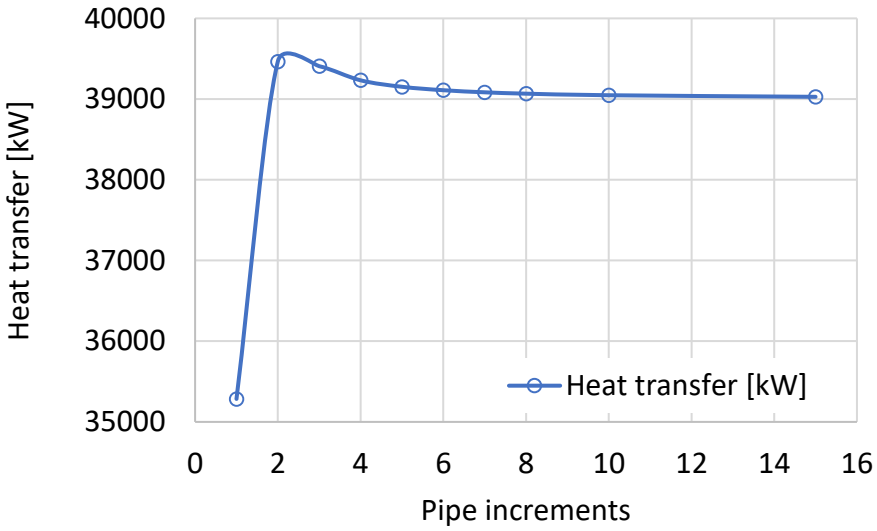

Figure C-2: Mesh independence study for the condensing zone

By changing the increments, one can see that the total heat transfer of condensing zone is influenced. As the increments are increased, the result becomes independent from the number of increments used. The number of increments was therefore chosen to be 5 since this would result in 0.3 % difference from a result that is not increment dependent.

2. Feedwater heater component's tubesheet

The tubesheet of the heater used a pipe component connected to a node through a composite heat transfer element to model the heat transfer. The heat transfer will however only occur when a temperature difference is encountered, which is the case during transient scenarios.

A node independence study was done on the tubesheet component. The network was set up using the element as shown in Figure 3.38 with two boundary conditions on either side of the pipe element. The conditions were set to what one would typically encounter in a large coal-fired power

station. The transient scenario involved dropping the inlet temperature of the feedwater by 20 °C and recording the time it took for the node to drop by 18 °C. The results are displayed in Figure C-3.

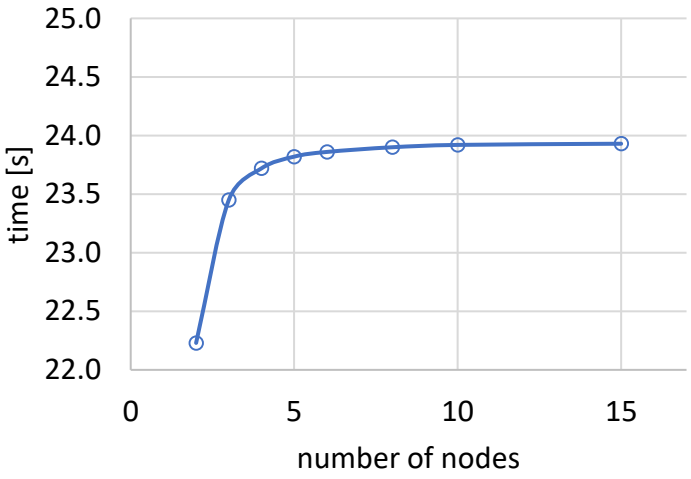

Figure C-3: Mesh independence for tubesheet

From the study, one can see that by using a maximum number of nodes the time it took for the downstream node to drop by 18 °C was 24.93 seconds. The time it took for 5 nodes was 23.82 seconds, which is a 0.4 % error which is sufficient. Thus, 5 nodes were chosen for the tubesheet heat transfer element.

3. Turbine component's shaft and casing

A node independence study was also done on the turbine's shaft and casing components. The network was set up by using the turbine component with the shaft and casing at atmospheric temperature. The steam is sent through the turbine at normal boiler outlet conditions. The outlet temperature of the steam was then recorded for various heat transfer nodes and the results are in Figure C-4.

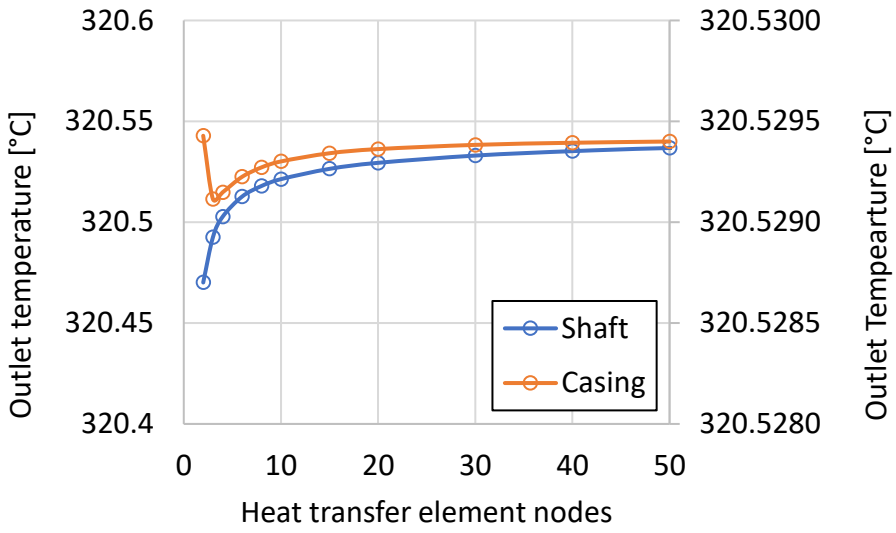

Figure C-4: Mesh independence study for the turbine shaft

From Figure C-4 one can see that the outlet temperature results only change by a few decimals of a degree for various nodes for the shaft. The casing's results showed even less of a change. It can therefore be concluded that the nodes will not make an impact on the overall results and a total number of 5 nodes for each heat transfer element was chosen.

Appendix D. Feedwater heater geometry validation

The feedwater heater component's geometry has been validated using a simplified 3D CAD model of a horizontal heater. Various configurations were tested where the inputs for each configuration were kept the same for the Flownex model and the 3D CAD model.

1. Case 1

Case 1 involved setting the heater geometry to not include a drain cooling zone. This meant that the liquid level was spanned the entire length of the shell for each level instance.

Table D-1: Case 1 FWH geometrical validation

FWH geometry	
Shell	[m]
Diameter:	2
Length:	10
Tubes	[m]
Diameter:	0.03
Pitch:	0.06
Bundle to shell clearance	0.25
DC zone	[0-1]
Length:	0
Height:	0

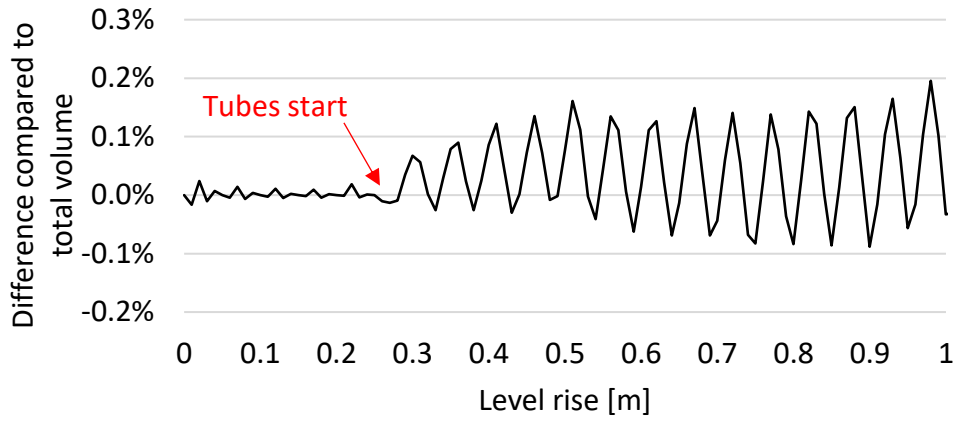

Figure D-1: Case FWH geometrical validation

2. Case 2

Case 2 involved setting the heater geometry to include a drain cooling zone. The drain cooling zone spanned the entire length of the shell but its height was limited to one quarter of the diameter of the shell.

Table D-2: Case 2 FWH geometrical validation

FWH geometry	
Shell	[m]
Diameter:	2
Length:	10
Tubes	[m]
Diameter:	0.03
Pitch:	0.06
Bundle to shell clearance	0.25
DC zone	[0-1]
Length:	1
Height:	0.25

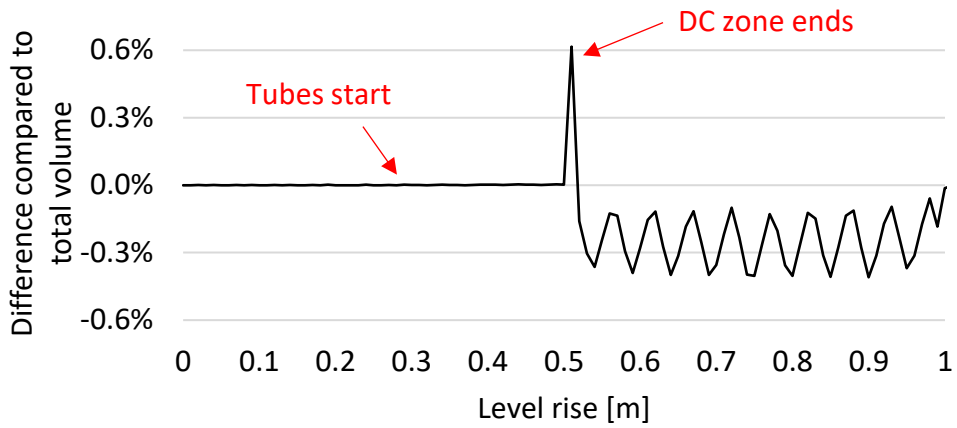

Figure D-2: Case 2 FWH geometrical validation

3. Case 3

Case 3 involved setting the heater geometry to include a drain cooling zone. The drain cooling zone spanned the half the length and half the diameter of the shell.

Table D-3: Case 3 FWH geometrical validation

FWH geometry	
Shell	[m]
Diameter:	2
Length:	10
Tubes	[m]
Diameter:	0.03
Pitch:	0.06
Bundle to shell clearance	0.25
DC zone	[0-1]
Length:	0.5
Height:	0.5

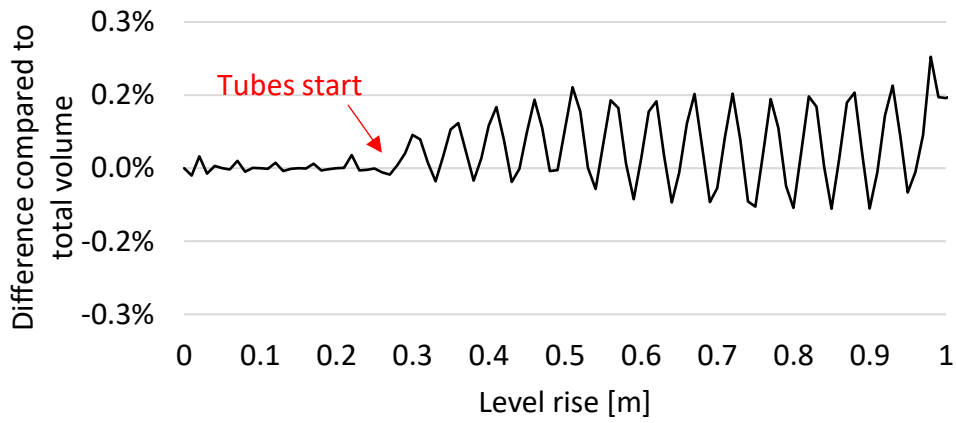

Figure D-3: Case 3 FWH geometrical validation

4. Case 4

Case 4 involved setting the heater geometry to include a drain cooling zone. The drain cooling zone spanned the half the length and one quarter the diameter of the shell.

Table D-4: Case 4 FWH geometrical validation

FWH geometry	
Shell	[m]
Diameter:	2
Length:	10
Tubes	[m]
Diameter:	0.03
Pitch:	0.06
Bundle to shell clearance	0.25
DC zone	[0-1]
Length:	0.5
Height:	0.25

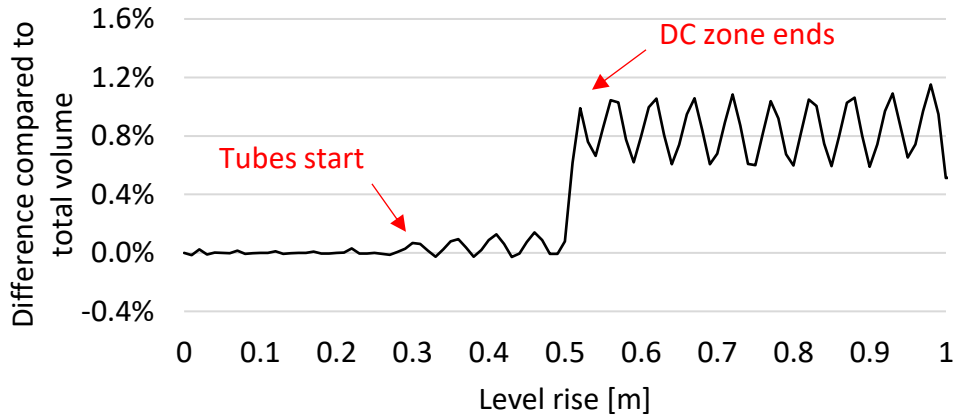

Figure D-4: Case 4 FWH geometrical validation

5. Case 5

Case 5 involved changing most of the parameters from the previous cases.

Table D-5: Case 5 FWH geometrical validation

FWH geometry	
Shell	[m]
Diameter:	1.6
Length:	8
Tubes	[m]
Diameter:	0.025
Pitch:	0.05
Bundle to shell clearance	0.1
DC zone	[0-1]
Length:	0.5
Height:	0.3

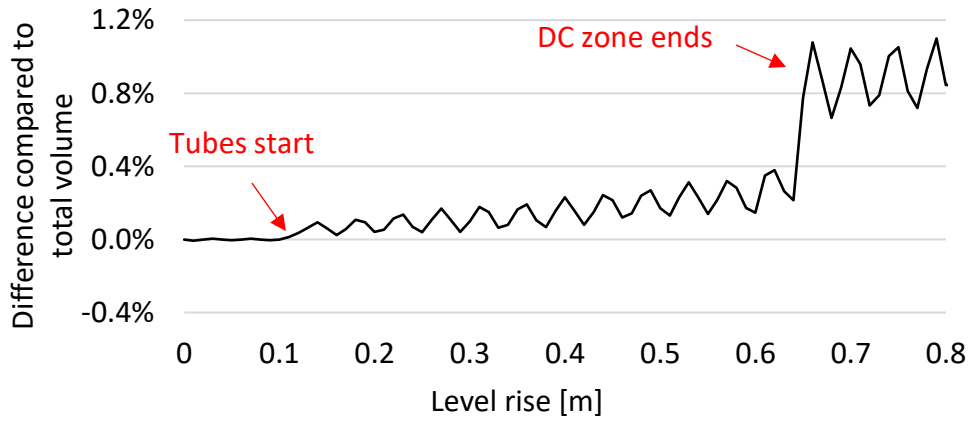

Figure D-5: Case 5 FWH geometrical validation